

#5

~~CONFIDENTIAL~~

AD 333 298

*Reproduced  
by the*

**ARMED SERVICES TECHNICAL INFORMATION AGENCY  
ARLINGTON HALL STATION  
ARLINGTON 12, VIRGINIA**



Office of the Secretary of Defense *5 USC sec 552 and*  
Chief, RDD, ESD, WHS  
Date: 26 Apr 2013 Authority: EO 13526  
Declassify:   A   Deny in Full: \_\_\_\_\_  
Declassify in Part: \_\_\_\_\_  
Reason: \_\_\_\_\_  
MDR: 12-M-3148

~~CONFIDENTIAL~~

DECLASSIFIED IN FULL  
Authority: EO 13526  
Chief, Records & Declass Div, WHS  
Date: **26 APR 2013**

*2-2*  
**12-M-3148**

NOTICE: When government or other drawings, specifications or other data are used for any purpose other than in connection with a definitely related government procurement operation, the U. S. Government thereby incurs no responsibility, nor any obligation whatsoever; and the fact that the Government may have formulated, furnished, or in any way supplied the said drawings, specifications, or other data is not to be regarded by implication or otherwise as in any manner licensing the holder or any other person or corporation, or conveying any rights or permission to manufacture, use or sell any patented invention that may in any way be related thereto.

Page determined to be Unclassified  
Reviewed Chief, RDD, WMS  
IAW EO 13526, Section 3.5  
Date:

26 APR 2013

[Redacted]

[Redacted]

333 298



THE GENERAL MILLS ELECTRONICS GROUP

DECLASSIFIED IN FULL  
Authority: EO 13526  
Chief, Records & Declass Div, WHS  
Date: 26 APR 2013



~~CONFIDENTIAL~~

ORIGINAL CONTAINS COLOR PHOTOS AND ASTIA  
REPRODUCTIONS WILL BE IN BLACK AND WHITE.  
ORIGINAL MAY BE SEEN IN ASTIA HEADQUARTERS.

~~DO NOT REPRODUCE~~  
~~FOR PUBLICATION~~

This document consists of 150 pages and is number 1  
of 14 copies, series 4, and the following attachments.

NINTH QUARTERLY  
PROGRESS REPORT  
ON  
DISSEMINATION OF SOLID  
AND LIQUID BW AGENTS

(Unclassified Title)

For Period June 4, 1962 - September 4, 1962  
Contract No. DA-18-064-CML-2745

~~CONFIDENTIAL~~  
~~FOR PUBLICATION~~

Prepared for:

U. S. Army Biological Laboratories  
Fort Detrick, Maryland

Submitted by:

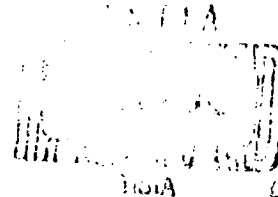
*G. R. Whitnah*  
G. R. Whitnah  
Project Manager

Report No: 2344  
Project No: 82408  
Date: October 19, 1962

Approved by:

*S. E. Jones*  
S. E. Jones, Director  
Aerospace Research

Engineering and Research  
2003 East Hennepin Avenue  
Minneapolis 13, Minnesota



~~CONFIDENTIAL~~

DECLASSIFIED IN FULL  
Authority: EO 13526  
Chief, Records & Declass Div, WHS  
Date: 26 APR 2013



## FOREWORD

Staff members of the Aerospace Research Department and Engineering Department who have participated in directing and performing the work reported herein include Messrs. S. P. Jones, Jr., G. Whitnah, M. Sandgren, A. Anderson, R. Lindquist, J. McGillicuddy, J. Upton, C. Hagberg, W. L. Torgeson, S. Steinberg, P. Stroom, G. Morfitt, J. Walters, A. T. Bauman, T. Petersen, D. Harrington, R. Ackroyd, D. Kedi, B. Schmidt, G. Lunde, R. Dahlberg, R. Kendall, A. Kydd, E. Knutson, J. Unga, D. Stender, H. Kuhlman, G. Granley, J. Pilney, A. Johnson, and O. Fackler.

Page determined to be Unclassified  
Reviewed Chief, RDD, WHS  
IAW EO 13526, Section 3.5  
Date: 6 APR 2013

~~CONFIDENTIAL~~

## ABSTRACT

This Ninth Quarterly Progress Report covers the period from June 4, 1962 to September 4, 1962. Accomplishments are reported in all phases of the research and development program pertaining to the line-source dissemination of BW agents.

Theoretical and experimental results relative to the studies of the mechanics of dry powders are presented for: 1) the applied stresses and energies required for the compaction of powders, 2) shear strength of compacted powders, and 3) bulk tensile strength and bulk density of compacted powders as a function of compressive load and distance from the face of the piston.

Data on aerosol decay as affected by relative humidity are reported for five powders. A statistical analysis of the behavior of aerosols is presented to explain the phenomena observed in the aerophilometer.

Tests on dissemination and deagglomeration, using the wind tunnel, are described which establish an upper limit of approximately  $0.58 \text{ g/cm}^3$  density for compacted Sm which can be aerosolized efficiently by the aerodynamic breakup mechanism. A related discussion reports some preliminary data on the effects of storage on the aerodynamic breakup of compacted Sm.

Wind tunnel evaluation of a shroud for the discharge tube of the airborne dry agent disseminator is discussed.

Work with the full-scale experimental equipment for feeding and metering both compacted and uncompact powder is reported.

Progress is reported on the design and fabrication of the first-generation airborne dry BW agent disseminating store.

An apparatus is described which is used for inserting charges of compacted powder into the experimental model of the dry agent disseminator. Other techniques for filling the disseminator are discussed.

Successful flight tests of the General Mills, Inc. liquid agent disseminating store on F-105 and F-100D airplanes at Eglin Air Force Base are reported.

iii

~~CONFIDENTIAL~~

DECLASSIFIED IN FULL  
Authority: EO 13526  
Chief, Records & Declass Div, WHS  
Date: 26 APR 2013

~~CONFIDENTIAL~~

## TABLE OF CONTENTS

Section	Title	Page
1.	INTRODUCTION	1-1
2.	THEORETICAL AND EXPERIMENTAL STUDIES OF THE MECHANICS OF DRY POWDERS	2-1
2.1	Experimental Compaction Studies	2-1
2.1.1	Apparatus	2-1
2.1.2	Experimental Results and Discussion	2-2
2.2	Triaxial Shear Tests	2-7
2.3	Bulk Tensile Strength of Compressed Powders	2-15
2.4	Shear Strength of Compressed Powders by the Sliding Disk Method	2-26
2.5	Bulk Density of Compressed Powders	2-27
3.	AEROSOL STUDIES	3-1
3.1	Study of the Effects of Environmental Humidity on Aerosol Decay	3-1
3.2	Considerations on Light-Scattering Noise Levels	3-8
3.3	Mathematical Analysis of Fluctuations in the Light-Scattering Signal	3-10
3.4	A Swirl Powder Dispenser	3-20
3.5	Conclusions and Plans for Future Work	3-22
4.	DISSEMINATION AND DEAGGLOMERATION STUDIES	4-1
4.1	General	4-1
4.2	Aerosol Concentration Measurements	4-1
4.3	Shroud Investigation-Prototype Dry Agent Disseminator	4-5
4.4	Wind Tunnel Boundary Layer	4-12
4.5	<u>Sm</u> Storage Test	4-14
5.	CONTINUATION OF EXPERIMENTS WITH THE FULL-SCALE FEEDER FOR COMPACTED DRY AGENT SIMULANT MATERIALS	5-1
5.1	Tests at 0.65 g/cm <sup>3</sup> Density	5-1
5.2	Wind-Tunnel Dissemination of Talc Discharged from Feeder	5-1
5.3	Operation with Uncompacted Talc	5-2

~~CONFIDENTIAL~~

~~CONFIDENTIAL~~

TABLE OF CONTENTS (Continued)

<u>Section</u>	<u>Title</u>	<u>Page</u>
6.	DESIGN AND FABRICATION OF THE FIRST-GENERATION PROTOTYPE DRY AGENT DISSEMINATING STORE	6-1
6.1	Store Structure	6-1
6.2	Rotary Actuator Assembly	6-6
6.3	Cockpit Control Panel	6-7
6.4	Aft Actuator Control Panel	6-8
6.5	Dry Nitrogen System	6-8
7.	FILLING THE DRY AGENT DISSEMINATING STORE	7-1
7.1	Introduction	7-1
7.2	Loading Fixture	7-2
7.3	Multiple Sealed Packages	7-5
8.	FLIGHT TESTING OF LIQUID AGENT DISSEMINATING STORE	8-1
9.	SUMMARY AND CONCLUSIONS	9-1
10.	REFERENCES	10-1
	APPENDIX A. LAYOUT, EJECTION TUBE SHROUD	A-1
	APPENDIX B. CONTROL BOX	B-1

DECLASSIFIED IN FULL  
Authority: EO 13526  
Chief, Records & Declass Div, WHS  
Date:

26 APR 2013

~~CONFIDENTIAL~~

~~CONFIDENTIAL~~

### LIST OF ILLUSTRATIONS

Figure	Title	Page
2.1	Compaction Apparatus	2-3
2.2	Compaction of Cornstarch-Compaction Rate 0.020 in./min, Initial Specific Volume 1.71 cm <sup>3</sup> /g	2-4
2.3	Compaction Stress as a Function of Powder Specific Volume-Compaction Rate 0.020 in./min	2-6
2.4	Compaction Characteristics of Various Powdered Materials at 0.200 in./min Compaction	2-8
2.5	Exploded View of Triaxial Test Sample Preparation Assembly	2-10
2.6	Load-Strain Curve for Compacted Saccharin ( $\rho_0 = 0.65 \text{ g/cm}^3$ )	2-12
2.7	Compacted Saccharin Failed in Compression ( $\rho_0 = 0.65 \text{ g/cm}^3$ )	2-12
2.8	Shear Locus Curve Illustrating the Relationship between Bulk Shear Strength $\tau_0$ and Bulk Tensile Strength $\sigma_{t0}$	2-13
2.9	Bulk Tensile Strength for Saccharin as a Function of Distance "L" from Compressive Force at a Compressive Load of 1454 g	2-16
2.10	Bulk Tensile Strength for Saccharin as a Function of Distance "L" from Compressive Force at a Compressive Load of 2130 g	2-17
2.11	Bulk Tensile Strength for Saccharin as a Function of Distance "L" from Compressive Force at a Compressive Load of 2919 g	2-18
2.12	Bulk Tensile Strength for Cornstarch as a Function of Distance "L" from Compressive Force at a Compressive Load of 1454 g	2-19
2.13	Bulk Tensile Strength for Cornstarch as a Function of Distance "L" from Compressive Force at a Compressive Load of 2130 g	2-20

~~CONFIDENTIAL~~

~~CONFIDENTIAL~~

LIST OF ILLUSTRATIONS (Continued)

Figure	Title	Page
2. 14	Bulk Tensile Strength for Cornstarch as a Function of Distance "L" from Compressive Force at a Compressive Load of 2919 g	2-21
2. 15	Bulk Tensile Strength for Sm as a Function of Distance "L" from Compressive Force at a Compressive Load of 2130 g	2-22
2. 16	Bulk Tensile Strength for Sm as a Function of Distance "L" from Compressive Force at a Compressive Load of 2919 g	2-23
2. 17	Bulk Tensile Strength for Powdered Milk as a Function of Distance "L" from Compressive Force at three Compressive Loads	2-24
2. 18	Comparison of Bulk Tensile Strength of Powders at the Same Compressive Load of 2919 g	2-25
2. 19	Variation of Bulk Density of Talc with Total Plug Length	2-28
2. 20	Bulk Density of Talc (Mistron Vapor) as a Function of Distance from Piston at Various Compressive Loads	2-29
3. 1	Effect of Humidity on Decay of Talc Aerosols (= 52 mg Samples)	3-3
3. 2	Effect of Humidity on Decay of Saccharin Aerosols (= 57 mg Samples)	3-4
3. 3	Effect of Humidity on Decay of Cornstarch Aerosols (= 550 mg Samples)	3-5
3. 4	Effect of Humidity on Decay of Powdered Milk Aerosols (= 550 mg Samples)	3-6
3. 5	Effect of Humidity on Decay of Powdered Sugar Aerosols (= 530 mg Samples)	3-7
3. 6	Proposed Mechanism for Anomalous Humidity Effect	3-8
3. 7	Copies of Light-Scattering Records: Top - Talc Aerosol, Bottom - Saccharin Aerosol	3-9

~~CONFIDENTIAL~~

LIST OF ILLUSTRATIONS (Continued)

Figure	Title	Page
3.8	Noise Levels for Various Scattering Agencies	3-11
3.9	Swirl Powder Dispenser	3-21
4.1	Concentration of Fine Sm Aerosol Cloud in Wind Tunnel as a Function of Bulk Density-Sampling Probe at 0.5 inches from Wall	4-3
4.2	Pressure Required to Compact Sm Having a Mass Median Diameter of 6.2 Microns	4-4
4.3	Concentration Profile of Fine Aerosol Cloud Generated in Wind Tunnel with Mach Number 0.5 Air Stream	4-6
4.4	Deposition of Iron Oxide on Trailing Edge of Shroud and on Tunnel Wall	4-8
4.5	Modified Model Disseminator Shroud	4-10
4.6	Dissemination Flow Pattern of Modified Shroud	4-11
4.7	Concentration of Viable Organisms on Wind Tunnel Wall	4-13
4.8	Wind Tunnel Boundary-Layer Profile with Mach Number 0.5 Free Stream	4-15
4.9	Wind Tunnel Boundary-Layer Profile with Mach Number 0.8 Free Stream	4-16
5.1	Powder Flow Rate Curve for Second Experimental Unit	5-3
5.2	Powder Flow Rate Curves for Second Experimental Unit	5-4
6.1	Welding an End Ring on Outer Shell of Center Section	6-2
6.2	Strong Back Casting and Outer Shell of Center Section	6-3
6.3	Bayonet Rings on Center and Tail Sections	6-4
6.4	Welding an End Ring on Inner Tank	6-5

viii

~~CONFIDENTIAL~~

DECLASSIFIED IN FULL  
Authority: EO 13526  
Chief, Records & Declass Div, WWS  
Date: 26 APR 2013

~~CONFIDENTIAL~~

LIST OF ILLUSTRATIONS (Continued)

<u>Figure</u>	<u>Title</u>	<u>Page</u>
7.1	Loading Tube Assembly	7-2
7.2	Loading Fixture for Use with Prototype Dry Agent Disseminating Store	7-4
7.3	Loading Tube Piston	7-4
7.4	Loading Tube Disconnected from Lifter Arms	7-6
7.5	Operating Controls for Loading Tube	7-6

~~CONFIDENTIAL~~

DECLASSIFIED IN FULL  
Authority: EO 13526  
Chief, Records & Declass Div, WHS  
Date: 26 APR 2013



~~CONFIDENTIAL~~

NINTH QUARTERLY PROGRESS REPORT  
ON  
DISSEMINATION OF SOLID AND LIQUID BW AGENTS

1. INTRODUCTION

This Ninth Quarterly Progress Report covers the work accomplished during the three-month period ending approximately September 4, 1962. This work was done at General Mills, Inc. (GMI) under Contract DA-18-064-CML-2745 which is a comprehensive research and development program on the dissemination of solid and liquid BW agents.

This report presents some more of the results of the theoretical and experimental studies of the mechanics of dry powders. The objective of this part of the program is to obtain basic information for application in the engineering development of BW munitions and related support equipment. Progress is also reported on the development of an airborne munition for disseminating dry BW agent from a compacted state. This program has reached the stage where fabrication of the first-generation airborne unit is underway.

Also presented in this report is a brief summary of the results of flight testing the GMI liquid agent disseminating store on the F-105 and F-100D airplanes. These flight tests were conducted by the BW/CW Weapons Group at Eglin Air Force Base, Florida with GMI providing technical assistance. A test report is being prepared by the BW/CW Weapons Group.

~~CONFIDENTIAL~~

DECLASSIFIED IN FULL  
Authority: EO 13526  
Chief, Records & Declass Div, WHS  
Date:

26 APR 2013

## 2. THEORETICAL AND EXPERIMENTAL STUDIES OF THE MECHANICS OF DRY POWDERS

One of the basic goals of our investigation of the mechanics of powders is the development of means for measuring important physical properties of powdered materials. There are two main areas of interest in regard to the mechanical behavior of powders: 1) the bulk properties and characteristics of powders, which are particularly important with respect to the compaction process, and 2) the aerosolization behavior of compactible powders.

Considerable progress has been made in developing devices and techniques for measurement of the bulk properties of powders. A newly developed technique for precise experimental evaluation of the compaction characteristics of powders is described below. Also, further studies of the shear strength, bulk tensile strength, and bulk density of powders are reported in subsequent sections of this report.

Although the processes of breakup and aerosolization of compacted powders must be closely related to bulk properties, considerable difficulty has been experienced in establishing the nature of this relationship. For this reason, several new concepts are being studied in which pneumatic or hydrodynamic stresses would be employed in experiments to define the mechanical properties of powders. One such approach is discussed in Section 2.2 of this report.

### 2.1 Experimental Compaction Studies

#### 2.1.1 Apparatus

A study of the compaction characteristics of various powders has been in progress during the past nine months as part of a comprehensive investigation of the mechanical behavior of dry powders. In the course of this work, several devices have been developed for measuring the applied stresses and energies required for compaction of powders; each of these

has been found to be deficient in one or more ways. An improved device for experimental study of the compaction characteristics of powders has been developed during the current report period and has been found to be completely satisfactory. This device is shown in Figure 2.1. It can be seen from the figure that the piston-cylinder configuration utilized in previous compaction devices has been retained in the new design. However, the new compaction unit is much more rigid than earlier models and, through use of an axial-circulating ball bearing for the piston, is less subject to frictional effects.

The material to be compacted is placed in a machined brass receptacle that fits into a recess in the base of the compaction unit, thus insuring proper alignment with the piston.

Tests are carried out by using the compaction unit shown in Figure 2.1 in conjunction with an Instron test machine. By utilizing the Instron machine for control of the sample deformation rate and for measurement and recording of the load applied to the powder, a very high degree of precision and reproducibility can be achieved in compaction experiments.

Compaction tests under controlled humidity conditions may be carried out by enclosing the compaction unit in a sealed plastic bag after prior conditioning of powder and apparatus in a dry box.

### 2.1.2 Experimental Results and Discussion

A number of experiments have been carried out with the apparatus described above. Because of the preliminary nature of these tests, which were carried out primarily for the purpose of evaluating the new compaction device, no attempt was made to control humidity. (Future tests will be conducted under controlled humidity conditions, as described above.)

A complete load-strain curve for cornstarch, as recorded on the Instron machine, is shown in Figure 2.2. This curve is quite typical of results obtained in tests of several powders. In this test, 0.72 grams of cornstarch

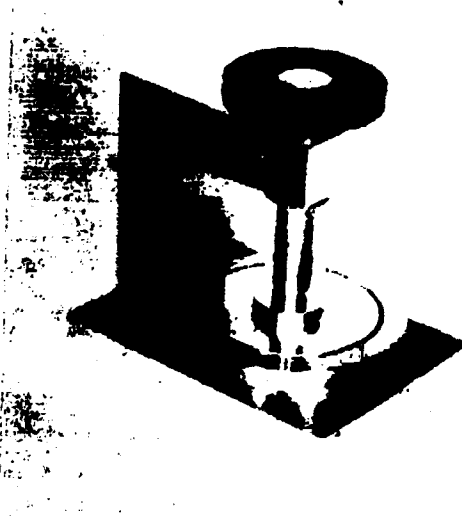


**Figure 2.1** Compaction Apparatus

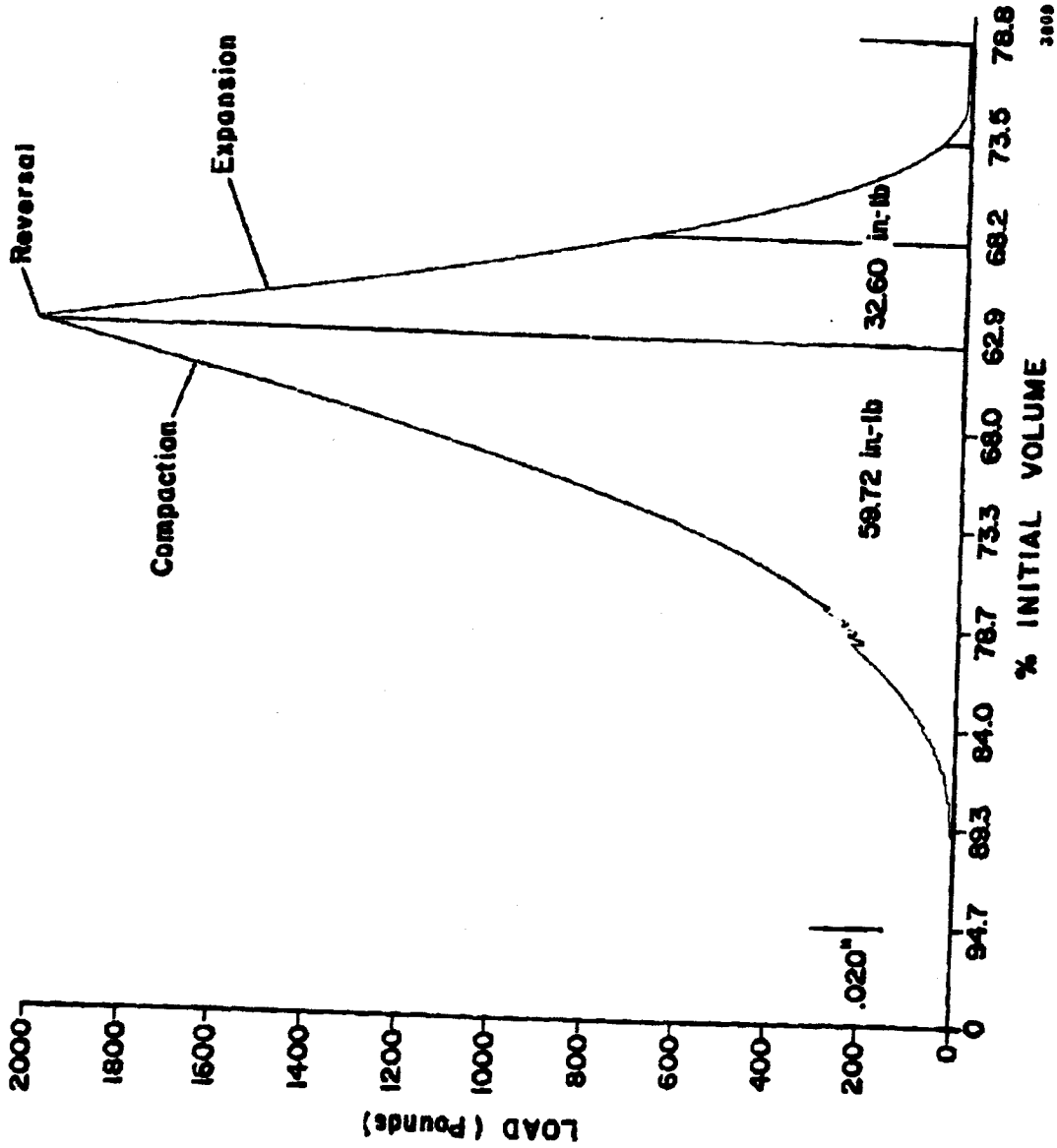


Figure 2.2 Compaction of Cornstarch - Compaction Rate 0.020 in./min,  
Initial Specific Volume 1.71 cm<sup>3</sup>/g

with an initial density of  $0.585 \text{ g/cm}^3$  were compacted at a rate of 0.02 in./min until the load reached 2000 pounds; then the cross-head direction was reversed and the elastic recovery of the sample was determined. The area under the compaction portion of the curve represents the total work (or energy) expended in an unidirectional compaction process. The net work absorbed by the powder is found by subtracting the area under the right-hand portion of the curve, which corresponds to the elastic energy stored in the compressed powder sample. In this case, the energy recovered was found to be about 55 percent of the total energy absorbed by the powder during compaction.

Compaction data for talc, saccharin, and cornstarch - as obtained with the new apparatus - are plotted versus specific volume in Figure 2.3. The data are in quite good agreement with previous results for these powders over the range of densities attainable in the earlier tests (see Table 2.1). It can be seen, however, that a considerable departure from the power-law relationship found in past tests occurs under high stresses. It should be emphasized that the high stresses applied to the samples in these tests are well beyond the practicable compaction range for visible materials. It is nevertheless desirable to establish the range of densities for which the empirical power-law relationship

$$\sigma = k \cdot \rho^m \quad (1)$$

is a valid representation of the relationship between stress and density for compactible materials. The constants  $k$  and  $m$  in Equation (1), as determined with the new test technique, are presented in Table 2.1, together with constants from previous tests.

Previous experiments with cornstarch and powdered milk indicate that these powders exhibit a "stick-slip" behavior when compacted rapidly. Some evidence of this behavior can be seen in Figure 2.2 (cornstarch) at a load of about 200 pounds. For the most part, however, it is clear that the

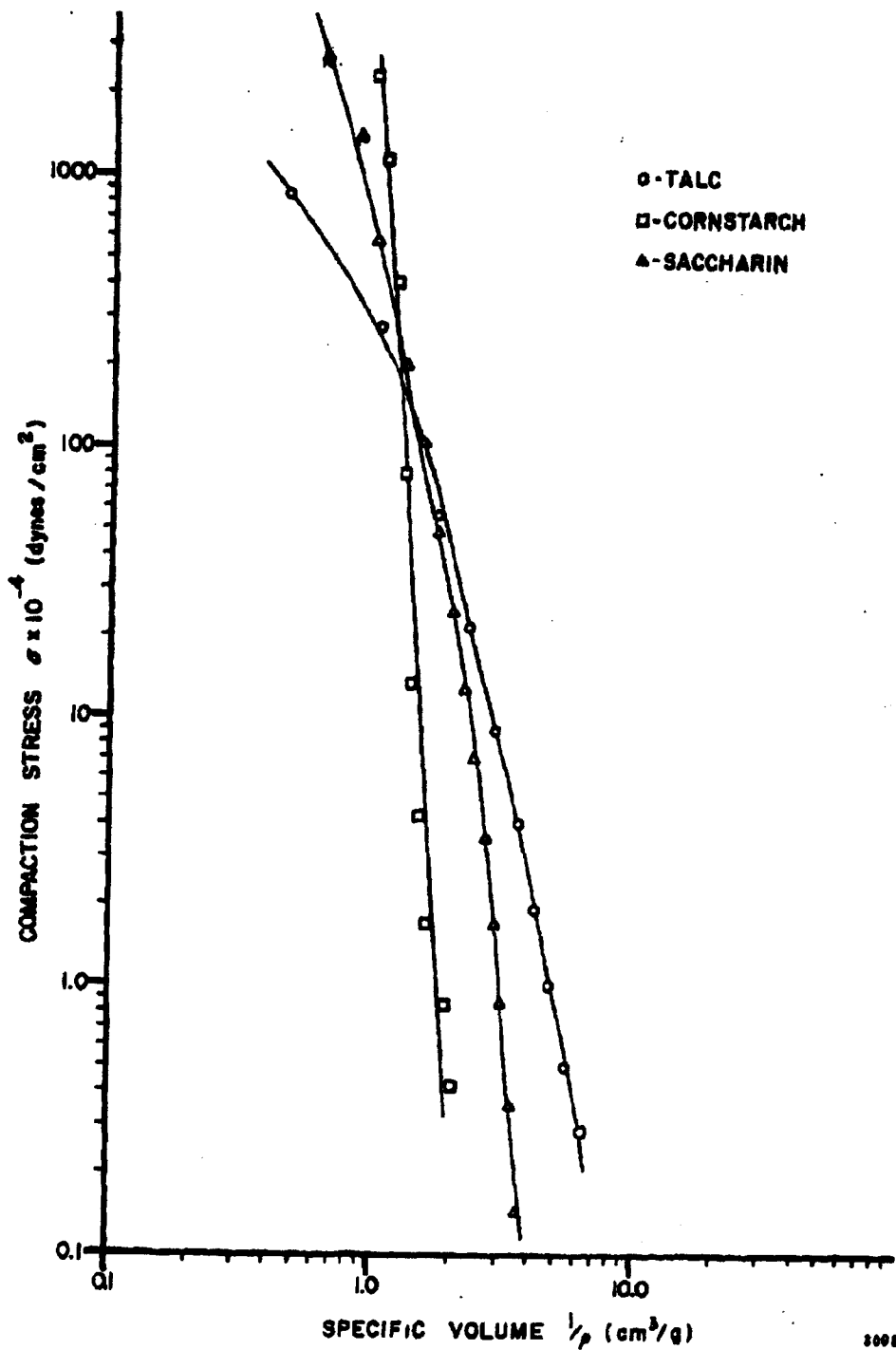


Figure 2.3 Compaction Stress as a Function of Powder  
 Specific Volume-Compaction Rate 0.020 in./min

Table 2.1 Compaction Constants for Three Powders

Powder	m*	m	k*	k
Talc	- 6.50	- 6.75	$4.42 \times 10^7$	$2.35 \times 10^7$
Saccharin	- 7.70	- 6.50	$2.21 \times 10^7$	$1.72 \times 10^7$
Cornstarch	-20.8	-18.80	$1.67 \times 10^8$	$1.29 \times 10^8$

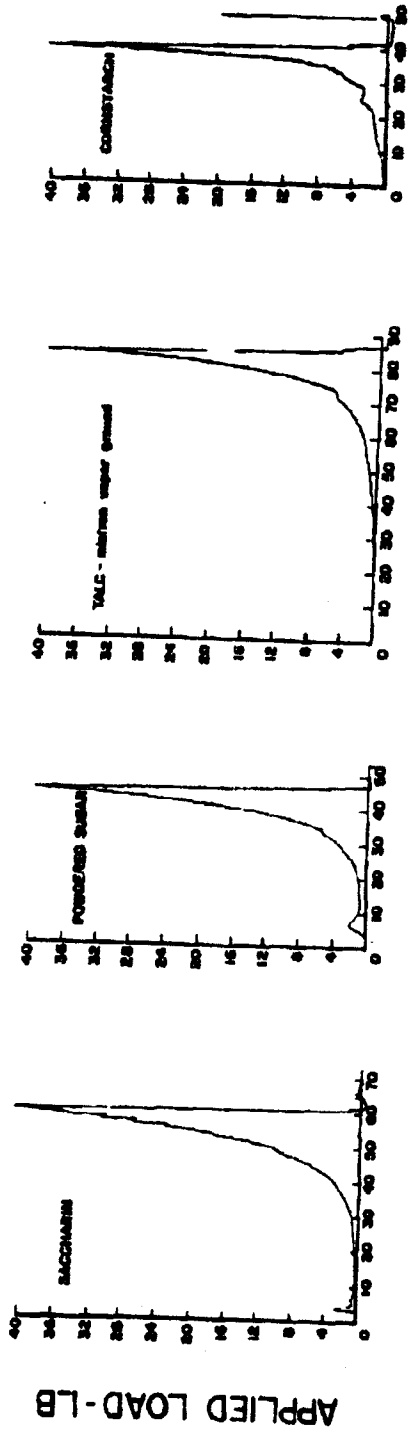
\*Indicates previous results.

compaction process for cornstarch is free of irregularities at a compaction rate of 0.02 in./min. On the other hand, tests conducted at a compaction rate of 0.2 in./min for eight powders including cornstarch exhibited much less regular behavior (see Figure 2.4). In these tests, powdered milk and saccharin as well as cornstarch displayed "stick-slip" behavior as can be seen from the figures. These results are presented with reservations, however, since it is possible that the irregularities may in part be due to air entrapment in the samples as a result of the high compaction rate, plus the fact that the piston used in these tests was not vented. Effects of compaction rate will be investigated in future tests with suitable precautions to prevent air entrapment.

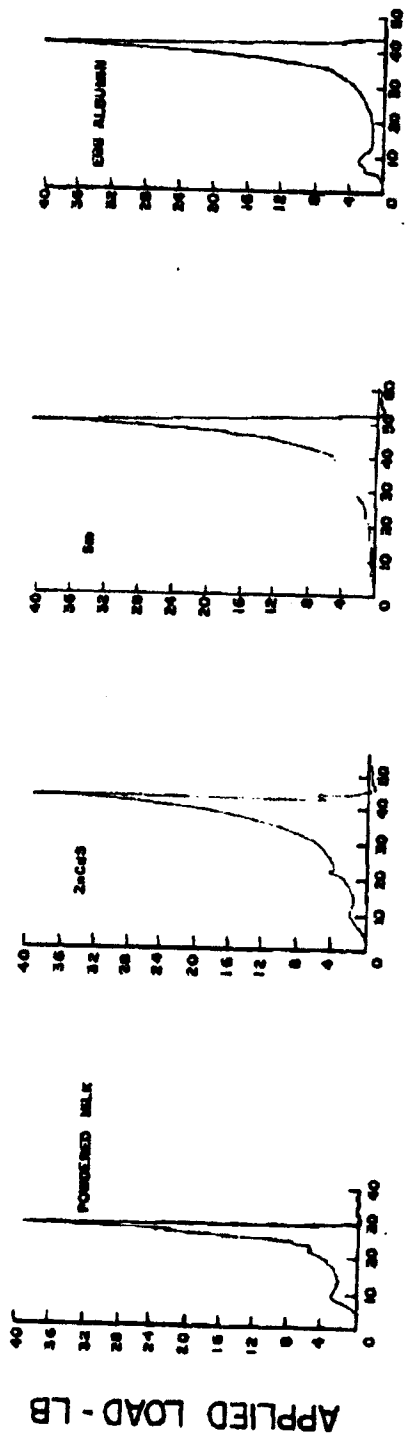
## 2.2 Triaxial Shear Tests

Considerable progress has been made in improving the triaxial technique for determining the shear strength of a compacted powder. As pointed out in the Eighth Quarterly Report<sup>1</sup>, the conventional triaxial test method leads to experimental difficulties with compactible materials because the membrane used to seal the powder sample prevents a natural shear failure





DISPLACEMENT - % INITIAL SAMPLE THICKNESS



DISPLACEMENT - % INITIAL SAMPLE THICKNESS

Figure 2.4 Compaction Characteristics of Various Powdered Materials at 0.200 in./min Compaction

of the sample. In order to eliminate this effect, a modified sample preparation procedure has been evolved that does not require use of a rubber membrane.

An exploded view of the assembly used for sample preparation is shown in Figure 2.5. The powder sample is compacted within a segmented cylindrical section, which is supported by means of an external housing as shown in the exploded view. The center segment is split into three 120-degree sections to facilitate removal after compaction of the sample. The test specimen is prepared by filling the cylinder with a known mass of powder which is then compacted by means of pistons forced into the cylindrical chamber from each end. Each piston is advanced at the same rate during compaction of the sample to center the compacted material in the cylinder. The final average density of the sample is fixed by accurately defining the distance between the pistons at the completion of the compaction process. For loose powders, extension units are placed at each end of the assembly shown in Figure 2.5 to permit initial compaction of the powder into the central section of the cylinder.

After compaction, the pistons are removed and threaded end plugs are installed in each end cylinder to give support to the compacted powder column. The entire assembly is then placed in the Instron test machine and a load of about 50 pounds is applied to the end plugs. (This load is not applied to the powder, but is carried by the central cylinder.) The housing may now be removed, after which the load is gradually released. Because of the elastic nature of the compacted powder, a small gap will generally appear between the center cylindrical segments and the upper-end cylinder, thus simplifying removal of the segmented center cylinder. (The center section is made of magnetic stainless steel; thus, the center-section segments can be readily removed with a weak magnet.) If this procedure is followed carefully, the exposed powder will be free of cracks or other imperfections.

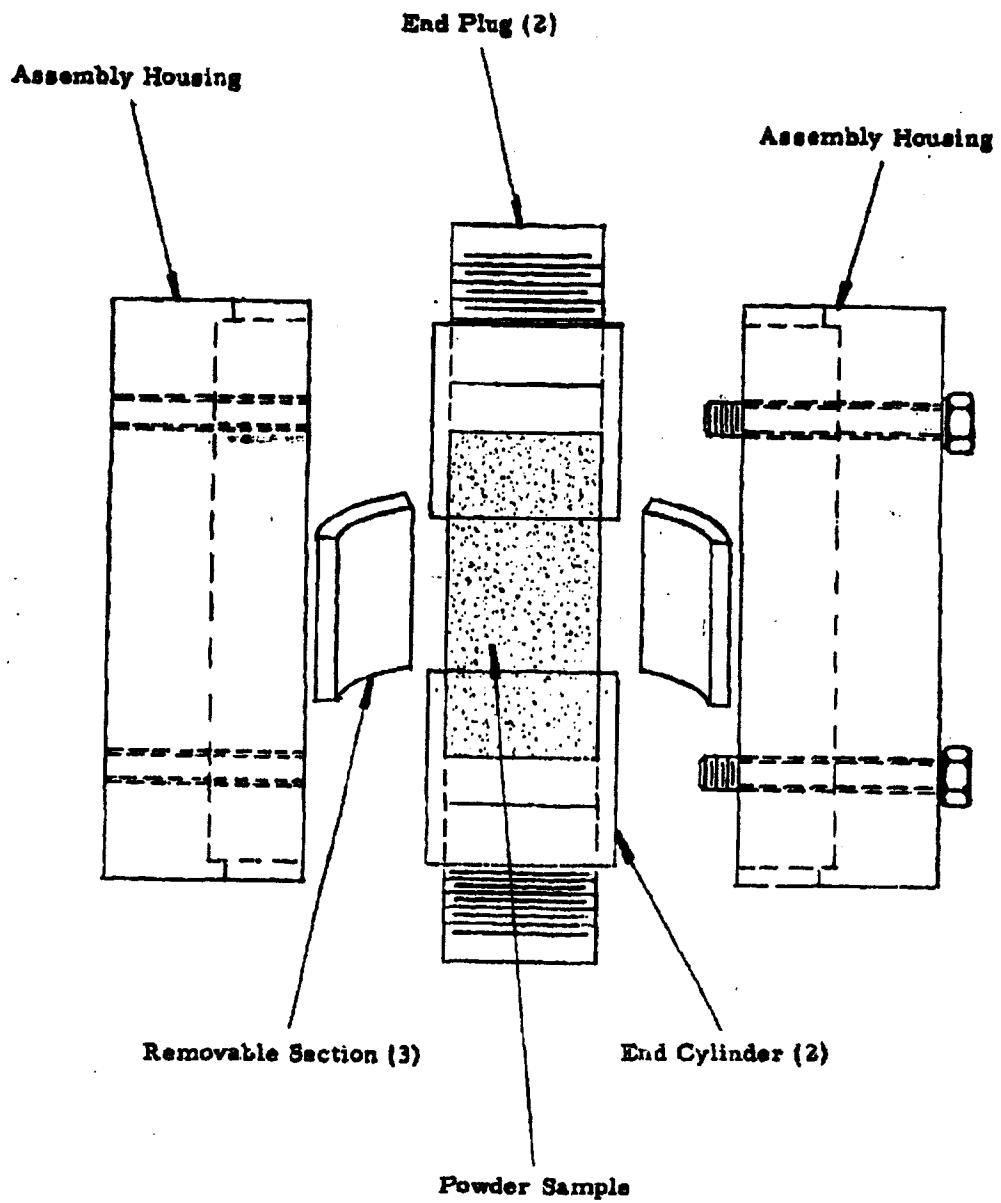


Figure 2.5 Exploded View of Triaxial Test Sample Preparation Assembly

The shear strength of saccharin compacted to an average density of  $0.65 \text{ g/cm}^3$  by the above technique has been obtained by tests conducted in the Instron test machine. The load-strain diagram for a typical test is shown in Figure 2.6. It is apparent that the sample failure is very well defined, the load falling from about 6.7 to 0.5 pounds as the sample fails in shear. By stopping the machine at the instant of failure, it is possible to remove the fractured test sample intact. The typical appearance of a sheared sample is illustrated by Figure 2.7. The shear planes are clearly evident in the photograph.

This technique is currently being extended to permit triaxial tests in a pressurized chamber<sup>1</sup>. A thin loose-fitting membrane, enclosing the entire sample assembly, will be used in these tests. By venting the interior of the membrane to ambient pressure, the desired lateral stress on the sample will be achieved; however, the loose membrane will be free to deform as the sample shears. It is believed that this modification of the earlier test technique will result in clear-cut failure of the test specimens.

In order to fully define the shear strength of a compacted powder, it is necessary to examine the tensile shear strength of the powder as well as its compressive shear strength. The reason for this is evident from a study of Figure 2.8. Compressive shear tests are capable of establishing the portion of the shear locus B-C on the figure. However, the pure shear strength of the powder  $\tau_c$  cannot be determined by the compressive triaxial technique, since a tensile stress must be applied to the sample in order to perform tests in the region A-B of Figure 2.8. In principle, the triaxial test can be performed in this region by applying a gradually increasing axial tension to the sample while maintaining a constant chamber pressure as before. Attempts to conduct such a test at zero chamber pressure have not succeeded, however, because sample failure invariably occurs in the plane of one of the end cylinders. Since sample failure in tension should occur as a result of combined tension and shear, it is to be expected that the sample

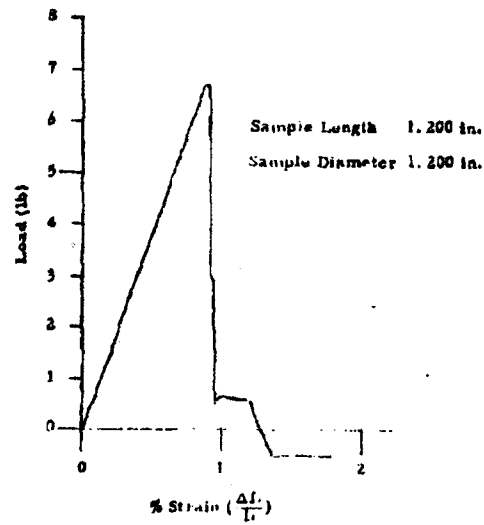


Figure 2.6 Load-Strain Curve for Compacted Saccharin ( $\rho_0 = 0.65 \text{ g/cm}^3$ )

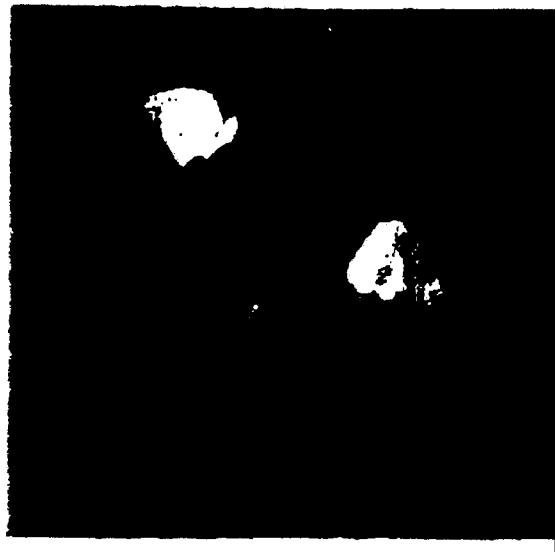


Figure 2.7 Compacted Saccharin Failed in Compression ( $\rho_0 = 0.65 \text{ g/cm}^3$ )

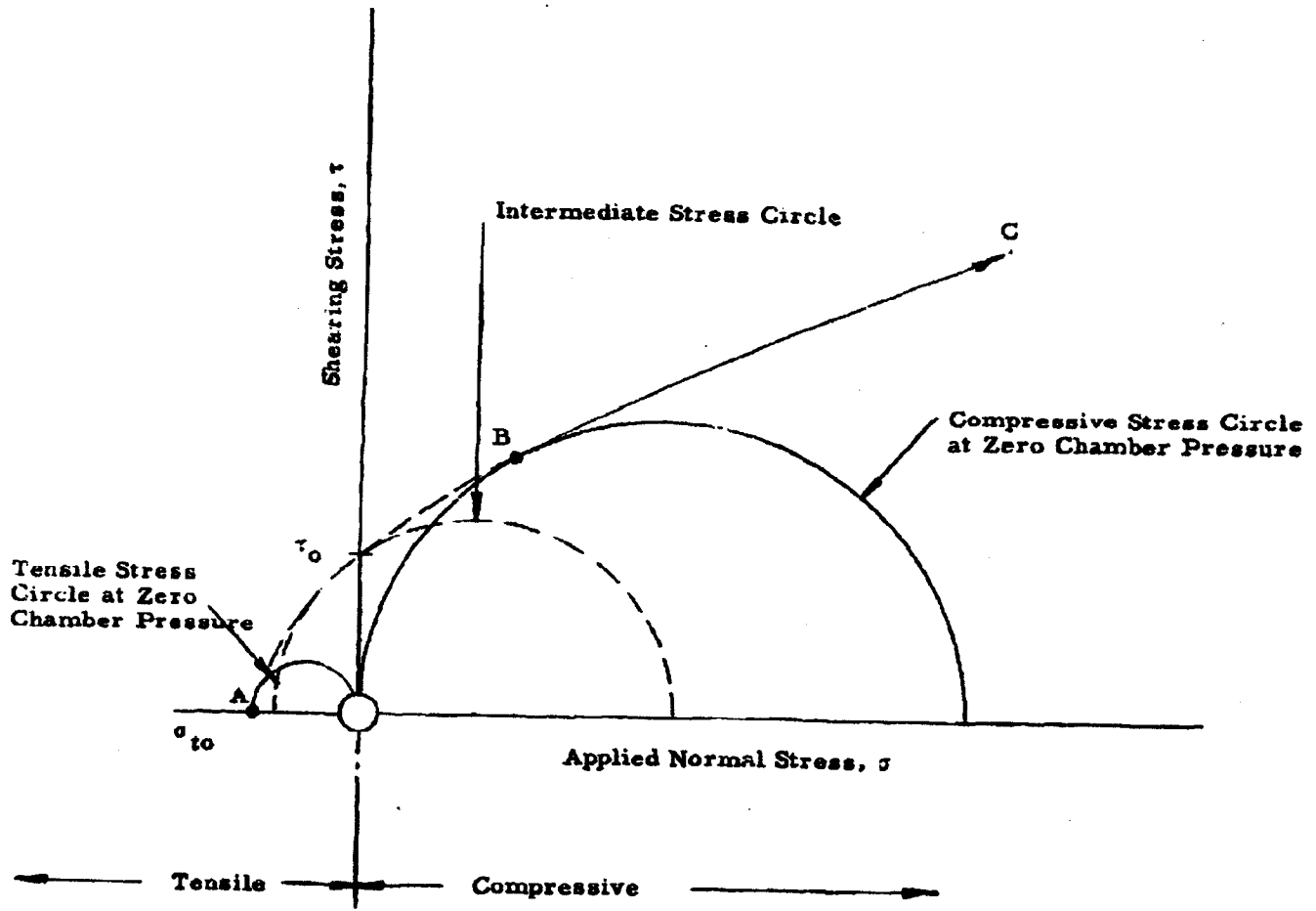


Figure 2.8 Shear Locus Curve Illustrating the Relationship between Bulk Shear Strength  $\tau_0$  and Bulk Tensile Strength  $\sigma_{t0}$

should fail in the manner typified by Figure 2.7 for the compressive case. Presumably, the type of failure actually observed is due in part at least to the constraining effect of the end cylinder.

It is believed that measurements of bulk tensile strength should, if possible, be carried out in such a way that fracture occurs in the central region of the powder sample rather than at one end. A "natural" tensile failure may be possible if the test specimen is compacted so that the center section has a reduced cross-sectional area. Experiments with a reduced-area sample will be tried as soon as the modified center-section cylinder can be fabricated.

A completely different means of evaluating the tensile strength of a compacted powder is now under investigation. In the proposed test, a compacted powder sample is placed in a pressure chamber and the pressure in the chamber is gradually increased to a preselected value. After equilibrium is established, the chamber is depressurized at a controlled rate. The gas entrapped within the pores of the powder sample will flow toward the surface of the sample. The resulting viscous stresses at the powder surface will tend to break the relatively weak bonds holding the particles together. If properly carried out, this test should permit detection of a "threshold" condition at which erosion of the powder surface begins. From this information, it may be possible to compute the average strength of inter-particle bonds.

This possible means of experimentally determining the tensile strength of compacted powders is based on the following observations: 1) Experience has shown that air entrapment occurs within a powder bed when compaction takes place rapidly. This is because time is required for the air contained in the void spaces to percolate through the powder. Also, experiments have shown that compacted powder samples subjected to a pressurized gas environment expand significantly when the pressure is suddenly released. 2) Even when compacted under high stresses most powders have void spaces amounting to 30 to 50 percent of the total volume of a powder sample.

Thus, it is clear that a very considerable mass of gas, capable of supplying a large amount of mechanical energy, can be stored in a powder sample at pressures of several atmospheres.

It is apparent that this concept may also provide a means for aerosolization of compacted powders. This possibility will be explored in the tests now being planned.

### 2.3 Bulk Tensile Strength of Compressed Powders

In the development of a method for the measurement of bulk tensile strengths of compressed powders<sup>1, 2</sup>, we have previously confined our study to zinc cadmium sulfide. In order to determine the effectiveness of our method in the measurement of the tensile strength of other powders, we have extended our study to include saccharin, cornstarch, powdered milk, Sm, and talc. Again we have confined our study to three compressive loads, 1454, 2130, and 2919 grams, and to a compression time of 1-1/2 hours. All measurements were made in a controlled environment of 15 percent relative humidity. The results obtained are presented in Figures 2.9 through 2.17. Diameter of the powder plug was 0.75 inches. Although talc was included in our study, no valid measurements were obtained. It was found that upon removal of the spring clips holding the column segments together, the release of elastic energy in the talc plug caused the column segments to spring apart fracturing the column of powder prior to measurement of the tensile strength. The present apparatus will have to be modified to overcome this problem. Figure 2.18 is a presentation of the variation of tensile strengths of various powders at the same compressive load. In this manner the powders can be characterized according to their relative tensile strengths fulfilling, in part, the purpose of the current study.

It is seen that the data do not follow the simple exponential relationship proposed earlier<sup>1, 2</sup>:

$$\sigma = \sigma_0 e^{-kL}$$



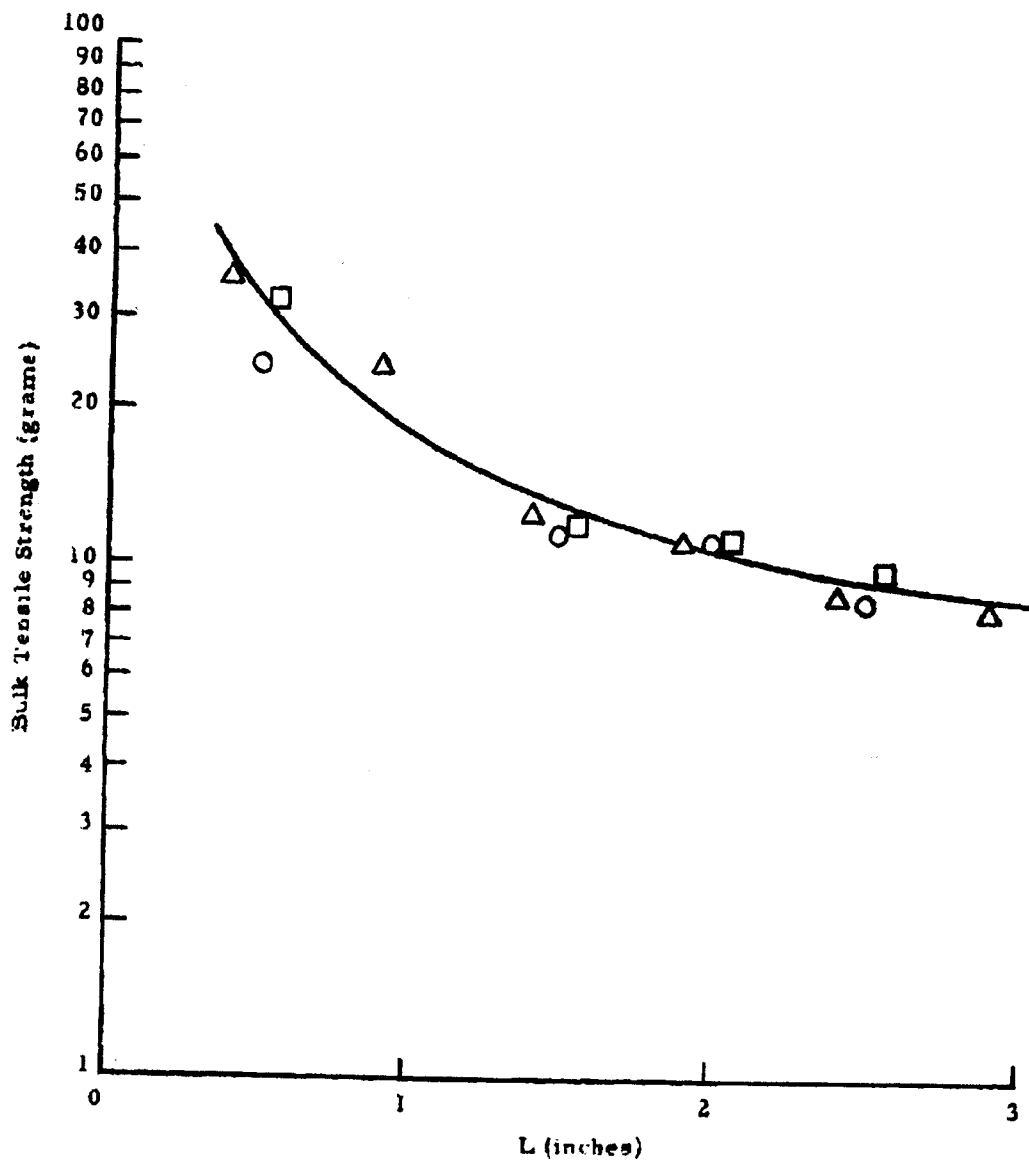


Figure 2.9 Bulk Tensile Strength for Saccharin as a Function of Distance "L" from Compressive Force at a Compressive Load of 1454 g

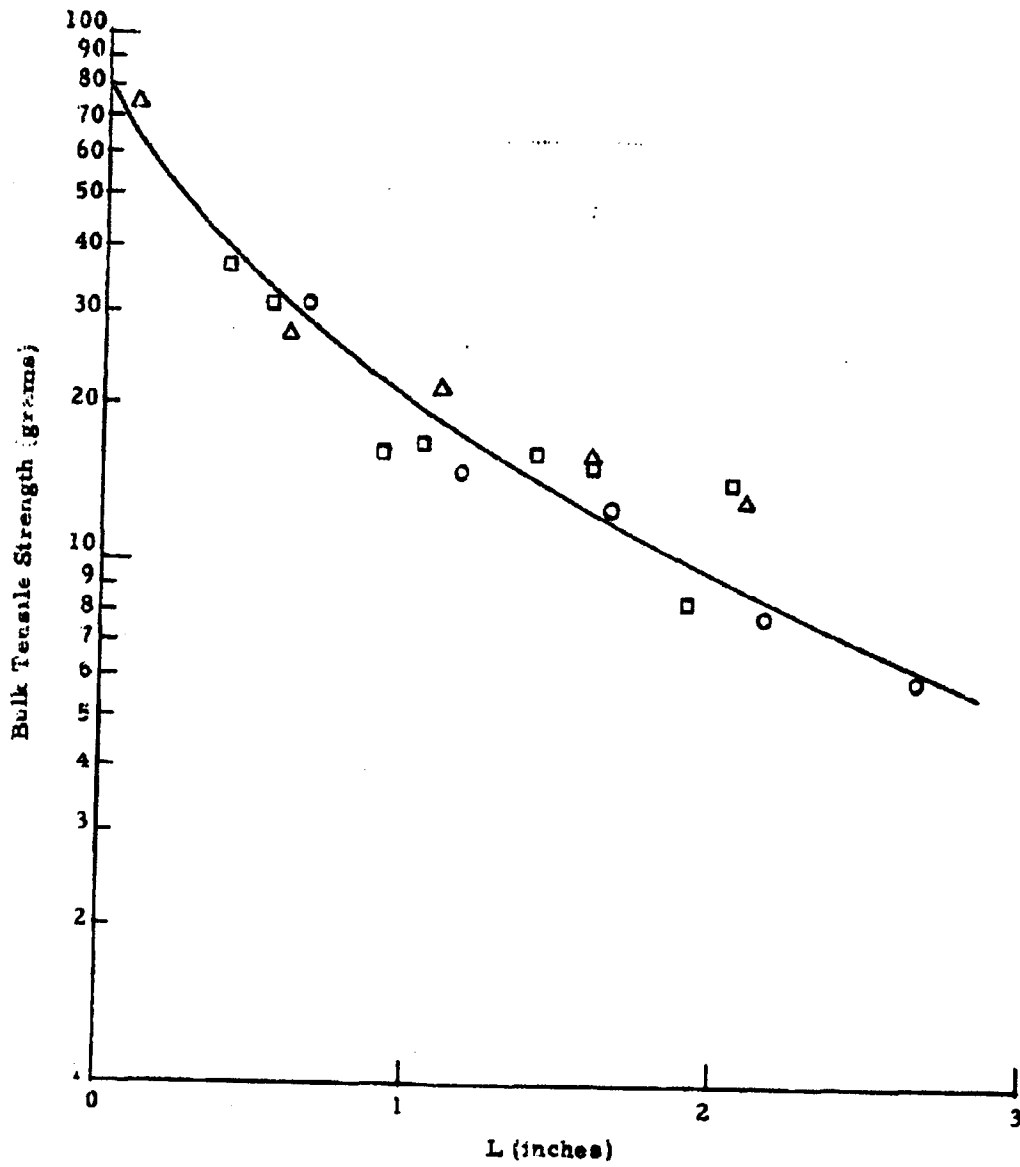


Figure 2.10 Bulk Tensile Strength for Saccharin as a Function of Distance "L" from Compressive Force at a Compressive Load of 2130 g

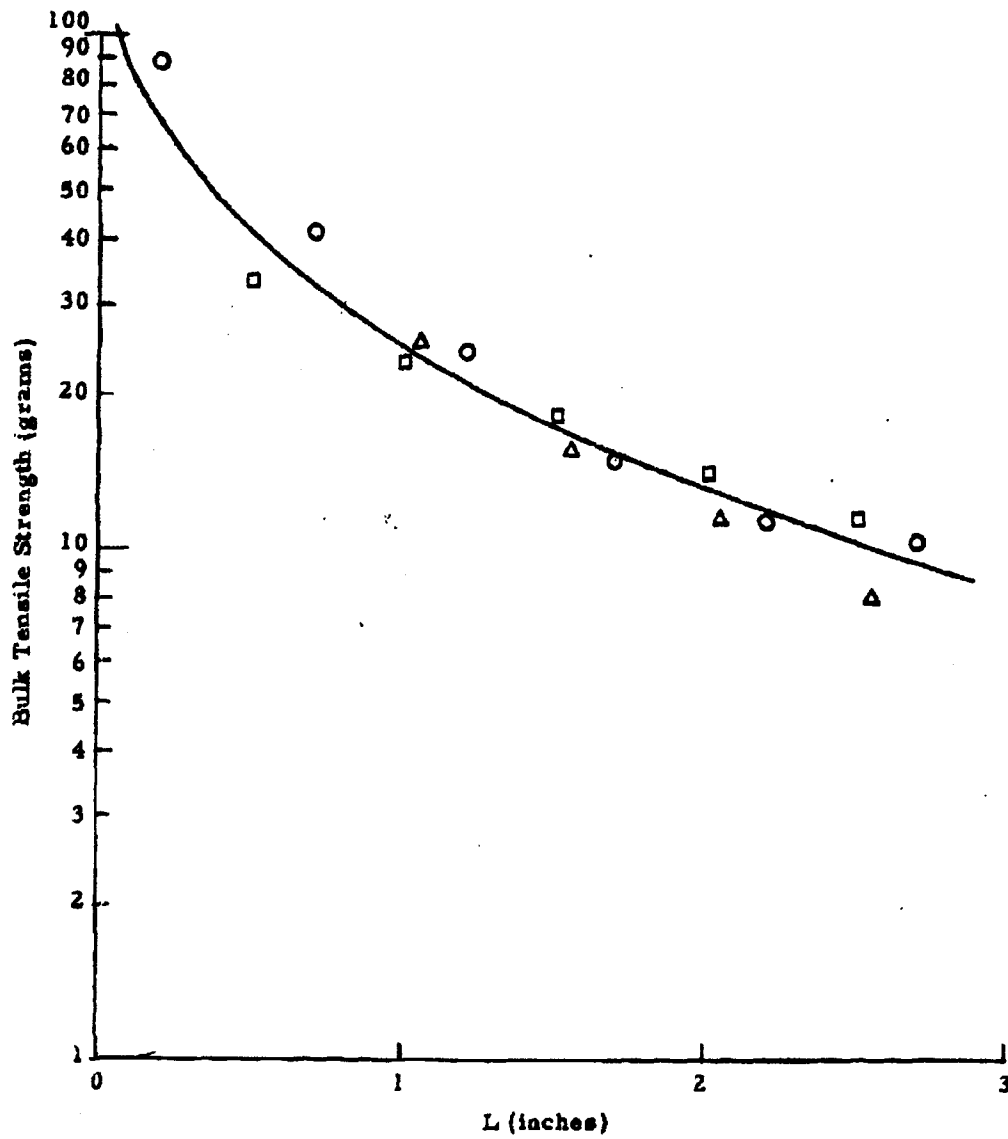


Figure 2.11 Bulk Tensile Strength for Saccharin as a Function of Distance "L" from Compressive Force at a Compressive Load of 2919 g

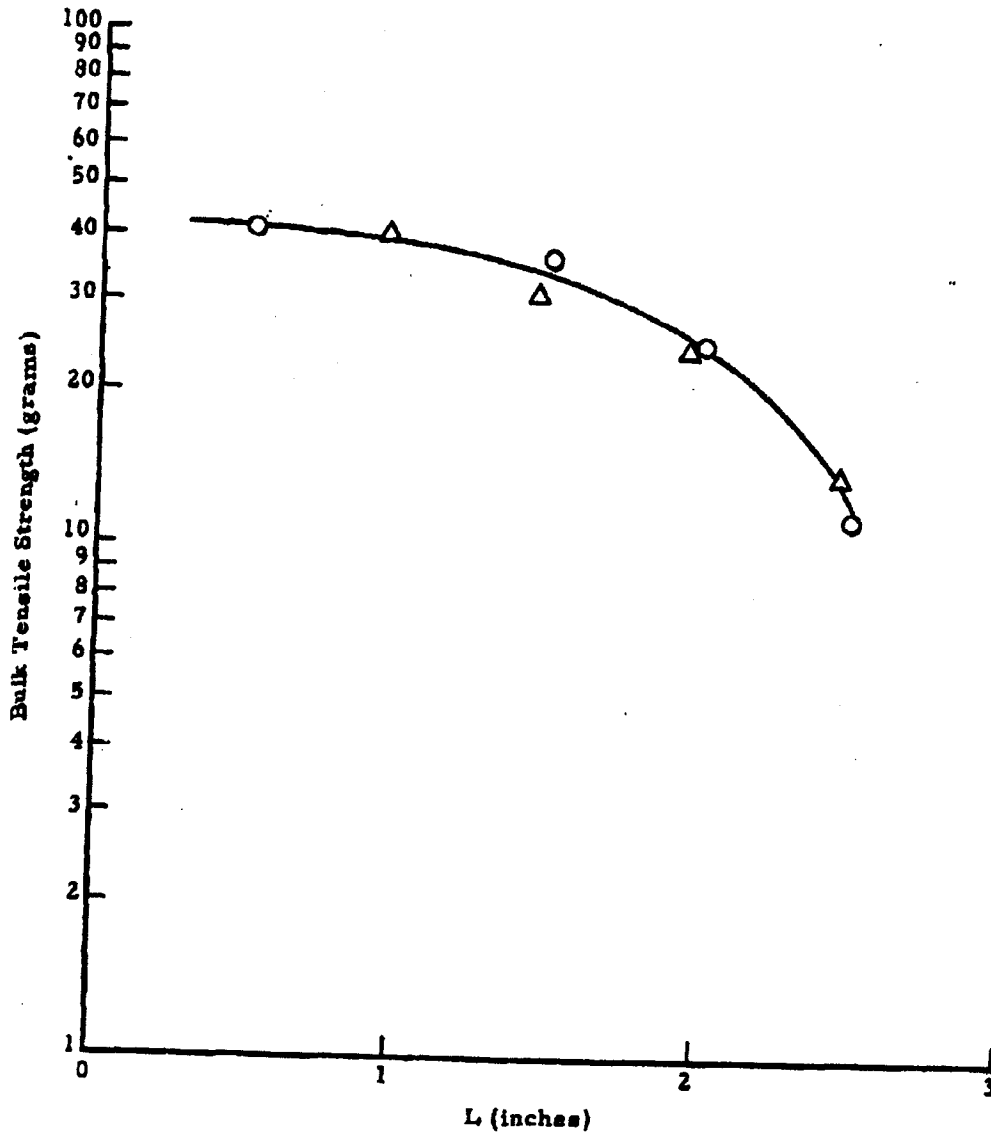


Figure 2.12 Bulk Tensile Strength for Cornstarch as a Function of Distance "L" from Compressive Force at a Compressive Load of 1454 g

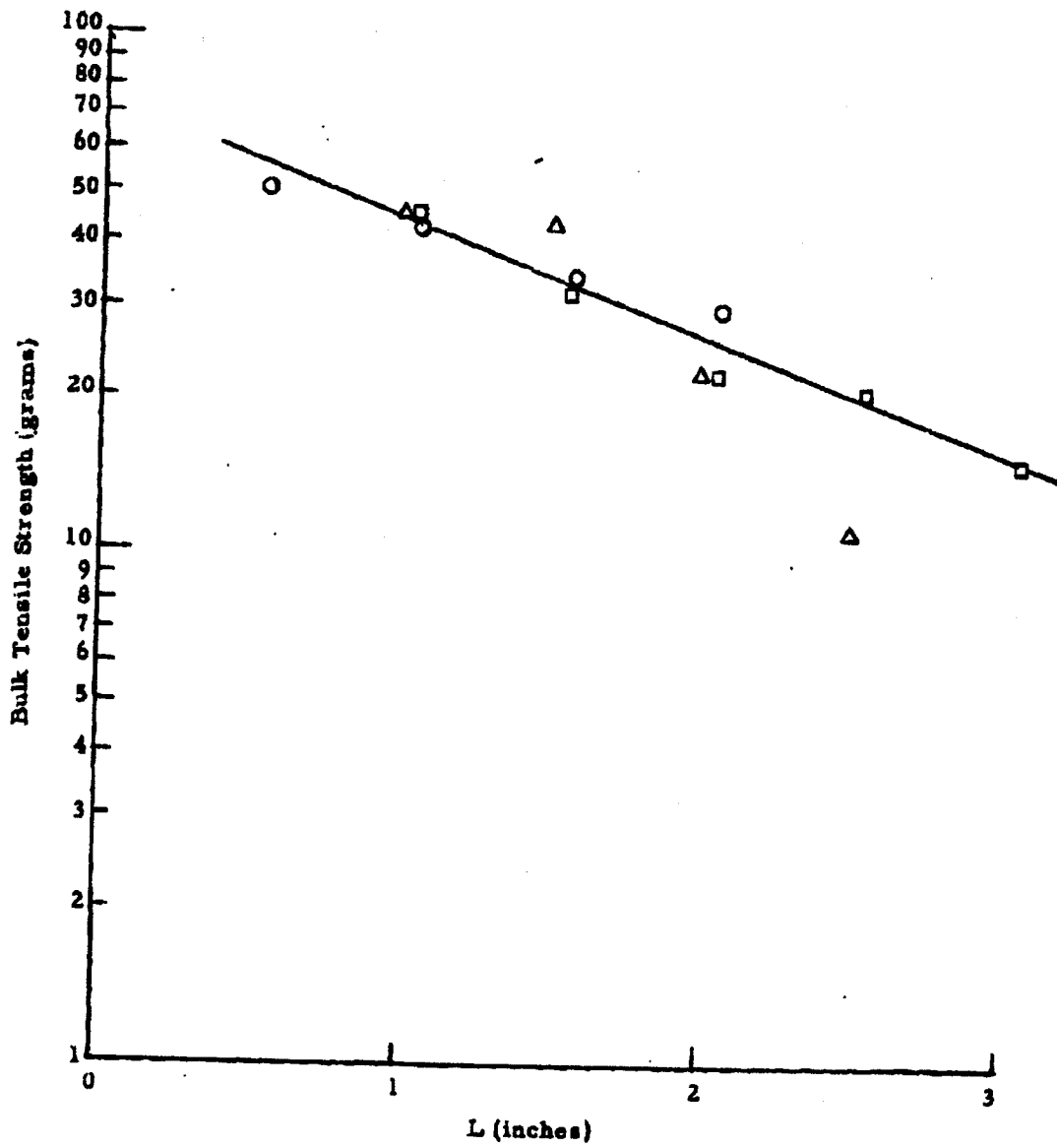


Figure 2.13 Bulk Tensile Strength for Cornstarch as a Function of Distance "L" from Compressive Force at a Compressive Load of 2130 g

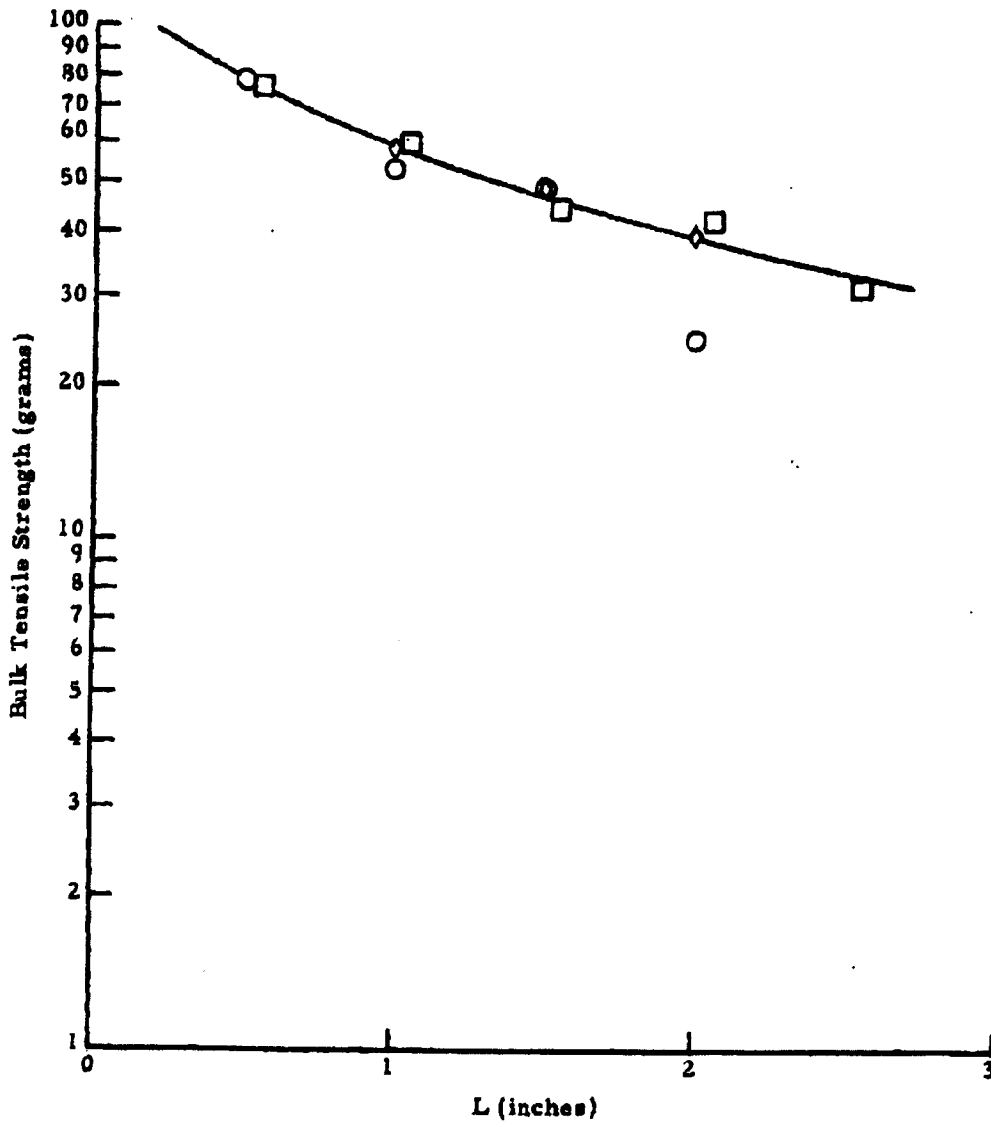


Figure 2.14 Bulk Tensile Strength for Cornstarch as a Function of Distance "L" from Compressive Force at a Compressive Load of 2919 g

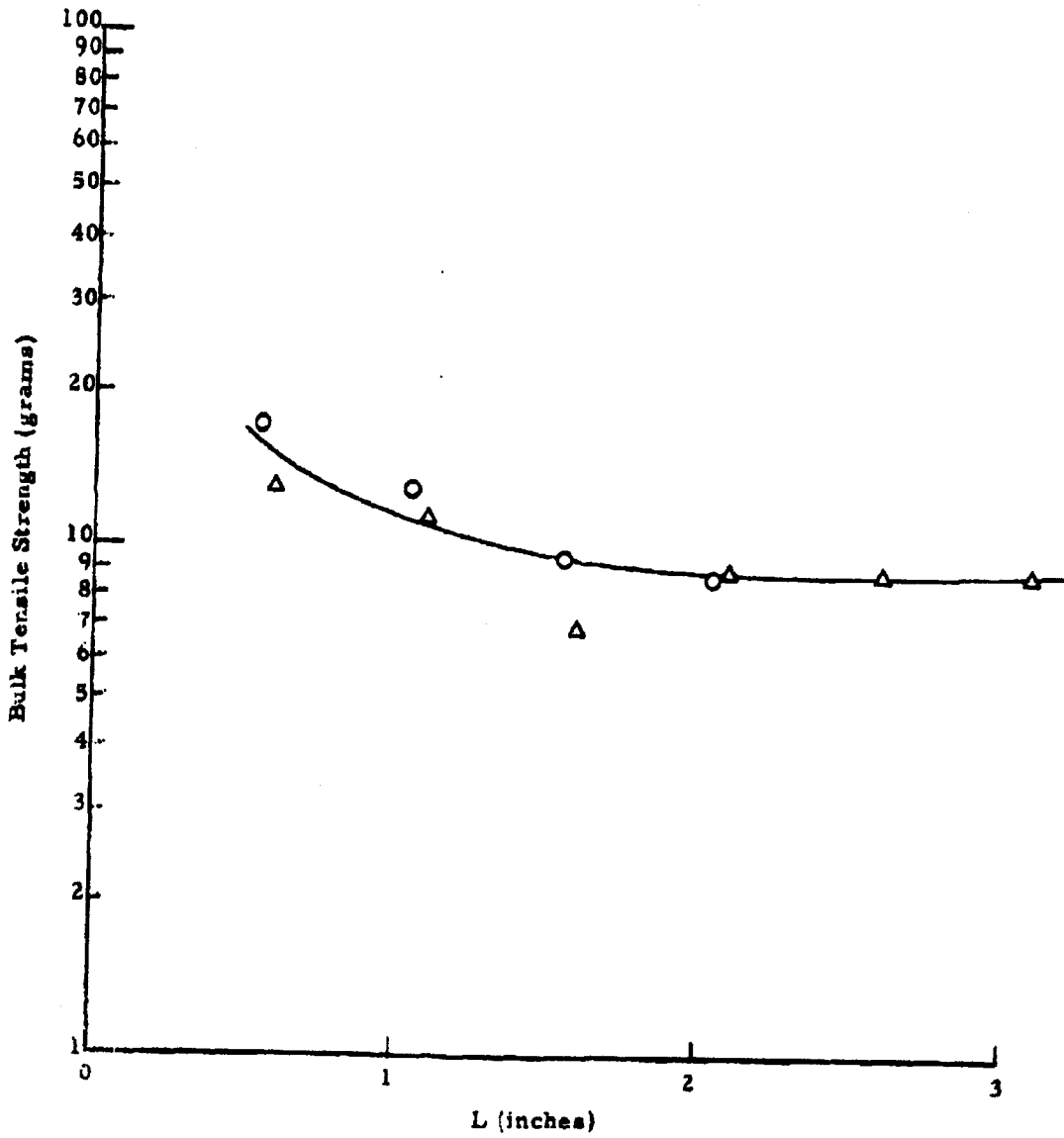


Figure 2.15 Bulk Tensile Strength for  $S_m$  as a Function of Distance "L" from Compressive Force at a Compressive Load of 2130 g

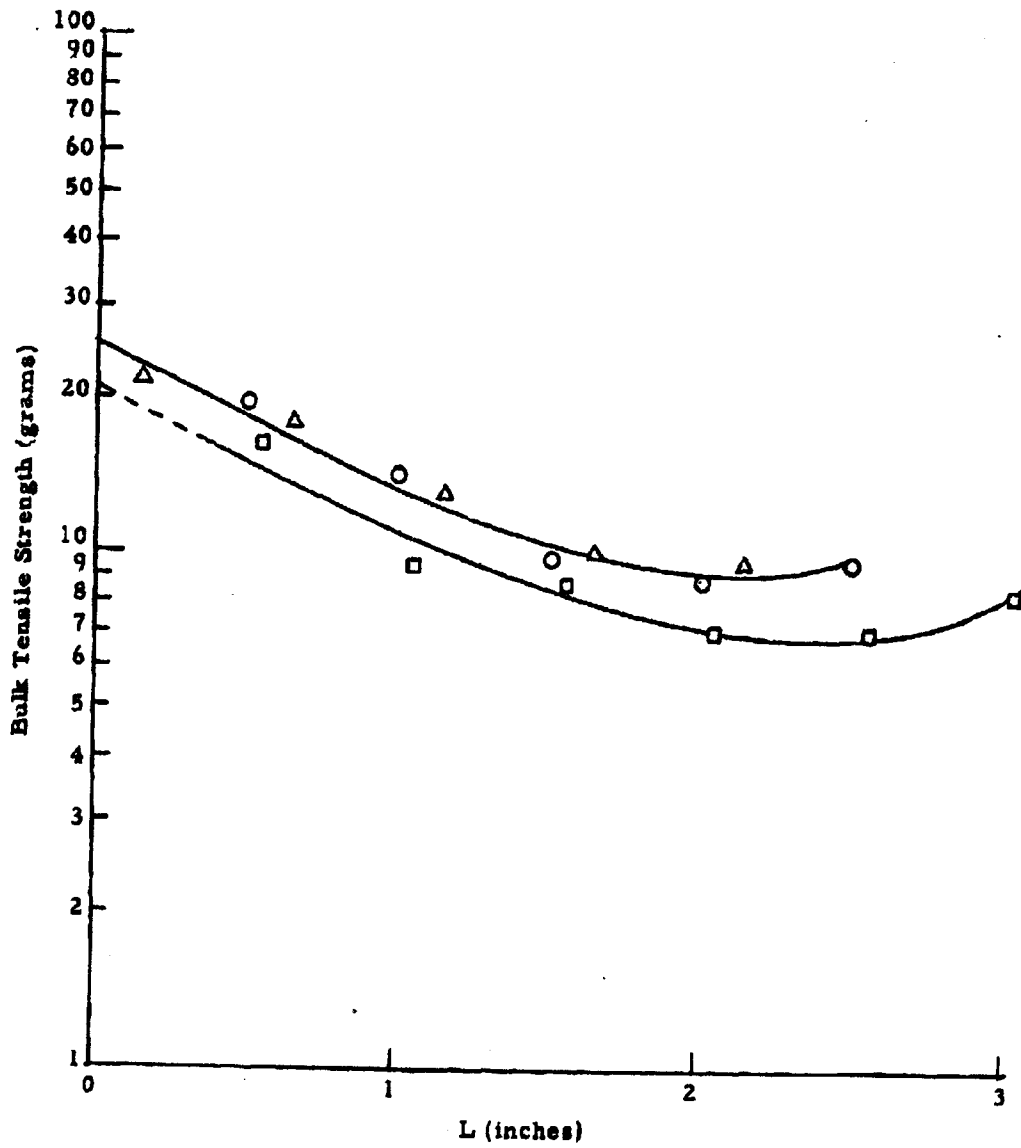


Figure 2.16 Bulk Tensile Strength for  $S_m$  as a Function of Distance "L" from Compressive Force at a Compressive Load of 2919 g



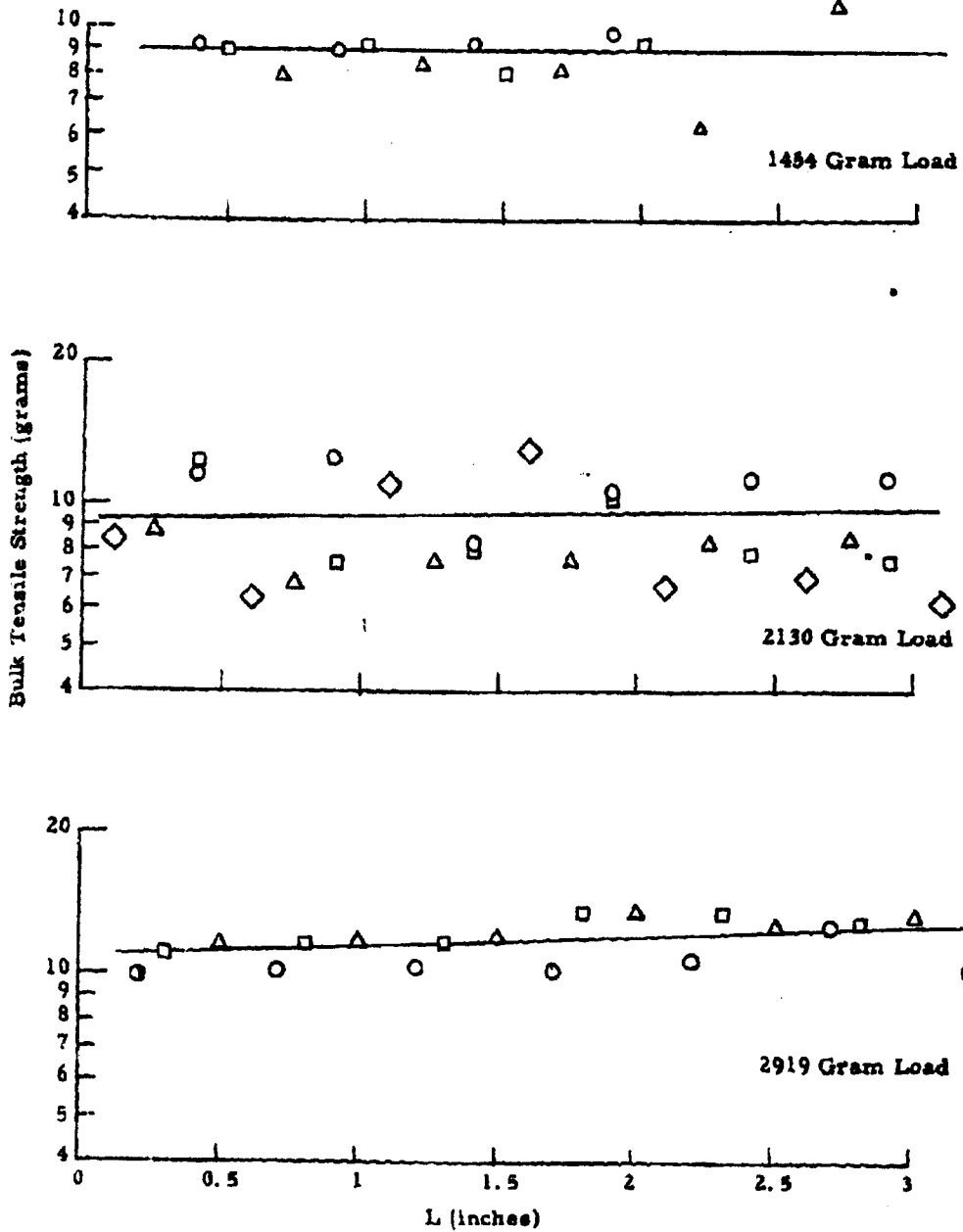


Figure 2.17 Bulk Tensile Strength for Powdered Milk as a Function of Distance "L" from Compressive Force at Three Compressive Loads

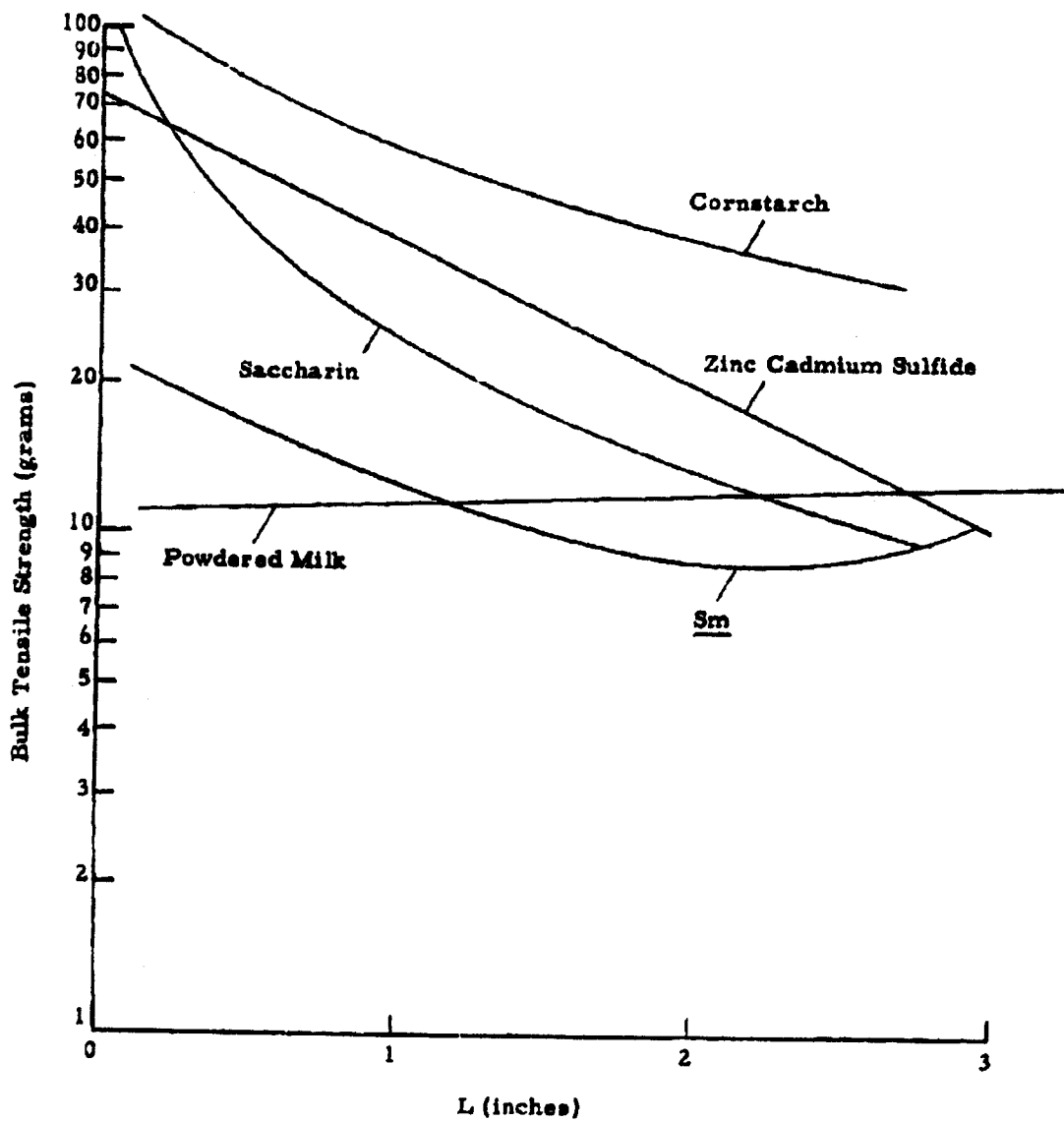


Figure 2.18 Comparison of Bulk Tensile Strength of Powders at the Same Compressive Load of 2919 g

where:

$\sigma$  = bulk tensile strength of a column of compressed powder at a distance  $L$  from the piston

$\sigma_0$  = bulk tensile strength of the compressed powder immediately below the piston

$k$  = constant

$L$  = distance from piston to fracture plane

If this deviation from current proposed theory continues throughout subsequent experimentation, it will be proposed that the bulk tensile strength may follow the relationship:

$$\sigma = \sigma_0 e^{-kL} + \sigma_0 e^{+kL}$$

indicating that the experimental values obtained are in reality the sum of two exponentials, with equal slopes but opposite in sign. This would represent a buildup of tensile strength from the bottom of the column of compressed powder as well as at the head of the compressive piston. Studies including variations in total column length as well as bulk density determinations will help to elaborate upon this.

#### 2.4 Shear Strength of Compressed Powders by the Sliding Disk Method

An extensive test program is now in progress in which the shear strengths of a number of powders are being determined as a function of compressive load over a wide range of relative humidity environments. For reasons of continuity the reporting of these results will be delayed pending the completion of this study.

## 2.5 Bulk Density of Compressed Powders

During the previous quarter<sup>1</sup>, a study of the bulk density variation in a compressed column of saccharin was made at various compressive loads. This study has been extended, for comparative purposes, to talc. The apparatus and techniques are identical to those previously described<sup>1</sup> in which the loose bulk powder is used to fill a segmented column 5-3/32 inch ID which, following compression of the powder, is then cut into one-inch segments to determine the density variation throughout the column. In the apparatus described the total column length of uncompacted powder was 20 inches. A few preliminary experiments indicated that the talc was sufficiently more compressible than saccharin to necessitate a 5-inch extension of the fill tube in order to obtain column lengths of the compressed powder comparable to those obtained for saccharin. With this revision in the apparatus the column of uncompacted talc is now 25 inches in length. The data obtained are presented in Figures 2.19 and 2.20. Figure 2.19 shows the effect of increasing the powder column length. The broken lines represent results obtained using a 20-inch column length prior to compaction, whereas the solid lines represent results with a 25-inch column length. Figure 2.20 represents the completed study for talc. The plot for each compressive load represents the average of two independent determinations.

The behavior of talc differed from that of saccharin in two distinct ways: 1) the decrease in density down the column is significantly greater for talc than for saccharin, and 2) talc displays a considerable release of elastic energy following the removal of the compressive force. This difference was also noted in the bulk tensile strength measurements discussed earlier in this report.

Our continued study of the radial variation of the bulk density in a column of compressed powder indicates that the differences in density previously reported<sup>1</sup> between the inner core and the outer annular segment were due to experimental error. Refined experimental techniques show the absence of significant variations in the radial distribution of bulk densities of compressed powders.

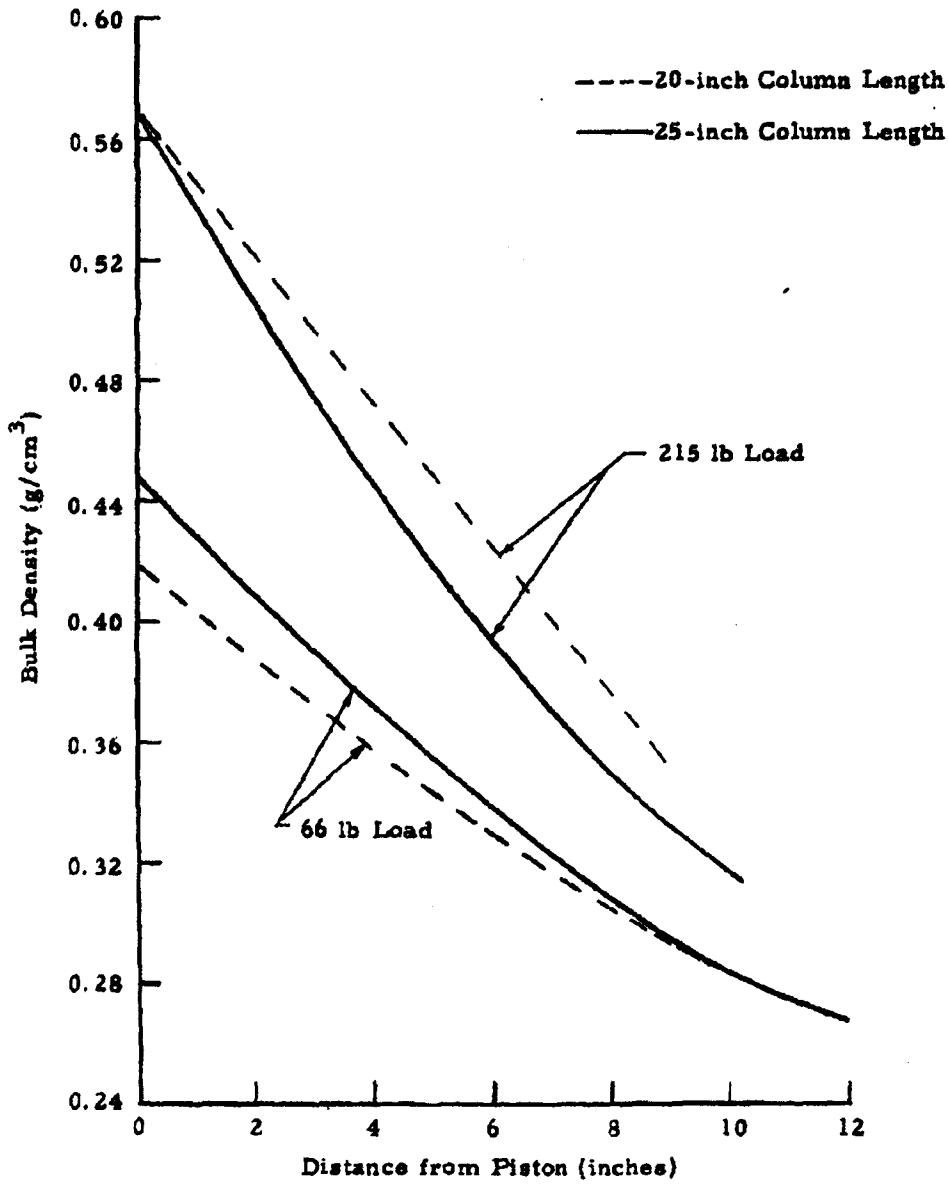


Figure 2.19 Variation of Bulk Density of Talc with Total Plug Length

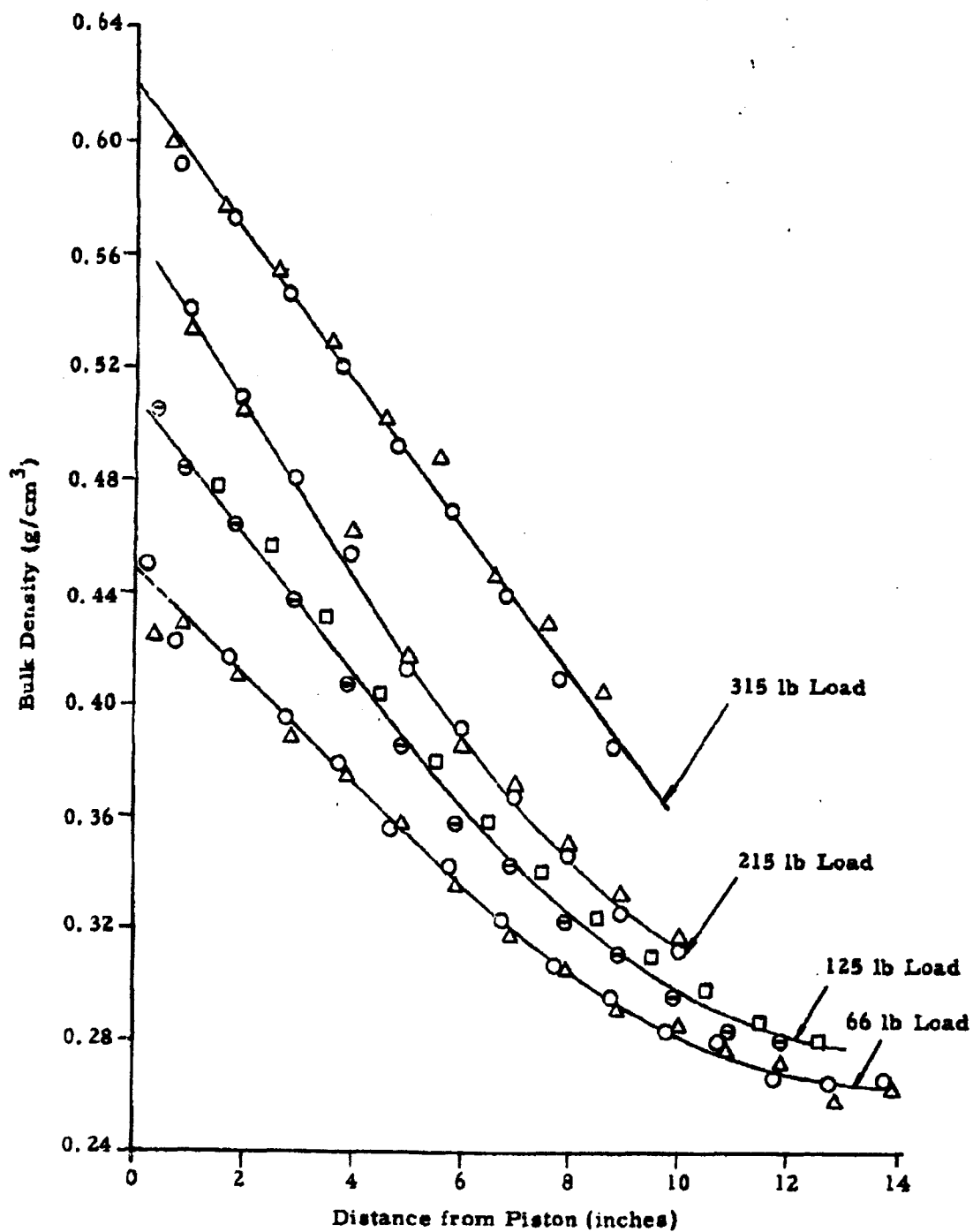


Figure 2.20 Bulk Density of Talc (Mistron Vapor) as a Function of Distance from Piston at Various Compressive Loads

### 3. AEROSOL STUDIES

The aerosol studies of the present quarter have proceeded along those mentioned at the conclusion of the last report<sup>1</sup>. A number of runs have been made at three humidity conditions - less than 5 percent, about 50 percent, and greater than 95 percent - for each of five different powders. The possibility of obtaining more direct information on the aerosol condition by analysis of the noise level on the light-scattering signals has been investigated, with positive results. Some time was devoted to the problem of obtaining an initially well-dispersed aerosol, resulting in the development of an alternate method of dispersing powders. Further work, chiefly involving ion injection, is outlined in the concluding section.

#### 3.1 Study of the Effects of Environmental Humidity on Aerosol Decay

As a preliminary step in the study of humidity effects on the decay of aerosols, runs have been made at three humidity conditions. One series of runs made use of normal room humidity conditions that were in the range of 45 to 50 percent during the period covered. In a second series of runs, a low humidity condition was obtained by placing a pan containing molecular sieve desiccant on the floor of the chamber near the fan. After the chamber was closed and the fan turned on, a check with an infrared hygrometer showed that the humidity was reduced to less than 5 percent after 1-1/2 hours. A third series of runs was made with a pan of water in place of the pan of desiccant. The hygrometer showed that the chamber humidity rose to greater than 95 percent 1-1/2 hours after closing the chamber.

Five powders - talc, saccharin, cornstarch, powdered sugar, and powdered milk - were run at each of the three humidity conditions. The stirring fan, with the small (4-inch) blade, was operated at 35 volts throughout each run so that the decay observed was in each case "turbulent" decay. The powder dispersing system was operated as described in the last report.

No attempt was made to precondition the powder samples prior to dispersing. Only one of the two light-scattering units was used in this work, since it was shown in the last report that the two signals were identical for the stirred settling case.

The light-scattering data from the humidity runs are shown in Figures 3.1 through 3.5. The runs for talc and saccharin were repeated; these showed generally good reproducibility. It will be noted that the five powders fall into two categories as regards the effect of humidity on aerosol decay.

Saccharin is the prototype for the powders of the first category. The decay rate for saccharin was about the same in the 5 and 50 percent relative humidity environments, but was somewhat larger at 95 percent relative humidity. Cornstarch and powdered milk behaved similarly.

Powders of the second category, talc and powdered sugar, exhibited a different behavior. For talc the decay rates were about equal for the two extreme humidity conditions and less for the intermediate humidity condition. In summary, the decay rate for powders of the second category first decreased, then increased with increasing humidity; whereas powders of the first category exhibited decay rates that increased monotonically with increasing humidity.

The behavior of aerosols exposed to various humidities is difficult to interpret in terms of fundamental decay processes. The behavior of powders of the first category seems quite reasonable, i. e., increased humidity increases either or both the agglomeration rate and rate of loss to walls. However, the behavior of powders of the second category is more difficult to explain. For the latter category, the eminent possibility would seem to be that increasing humidity enhances one of the rates and retards the other, one rate dominating at one extreme humidity condition with the other rate dominating at the other extreme. Thus, if a hypothetical decay rate parameter  $\lambda$  is comprised of two parts,  $\lambda_{\text{settling}} + \lambda_{\text{agglomeration}}$ , the observed behavior could be accounted for as indicated in Figure 3.6. For the present,



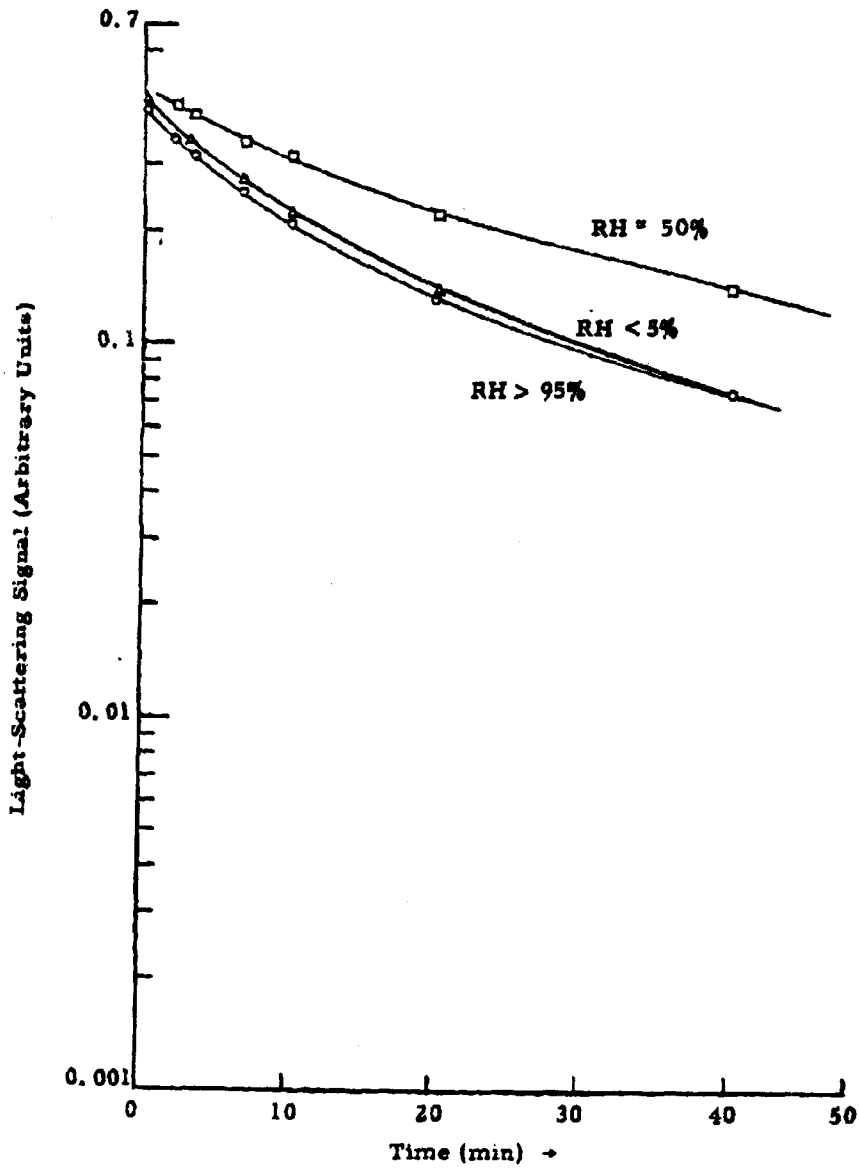


Figure 3.1 Effect of Humidity on Decay of Talc Aerosols (= 52 mg Samples)

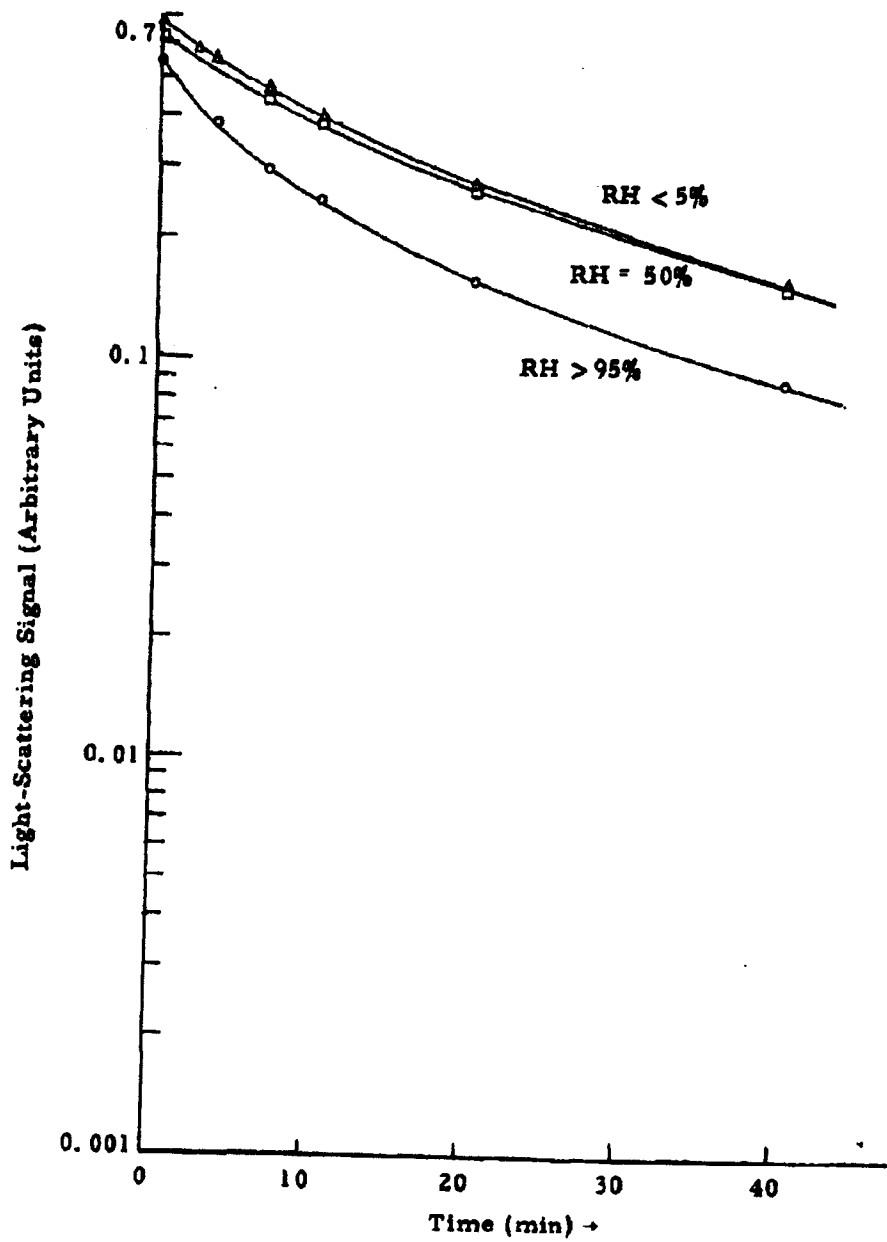


Figure 3.2 Effect of Humidity on Decay of Saccharin Aerosols (= 57 mg Samples)

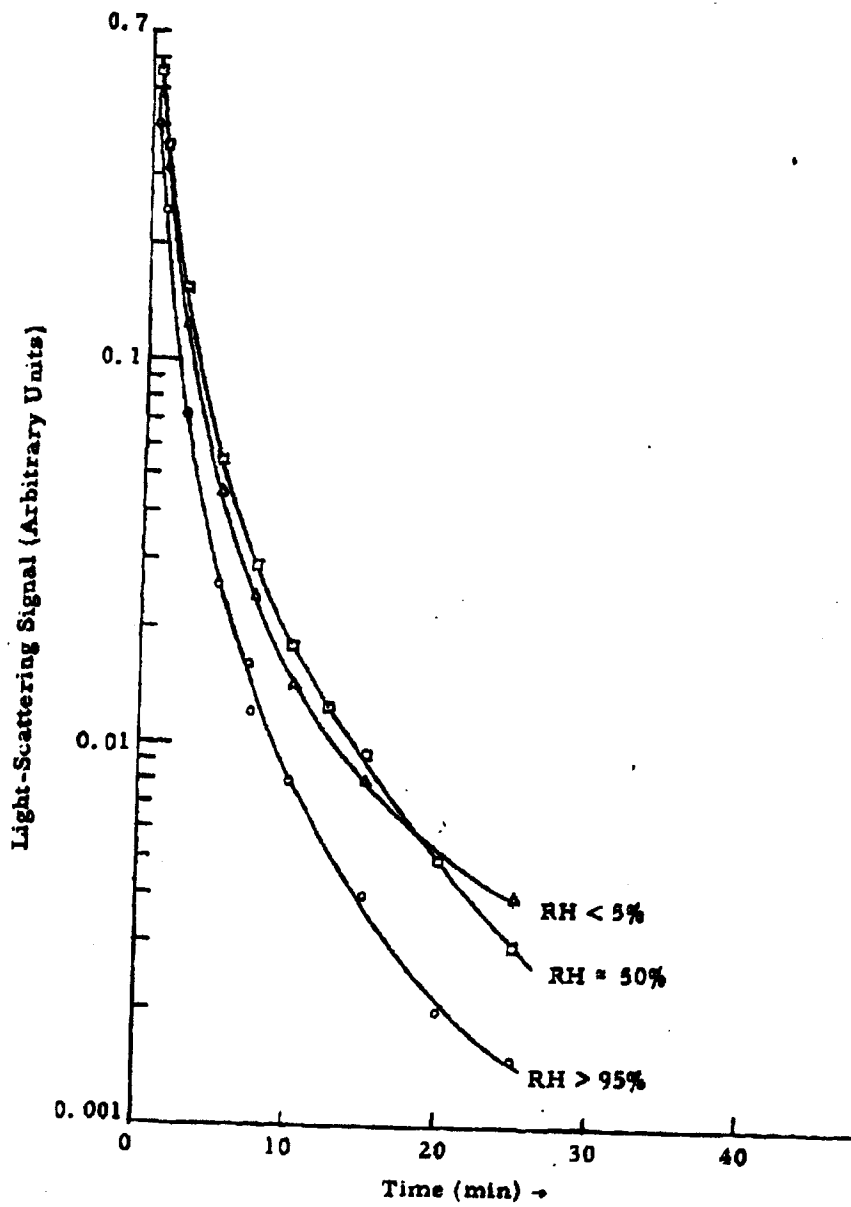


Figure 3.3 Effect of Humidity on Decay of Cornstarch Aerosols ( =550 mg Samples)

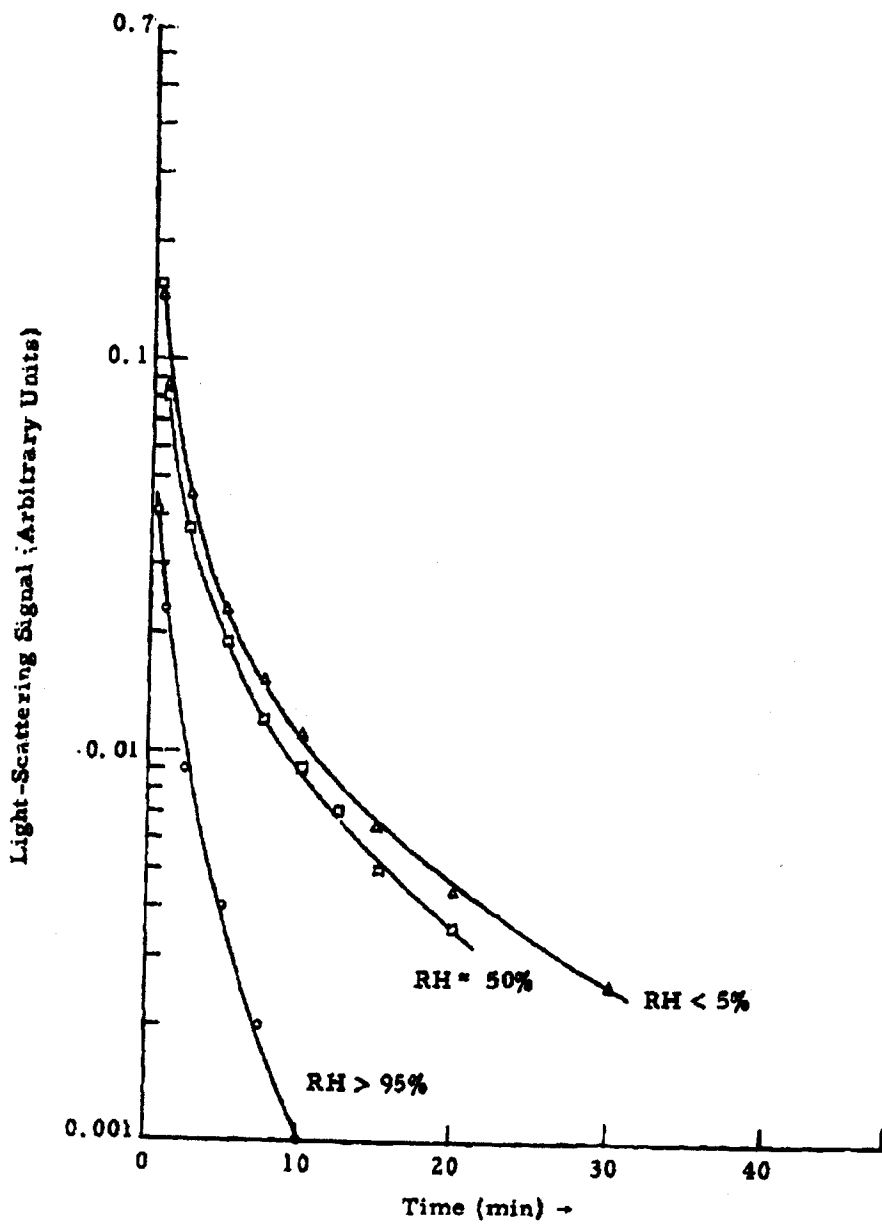


Figure 3.4 Effect of Humidity on Decay of Powdered Milk Aerosols ( \* 550 mg Samples)

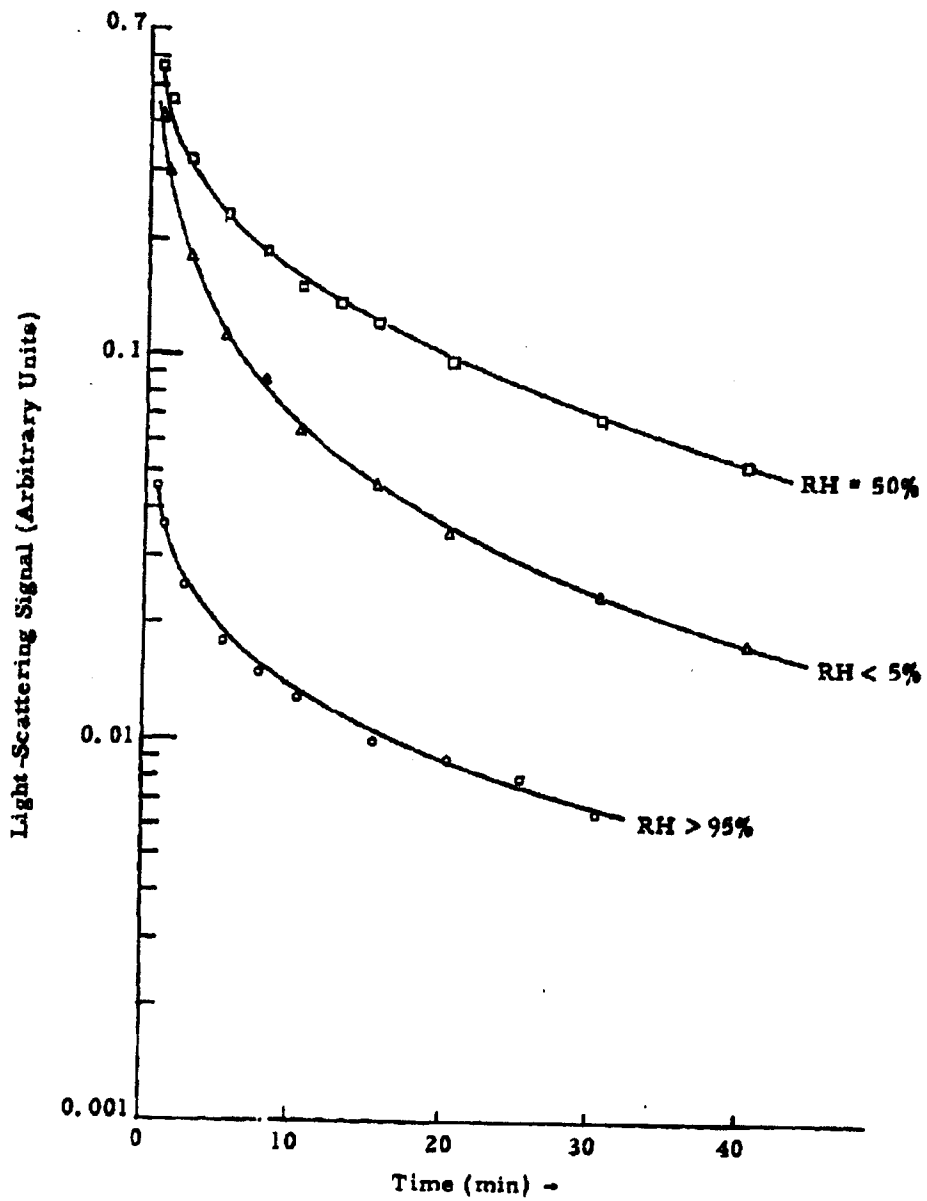


Figure 3.5 Effect of Humidity on Decay of Powdered Sugar Aerosols (4 530 mg Samples)

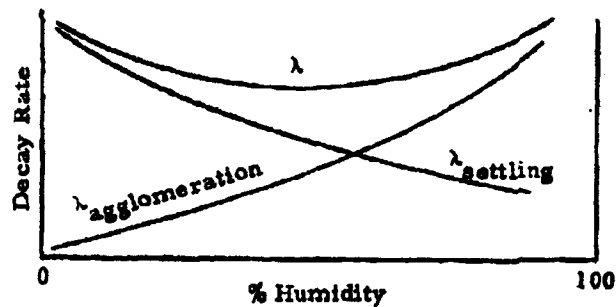


Figure 3.6 Proposed Mechanism for Anomalous Humidity Effect

we shall not speculate further on the mechanisms behind the humidity effects. Certain theoretical considerations that may be pertinent are forthcoming and further experimental work is planned in this area.

### 3.2 Considerations on Light-Scattering Noise Levels

It was noticed during the work of the last quarter that the noise levels on the light-scattering records were consistently higher for talc aerosols than for saccharin aerosols. Some of the work of this quarter was devoted to investigating this phenomenon. Actual copies of typical records are shown in Figure 3.7. The important point to be noted is that for a given scattering signal, the noise level (breadth of trace) for talc is about twice that for saccharin.

The noise observed may have one or more origins. Fluctuations may arise from the light source, from the aerosol within the scattering volume, from the photomultiplier tube, or from various points in the amplification system. In order to study these points, two systems of illumination other

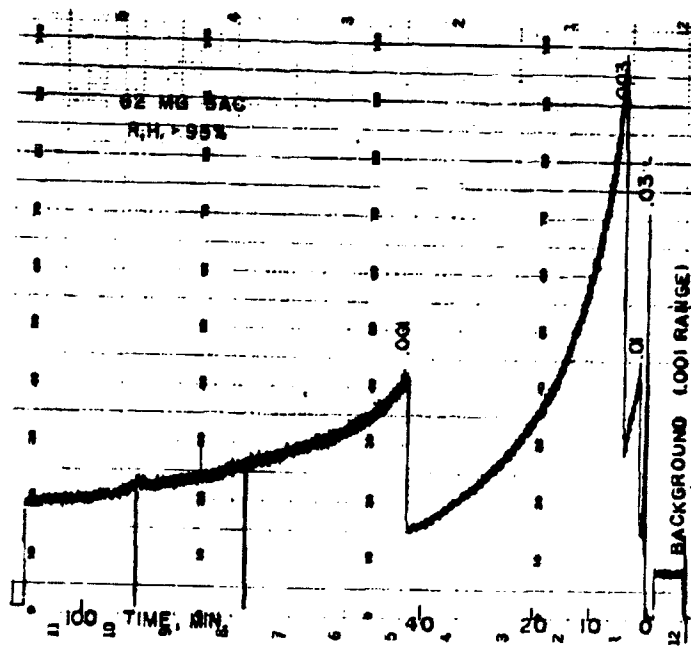
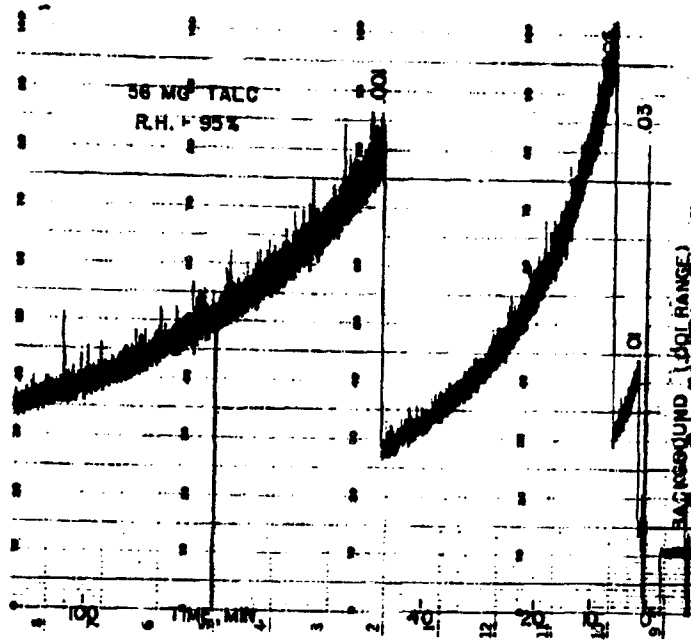


Figure 3.7 Copies of Light-Scattering Records:  
Top-Talc Aerosol, Bottom-Saccharin Aerosol

than the usual light scattered from an aerosol were tried. The first made use of a radioactive standard light source that was taped inside the chamber to the window facing the photomultiplier tube. Masks were used to control illumination. The second method of illumination consisted of light scattered from a bottle of distilled water placed in the chamber at the scattering volume. Illumination was controlled by adjusting the voltage of the light source. The noise resulting from these two methods of illumination, together with noise levels from talc and saccharin aerosols, are shown in Figure 3.8.

Figure 3.8 shows that the noise levels from the two auxiliary methods of illumination, the radioactive light source and scattering from distilled water, are very nearly equal up to about 1 mv signal. Both aerosol noise levels are somewhat higher. Since the fluctuations in the scattered light are independent of those fluctuations operative without the aerosol<sup>4</sup>, we have

$$(\text{observed fluctuation})^2 = \left( \text{fluctuation due to aerosol} \right)^2 + \left( \text{intrinsic fluctuations} \right)^2 .$$

### 3.3 Mathematical Analysis of Fluctuations in the Light-Scattering Signal

The experimentally discovered phenomena of fluctuations in the light-scattering signal have motivated further theoretical analysis which will be presented in this section. In the process we shall rephrase certain parts of the work presented in the last quarterly report<sup>1</sup> and extend certain definitions given there.

<sup>4</sup>The fact that the two auxiliary methods of illumination yield the same noise level indicates that this "intrinsic noise" arises in the photomultiplier tube or the subsequent electronics. A simple calculation based on the theory of the shot effect indicates that the origin is in fact shot noise in the photomultiplier tube.



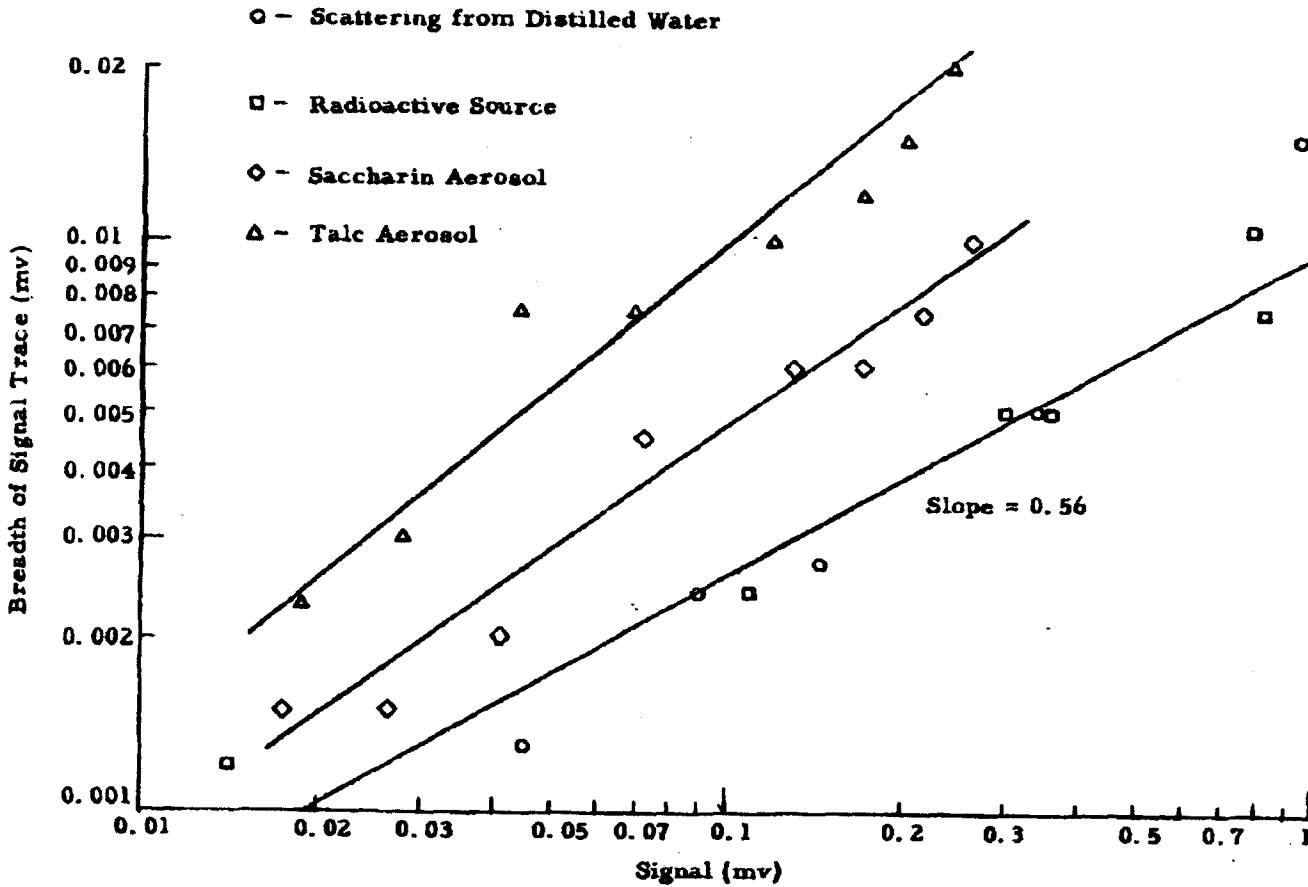


Figure 3.8 Noise Levels for Various Scattering Agencies

Let  $N(t)$  be the number of particles in the aerosol at time  $t$ . The corresponding cumulative particle size distribution  $N(d, t)$  and particle size distribution  $N'(d, t)$  are defined as before<sup>3</sup>, as are the fractional distributions  $n(d, t)$  and  $n'(d, t)$ .

The analysis that follows will emphasize the randomness associated with aerosols, a point of view which in light of experience is more in accord with facts than an analysis emphasizing the regularities of aerosols. We assume that at any particular instant  $t$ , the  $N(t)$  particles are distributed randomly throughout the chamber, the distribution being in a constant state of flux because of air currents. At any particular time  $t$  certain particles find themselves in the light-scattering volume<sup>4</sup>  $\delta V$ , while at some later time other particles are so located. We assume that this constant exchange of light-scattering samples is equivalent to random sampling of the aerosol. The following analysis also requires that many samples be taken over an interval of time during which  $N(t)$  is approximately constant. An oscilloscope study has shown that this requirement is probably satisfied for the aerosols under study.

Under the assumptions just made, the aerosol sampling process obeys Poisson statistics\*, wherein the probability  $p(m)$  that exactly  $m$  particles are located in a sample of volume  $\delta V$  picked at random is

$$p(m) = \frac{1}{m!} \left[ N(t) \frac{\delta V}{V} \right]^m \cdot \exp \left[ -N(t) \frac{\delta V}{V} \right]. \quad (2)$$

If many independent samples of size  $\delta V$  are taken, the expected average  $\bar{m}$  of  $m$  is

$$\bar{m} = \sum_{m=0}^{\infty} mp(m) = N(t) \frac{\delta V}{V}, \quad (3)$$

\* See, for example, the discussion of Poisson's distribution in Feller, An introduction to the theory of probability and its application, Vol. I, 2nd edition, John Wiley & Sons.

while the expected mean square fluctuation  $\overline{(m - \bar{m})^2}$  is

$$\begin{aligned} \overline{(m - \bar{m})^2} &= \overline{m^2} - \bar{m}^2 = \sum_{m=0}^{\infty} m^2 p(m) - \bar{m}^2 \\ &= (\bar{m} + \bar{m}^2) - \bar{m}^2 = \bar{m} \end{aligned} \quad (4)$$

The light scattered may now be calculated on a statistical basis\*. Suppose that at time  $t$  it is known that there are exactly  $m$  particles in  $\delta V$ . The light scattered is<sup>4</sup>

$$(I_s)_m = I \cdot \delta \Omega \cdot \sum_{i=1}^m \sigma(d_i) \quad (5)$$

where  $d_i$  is the diameter of the  $i^{\text{th}}$  particle and  $\sigma(d_i)$  is the corresponding scattering cross-section. The  $d_i$ , however, must be predicted by statistics. If the  $i^{\text{th}}$  of the  $m$  particles is regarded as picked at random, the probability that its diameter is in the range  $(d_i, d_i + \delta d_i)$  is just  $n'(d_i, t)$ . The average value  $\overline{(I_s)_m}$  of  $(I_s)_m$  is found by averaging  $(I_s)_m$  over all possible values of each  $d_i$ . Thus

$$\begin{aligned} \overline{(I_s)_m} &= \underbrace{\iint \dots \int}_{m \text{ integrals}} (I_s)_m \cdot n'(d_1, t) n'(d_2, t) \dots n'(d_m, t) \delta d_1 \delta d_2 \dots \delta d_m \\ &= I \delta \Omega \iint \dots \int \left[ \sum_{i=1}^m \sigma(d_i) \right] n'(d_1, t) n'(d_2, t) \dots n'(d_m, t) \delta d_1 \delta d_2 \dots \delta d_m \end{aligned}$$

\*The analysis given here is modeled on the analysis of the shot effect by S. O. Rice, *Mathematical analysis of noise*, Bell System Technical Journal, Vol. 23 & 24; The reasoning is further elucidated in Lindsay and Margonau, *Foundations of physics*, Dover Press.

$$\begin{aligned}
&= I_0 \cdot \sum_{i=1}^m \left[ \int \sigma(d_1) n'(d_1, t) \delta d_1 \right] \cdot \underbrace{\int n'(d_1, t) \delta d_1 \dots \int n'(d_m, t) \delta d_m}_{i^{\text{th}} \text{ integral missing}} \\
&= I_0 \sum_{i=1}^m \int \sigma(d_1) n'(d_1, t) \delta d_1. \tag{6}
\end{aligned}$$

The latter step makes use of

$$\int n'(d_1, t) \delta d_1 = \int n'(d_2, t) \delta d_2 = \dots = 1.$$

Similarly, the  $m$  integrals in the sum differ only in integration variable, so that

$$\begin{aligned}
\overline{(I_s)}_m &= m \int \sigma(d) n'(d, t) \delta d \\
&= m \bar{\sigma} \tag{7}
\end{aligned}$$

where use has been made of the definition of the average cross-section  $\bar{\sigma}$ .

At this point the restriction to  $m$  particles may be lifted. The average scattered light  $\overline{I_s}$  is given by

$$\begin{aligned}
\overline{I_s} &= \sum_{m=0}^{\infty} p(m) \cdot \overline{(I_s)}_m \\
&= I_0 \bar{\sigma} \sum_{m=0}^{\infty} mp(m) \\
&= I_0 \bar{m} \bar{\sigma} \tag{8}
\end{aligned}$$

The calculation scheme used is somewhat overpowerful for this problem, the result of which could have been seen directly. The same method, however, may be used for the more subtle problem of calculating the fluctuation of  $I_s$ .

The fluctuation of  $I_s$  is found by calculating  $\overline{I_s^2}$  and making use of the identity:

$$\overline{(I_s - \bar{I}_s)^2} = \overline{I_s^2} - \bar{I}_s^2 \quad (9)$$

The expression for  $I_s^2$  for the case where  $m$  particles are assumed is

$$(I_s^2)_m = (I_s)_m \cdot (I_s)_m = \left[ I_0 \sum_{i=1}^m \sigma(d_i) \right] \cdot \left[ I_0 \sum_{j=1}^m \sigma(d_j) \right] \quad (10)$$

Averaging over the variety of particle sizes gives:

$$\overline{(I_s^2)_m} = (I_0)^2 \sum_{i=1}^m \sum_{j=1}^m \int \dots \int \sigma(d_i) \sigma(d_j) n'(d_1, t) n'(d_2, t) \dots n'(d_m, t) \delta d_1 \delta d_2 \dots \delta d_m \quad (11)$$

The double sum contains two distinct types of terms, as seen in

$$\begin{aligned} \overline{(I_s^2)_m} &= (I_0)^2 \sum_{i=1}^m \int [\sigma(d_i)]^2 n'(d_i, t) \delta d_i \\ &+ (I_0)^2 \sum_{i=1}^m \sum_{j=1}^m \int \sigma(d_i) n'(d_i, t) \delta d_i \cdot \int \sigma(d_j) n'(d_j, t) \delta d_j \quad (12) \\ &\quad i \neq j \end{aligned}$$

There are  $m$  terms of the first type, whereas the remaining  $m^2 - m$  terms are of the second type. Thus

$$\overline{(I_s^2)}_m = (I_{80})^2 m \overline{\sigma^2} + (I_{80})^2 m(m-1) \overline{\sigma^2}. \quad (13)$$

Again lifting the restriction to  $m$  particles:

$$\begin{aligned} \overline{I_s^2} &= \sum_{m=0}^{\infty} p(m) \cdot \overline{(I_s^2)}_m \\ &= (I_{80})^2 \overline{\sigma^2} \sum_{m=0}^{\infty} m p(m) + (I_{80})^2 \overline{\sigma^2} \sum_{m=0}^{\infty} m(m-1) p(m) \\ &= (I_{80})^2 \left[ \overline{m} \overline{\sigma^2} + \overline{m^2} \overline{\sigma^2} \right]. \end{aligned} \quad (14)$$

The mean square fluctuation  $\overline{(I_s - \overline{I_s})^2}$  is therefore

$$\overline{(I_s - \overline{I_s})^2} = (I_{80})^2 \overline{m} \overline{\sigma^2}, \quad (15)$$

and the fractional root mean square fluctuation is

$$\frac{1}{\overline{I_s}} \left[ \overline{(I_s - \overline{I_s})^2} \right]^{\frac{1}{2}} = \frac{1}{\sqrt{\overline{m}}} \frac{\sqrt{\overline{\sigma^2}}}{\overline{\sigma}}. \quad (16)$$

This completes the calculation of the fluctuation. It is to be noted that in the case of a monodisperse aerosol,  $\overline{\sigma^2} = \sigma^2$  so that the fluctuation provides a direct measure of

$$\overline{m} = N(t) \frac{\delta V}{V}. \quad (17)$$

If the aerosol is polydisperse, we have  $\overline{\sigma^2} \geq \sigma^2$  so that polydispersity increases the fluctuation, as one might expect. The formula shows the form of the dependence.

The formula for the fluctuation is general in that the distribution  $n'(d, t)$  from which it is derived has been left quite arbitrary. More specific results are available if a specific form for  $n'(d, t)$  is assumed. Before taking the full step, assuming  $n'(d, t=0)$  is logarithmic normal, we digress slightly to arrive at an unexpected result. It will now be assumed<sup>5</sup> that

$$\sigma(d) = \frac{d^2}{6\pi} \quad (18)$$

and that

$$N'(d, t) = N'(d, 0) \cdot \exp \left[ -\frac{v(d)}{H} t \right] \quad (19)$$

In consequence

$$\begin{aligned} N(t) &= \int N'(d, t) \delta d \\ &= \int N'(d, 0) \exp \left[ -\frac{v(d)}{H} t \right] \delta d, \end{aligned} \quad (20)$$

and

$$\begin{aligned} n'(d, t) &= \frac{N'(d, t)}{N(t)} \\ &= \frac{N'(d, 0) \cdot \exp \left[ -\frac{v(d)}{H} t \right]}{\int N'(d, 0) \cdot \exp \left[ -\frac{v(d)}{H} t \right] \delta d} \quad (21) \end{aligned}$$

The expression for the average scattered light, Equation (8), is

$$\begin{aligned} \bar{I}_s &= I_0 \bar{\sigma} = I_0 N(t) \frac{\delta V}{V} \int \sigma(d) n'(d, t) \delta d \\ &= I_0 \frac{\delta V}{V} \int \sigma(d) N'(d, t) \delta d \end{aligned} \quad (22)$$

The rate of change of  $\bar{I}_s$  is

$$\frac{d\bar{I}_s}{dt} = I_0 \frac{\delta V}{V} \int \sigma(d) \frac{\partial}{\partial t} N'(d, t) \delta d \quad (23)$$

Now,

$$\begin{aligned} \frac{\partial}{\partial t} N'(d, t) &= N'(d, 0) \frac{\partial}{\partial t} \exp \left[ -\frac{v(d)}{H} t \right] \\ &= -N'(d, 0) \frac{v(d)}{H} \exp \left[ -\frac{v(d)}{H} t \right] \\ &= -\frac{v(d)}{H} \cdot N'(d, t) \end{aligned} \quad (24)$$

It may be noted, however, that

$$\frac{v(d)}{H} = \frac{\rho g d^2}{18 \eta H} = \frac{\rho g}{3 \eta H} \cdot \frac{d^2}{6 \pi} = \frac{\rho g}{3 \eta H} \sigma(d) \quad (25)$$



so that

$$\begin{aligned}
 \frac{d\bar{I}_s}{dt} &= - \frac{\pi \rho g}{3\eta H} I_{80} \frac{\delta V}{V} \int [\sigma(d)]^2 N'(d, t) \delta d \\
 &= - \frac{\pi \rho g}{3\eta H} I_{80} \frac{\delta V}{V} N(t) \int [\sigma(d)]^2 n'(d, t) \delta d \\
 &= \frac{\pi \rho g}{3\eta H} \overline{m \sigma^2} I_{80} \quad . \quad (26)
 \end{aligned}$$

But  $(I_{80})^2 \overline{m \sigma^2}$  is the mean square fluctuation. Thus

$$\frac{d\bar{I}_s}{dt} = - \frac{\pi \rho g}{3\eta H} \frac{1}{I_{80}} \overline{(I_s - \bar{I}_s)^2} \quad . \quad (27)$$

In other words, the rate of change of the light scattering is proportional to the fluctuation. The remarkable point is that the expression is quite independent of the initial particle size distribution  $N'(d, 0)$ . This relation may afford a means of directly checking the degree of validity of the assumed relations:

$$\sigma(d) = \frac{d^2}{6\pi}$$

and

$$N'(d, t) = N'(d, 0) \cdot \exp \left[ - \frac{v(d)}{H} t \right] \quad . \quad (28)$$

It may also be noted that, under the hypotheses introduced:

$$\frac{d}{dt} \ln \bar{I}_s = - \frac{\pi \rho g}{3\eta H} \frac{\overline{\sigma^2}}{\bar{\sigma}} \quad (29)$$

which may help to clarify the significance of the logarithmic derivative. It is independent of  $\bar{m}$  as, of course, it should be for nonagglomerative decay.

If it is assumed that the initial particle size distribution is logarithmic normal, it may be seen that the various expressions take on the form of the turbulent settling integral discussed in the last report. This point will be reported on at a later date.

### 3.4 A Swirl Powder Dispenser

It was mentioned previously<sup>6</sup> that the present method of dispersing powders in the aerosol decay chamber leaves something to be desired. During the present report period, a new dispersing system was designed. The new dispersing system differs from the old system in that 1) it is intended to introduce the powder over a period of several seconds rather than in a sudden burst as did the old dispenser; and 2) the new dispenser is designed to partially aerosolize the powder before injection.

The swirl dispenser, shown schematically in Figure 3.9, consists of a shallow cylindrical chamber which is mounted edgewise on the aerosol chamber wall. Dry nitrogen is admitted into the cylindrical dispenser chamber (which is two inches in diameter and about one-half inch deep) through two tangential jets (711 microns in diameter) in such a way that the powder is made to swirl. There are two exit ports, each 1016 microns in diameter, that form a 45-degree angle with the tangent to the powder chamber. Therefore, powder particles must negotiate a sharp 45-degree turn in order to leave the dispenser. The ratio of outlet port area to inlet port area is about 2:1; therefore, at equilibrium flow conditions, the pressure in the dispersing chamber is one-half the supply pressure. Both inlet and exit flow are sonic, provided the supply pressure is greater than 45 psi. Flow rate is of the order of liters of free gas per second.

An experimental model of the new dispenser-produced aerosols that in general were considerably more stable than those produced by the old dispenser. The major drawback of the swirl dispenser is that a powder residue

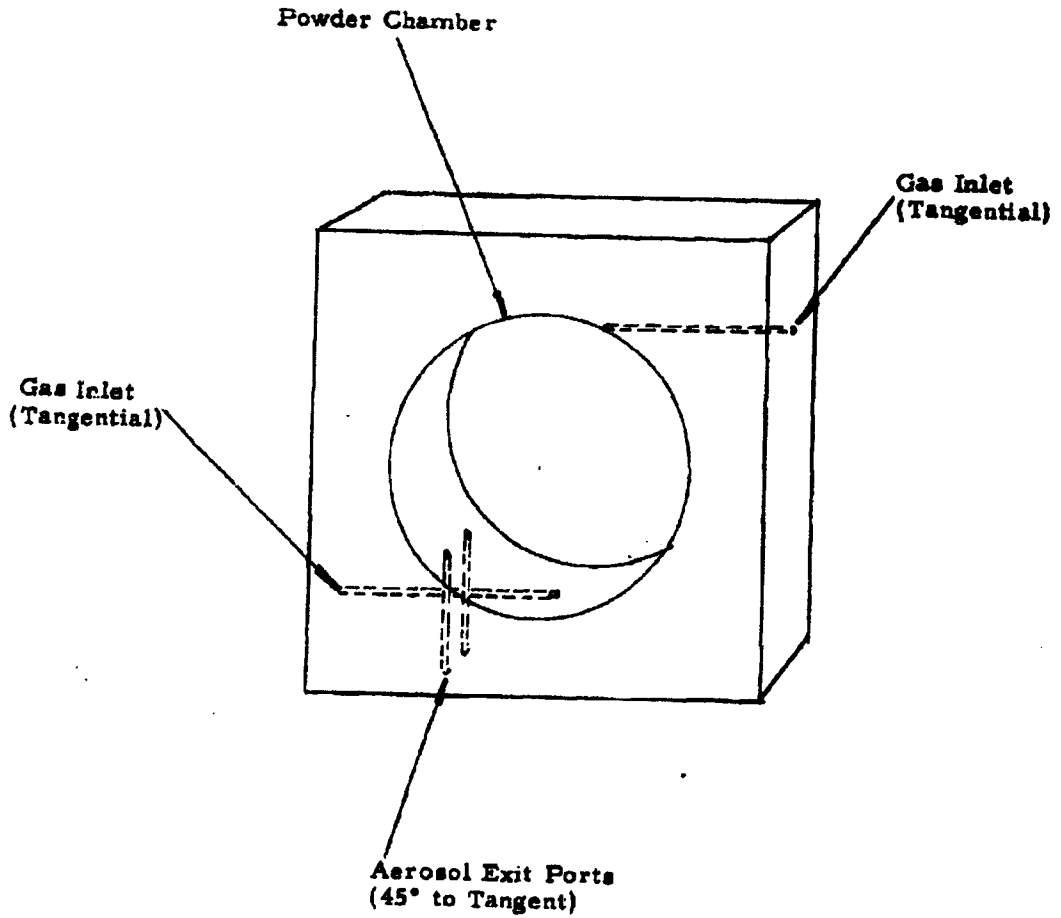


Figure 3.9 Swirl Powder Dispenser

coats, or in the case of some powders, actually cakes up the inside of the disperser. A carefully made model with polished internal surfaces may alleviate these difficulties. While the swirl disperser may not be the ultimate dispersing system, it at least provides an alternative method of dispersing powders.

### 3.5 Conclusions and Plans for Future Work

The experimental work of this quarter has revealed some pronounced effects of humidity on the stability of aerosols. One surprising feature is that for some powders the decay rate does not vary monotonically for increasing humidity. Some of the humidity runs will be repeated using the new dispersing technique described in Section 4.

Investigations up to this point have involved injecting particles into an atmosphere containing a background level of about  $10^3$  ions/cm<sup>3</sup>. Future work is planned where this ion concentration may be pushed up to  $10^6$ /cm<sup>3</sup> by means of a Whitby-type ion generator. This device produces either positive, negative, or equal amounts of positive and negative ions.

One may expect that work with different ion concentrations will add considerably to our knowledge of aerosol stability. Ion injection may prove a useful experimental tool in determining the relative importance of decay processes, since injection of ions of one sign only will clearly favor aerosol decay by precipitation on walls, whereas injection of ions of both signs would favor agglomeration. The literature on charged aerosols is rather extensive and should prove helpful in interpreting experimental results.

~~CONFIDENTIAL~~

#### 4. DISSEMINATION AND DEAGGLOMERATION STUDIES

##### 4.1 General

During this period the blow-down wind tunnel was utilized in three separate investigations related to the dissemination of dry, finely-divided materials. Major emphasis was devoted to defining the maximum bulk density of Sm which could be efficiently aerosolized by the aerodynamic break-up mechanism. For these tests the concentration of the fine aerosol cloud was determined over a range of bulk densities. When used in conjunction with our other methods of assessing the aerosol, i. e., filter and impactor samples for observation of small and large agglomerates respectively, this method serves to establish the point where dissemination becomes inefficient as bulk density is increased. Secondly, an investigation was conducted to determine the aerodynamic performance of the ejector shroud component of the prototype dry agent disseminator, so as to minimize the contamination of the store. Thirdly, a study was made of the effect of storing Sm in a compacted state.

##### 4.2 Aerosol Concentration Measurements

In studying the performance of the GMI-3 disseminator in the wind tunnel at a flow rate of 30 lb/min by use of the full-flow impactor, it was found that the quantity of Sm in the form of large agglomerates (100 to 500 microns) increased rapidly when the bulk density was increased above 0.60 g/cm<sup>3</sup>. However, at these high densities it was impossible to determine directly the quantity of material comprising these agglomerates, since many of them were impacted on the tunnel wall opposite the point of ejection. Therefore, it was found advantageous to sample the fine aerosol, which was essentially deagglomerated, to determine its change in concentration.

4-1

~~CONFIDENTIAL~~

DECLASSIFIED IN FULL  
Authority: EO 13526  
Chief, Records & Declass Div, WMS  
Date: 26 APR 2013

~~CONFIDENTIAL~~

Impactor tests have shown that the large agglomerates were heavily concentrated in the top half of the tunnel, opposite the point of dissemination. Also, it was found that the fine deagglomerated aerosol cloud was located along the bottom wall. In order to sample the fine aerosol, the high-velocity sampling probe was located at 0.5 inch from the bottom wall and samples were collected on Millipore filters. The quantity of Sm collected was determined by measuring the turbidity of the samples with a calibrated Bausch and Lomb spectrophotometer (light extinction method).

In Figure 4.1 the results of this work are given for free stream Mach numbers 0.5 and 0.8. The measurements indicate that the concentration of the fine, deagglomerated aerosol is essentially independent of the bulk density in the range 0.33 to 0.57 g/cm<sup>3</sup>. However, above this range the quantity of material in the fine aerosol cloud decreases with increasing bulk density. Conversely, the results indicate that as the bulk density exceeds 0.57 g/cm<sup>3</sup>, a greater quantity of the material is comprised of large agglomerates which do not readily break up.

Notice that the two curves break at approximately the same bulk density. This was a rather unexpected result since the maximum aerodynamic force exerted on agglomerates during dissemination is proportional to the square of the free stream velocity. At Mach number 0.8 the deagglomeration force is about 2.5 times that at Mach number 0.5. An explanation for this behavior is that the strength of the large agglomerates increases rapidly with bulk density in the region of the break point. Figure 4.2 shows the force required to compact this lot of Sm to bulk densities up to 0.61 g/cm<sup>3</sup>. The curve is an exponential that increases rapidly with increasing bulk densities above the 0.55 g/cm<sup>3</sup> level.

The experimental technique employed in this study, measurement of the deagglomerated aerosol concentration, depends on the classification of material into large agglomerates and a fine aerosol. In order to determine whether the samples collected were representative of the fine aerosol concentration and to determine the effect of sampling probe position, the

~~CONFIDENTIAL~~

DECLASSIFIED IN FULL  
Authority: EO 13526  
Chief, Records & Declass Div, WHS  
Date: 26 APR 2013

CONFIDENTIAL

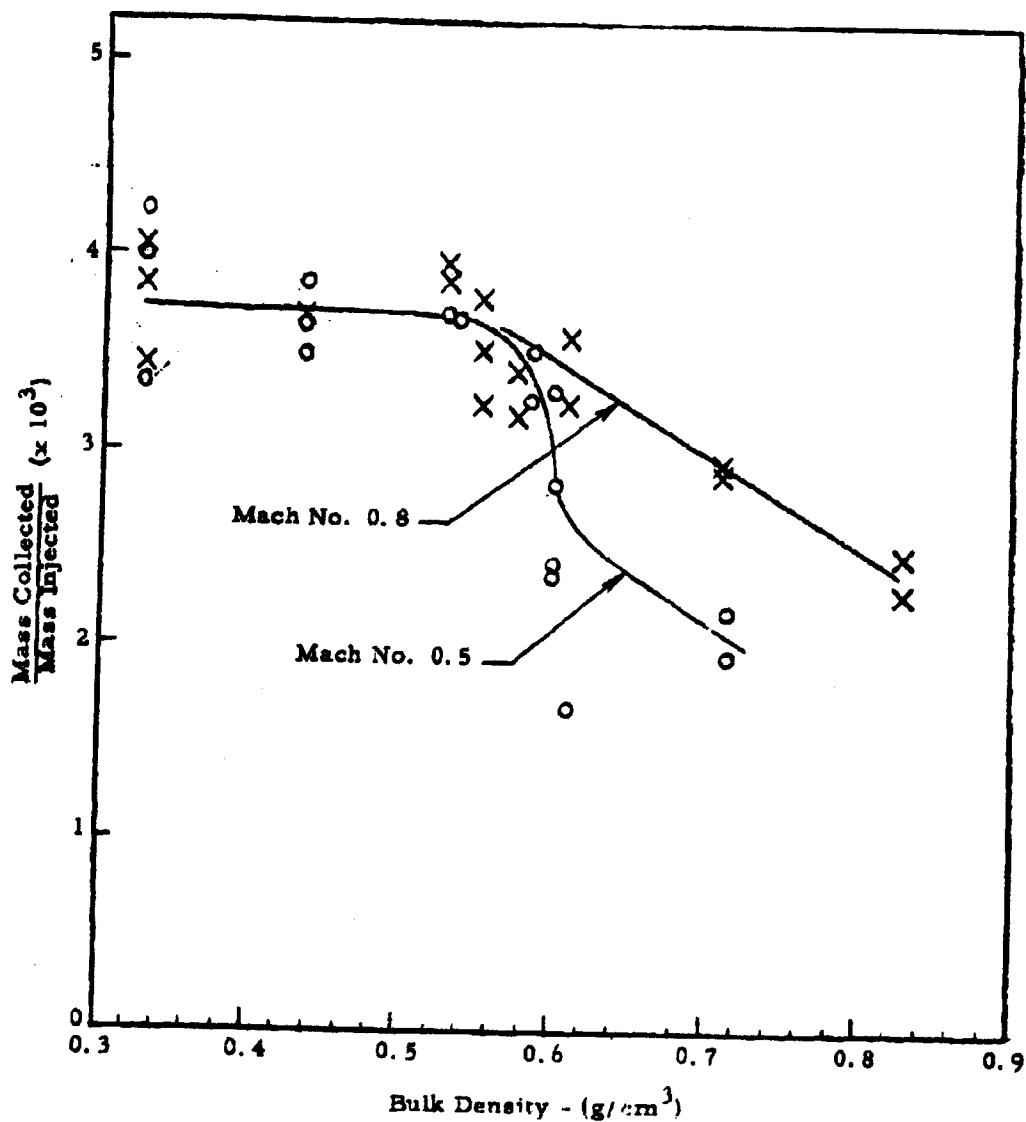


Figure 4.1 Concentration of Fine Sm Aerosol Cloud in Wind Tunnel as a Function of Bulk Density - Sampling Probe at 0.5 inches from Wall

CONFIDENTIAL

DECLASSIFIED IN FULL  
Authority: EO 13526  
Chief, Records & Declass Div, WHS  
Date: 26 APR 2013

~~CONFIDENTIAL~~

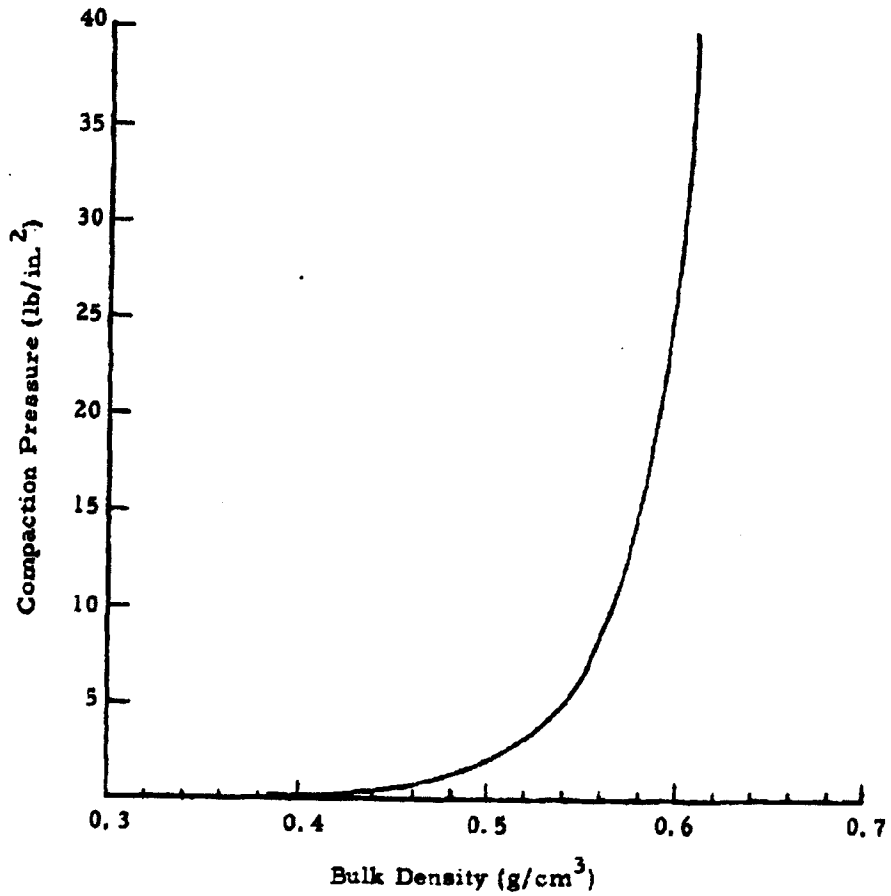


Figure 4.2 Pressure Required to Compact Sm having a Mass Median Diameter of 6.2 Microns

~~CONFIDENTIAL~~

DECLASSIFIED IN FULL  
Authority: EO 13526  
Chief, Records & Declass Div, WHS  
Date: 26 APR 2013



~~CONFIDENTIAL~~

concentration gradient within the fine aerosol cloud was measured for the two bulk densities 0.33 and 0.57 g/cm<sup>3</sup>. The results are shown in Figure 4.3. The concentration of the aerosol cloud was essentially the same for the two cases, indicating that the quantity of material that was deagglomerated during dissemination was similar. There appears to be some difference in the gradient at the 0.75-inch distance; however, this should have only a small effect on the whole fine aerosol cloud. The difference in the absolute values shown in Figures 4.1 and 4.3 is due to an essentially systematic error in the data of Figure 4.1. Since this study is concerned with relative changes in concentration, such an error does not affect the interpretation of the data.

It can be concluded from this study that the maximum S<sub>m</sub> bulk density which is feasible for dissemination is about 0.58 g/cm<sup>3</sup>. It is important to realize that the S<sub>m</sub> simulant was not stored in the compacted state for this work. Recent data indicate that storage of the compacted material will somewhat reduce this value (see Section 4.5).

#### 4.3 Shroud Investigation - Prototype Dry Agent Disseminator

In planning the prototype dry agent disseminator, it was decided that the agent should be injected into the air stream at a substantial distance outward from the disseminator store to prevent excessive contamination of the unit. Wind tunnel studies have shown that the agent aerosol cloud will flow along the skin of the store if the orifice is positioned flush with the surface.

The original shroud design is shown in our previous report<sup>7</sup>. It projects outward five inches from the store. Because the requirements that the shroud must contain a valve mechanism and that the cord length could not exceed ten inches, an elliptical cylinder configuration was chosen. This shape is not the most satisfactory from the aerodynamic standpoint, and therefore, a plate was designed for the end of the shroud which would prevent the aerosol from flowing into the low-pressure separation region along the trailing edge.

~~CONFIDENTIAL~~

**CONFIDENTIAL**

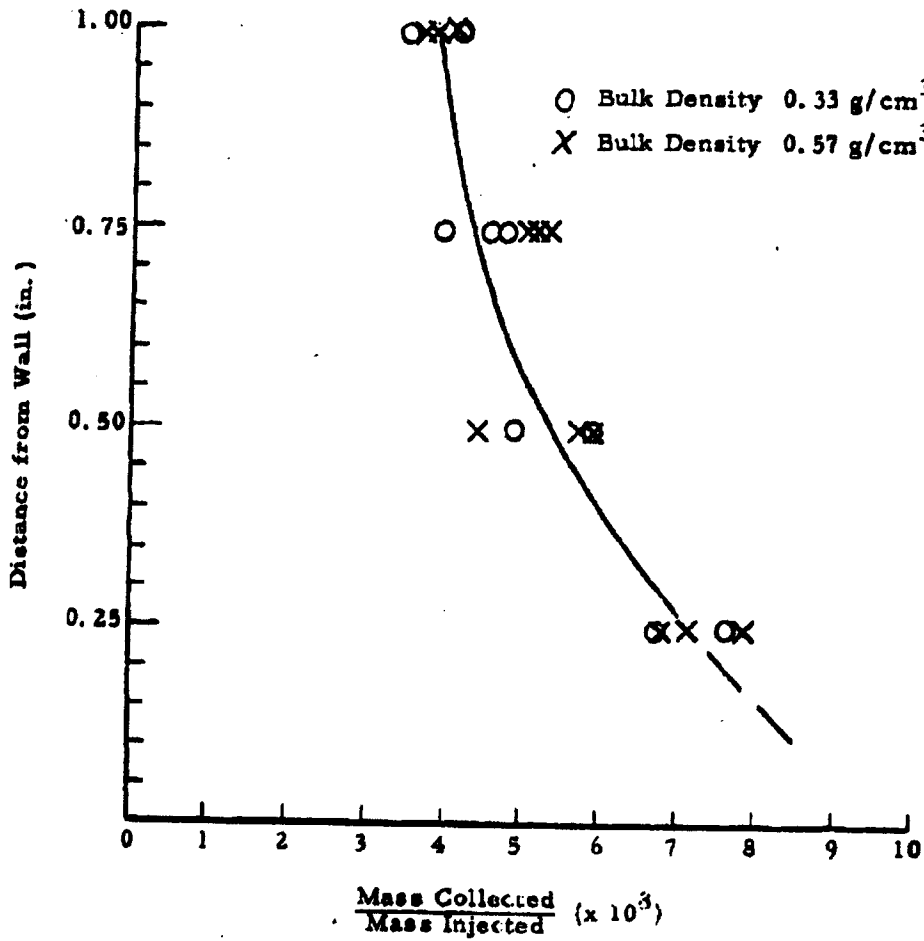


Figure 4.3 Concentration Profile of Fine Aerosol Cloud Generated in Wind Tunnel with Mach Number 0.5 Air Stream

**CONFIDENTIAL**

~~CONFIDENTIAL~~

Very little information on such an application is available in the literature. Consequently, it was necessary to investigate its performance in the blow-down wind tunnel. A model of the shroud was constructed to a scale of one-fifth the actual size. The cross-sectional area of the model was approximately 11 percent of that of the tunnel, allowing a free stream Mach number of 0.65 to be investigated without choking the flow at the model. To simulate the prototype unit, the ratio of the wall boundary-layer thickness to model length was made similar to the actual case. The boundary-layer thickness was measured and found to be in agreement with our previously calculated values. The Reynolds number of the shroud is another important parameter. However, it was impossible to simulate the prototype in this respect. The Reynolds number based on the length of the shroud from the leading edge will be about  $36.7 \times 10^6$  for the prototype unit, while the maximum we could obtain from the model was  $2.1 \times 10^6$ . Since flow separation is retarded with increased Reynolds number, the results from the wind tunnel study can be considered conservative, i. e., the prototype should perform better than the model.

The investigation was primarily based on photographic observations of the aerosol flow pattern and powder deposits on the tunnel wall and model. Aerosols were generated from four materials: talc, zinc cadmium sulfide, iron oxide pigment, and Sm. The pigment was most helpful when studying the powder deposits, while Sm and talc were especially suitable for observing the aerosol flow pattern during the tests.

The first runs were conducted without the end plate mounted on the shroud. The resulting flow pattern was unsatisfactory as a portion of the aerosol flowed downward along the back of the shroud before moving in the downstream direction. There was a large amount of powder deposited on the tunnel wall with this configuration.

By adding the end plate to the shroud the amount of material deposited on the back of the model and tunnel was significantly reduced, although this arrangement was still considered unsatisfactory. Figure 4.4 shows the

~~CONFIDENTIAL~~

**CONFIDENTIAL**

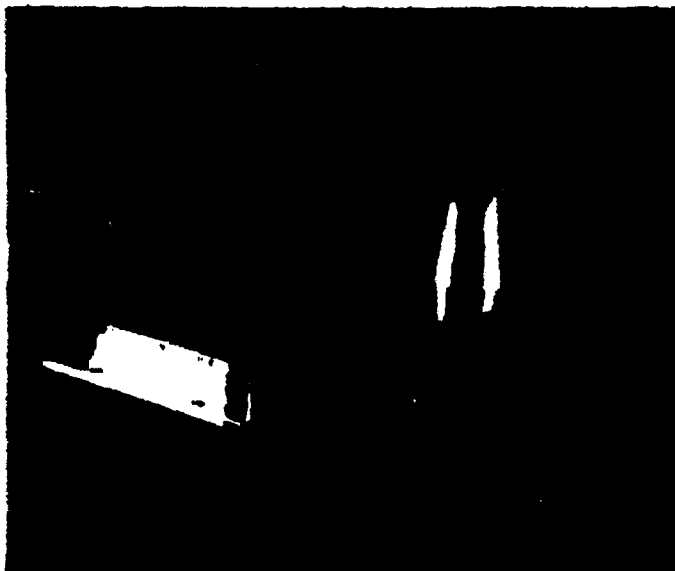


**Figure 4.4 Deposition of Iron Oxide on Trailing  
Edge of Shroud and on Tunnel Wall**

DECLASSIFIED IN FULL  
Authority: EO 13526  
Chief, Records & Declass Div, WHS  
Date: 26 APR 2013

**CONFIDENTIAL**

~~CONFIDENTIAL~~

model and tunnel wall deposits. Note that on the wall there appears to be two deposit areas. One is located at the back of the shroud while the second begins about three inches downstream of the shroud and continues downward along the tunnel. The explanation for this pattern is that the material was collected on the model because a portion of the aerosol flowed directly into the separation region along the back of the shroud, while the wall deposit resulted from turbulent mixing downstream of the shroud.

Modifications were made to the original model to reduce the effect of flow separation. Roughness elements such as fine emory cloth and wires were secured to the forward surface of the model to generate a turbulent boundary layer on the model and thereby retard the separation point on the model. However when these tests were made, much more material was deposited on the base wall. In actuality these turbulence generators caused more severe separation because they were too thick for the existing boundary layer.

In another case, air was injected into the separation region behind the shroud to increase the pressure. These tests showed that by this technique all material deposits on back of the shroud and on the wall directly behind the shroud could be eliminated. However, the only solution for reducing the downstream wall deposit was to add a faring to the back of the shroud which would reduce turbulent mixing.

Figure 4.5 shows the model faring modification that was tested. The length was increased by 50 percent. Observations and motion pictures such as shown in Figure 4.6 indicated this configuration was a substantial improvement over the original one.

As a result of this wind tunnel study, the shroud design for the prototype unit was modified. The dimensions for the new shroud are given in GMI drawing SK 29100-795 in Appendix A.

To estimate the amount of material that might collect on the disseminator store using the improved shroud design, a known quantity of viable Sm was injected into the wind tunnel. Three areas of the tunnel were washed

~~CONFIDENTIAL~~

~~CONFIDENTIAL~~

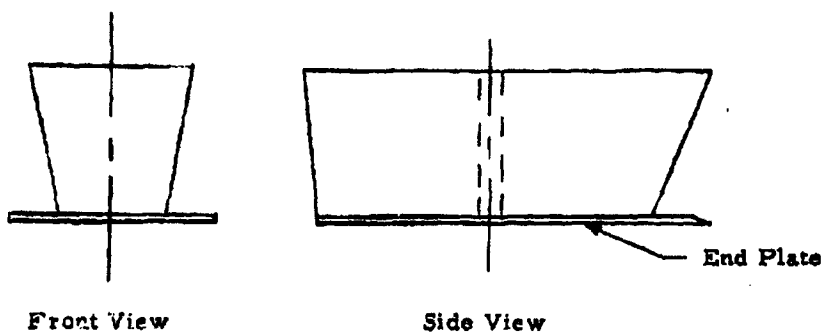


Figure 4.5 Modified Model Disseminator Shroud

~~CONFIDENTIAL~~

DECLASSIFIED IN FULL  
Authority: EO 13526  
Chief, Records & Declass Div, WMS  
Date: 26 APR 2013



Figure 4.6 Dissemination Flow Pattern of Modified Shroud

~~CONFIDENTIAL~~

down and the samples were assayed using standard techniques. Figure 4.7 shows the concentration of viable organisms on the wall as a function of distance from the injection point. The contamination increase, beginning about nine inches downstream of the ejection point, indicates that turbulent mixing becomes important in this region. If the scale model had been made with a portion of the under side of the store, the tapered tail section would begin at about six inches downstream of the point of dissemination. Since the store begins to taper well ahead of the region where contamination increase was observed, it is believed that the condition will be much more favorable on the prototype unit. The total organism count on the tunnel wall over the 0 to 8-inch length was found to be  $5 \times 10^3$  organisms when the wind tunnel was operated at Mach number 0.5. Since  $15.1 \times 10^{11}$  organisms were aerosolized during this run, about  $3.3 \times 10^{-7}$  percent of the material disseminated may collect on the store. It should be emphasized that this is only a rough prediction of the contamination that could be expected on the actual store. It is extremely difficult to simulate the actual flow conditions around such a store with a sealed-down model. However, we believe that if any difference exists between the prototype and the model, the prototype store will have the better performance.

#### 4.4 Wind Tunnel Boundary Layer

In the above shroud investigation it was pointed out that the ratio of boundary-layer thickness to shroud length was important in scaling the model. Therefore, the boundary-layer profile was measured at Mach numbers 0.5 and 0.8 and compared with a theoretical calculation similar to that discussed in our earlier report<sup>8</sup>.

The velocity profile was determined by measuring the stagnation pressure at numerous points in the air stream and the static pressure at the tunnel wall. The temperature within the boundary layer was assumed constant. A double impact probe was made from 0.032-inch outside diameter tubing such that for each run two stagnation pressures were measured, one in the free stream and the other within the boundary layer.



~~CONFIDENTIAL~~

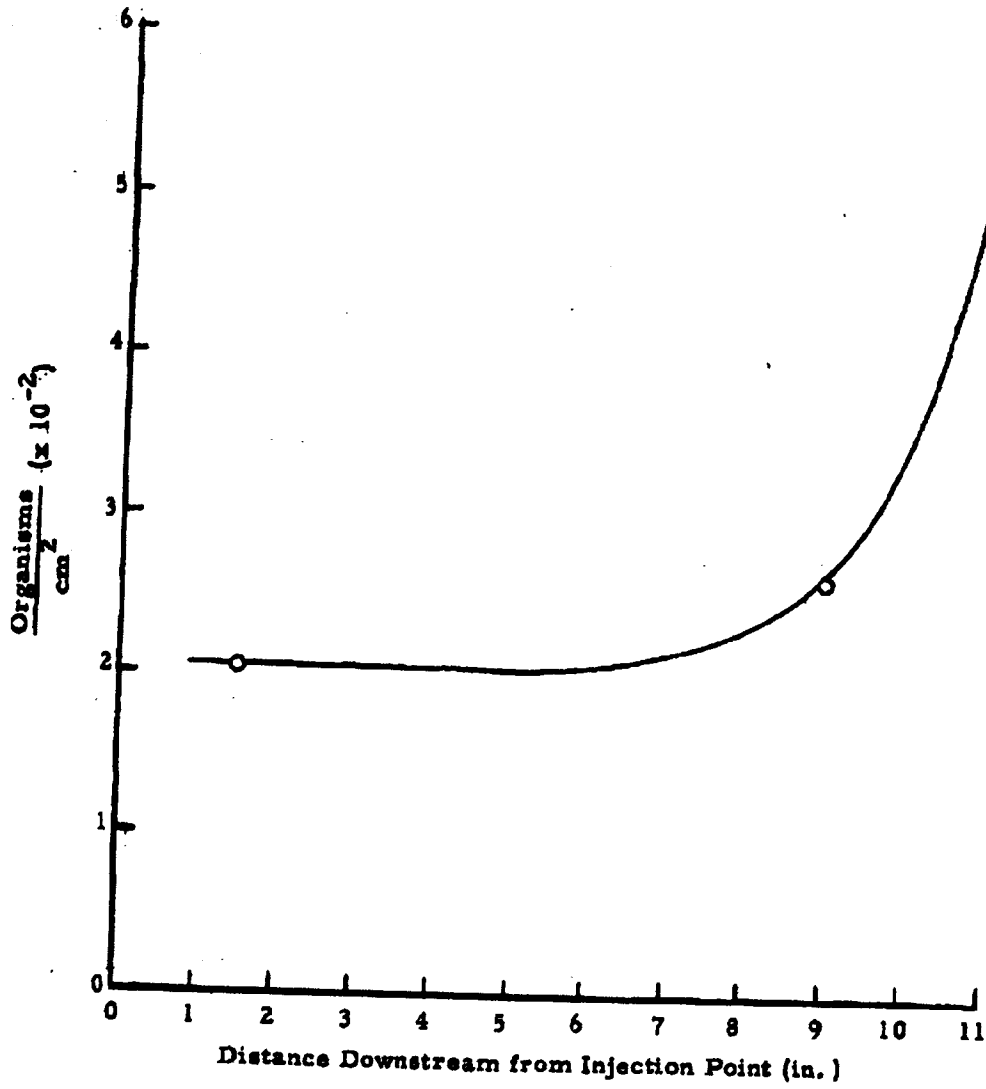


Figure 4.7 Concentration of Viable Organisms on Wind Tunnel Wall

~~CONFIDENTIAL~~

DECLASSIFIED IN FULL  
Authority: EO 13526  
Chief, Records & Declass Div, WMS  
Date: 26 APR 2013

~~CONFIDENTIAL~~

The resulting boundary-layer profiles are shown in Figures 4.8 and 4.9 for free stream Mach numbers 0.5 and 0.8, respectively. The velocity, plotted on the abscissa, is normalized to the free stream velocity. Notice that the measured boundary-layer thickness is similar to the calculated value in both cases and that the free stream velocity is quite uniform. Within the boundary layer, a difference between the theoretical and measured profile may be due to stagnation probe errors or the fact that the boundary layer is in transition from the laminar to the turbulent boundary condition. Correction factors were calculated to determine the probe error, which was found negligible. Using the Reynolds number based on tunnel length (Reynolds number =  $1.77 \times 10^6$  for Mach number 0.5; Reynolds number =  $2.82 \times 10^6$  for Mach number 0.8) as the criterion for judgment, it is thought that the boundary layer is in transition between the purely laminar and turbulent conditions.

#### 4.5 Sm Storage Test

The influence of storage on the physical properties of compacted powders is considered an important parameter in dissemination. In the case of noncompacted Sm, storage periods on the order of one year have very little detrimental effect on the aerosolization of the material. In our dissemination tests, only small amounts of strong agglomerates have been observed in material that has been stored at a temperature of 0°F for long periods.

A study was conducted to determine whether storage of Sm in the compacted form would reduce the aerosolization efficiency during dissemination. Therefore Sm was compacted to densities ranging from 0.52 to 0.60 g/cm<sup>3</sup> in a dry box and stored in a deep freeze. After ten weeks the material was disseminated with the GMI-3 fixture at a flow rate of about 30 lb/min into the wind tunnel at Mach number 0.5.

Our standard methods of assessing the aerosol were used which included the full-flow impactor and the sampling probe. There was a definite change in the characteristics of the material - over the full density range covered

~~CONFIDENTIAL~~

~~CONFIDENTIAL~~

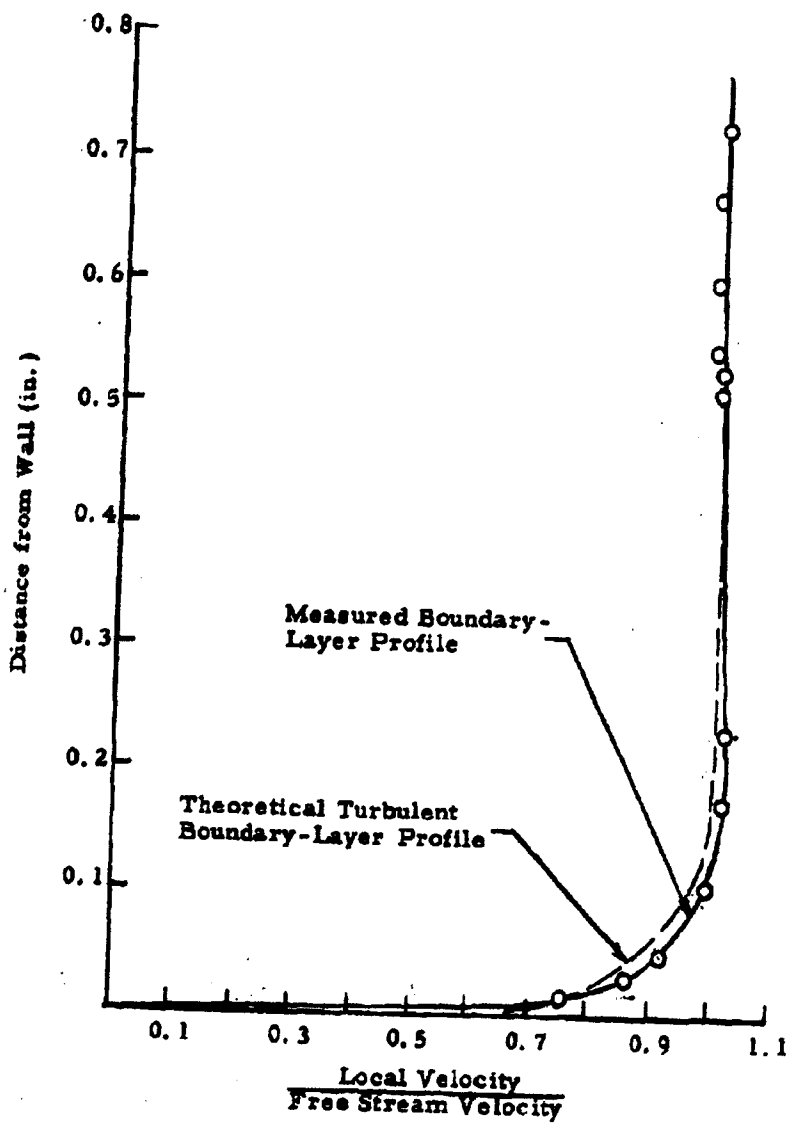


Figure 4.8 Wind Tunnel Boundary-Layer Profile with Mach Number 0.5 Free Stream

~~CONFIDENTIAL~~

DECLASSIFIED IN FULL  
Authority: EO 13526  
Chief, Records & Declass Div, WWS  
Date: 26 APR 2013

~~CONFIDENTIAL~~

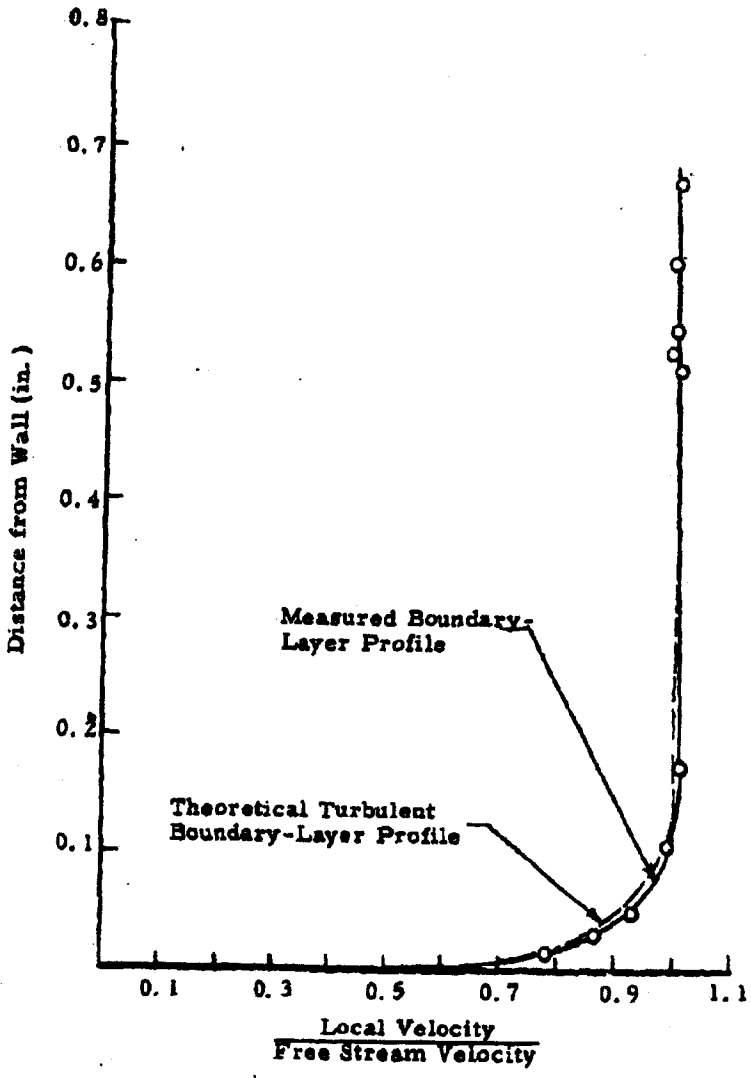


Figure 4.9 Wind Tunnel Boundary-Layer Profile with Mach Number 0.8 Free Stream

~~CONFIDENTIAL~~

DECLASSIFIED IN FULL  
Authority: EO 13526  
Chief, Records & Declass Div, WHS  
Date: 26 APR 2013

~~CONFIDENTIAL~~

there was an increase in agglomerates present in the aerosols. Material stored at density  $0.60 \text{ g/cm}^3$  did not aerosolize satisfactorily. An excessive amount of large agglomerates (100 to 500 microns) were observed on the impactor plate. Results with this particular material were similar to those obtained at  $0.65 \text{ g/cm}^3$  when the material was not stored in the compacted condition.

Material stored at  $0.54 \text{ g/cm}^3$  aerosolized satisfactorily. In analyzing the filters for small scale agglomeration (5 to 20 microns), it was found that because of agglomeration in the 5 to 20-micron range an estimated 14 percent of the useful 1 to 5-micron material was lost<sup>9</sup>.

Based on these storage investigations, it appears that the maximum bulk density that can be stored for relatively long periods and subsequently disseminated satisfactorily is about  $0.55 \text{ g/cm}^3$ . Thus, the effect of storage will tend to reduce the maximum density that can be feasibly disseminated as shown in Figure 4.1.

A larger and more detailed study of the effects of storage on the characteristics of compacted Sm has been planned for the future. It will continue for a year so as to provide data for a relatively long-storage period. In the investigation, information will also be obtained on the viability of the stored Sm.

~~CONFIDENTIAL~~

5. CONTINUATION OF EXPERIMENTS WITH THE FULL-SCALE FEEDER FOR COMPACTED DRY AGENT SIMULANT MATERIALS

5.1 Tests at 0.65 g/cm<sup>3</sup> Density

During the period covered by this report, the full-scale experimental feeder was operated successfully with a load of talc compacted to a density of 0.65 g/cm<sup>3</sup>. The schedule permitted only one series of runs to be made at this density. The feeder was then removed from the test stand so preparations could be made for testing the second experimental unit<sup>10</sup>, which is similar in design to the first-generation airborne dry agent disseminator.

The arrangement used in conducting this series of runs at 0.65 g/cm<sup>3</sup> density was the same as was used in the work that has been reported previously<sup>11,12</sup>. In a series of 16 runs with the feeder driven at 24 rpm, the average feed rate was determined to be 53 lb/min. Approximately 320 pounds of talc were fed during these runs. Air was supplied to the feeder at rates ranging from 4 to 10 std cfm. The pressure as measured inside the feeder varied from 3 cm Hg at 4 std cfm air rate to 8 cm Hg at 10 std cfm.

The driving torque was observed to vary between 18 and 27 ft-lb. At a speed of 24 rpm, the 27 ft-lb torque requirement results in an input of 0.12 hp to drive the feeder.

5.2 Wind-Tunnel Dissemination of Talc Discharged from Feeder

This series of runs was also used to provide a sample of talc that was disseminated in the high-speed wind tunnel to observe subsequent breakup into basic particles. Virgin talc at an initial compacted density of 0.5 g/cm<sup>3</sup> was desired for this sample, whereas a higher density was to be used for the actual test runs. The virgin material was loaded so as to discharge first when the feeder was operated.

~~CONFIDENTIAL~~

~~CONFIDENTIAL~~

The material sampled from the feeder discharge was disseminated in the wind tunnel using the GMI-3 disseminator and standard techniques. The tunnel was operated at Mach 0.5, and aerosol samples were obtained with the full-discharge impactor on one run and the high velocity sampling probe on the other.

The impactor has a cutoff point at about 6 microns. Essentially no large agglomerated material was found on the impactor, indicating that the talc was deagglomerated very well. The material collected on the filter in the sampling probe was examined under the microscope. There was no significant agglomeration. A majority of the material was collected in the form of basic particles, and the agglomerates that were observed consisted mainly of doublets and triplets.

### 5.3 Operation with Uncompacted Talc

Because of the emphasis which has been placed on disseminating compacted agents, all of the experiments with the first full-scale experimental feeder were conducted with compacted powder. When the second experimental feeder was completed, a few days were devoted to operating the unit with uncompacted talc. The loose bulk powder was loaded into the disseminator with the unit standing on end. It was possible to put 150 pounds of talc into the unit for each of two test series. The average density was calculated to be approximately  $0.25 \text{ g/cm}^3$ .

The observations made during these tests with uncompacted talc are not sufficient to justify detailed discussion of the results. However, the unit was capable of feeding the powder in a fairly uniform manner and for this reason the data are presented here to document the tests.

The results are summarized in Table 5.1 and in Figures 5.1 and 5.2. Only the first run with the first loading is documented because the remainder of the material was expended in miscellaneous experimental operation of the unit. Attempts to get high powder flow rates by operating at 37 rpm

~~CONFIDENTIAL~~

DECLASSIFIED IN FULL  
Authority: EO 13526  
Chief, Records & Declass Div. WHS  
Date: 12 6 APR 2013

~~CONFIDENTIAL~~

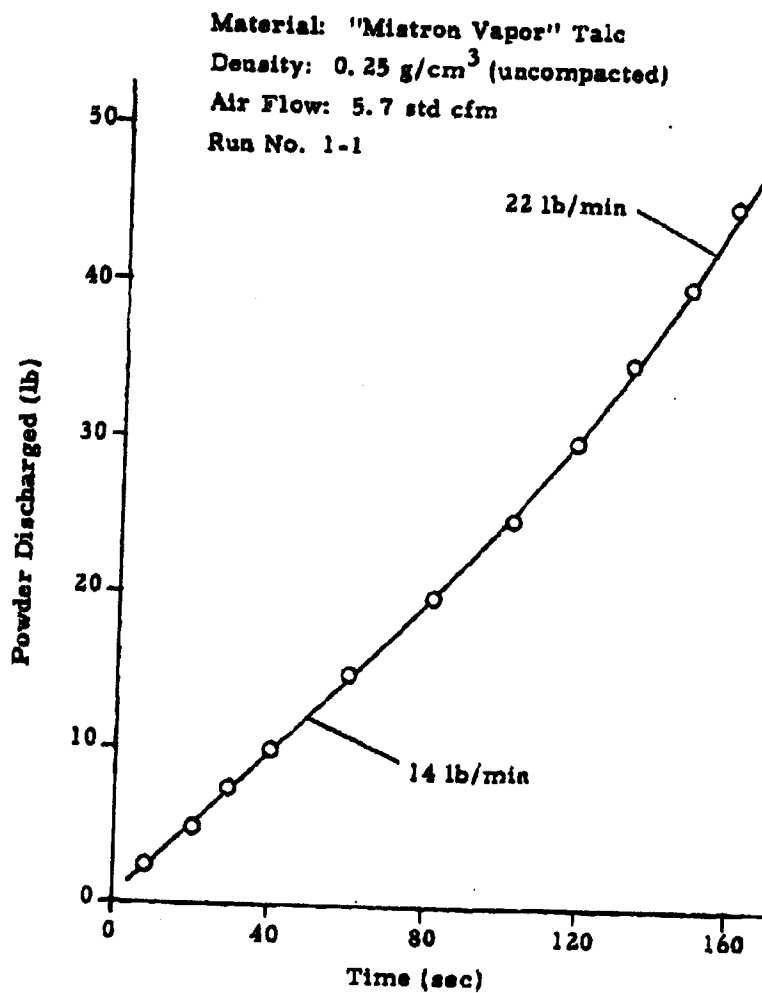


Figure 5.1 Powder Flow Rate Curve for Second Experimental Unit

~~CONFIDENTIAL~~



**CONFIDENTIAL**

Material: "Mistron Vapor" Talc  
Density: 0.25 g/cm<sup>3</sup> (uncompacted)  
Run Nos. as labeled

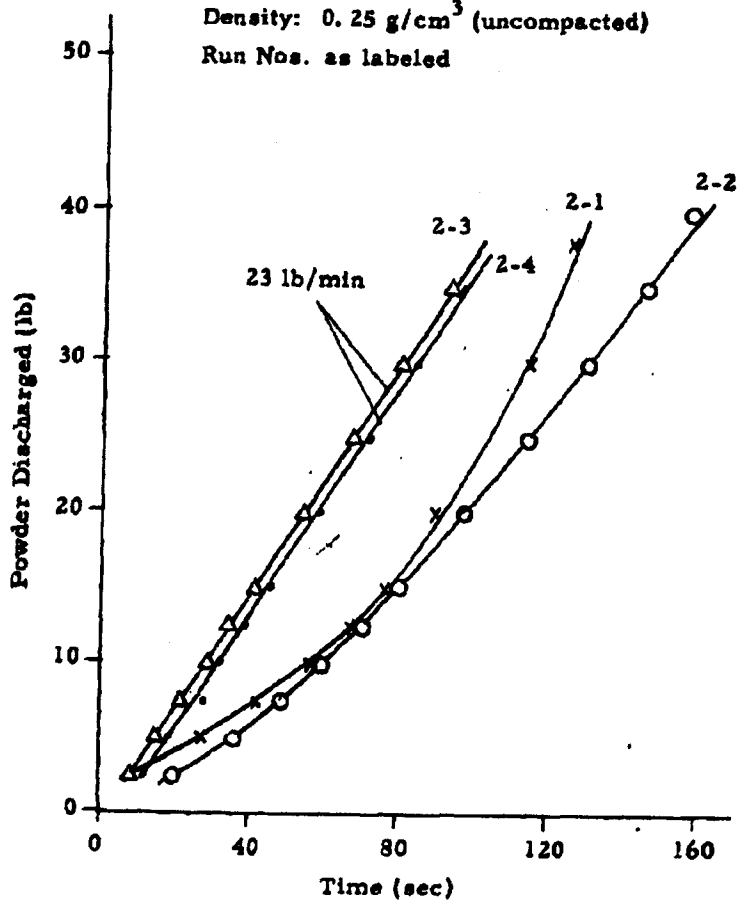


Figure 5.2 Powder Flow Rate Curves for Second Experimental Unit

5-4

**CONFIDENTIAL**

DECLASSIFIED IN FULL  
Authority: EO 13526  
Chief, Records & Declass Div, WMS  
Date: 26 APR 2013

~~CONFIDENTIAL~~

in runs 2-1 and 2-2 were not successful; the drive belt used to drive the disseminator slipped on the input pulley to the gear reduction unit in the test stand. Operation at 25 rpm resulted in a fairly uniform discharge rate for run 1-2 and identical rates for runs 2-3 and 2-4. The rate of 23 lb/min for runs 2-3 and 2-4 agreed well with the rate at the end of run 1-1.

The maximum torque observed during these trials was approximately 30 ft-lb.

Table 5.1 Summary of Data Obtained While Operating the Second Experimental Unit with Uncompacted Talc

Run No.	Q	Speed (rpm)	Rate (lb/min)
1-1	5.7	25	14-22
2-1	3.1	37*	8.5-34.5
2-2	4.0	37*	10-19.5
2-3	3.5	25	23
2-4	3.1	25	23

\* The rpm was not constant because of belt slippage on drive pulley.

~~CONFIDENTIAL~~

**6. DESIGN AND FABRICATION OF THE FIRST-GENERATION PROTO-TYPE DRY AGENT DISSEMINATING STORE**

The general configuration for the first-generation airborne dry agent disseminating store was described in the Eighth Quarterly Progress Report<sup>13</sup>. During the period covered by this report, work has progressed on the design, fabrication, and procurement of all parts of the disseminator.

**6.1 Store Structure**

During the reporting period, a purchase order was placed with Fletcher Aviation Company of El Monte, California for fabrication of the outer and inner tank structures. Parts being fabricated by Fletcher include:

- 1) The outer tank skin
- 2) The strong back casting
- 3) Tank reinforcement rings
- 4) Bayonet attachment rings
- 5) Inner tank

Fletcher Aviation Company will also install the foam insulation between the inner and outer tank.

Figures 6.1 through 6.4 show fabrication in process at Fletcher Aviation Company. In Figure 6.1, an end ring is being welded on an outer tank center section. The four holes in the tank section are for the lug attachments. Figure 6.2 shows an outer tank center section and a strong back casting. Bayonet rings on tank center and tail sections can be seen in Figure 6.3. Figure 6.4 shows an end ring being welded on an inner tank.

Three store structures have been ordered -- one for the airborne store for flight tests, and two for laboratory structural tests. The structural tests are scheduled for the latter part of October, 1962.



Figure 6.1 Welding an End Ring on Outer Shell at Center Section



3005  
Figure 6.2 Strong Back Casting and Outer Shell of Center Section



Figure 6.3 Bayonet Rings on Center and Tail Sections

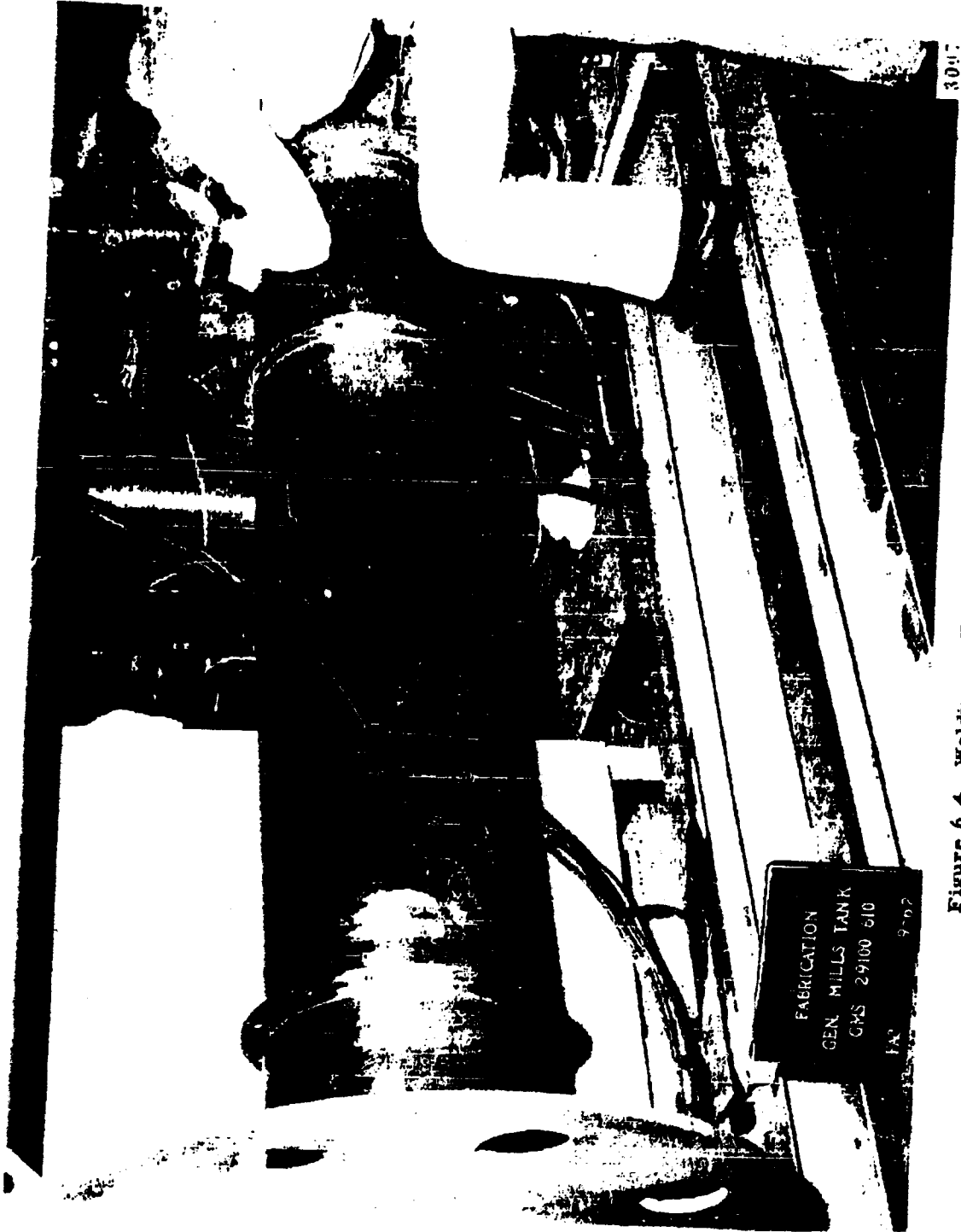


Figure 6.4 Welding an End Ring on Inner Tank

## 6.2 Rotary Actuator Assembly

During the reporting period, the design of the rotary actuator was completed and all parts were released for fabrication. At the close of the period about 75 percent of the designed parts had been fabricated and all of the purchased items, including the drive motor, had been received.

A method of mounting the motor leads within the actuator housing was developed. This permits the motor shell and support to rotate with respect to the outer shell during the change of gears for speed selection.

During the shifting of drive speeds, the motor pinion becomes completely disengaged from one driven gear before engaging the next. Since all gears are in a completely random rotational position, there is a possibility of interference when attempting a new gear mesh. To overcome the problem, if it should occur, a system was developed to "jog" the motor armature (and shaft and gear) when in the disengaged position. By means of a switch and set of relays, a short electrical impulse is delivered to the drive motor producing the jog.

Two types of dry lubricants have been tested on the motor pinion and gears in the speed change unit. Teflon coating provided adequate lubrication but tended to flake off during operation. A mixture composed of molybdenum disulfide and graphite in a resin binder also provided adequate lubrication.

Special effort has gone into the design of the coupling required between the actuator output and the drive screw of the tank feed mechanism. The coupling must be very compact because of the limited space and must have a relatively large torque and horsepower capacity. The evolved design is a segmented type coupling with elastomeric inserts and permits some angular and radial misalignment as well as axial motion.



### 6.3 Cockpit Control Panel

Since the solid agent disseminator functions in a manner quite differently from the liquid agent unit, it has been necessary to design a new control panel for the airplane cockpit. An assembly drawing of this control box is presented in Appendix B. The panel contains two toggle switches and three indicator lights.

When operated, the master switch connects 28 volt d-c airplane power to the disseminator electrical system. This is accomplished by energizing a relay with the switch action; the closing of the relay contacts connects the generator output to the system. The relay and generator are in the disseminator store. The second toggle switch, the arming switch, is provided with a guard. It is impossible to disseminate until this switch is operated. In addition to arming the circuit, closing this switch also fires the squibs that blow out the safety seal in the discharge tube through which the agent is disseminated. The arming switch is wired in series with the master switch.

The top indicator light becomes illuminated when the store generator malfunctions. The center indicator light shows when the discharge valve is open, and the bottom indicator light comes on when dissemination occurs. These indicators are the "push-to-test" type and can be tested after the master switch is closed.

The control box is also used as a junction box through which the disseminator is connected to the armament circuit used to initiate dissemination. The "pickle" switch on the control stick is used for dissemination.

At the end of the reporting period, approximately 50 percent of the components for the control box had been received.

#### 6.4 Aft Actuator Control Panel

This control panel is located within the store just aft of the actuator assembly and is reached through an access door. Its purpose is to provide extra-cockpit control of the actuator and tank drive mechanism positions during servicing. The unit contains a toggle switch to cut out the normal automatic operation of the drive system and permit local manual control. Two pushbutton switches initiate the inward and outward motions of the drive pistons - essentially forward and reverse controls. Two indicator lights signal when the pistons have reached either extreme position. A separate pushbutton switch is used to stop the actuator. Provision is also made for the switch to jog the motor armature for gear meshing if this feature proves to be necessary.

#### 6.5 Dry Nitrogen System

The dry nitrogen system was described in the Eighth Quarterly Progress Report<sup>14</sup>. During the past quarter, effort was devoted to fabrication and procurement of the various components in the gas system. An order was placed with Tavco, Inc. of Santa Monica, California to furnish the pressure vessel with electrical heater and an integral valve and pressure regulator assembly containing the following: high-pressure relief valve, charging valve, manual shutoff valve, solenoid valve, ground checkout valve, pressure regulator, low-pressure relief valve, ground checkout discharge port, and high and low-pressure gages.

Two methods of filling the system with high-pressure nitrogen were investigated: 1) using a compressor to pump nitrogen from 2200 or 2400-psi cylinders into the pressure vessel, and 2) using 6000-psi cylinders to top off after partial filling with standard cylinders. The method of cascading high-pressure nitrogen vessels into the system vessel was considered most practical for filling the first-generation flying model. Two ground carts will

be employed, one cart carrying three manifolded 2400-psi bottles, and the other transporting a 6000-psi bottle. The 2400-psi bottles will be used to fill the system vessel part way and to check out the system. The 6000-psi bottle will be used to top off the system vessel. The combination of the three 2400-psi bottles and the 6000-psi bottle will fully charge three system vessels to 3000 psi, while allowing one minute flow for calibration and checkout of the system.

~~CONFIDENTIAL~~

## 7. FILLING THE DRY AGENT DISSEMINATING STORE

### 7.1 Introduction

Ever since the conception of an airborne store for disseminating dry agent material from a compacted state, it has been recognized that filling such a disseminator would present problems quite different from those associated with filling a material that could be handled in a fluid state. As work has progressed on the development of the disseminator itself, a concurrent effort has been devoted to developing a suitable filling procedure. Early in the program it was evident that a method employing an auxiliary loading tube would very likely work. Consequently, a suitable device was designed and fabrication of this loader was completed during this reporting period. Effort has also been expended in an attempt to devise a suitable method of encapsulating the compacted dry agent in a manner that would permit manual loading of the disseminator without requiring the use of auxiliary loading equipment.

At a meeting at Fort Detrick on June 20-21, 1962, the subject of filling the dry agent disseminator was discussed with personnel from the Process Development Division. These people felt that the disseminator design was compatible with the general requirements for filling dry agents. However, they expressed the view that the use of the auxiliary loading device, which was described for them by the GMI engineers, would require rather elaborate plant loading facilities. They recommended compacting the agent in sealed packages that could be loaded into the disseminator by one man. The use of sealed packages would eliminate the need for decontaminating the unit after filling. They already have experience with filling similar packages for other applications. Consequently, an increased effort has been devoted to the search for a packaging material that will provide a sealed container and yet will break up and pass through the disseminator along with the agent without clogging the disaggregator or plugging the discharge orifice.

~~CONFIDENTIAL~~

**CONFIDENTIAL**

7.2 Loading Fixture

The loading tube, which has been fabricated for the purpose of placing a charge of compacted dry powder material in the dry agent disseminating store, is shown schematically in Figure 7.1. A photograph of the complete loading fixture comprised of the loading tube, pneumatic controls, and portable, adjustable mount is shown in Figure 7.2. The loading fixture is described in the following paragraphs.

The basic components of the loading device are the outer tube, the inner tube, the piston, and the gas supply system. The piston and the charge of compacted powder are contained within the inner tube. This tube, in turn, is contained by the outer tube. Means are provided for admitting gas under pressure to either the space behind the piston or the space behind the inner tube.

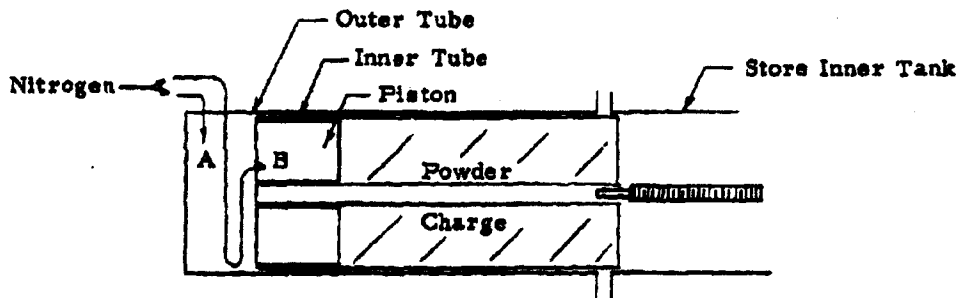


Figure 7.1 Loading Tube Assembly

DECLASSIFIED IN FULL  
Authority: EO 13526  
Chief, Records & Declass Div, WNS  
Date: 26 APR 2013

**CONFIDENTIAL**

~~CONFIDENTIAL~~

In operation the loading tube assembly is aligned with the store, and the outer tube of the loader is attached to the flange of the store inner tank (Figure 7.1). The inner tube, with powder charge and piston, is pushed into the store by applying gas pressure in space "A" (Figure 7.1). The small central tube is fastened to the inner tube and serves to guide the store drive screw as the powder charge is inserted. The inner tube hits a stop block when the powder face comes within 1/8 inch of the disaggregator blades. Space "A" is then vented to the atmosphere and space "B" is pressurized. Pressure in space "B" forces the piston and consequently the powder charge out of the inner tube, but since the powder face is against the disaggregator disk the powder cannot move and the inner tube retracts into the outer tube leaving the powder charge in the store inner tank.

The tubes and piston are made entirely of aluminum. The outer surfaces of the inner tube, central tube, and piston are Teflon-coated to prevent aluminum from rubbing against aluminum.

Seals are incorporated to prevent gas leakage past the inner tube and the piston. In order to obtain a seal with the required flexibility, rubber tubing of 35 durometer hardness was used in making the large diameter seals. Conventional O-rings are used in the piston to seal on the central tube. Since less than 1 psi pressure is required to move the inner tube into the store, a single seal has proven adequate on the inner tube. However, the 35 psi pressure required to force the powder out of the inner tube necessitated using two seals on the piston. The piston is shown in Figure 7.3. The flat on the piston matches a corresponding surface on the inner tube and provides clearance for a guide mounted on the inside wall of the store.

The pressure line to feed the space behind the piston is a flexible coil of 3/8 inch nylon tubing. The connection inside the outer tube is a swivel so the tubing can swing from a tangential to an axial direction as the inner tube is forced out of the outer tube. The other end of the nylon tube is attached to the back of the inner tube by a quick connect coupling. This coupling is readily accessible when the inner tube is completely withdrawn from the outer tube for the purpose of changing inner tubes.

C  
O  
N  
F  
I  
D  
E  
N  
T  
I  
A  
L

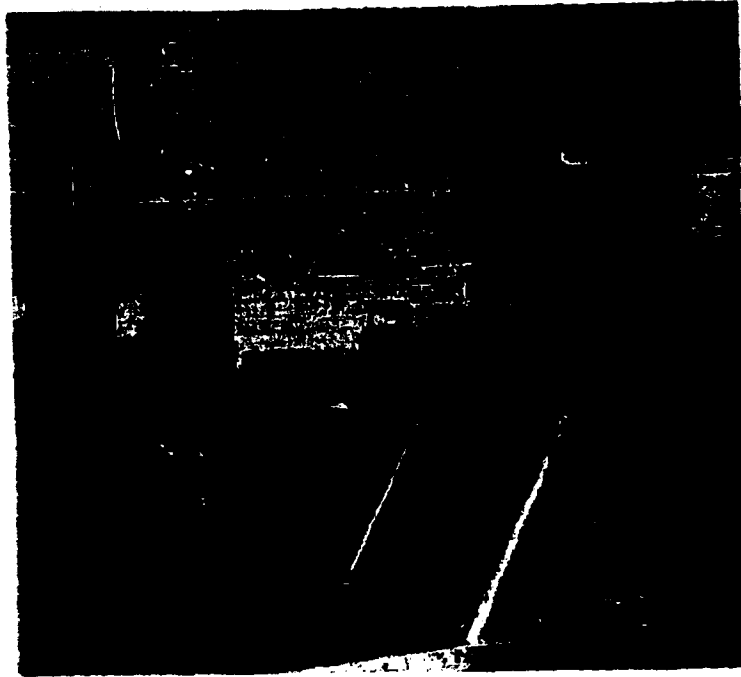


Figure 7.2 Loading Fixture for Use with Prototype Dry Agent Disseminating Store

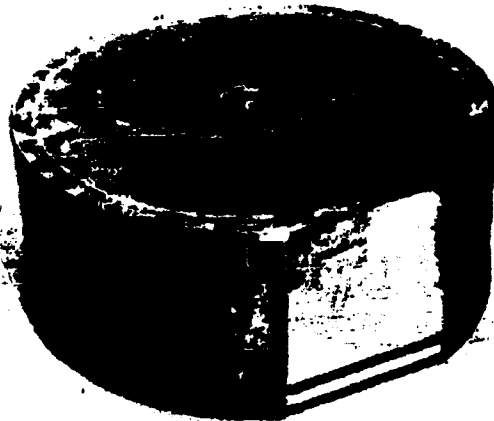


Figure 7.3 Loading Tube Piston

7-4

~~CONFIDENTIAL~~

3025

DECLASSIFIED IN FULL  
Authority: EO 13526  
Chief, Records & Declass Div, WHS  
Date: 26 APR 2013

~~CONFIDENTIAL~~

A Colson C/U Half-Ton Lifter was purchased and modified to provide a mount for the loading tube and pneumatic controls. The loading tube is supported in a gimbal ring (see Figure 7.2) that can be translated laterally by means of a hand crank. These features facilitate aligning the loading tube with the store.

The gimbal is mounted in the lifter arms in such a way that the loading tube can be easily removed as shown in Figure 7.4. This is done so the tube can be positioned vertically for filling, and then the lifter can be moved out of the way.

A pressure regulator, pressure gage, and three-position four-way valve are located on the loading fixture as shown in Figure 7.5. Gas for operating the loader can be supplied to the pressure regulator from either an air compressor or high pressure gas cylinders. The use of dry nitrogen is recommended for use with agents which must be kept dry.

The pressure regulator is required since the two major operations that must be performed require substantially different pressures. The regulator also allows control of the speed of the two operations. Pressure control is most important in the second operation of retracting the inner tube which requires about 6,000 lb force or about 30 psi. As the powder charge moves out of the inner tube, the required force diminishes, and during the course of this operation it is necessary to continually decrease the pressure to maintain a reasonable retracting speed.

### 7.3 Multiple Sealed Packages

The concept of filling the disseminator with six or eight sealed packages of compacted agent offers many advantages as compared to the use of an auxiliary loading device. Some of these advantages are:

- 1) The amount of support equipment required would be reduced significantly.
- 2) The loading plant facilities would be less elaborate.

~~CONFIDENTIAL~~

DECLASSIFIED IN FULL  
Authority: EO 13526  
Chief, Records & Declass Div, WHS  
Date: 26 APR 2013



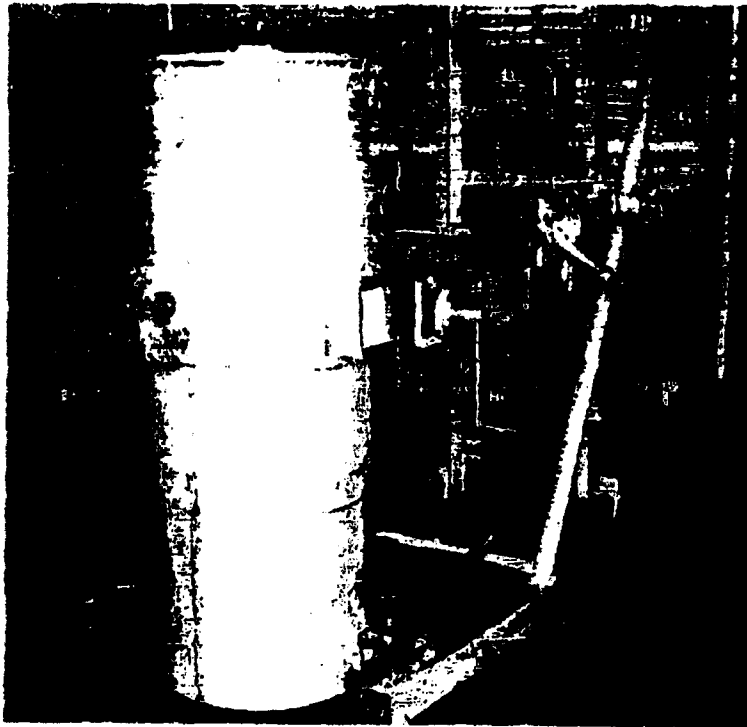


**Figure 7.4 Loading Tube Disconnected from Lifter Arms**



**Figure 7.5 Operating Controls for Loading Tube**

7-6  
**CONFIDENTIAL**

3029

DECLASSIFIED IN FULL  
Authority: EO 13526  
Chief, Records & Declass Div, WHS  
Date: 26 APR 2013

~~CONFIDENTIAL~~

- 3) It would be easier to make the filling operations safe for operating personnel.
- 4) The filling operation could probably be performed quicker.

Unfortunately, the requirement that the package or container must provide a biological seal and yet be capable of being broken up and fed through the disseminator along with the agent presents a formidable problem. Nevertheless, the advantages are attractive enough to warrant the effort that is being expended in an attempt to develop a package meeting the requirements.

In search for a suitable packaging technique three general encapsulating methods are being considered.

The first method is to form a suitable skin by applying the proper substance to the exterior surfaces of a compacted charge of agent. The second is to compact the agent in a container previously prepared from a rigid foam plastic material of the required properties. The third is to compact the agent in a bag made from a plastic film that can be caused to undergo chemical or physical changes inside of the disseminator so the film disintegrates or disperses before the disseminator is operated.

With reference to the first method of encapsulation, two techniques have been tried. One is to spray or paint the substance being investigated directly onto the compacted powder after removing the slug of powder from the mold. The other technique is to apply the encapsulating substance to the interior surface of the mold before introducing the powder and then cause the substance to transfer to the powder after compaction. This latter technique has been accomplished with wax that has been transferred by heating the mold. To date, neither of these techniques has produced a satisfactory encapsulation.

The foam plastic approach uses the blades of the disaggregator within the disseminator to shave off the foam container and the compacted powder simultaneously. The container must be broken into small pieces that will flow through the discharge opening without plugging the hole. To obtain a

7-7

~~CONFIDENTIAL~~

DECLASSIFIED IN FULL  
Authority: EO 13526  
Chief, Records & Declass Div, WHS  
Date: 26 APR 2013

~~CONFIDENTIAL~~

gas-tight container, the unicellular type foam was selected. A foam container was fabricated and loaded with compacted talc and then tested in the Second Experimental (disseminator) Unit. The test demonstrated that the unit is capable of digesting a type of foam plastic, but that it will be necessary to incorporate a feature in the disseminator to prevent relatively large pieces of foam from plugging the orifice. The effort on this approach has been toward producing a foam material that was sufficiently strong yet adequately friable. Fortunately, the Chemical Activity of General Mills Central Research Laboratory has had considerable experience in the development of foam plastics. With their cooperation in this particular investigation, we believe some progress was made toward developing a suitable encapsulating material.

The plastic film approach to encapsulation considered the use of a film that would have poor resistance to certain environmental conditions. For instance, if a quantity of agent were compacted into a bag made of film, sealed, and placed in the disseminator, which in turn was sealed, a change of temperature or a change of gas within the disseminator might deteriorate the film so it would crumble or vaporize. Accordingly, a survey of possible films was conducted. The consensus pointed to polypropylene film brought to low temperature (-20°F) at which time the film should become brittle enough to fracture into small pieces. However, samples of polypropylene film which were subjected to cold box tests down to -50°F and -109°F (dry ice temperature) did not react as desired. Other possibilities in this area of disintegrating films are currently being investigated.

7-8

~~CONFIDENTIAL~~

DECLASSIFIED IN FULL  
Authority: EO 13526  
Chief, Records & Declass Div, WHS  
Date: 26 APR 2013

~~CONFIDENTIAL~~

8. FLIGHT TESTING OF LIQUID AGENT DISSEMINATING STORE

During the period from August 13 to 29, 1962, GMI provided technical assistance in connection with flight testing of the GMI liquid agent disseminating store by the BW/CW Weapons Group at Eglin Air Force Base, Florida. These tests were conducted to investigate the airworthiness of the store and to evaluate performance of the F-105 and F-100D airplanes with the GMI disseminating store attached. A report covering this test project is being prepared by the BW/CW Weapons Group. On the basis of the verbal reports of the test pilots and the personal observations of GMI representatives, it can be said that the store functioned entirely satisfactorily and the airplanes performed normally with the store attached.

In order to establish the maximum performance conditions for the F-105 airplane to be used in the flight tests, the GMI store was shipped to the Republic Aviation Corporation at Farmingdale, Long Island, New York. Here the store was mounted on an F-105 and flutter and vibration analysis and static stiffness measurements were made. These data were then used to compute the allowable flight conditions for the F-105 airplane with the GMI store attached. This work was accomplished in late July and early August. Upon completion of the measurements at Farmingdale, the GMI store was shipped to Eglin Air Force Base for flight testing.

Two flights were made with the disseminator on the F-105 airplane. For the first flight the unit was mounted at the left inboard wing station. The centerline station was used on the second flight. The airplane was flown at 400 knots indicated air speed and maneuvered at altitudes of 5,000 and 30,000 feet. The disseminator was filled with dyed water that was disseminated at 200 feet. The dissemination was photographed from an F-100D chase plane. Personnel in the chase plane reported that the aerosol stream was separated from the bottom aft of the airplane by a space of approximately one foot.

~~CONFIDENTIAL~~

~~CONFIDENTIAL~~

One flight was made with the disseminator mounted on the inboard wing station of an F-100D airplane. This airplane was flown at 300 knots indicated air speed and maneuvered at altitudes of 5,000 and 30,000 feet. Dissemination was made at 200 feet. This flight was also covered by photography from a chase plane.

The disseminator was filled with water containing methylene blue dye so the airplanes could be examined for contamination after each flight. The F-105 was found to be free of contamination after the first flight, but on the second flight a small amount of dye was found on the lower ventral (fin). No contamination was found upon examining the F-100D after operating the disseminator on this airplane.

8-2

~~CONFIDENTIAL~~

DECLASSIFIED IN FULL  
Authority: EO 13526  
Chief, Records & Declass Div, WHS  
Date: 26 APR 2013

~~CONFIDENTIAL~~

## 9. SUMMARY AND CONCLUSIONS

Work has progressed on our broad program of research and development on the dissemination of solid and liquid BW agents. Each area of work which is summarized in the following paragraphs is discussed in detail in the section referenced at the end of the paragraph.

Applied stresses and energies required for compaction of powders have been successfully measured using an improved piston-cylinder device in an Instron test machine. Values for the constants  $k$  and  $m$  in the equation  $\sigma = k \cdot p^m$  have been determined for talc, saccharin, and cornstarch. Previously reported difficulties with the triaxial shear test have been overcome by using a sample preparation procedure that does not require the use of the rubber membrane which prevented natural shear failure of the sample. Effort has been directed toward determination of the tensile shear strength of powders as well as compressive shear strength using the triaxial technique. The bulk tensile strength of saccharin, cornstarch, powdered milk, Sm, and talc has been measured as a function of compressive load and distance from the piston to the fracture plane. The bulk density of talc (Mistron Vapor) has been determined as a function of compressive load and distance from the piston (Section 2).

Aerosol decay has been investigated for three humidity conditions - less than 5 percent, approximately 50 percent, and greater than 95 percent - for five powders. Saccharin, cornstarch, and powdered milk exhibited decay rates that increased monotonically with increasing humidity; whereas, talc and powdered sugar exhibited decay rates that were higher for the two extreme humidity conditions than for the intermediate condition. It has been demonstrated experimentally that high frequency fluctuations on the light-scattering records have significance and are not merely system noise. A formula for the fluctuation has been derived mathematically. A new swirl disperser has been used to introduce powders into the aerosol decay chamber, and the aerosols thus produced were found to be more stable than those obtained with the rupturing-diaphragm disperser (Section 3).

9-1

~~CONFIDENTIAL~~

DECLASSIFIED IN FULL  
Authority: EO 13526  
Chief, Records & Declass Div, WHS  
Date: 26 APR 2013

~~CONFIDENTIAL~~

The high-speed wind tunnel dissemination studies have shown that the maximum bulk density to which S<sub>m</sub> can be compacted and yet be aerosolized efficiently by the aerodynamic breakup mechanism is about 0.58 g/cm<sup>3</sup>. This limiting density was the same for both Mach numbers 0.5 and 0.8. It is believed that any dependence upon Mach number is far overshadowed by the rapidly increasing strength of the compacted S<sub>m</sub> as the bulk density is raised above this value. Tests of compacted S<sub>m</sub> which had been stored at a low temperature for ten weeks indicate that when compacted material is to be stored for long periods, the maximum allowable density will be lowered to about 0.55 g/cm<sup>3</sup>. In making this determination a new technique was used wherein the change in concentration of the fine portion of the aerosol was measured. A wind tunnel study of the ejection tube shroud using a scale model has produced a design which is expected to eliminate contamination of the store (Section 4).

A powder flow rate of 53 lb/min has been achieved with the full-scale experimental feeder using talc compacted to a density of 0.65 g/cm<sup>3</sup>. The second experimental unit, which is a prototype of the airborne disseminator, has been completed and this unit has been operated with uncompacted talc. A sample of talc initially compacted to 0.55 g/cm<sup>3</sup> has been collected from the discharge of the full-scale feeder and subsequently disseminated satisfactorily in the high-speed wind tunnel at Mach number 0.5 using the GMI-3 fixture (Section 5).

Design and fabrication of the first-generation dry agent disseminating store progressed from the design study stage to actual fabrication and procurement of the various components. An order has been placed with the Fletcher Aviation Company of El Monte, California for fabrication of the main structural parts of the store. The speed-selection portion of the rotary actuator assembly has been tested. A cockpit control panel has been designed. The high-pressure vessel and associated valves and pressure regulator for the dry nitrogen system have been ordered from Tavco, Inc. of Santa Monica, California, who are specialists in this type of equipment. The cascading method, using 6000-psi nitrogen cylinders for "topping-off", has been selected for filling the nitrogen system (Section 6).

9-2

~~CONFIDENTIAL~~

DECLASSIFIED IN FULL  
Authority: EO 13526  
Chief, Records & Declass Div, WHS  
Date: 26 APR 2013

~~CONFIDENTIAL~~

A loading fixture has been fabricated for the purpose of inserting charges of compacted powder into the dry agent disseminating store. The material is first compacted into a cylindrical tube in the loading fixture and is then transferred to the store. As an alternate method of loading, an investigation has been started with the objective of perfecting a method of encapsulating quantities of compacted agent small enough to permit loading the store without the aid of special equipment. The problem is to find an encapsulating material which can be digested by the disseminator (Section 7).

In August the GMI liquid agent disseminating store was successfully flight tested on an F-105 and an F-100D airplane at Eglin Air Force Base. These tests were conducted by the BW/CW Weapons Group at Eglin to determine airworthiness of the store. The tests also demonstrated that there is no contamination of the airplanes when the store is mounted at a wing station. There was minor contamination of the lower ventril of the F-105 when the store was mounted on the centerline station (Section 8).

~~CONFIDENTIAL~~

DECLASSIFIED IN FULL  
Authority: EO 13526  
Chief, Records & Declass Div, WMS  
Date: 26 APR 2013



## 10. REFERENCES

- 1) General Mills, Inc. Electronics Div. Report No. 2322. Dissemination of solid and liquid BW agents (U), by G. R. Whitnah et al. Contract DA-18-064-CML-2745. Eighth Quarterly Progress Report (August 22, 1962). Confidential.
- 2) ----. Report No. 2300. Dissemination of solid and liquid BW Agents (U), by G. R. Whitnah et al. Contract DA-18-064-CML-2745. Seventh Quarterly Progress Report (June 22, 1962). Confidential.
- 3) ----. Report No. 2322, op. cit., pp. 3-2 and 3-3.
- 4) Ibid. p. 3-4.
- 5) Ibid. p. 3-6.
- 6) Ibid. p. 3-20.
- 7) Ibid. p. 7-2.
- 8) General Mills, Inc. Electronics Div. Report No. 2216. Dissemination of solid and liquid BW agents (U), by G. R. Whitnah et al. Contract DA-18-064-CML-2745. Fourth Quarterly Progress Report (August 10, 1961). (AD 325, 247). pp. 62-72. Confidential.
- 9) ----. Report No. 2264. Dissemination of solid and liquid BW Agents (U), by G. R. Whitnah et al. Contract DA-18-064-CML-2745. Sixth Quarterly Progress Report (Feb. 23, 1962). pp. 5-6 thru 5-19. Confidential.
- 10) ----. Report No. 2322, op. cit., pp. 7-13 and 7-14.
- 11) Ibid. pp. 6-1 thru 6-4.
- 12) General Mills, Inc. Report No. 2300, op. cit., pp. 6-2 thru 6-7.
- 13) ----. Report No. 2322, op. cit., pp. 7-1 thru 7-12.
- 14) Ibid. pp. 7-4 thru 7-7.

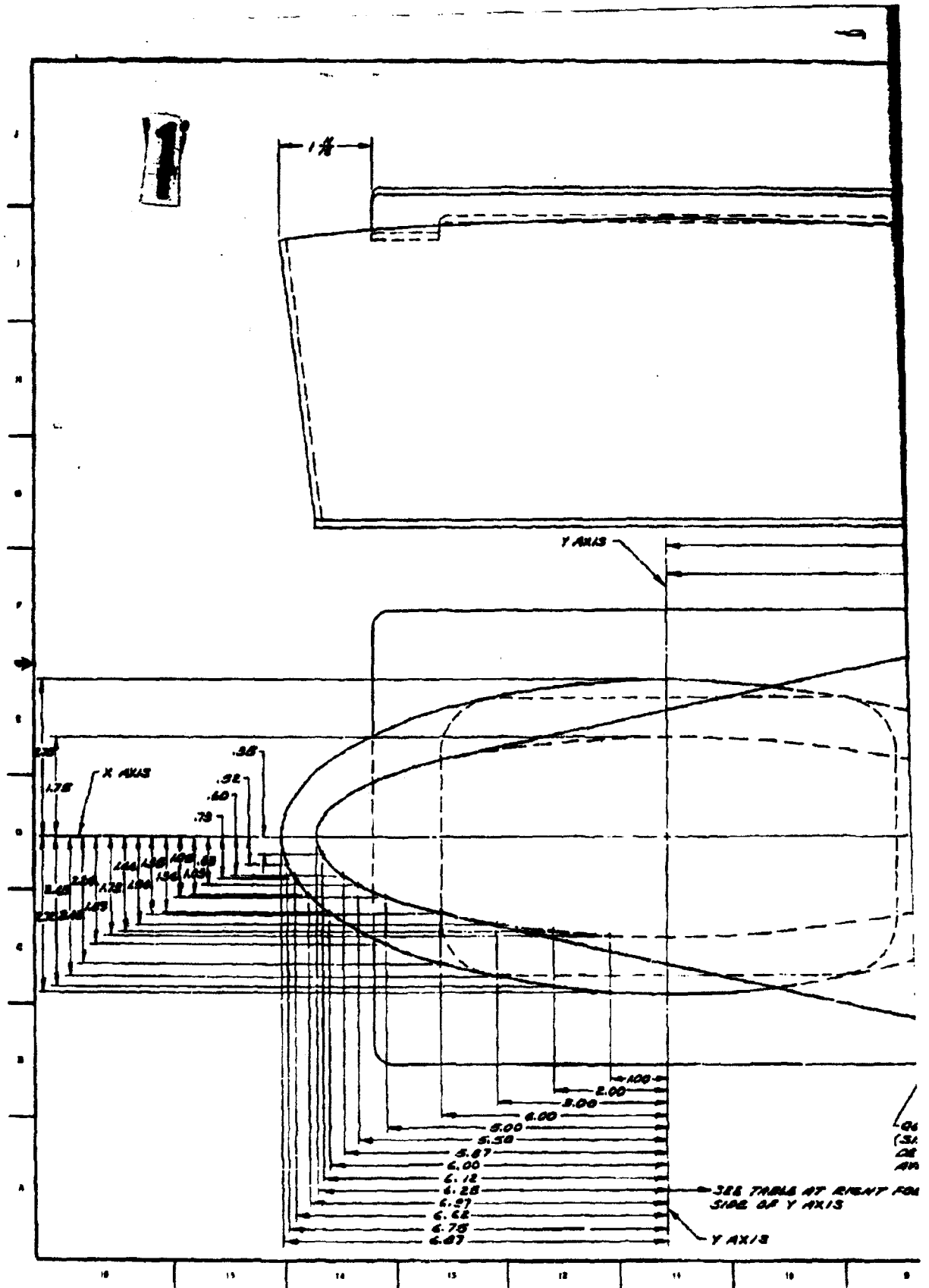
**APPENDIX A**

**LAYOUT,**

**EJECTION TUBE SHROUD**

A-1

Page determined to be Unclassified  
Reviewed Chief, RDD, WHS  
IAW EO 13526, Section 3.5  
Date: 26 APR 2013





**APPENDIX B**  
**CONTROL BOX**

B-1

Page determined to be Unclassified  
Reviewed Chief, RDD, WHS  
IAW EO 13526, Section 3.5  
Date: 26 APR 2013





#6

Page determined to be Unclassified  
Reviewed Chief, RDD, WHS  
IAW EO 13526, Section 3.5  
Date: 19 JUL 2013

~~AS- 332406~~

~~SECURITY REMARKING REQUIREMENTS~~

~~DOD 5200.1-R, DEC 78~~

~~REVIEW ON 28 AUG 82~~

Office of the Secretary of Defense <sup>5 USC sec 552</sup>  
Chief, RDD, ESD, WHS <sup>and</sup>  
Date: 19 Jul 2013 Authority: EO 13526  
Declassify:  Deny in Full: \_\_\_\_\_  
Declassify in Part: \_\_\_\_\_  
Reason: \_\_\_\_\_  
MDR: 12-M-3149

R-2  
12-M-3149



~~CONFIDENTIAL~~

AD 332 405

*Reproduced  
by the*

ARMED SERVICES TECHNICAL INFORMATION AGENCY  
ARLINGTON HALL STATION  
ARLINGTON 12, VIRGINIA



DECLASSIFIED IN FULL  
Authority: EO 13526  
Chief, Records & Declass Div, WHS  
Date: JUL 19 2013

~~CONFIDENTIAL~~

NOTICE: When government or other drawings, specifications or other data are used for any purpose other than in connection with a definitely related government procurement operation, the U. S. Government thereby incurs no responsibility, nor any obligation whatsoever; and the fact that the Government may have formulated, furnished, or in any way supplied the said drawings, specifications, or other data is not to be regarded by implication or otherwise as in any manner licensing the holder or any other person or corporation, or conveying any rights or permission to manufacture, use or sell any patented invention that may in any way be related thereto.

Page determined to be Unclassified  
Reviewed Chief, RDD, WHS  
IAW EO 13526, Section 3.5  
Date: JUL 19 2013

NOTICE:

~~THIS DOCUMENT CONTAINS INFORMATION  
AFFECTING THE NATIONAL DEFENSE OF  
THE UNITED STATES WITHIN THE MEAN-  
ING OF THE ESPIONAGE LAWS, TITLE 18,  
U.S.C., SECTIONS 793 and 794. THE  
TRANSMISSION OR THE REVELATION OF  
ITS CONTENTS IN ANY MANNER TO AN  
UNAUTHORIZED PERSON IS PROHIBITED  
BY LAW.~~

Page determined to be Unclassified  
Reviewed Chief, RDD, WHS  
IAW EO 13526, Section 3.5  
Date: JUL 19 2013

**332 405**

Page determined to be Unclassified  
Reviewed Chief, RDD, WHS  
IAW EO 13526, Section 3.5  
Date: JUL 19 2019



**THE GENERAL MILLS ELECTRONICS GROUP**



~~CONFIDENTIAL~~

This document consists of 198 pages,  
and is number 6 of 45 copies,  
series A and the following \_\_\_\_\_  
attachments.

**EIGHTH QUARTERLY  
PROGRESS REPORT  
ON  
DISSEMINATION OF SOLID  
AND LIQUID BW AGENTS  
(Unclassified Title)**

~~\_\_\_\_\_~~  
~~\_\_\_\_\_~~  
~~\_\_\_\_\_~~  
~~\_\_\_\_\_~~

For Period March 4, 1962 - June 4, 1962  
Contract No. DA-18-064-CML-2745

DECLASSIFIED IN FULL  
Authority: EO 13526  
Chief, Records & Declass Div, WHS  
Date: JUL 19 2013

Prepared for:

U. S. Army Biological Laboratories  
Fort Detrick, Maryland

Submitted by: G. R. Whitnah  
G. R. Whitnah  
Project Manager

Report No: 2322  
Project No: 82408  
Date: August 22, 1962

Approved by: S. P. Jones  
S. P. Jones, Director  
Aerospace Research

~~UPGRADED AT 10 YEAR INTER-  
VALS: AUTOMATICALLY  
DECLASSIFIED. DOD DIR 5200-10~~

Engineering and Research  
2003 East Hennepin Avenue  
Minneapolis 13, Minnesota

OCT 31 1962  
PSIA A

~~CONFIDENTIAL~~

Classified Reports

Page determined to be Unclassified  
Reviewed Chief, RDB, WHS  
IAW EO 13526, Section 3.5  
Date: JUL 19 2013

This document contains information that is  
not to be disseminated outside the  
organization. It is the property of the  
Department of Defense and is to be controlled  
and distributed in accordance with the  
Department of Defense Information Security  
Program (DIPSI) and the Department of  
Defense Information Security Manual (DODISMAN).  
Unauthorized disclosure of this information  
is prohibited.

This document contains information affecting  
the national defense of the United States  
within the meaning of the Espionage Laws,  
Title 18, United States Code, Sections 793  
and 794, and the transmission or revelation  
of its contents in any manner to an unauthorized  
person is prohibited by law.

ASTIA AVAILABILITY NOTICE

Qualified users may obtain copies of  
this document from ASTIA.

DOWNGRADED AS 25 YEAR  
DATE 10/10/2013

(This document was prepared manually  
and is not to be disseminated outside the  
organization. It is the property of the  
Department of Defense and is to be controlled  
and distributed in accordance with the  
Department of Defense Information Security  
Program (DIPSI) and the Department of  
Defense Information Security Manual (DODISMAN).  
Unauthorized disclosure of this information  
is prohibited.)

## FOREWORD

Staff members of the Research and Engineering Departments who have participated in directing and performing this work include Messrs. S. P. Jones, Jr., G. Whitnah, M. Sandgren, A. Anderson, V. W. Greene, R. Lindquist, J. McGillicuddy, J. Upton, W. L. Torgeson, S. Steinberg, P. Stroom, G. Morfitt, I. Hall, G. Beck, J. Walters, A. T. Bauman, T. Petersen, D. Harrington, R. Ackroyd, B. Schmidt, G. Lunde, R. Dahlberg, A. Kydd, E. Knutson, J. Unge, D. Stender, H. Kuhlman, O. Fackler, G. Granley, R. Hosking, and Miss M. Johnson.

Page determined to be Unclassified  
Reviewed Chief, RDD, WHS  
IAW EO 13526, Section 3.5  
Date: JUL 19 2013

~~CONFIDENTIAL~~

DECLASSIFIED IN FULL  
Authority: EO 13526  
Chief, Records & Declass Div, WHS  
Date:

JUL 19 2013

## ABSTRACT

This Eighth Quarterly Progress Report covers the work accomplished during the last reporting period on research and development related to the dissemination of BW agents.

The progress in theoretical and experimental studies of the mechanics of dry powders is reported. This work continues to produce basic information which is being applied in the design and development of an airborne disseminator.

Operation of the aerophilometer, with aerosols of dry powders, for the purpose of studying experimental techniques and determining operating parameters is discussed. This preliminary work is essential to carrying out the program on stability properties of aerosols.

Data on the effects of compaction and additives on the viability of Sm powder are presented.

The tests at Fort Detrick using the GMI-3 fixture and wind tunnel to generate aerosols in the 40-foot test sphere are described.

Results with the full-scale experimental equipment for feeding and metering compacted dry powders are reported.

The preliminary design of an airborne dry BW agent disseminating store is presented and described.

Successful flight tests of the liquid BW agent disseminating store on an A4D-1 airplane are discussed.

~~CONFIDENTIAL~~



~~CONFIDENTIAL~~

DECLASSIFIED IN FULL  
Authority: EO 13526  
Chief, Records & Declass Div, WHS  
Date:

JUL 19 2013

TABLE OF CONTENTS

Section	Title	Page
1.	INTRODUCTION	1-1
2.	THEORETICAL AND EXPERIMENTAL STUDIES OF THE MECHANICS OF DRY POWDERS	2-1
2.1	Compaction Experiments with Particulate Media	2-1
2.1.1	Piston-Cylinder Compaction Experiments	2-1
2.1.2	Hydrostatic Compaction Experiments	2-7
2.2	Powder Shear Strength Studies by the Triaxial Test Technique	2-11
2.2.1	Sample Preparation	2-11
2.2.2	Theoretical Density Variation	2-15
2.2.3	Test Procedure and Typical Test Results	2-16
2.3	Bulk Tensile Strength of Compressed Powders	2-24
2.4	Frictional Forces Between Powders and Plated Metal Surfaces	2-25
2.5	Bulk Density of Compressed Powders	2-31
2.5.1	Apparatus and Technique	2-35
2.5.2	Discussion of Data	2-35
2.6	Shear Strength of Powders by Sliding Disk Method	2-42
2.7	Future Areas for Study on the Characteristics of Powders	2-44
2.7.1	Bulk Density of Loose Powders	2-44
2.7.2	Measurement of Static Charge of Particulate Materials	2-50
2.7.3	Particle Size and Shape	2-50
2.7.4	Total Surface Area	2-50
3.	AEROSOL STUDIES	3-1
3.1	Terminology and Definitions	3-2
3.2	A Theoretical Calculation for Non-Agglomerative Aerosol Decay	3-4
3.3	Experimental Work	3-11
3.4	Conclusions and Plans for Immediate Future Work	3-21
4.	VIABILITY STUDIES	4-1
4.1	Presence of <u>B<sub>g</sub></u> Contaminants in <u>S<sub>m</sub></u> Powder	4-1
4.2	Effect of Agitation and Compaction on Viability of <u>S<sub>m</sub></u> Powder	4-1

~~CONFIDENTIAL~~

~~CONFIDENTIAL~~

DECLASSIFIED IN FULL  
Authority: EO 13526  
Chief, Records & Decls. Div, WHS  
Date:

JUL 19 2013

TABLE OF CONTENTS (Continued)

Section	Title	Page
5.	DISSEMINATION AND DEAGGLOMERATION STUDIES	5-1
5.1	General	5-1
5.2	Evaluation of the General Mills, Inc. Test Fixture Disseminating Dry <u>Sm</u> and Dried <u>Pasteurella Tularensis</u>	5-1
5.3	<u>Preliminary Results</u>	5-4
5.3.1	<u>Sm Tests</u>	5-4
5.3.2	<u>P. Tularensis Tests</u>	5-5
6.	CONTINUATION OF EXPERIMENTS WITH THE FULL- SCALE FEEDER FOR COMPACTED DRY AGENT SIMULANT MATERIALS	6-1
6.1	Introduction	6-1
6.2	Equipment Modifications	6-1
6.3	Test Results	6-2
6.4	Plans for Future Work	6-14
7.	DESIGN STUDIES ON A DRY AGENT DISSEMINATING STORE	7-1
7.1	General Arrangement for the Airborne Dry Agent Disseminating Store	7-1
7.1.1	Ram Air Turbine Generator	7-3
7.1.2	Dry Nitrogen System	7-4
7.1.3	Center Section	7-9
7.1.4	Rotary Actuator Assembly	7-11
7.2	Fabrication of the Second Experimental Unit	7-13
7.3	Fabrication of Loading Equipment for Use With the Second Experimental Unit	7-14
7.3.1	Hydraulic Press	7-15
7.3.2	Loading Fixture	
8.	TESTING OF THE LIQUID AGENT DISSEMINATING STORE	8-1
8.1	Structural Testing at Fletcher Aviation Company, El Monte, California	8-1
8.2	Flight Tests of Liquid Agent Disseminating Store at NATC, Patuxent River, Maryland	8-3

v  
~~CONFIDENTIAL~~

**CONFIDENTIAL**

DECLASSIFIED IN FULL  
Authority: EO 13526  
Chief, Records & Declass Div, WHS  
Date:

JUL 19 2013

**TABLE OF CONTENTS (Continued)**

<u>Section</u>	<u>Title</u>	<u>Page</u>
9.	SUMMARY AND CONCLUSIONS	9-1
10.	REFERENCES	10-1
APPENDIX A.	ASSEMBLY DRAWING - LIQUID AGENT DISSEMINATOR	A-1
APPENDIX B.	FLETCHER AVIATION COMPANY REPORT NO. 43.286 - QUALIFICATION TESTS, GENERAL MILLS TANK ASSEMBLY	B-1

**CONFIDENTIAL**

~~CONFIDENTIAL~~

DECLASSIFIED IN FULL  
Authority: EO 13526  
Chief, Records & Declass Div, WHS  
Date: JUL 19 2013

LIST OF ILLUSTRATIONS

Figure	Title	Page
2.1	Improved Piston-Cylinder Compaction Apparatus	2-2
2.2	Compaction Stress as a Function of Powder Specific Volume	2-4
2.3	Shape of Elastic Recovery versus Stress Curve	2-5
2.4	Compaction Behavior of Talc and Powdered Milk	2-6
2.5	Hydrostatic Compaction Apparatus	2-8
2.6	Density Variation in a Compacted Powder Column (Talc)	2-13
2.7	Test Specimen Density Distribution (Talc)	2-14
2.8	Triaxial Test Apparatus	2-17
2.9	Typical Load-Strain Curves for Talc ( $\rho = 0.65$ ; $p = 1$ psi)	2-18
2.10	Test Specimens Illustrating Shear Failure ( $\rho = 0.65$ ; $p = 1$ psi)	2-19
2.11	Load-Strain Curves for Talc ( $\rho = 0.65$ ; $p = 6$ psi)	2-21
2.12	Test Specimens After High Pressure Tests ( $\rho = 0.65$ ; $p = 6$ psi)	2-22
2.13	Triaxial Test Results for Talc at a Mean Sample Density, $\rho = 0.65$	2-23
2.14	Bulk Tensile Strength for Zinc Cadmium Sulfide as a Function of Distance "L" from Compressive Force at Various Total Plug Lengths, $L_t$ (Compressive Load A)	2-26
2.15	Bulk Tensile Strength for Zinc Cadmium Sulfide as a Function of Distance "L" from Compressive Force at Various Total Plug Lengths, $L_t$ (Compressive Load B)	2-27
2.16	Bulk Tensile Strength for Zinc Cadmium Sulfide as a Function of Distance "L" from Compressive Force at Various Total Plug Lengths, $L_t$ (Compressive Load C)	2-28

~~CONFIDENTIAL~~

~~CONFIDENTIAL~~

DECLASSIFIED IN FULL  
Authority: EO 13526  
Chief, Records & Declass Div, WHS  
Date:

JUL 19 2013

LIST OF ILLUSTRATIONS (Continued)

<u>Figure</u>	<u>Title</u>	<u>Page</u>
2. 17	Bulk Tensile Strength at $L_0$ for Zinc Cadmium Sulfide as a Function of Total Plug Length $L_t$ at Various Compressive Loads	2-29
2. 18	Bulk Density Apparatus Assembled for Filling	2-32
2. 19	Bulk Density Apparatus Assembled for Compaction of Bulk Powders	2-33
2. 20	Bulk Density Apparatus Assembled for Cutting of Individual Powder Segments	2-34
2. 21	Bulk Density of Precompacted Saccharin as a Function of Distance from Piston at Various Compressive Loads	2-36
2. 22	Bulk Density of Saccharin as a Function of Distance from Piston (a comparison of virgin saccharin with previously compacted saccharin)	2-38
2. 23	Bulk Density of Virgin Saccharin as a Function of Distance from Piston at Various Compressive Loads	2-39
2. 24	Variation in Bulk Density of Compacted Saccharin along the Radius of the Plug	2-40
2. 25	Variation in Bulk Density of Uncompacted Saccharin along the Radius of the Plug	2-41
2. 26	Sketch of a Probable Filling Mechanism in the Bulk Density Apparatus	2-43
2. 27	Variation of Shear Strength with Compressive Stress at 2 Percent Relative Humidity	2-45
2. 28	Variation of Shear Strength with Compressive Stress at 15 Percent Relative Humidity	2-46
2. 29	Variation of Shear Strength with Compressive Stress at 32 Percent Relative Humidity	2-47
2. 30	Variation of Shear Strength with Compressive Stress at 46 Percent Relative Humidity.	2-48

~~CONFIDENTIAL~~

**CONFIDENTIAL**

DECLASSIFIED IN FULL  
Authority: EO 13526  
Chief, Records & Declass Div, WHS  
Date: JUL 19 2013

LIST OF ILLUSTRATIONS (Continued)

Figure	Title	Page
2.31	Variation of Shear Strength with Compressive Stress at 69 Percent Relative Humidity	2-49
3.1	Theoretical Curves for Turbulent Settling	3-10
3.2	Experimental Curve for Light Scattering from Talc Aerosol	3-13
3.3	Experimental Curve for Scattered Light from Saccharin Aerosol	3-14
3.4	Experimental Curve for Scattered Light from Powdered Milk Aerosol	3-15
3.5	Experimental Curves for Light Scattered from K-Ferric Oxide Aerosol	3-18
5.1	Wind Tunnel Test Section Located in Glove Box of Spherical Test Chamber at Fort Detrick	5-3
6.1	Aerating Ring Installed in Center Section of Full-Scale Experimental Feeder	6-3
6.2	Arrangement for Collecting Powder without Direct Connection between Collection Drum and Discharge Tube	6-4
6.3	Air-to-Powder Ratios for Various Feeder Operating Conditions (actual test runs with talc are plotted)	6-6
6.4	Powder Discharge Rate	6-8
6.5	The Effect of Pre-Pressurizing on the Time Required to Establish Uniform Flow	6-10
6.6	Time Lag in Powder Flow	6-12
6.7	Powder Flow After Stopping Feeder Drive	6-13
7.1	Preliminary Tank Assembly	7-2
7.2	Dry Nitrogen Handling System	7-5

**CONFIDENTIAL**

~~CONFIDENTIAL~~

DECLASSIFIED IN FULL  
Authority: EO 13526  
Chief, Records & Declass Div, WHS  
Date: JUL 19 2013

LIST OF ILLUSTRATIONS (Continued)

<u>Figure</u>	<u>Title</u>	<u>Page</u>
7.3	Ratio of Nitrogen-to-Powder Flow Rates Obtained from Powder Feed Rate versus Available Nitrogen Flow Rates (Q)	7-8
7.4	Disseminator Dry Agent Test Model	7-10
8.1	GMI Liquid Agent Disseminating Store Mounted on Aero 7A Bomb Rack on A4D-1 Airplane (Side View)	8-5
8.2	GMI Liquid Agent Disseminating Store Mounted on Aero 7A Bomb Rack on A4D-1 Airplane (Front View)	8-6
8.3	GMI Liquid Agent Disseminating Store Spraying Water During Static Functional Test	8-7

x

~~CONFIDENTIAL~~

Page determined to be Unclassified  
Reviewed Chief, RDD, WHS  
IAW EO 13526, Section 3.5  
Date:

JUL 19 2013

**EIGHTH QUARTERLY PROGRESS REPORT  
ON  
DISSEMINATION OF SOLID AND LIQUID BW AGENTS**

**1. INTRODUCTION**

This is the Eighth Quarterly Progress Report on work accomplished on Contract Number DA-18-064-CML-2745. Under this contract, General Mills, Inc. is conducting a comprehensive research and development program on the dissemination of solid and liquid BW agents.

With the completion of the developmental model of the liquid agent disseminating store in April of this reporting period, the emphasis of work shifted almost entirely to areas relating to finely-divided solids. Consequently most of this report deals with progress in these areas. However, Section 8 does present some of the results of laboratory and field testing of the liquid agent disseminator.

On 22, 23 May, General Mills, Inc. was host to the Third Dissemination Coordination Meeting which was attended by representatives from Fort Detrick, Army Chemical Center, Chemical Corps Research and Development Command, Aerojet-General Corporation, Cornell Aeronautical Laboratories and General Mills, Inc. Some of the material covered in this progress report was also presented at this meeting.



## 2. THEORETICAL AND EXPERIMENTAL STUDIES OF THE MECHANICS OF DRY POWDERS

Studies of the mechanical properties and behavior of dry powders were continued during the period covered by this report. Experimental results on the compaction characteristics, shear strength, and tensile strength of various powders are presented.

### 2.1 Compaction Experiments with Particulate Media

Results obtained with an improved version of the piston-cylinder compaction apparatus and a hydrostatic compaction device are discussed and compared in the following sections.

#### 2.1.1 Piston-Cylinder Compaction Experiments

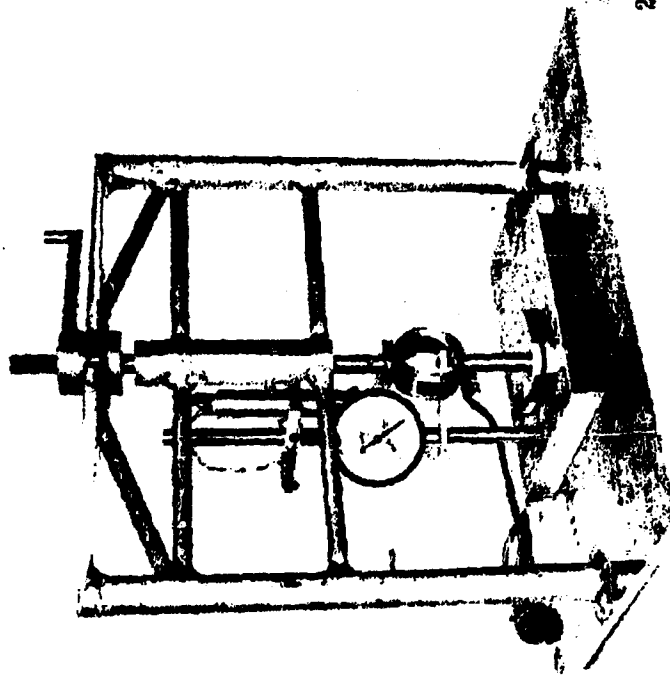
As pointed out in the last quarterly report (seventh), the initial piston-cylinder apparatus used in the compaction experiments was subject to several limitations and, consequently, an improved piece of apparatus (Figure 2.1\*) was fabricated. Powder is placed in the cylinder at the base of the apparatus. A surface stress is applied to the powder by a piston which is lowered by turning the crank at the top of the apparatus. An aluminum ring equipped with strain gages is used to measure the stress. Large-scale movement of the piston is measured by means of a Starrett dial indicator, and small-scale movement is measured by means of a sensitive differential transformer. The output of the strain gages and the differential transformer is recorded on a Sanborn recorder.

Using the experimental results obtained from the tests employing this piece of apparatus, a relationship between the bulk density of the powder and the stress necessary to obtain this density was obtained. These results

\* This is the same apparatus shown in the referenced report.

Page determined to be Unclassified  
Reviewed Chief, RDD, WHS  
IAW EO 13526, Section 3.5  
Date:

JUL 19 2013



2708

Figure 2.1 Improved Piston-Cylinder Compression Apparatus

Date: JUL 19 2013

are plotted in Figure 2. 2 for several different powders. The stress levels for these tests were considerably higher than those of earlier tests. The stress was increased monotonically during the tests.

A plot of the stress versus reciprocal density is a straight line on log-log paper which is in agreement with the previous results. An empirical formula of the form  $\sigma = k(1/\rho)^r$  can be used as a good fit to the data. The constants of this equation are given below for the powders tested:

Powder	r	k
Talc	- 6.50	$4.42 \times 10^7$
Saccharin	- 7.70	$2.21 \times 10^7$
Powdered Sugar	-11.5	$6.8 \times 10^6$
Powdered Milk	-35.9	$1.6 \times 10^9$
Cornstarch	-20.8	$1.67 \times 10^8$

At each compaction state a certain amount of energy is stored in the powder bed in the form of elastic energy as pointed out in an earlier report<sup>1</sup>. In the initial tests it was assumed that the material had linear elastic characteristics. It is now necessary to revise this assumption on the basis of more accurate measurements carried out with the improved apparatus. The general shape of the elastic recovery versus stress curve for powders such as talc, saccharin, and powdered sugar is shown in Figure 2. 3.

It is interesting to note that very little energy is recovered as the stress is reduced at high stress levels, but that most of the elastic recovery takes place at low stress levels. This implies that considerably less elastic energy is stored in the powder bed for a particular compaction state than was originally assumed.

JUL 19 2013

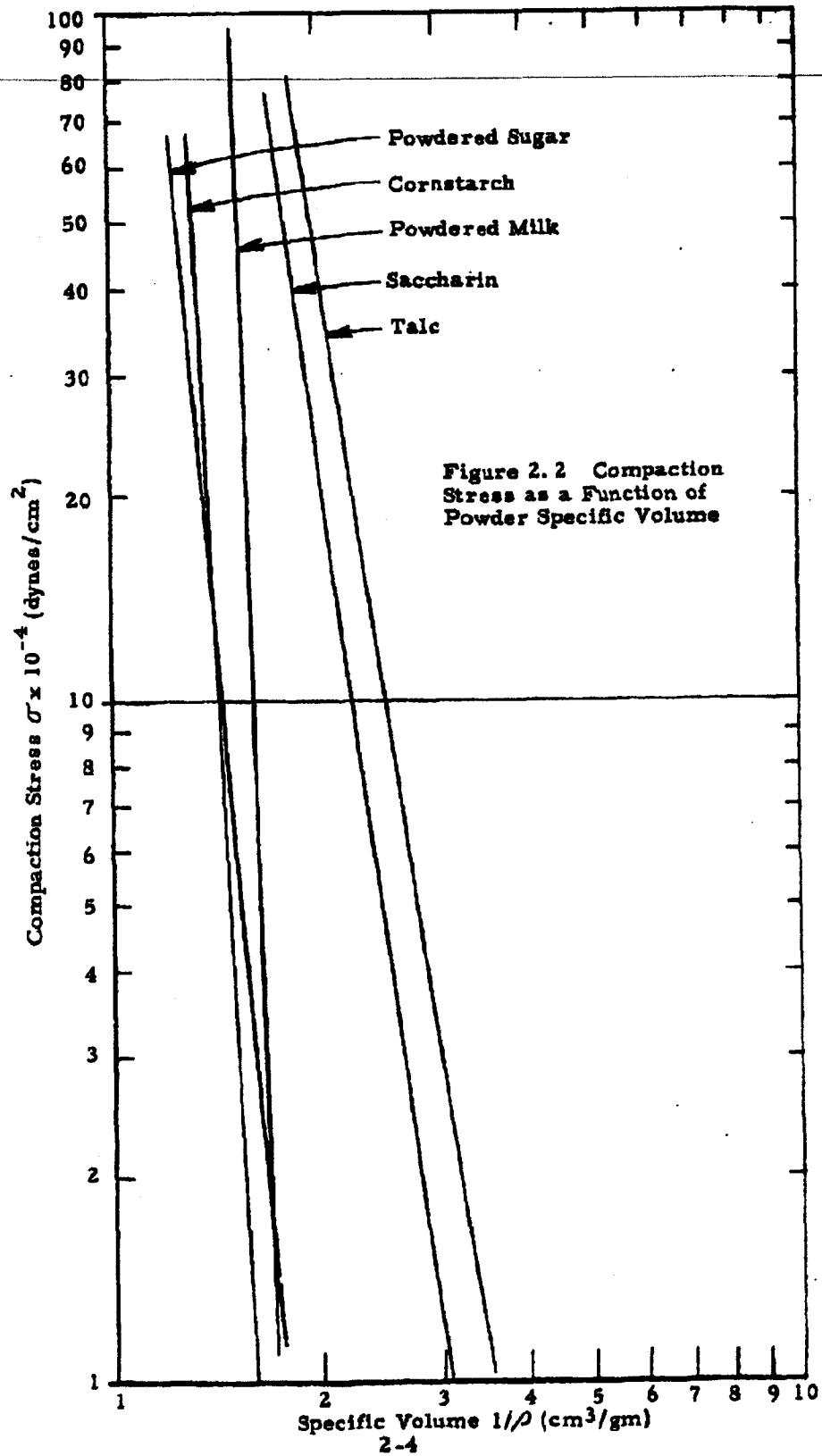


Figure 2.2 Compaction Stress as a Function of Powder Specific Volume

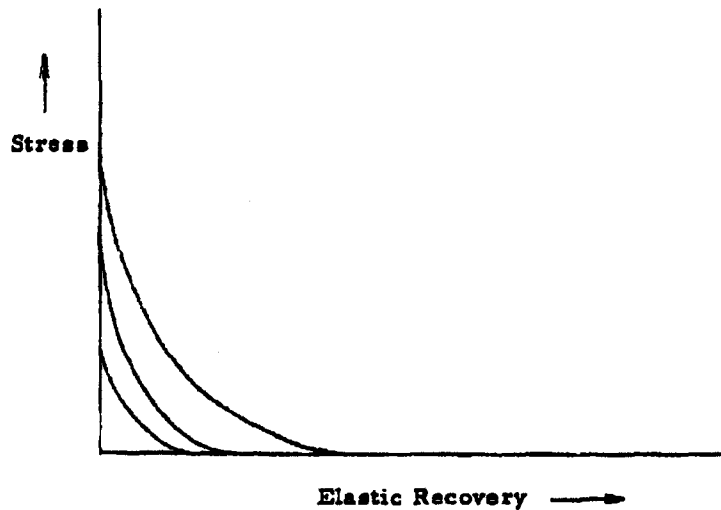


Figure 2.3 Shape of Elastic Recovery versus Stress Curve

Some difficulty was experienced in obtaining precise measurements of the elastic behavior of powder due to insufficient rigidity of the new compaction energy apparatus. At high stress levels the apparatus had a tendency to flex, making precise measurements of the elastic recovery of a powder difficult to obtain. However, the basic nature of the elastic recovery, illustrated in Figure 2.3, seems to be definitely established. In order to obtain more precise data, it will be necessary to modify the apparatus to make it more rigid.

In the process of testing the various powders it was noticed that powdered milk and cornstarch behaved in a unique manner during the compaction process. As the loading piston was gradually advanced, the stress was found to increase rapidly and then fall sharply to a lower level. In other words the powder seemed to compact in a stick-slip fashion. Figure 2.4 is a comparison of the recording traces showing the variation of stress as a function of time for talc and powdered milk as the powders were gradually compacted.

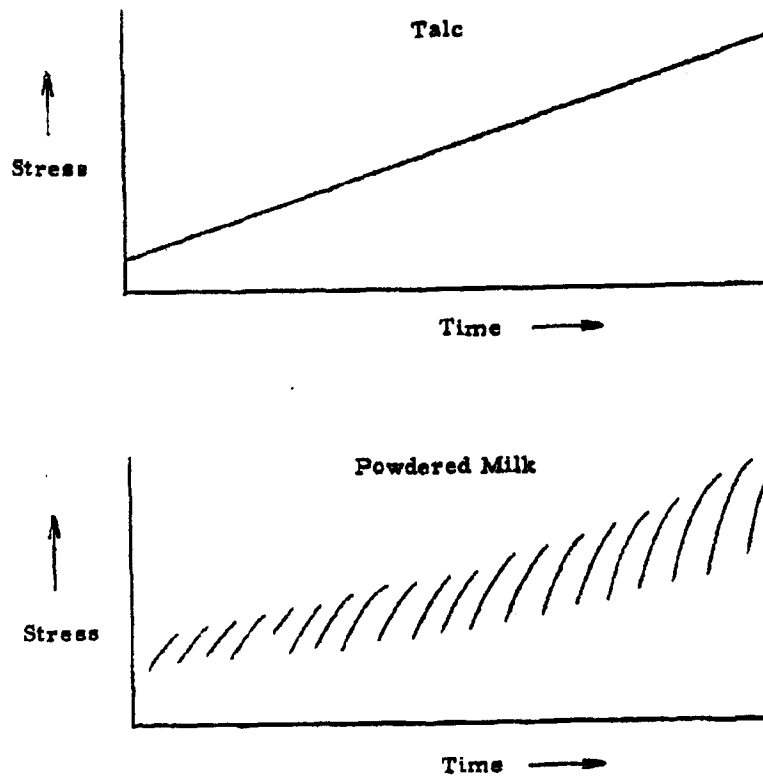


Figure 2.4 Compaction Behavior of Talc and Powdered Milk

The stick-slip phenomena observed with powdered milk and cornstarch diminishes at high stress levels. The stresses plotted in Figure 2. 2 for powdered milk and cornstarch were the values noted after the stress had fallen from the peak value. The magnitude of the stress peaks was influenced by the rate at which a force was applied. If the force was applied rapidly the peaks were quite small. This phenomenon, indicating that the rate at which surface stresses are applied may be an important factor in the compaction process, will be investigated in future tests.

An expression for the compaction energy as a function of density can be obtained from the stress-density curve (Figure 2. 2) and is of the form  $W = C\rho^n$ . However, from the previous discussion it is apparent that the stress necessary to reach a given compaction state, and hence the energy involved in the process, may depend on the path taken to reach that compaction state. For example, if a certain stress is applied and released several times in compacting a bed of powder, the energy of compaction might be different than if the stress were applied monotonically to reach the same compaction state. In those tests made to date in which the test procedure was varied, the results have not been significantly different. However, an investigation to precisely determine the effect of path on the compaction energy is planned for future work.

### 2. 1. 2 Hydrostatic Compaction Experiments

In the process of performing the piston-cylinder compaction experiments, the question arose as to how much the results depended upon the constraints and loading conditions imposed by the apparatus. In order to answer this question a hydrostatic compaction experiment was devised in which the constraints imposed by the apparatus were minimized. The apparatus is shown in Figure 2. 5.

A sample of powder was put into a polyethylene bag which was then hermetically sealed. The bag was inserted in the pressure chamber with the powder sample vented to the outside. The chamber was then filled with

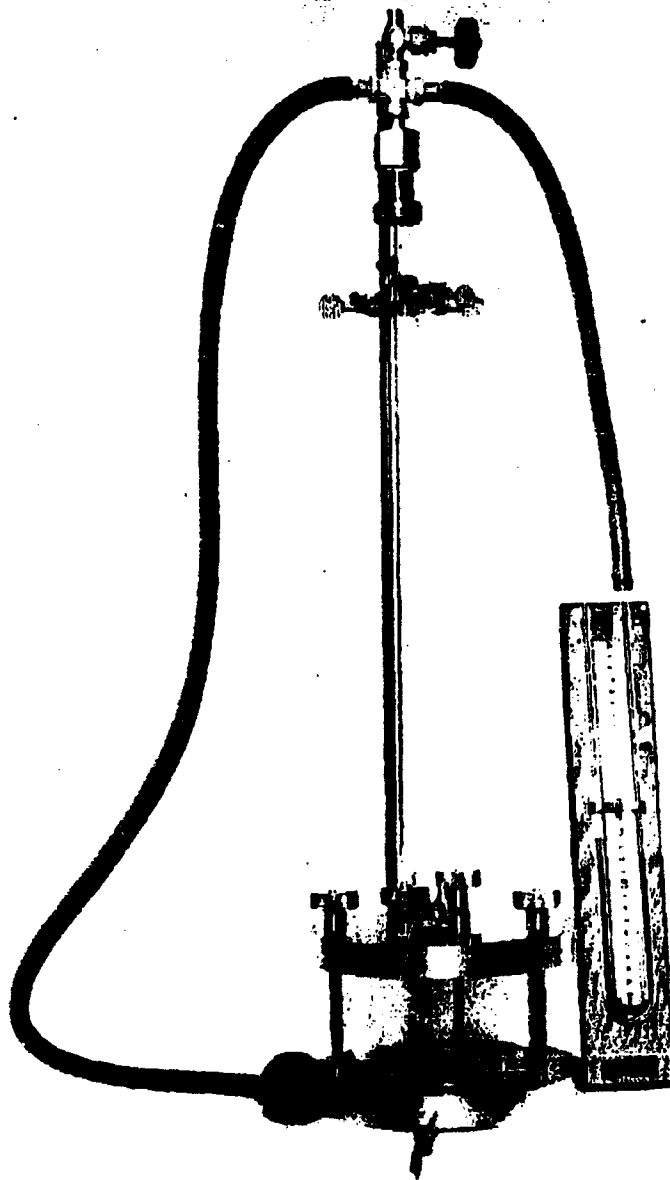


Figure 2.5 Hydrostatic Compaction Apparatus



water to a certain level in the calibrated tube used for measuring volume change. Then the pressure in the chamber was increased in small increments and the volume change was noted. It was interesting to note that considerable time was required for the system to come to equilibrium after the pressure was increased. Evidently the stress distribution in a powder bed undergoes a change during the compaction process. After the system reached a state of equilibrium, the hydrostatic pressure was released and the volume change caused by elastic recovery was noted. The shape of the elastic recovery versus stress curves was essentially the same as that shown in Figure 2.3.

From the data, a curve of stress versus the reciprocal density was plotted for the two powders tested (talc and saccharin) and a straight line on log-log paper was obtained. Thus, both the hydrostatic and piston-cylinder compaction tests yield a stress-density relationship which is described by the empirical formula:

$$\sigma = k \left( \frac{1}{\rho} \right)^r .$$

The constants for this equation for the two powders tested in the hydrostatic compaction apparatus are:

$$\text{talc: } k = 1.39 \times 10^6, r = -7.6;$$

and

$$\text{saccharin: } k = 1.95 \times 10^7, r = -6.24.$$

Values of the exponent  $r$  are in good agreement with those determined by the piston-cylinder method. The coefficient  $k$  for saccharin is also in good agreement with the results of earlier tests. However, the value of  $k$  for talc differed appreciably from that determined by the piston-cylinder method. This apparent discrepancy might be attributable to differences in

JUL 19 2013

the compaction process. At the conclusion of one of the hydrostatic experiments with talc, the stress was cycled several times. The result of this cycling caused the bulk density to increase with each succeeding cycle until a point was reached where the density did not seem to increase further. From this one can see that it is somewhat ambiguous to speak of the stress necessary to reach a certain compaction state without specifying the compaction process, at least for a powder like talc. Other powders may respond differently to the cycling process.

The hydrostatic compaction apparatus has several drawbacks, one being expansion of the chamber under pressure. This expansion necessitated calibration tests, resulting in a tare which has to be taken into account to determine the true volume change of the powder sample for various pressures. Some difficulty was also experienced in determining the exact volume of the powder sample, a value needed in order to calculate the bulk density. Nevertheless, it is believed that the results are meaningful and are in accord with our previous results.

In view of the fact that results from hydrostatic compaction tests seem to be in close agreement with the results obtained from the piston-cylinder tests, future compaction tests will be conducted utilizing the piston-cylinder arrangement because of the relative ease of conducting these tests.

The powders that have been investigated thus far seem to fall into two major groups. In the first group are powders such as powdered milk and cornstarch which display the above-mentioned stick-slip phenomena and compact very little even when subjected to high compressive stresses. In the second group are powders such as talc and saccharin which compact much more smoothly.

Future tests will be oriented to determine what factors are affecting the compacting characteristics of a powder. Factors such as the history of the powder, particle shape and size, electrostatic charge, and moisture content would seem to be among the most important factors to consider.

## 2.2 Powder Shear Strength Studies by the Triaxial Test Technique

Preliminary tests with the triaxial test apparatus described in a previous report<sup>2</sup> revealed deficiencies in the originally proposed test technique, which produced excessive scatter of the experimental data. To improve the reliability and reproducibility of the triaxial shear test, modifications were made in the method of sample preparation and in the means used to apply stresses to the test sample.

### 2.2.1 Sample Preparation

For incompactable materials, which exhibit dilatancy in shear, the preparation of homogeneous test samples is a straightforward matter. However, in the case of compactable materials, it does not appear to be possible to produce truly homogeneous, isotropic samples. Since the test sample has the form of a right circular cylinder, it is natural to compact the sample to the degree necessary for handling by employing a piston-cylinder apparatus. However, from prior study of the compaction process in a piston-cylinder device<sup>3</sup>, it is known that the compressive stresses applied to the powder decay exponentially with distance from the loading piston. Furthermore, the ratio of radial to axial stress appears to lie in the range 0.3 to 0.5 for most materials. From this it may be inferred that the density of the sample will decrease with distance from the loading piston and that the powder will compact non-isotropically. It is clear that the latter effect is not objectionable since it is typical of the behavior of a compactable powder. Non-uniform sample density is undesirable, however, since the shear strength of a powder will, in general, depend on the density.

Several techniques have been used to prepare samples for the triaxial shear test. The technique originally used was based upon the observation that a region of nearly constant density exists in a column of powder which

Date: JUL 19 2013

has been compacted in a vertically disposed piston-cylinder device. It was thought that a test sample obtained from this region would be ideal for tri-axial testing. However, it was found to be impossible to obtain a sufficient degree of compaction in this region to permit the minimal handling required for preparation of the test specimen. Thus, it became evident that a density gradient in the sample would have to be accepted for samples compacted in the piston-cylinder device. A series of experiments were carried out to determine the density variation along a powder column for loads sufficiently high to cause compaction to occur along the entire column. Typical results for talc are shown in Figure 2.6 for two applied loads. It is apparent that the density gradient is essentially constant over the length of the compacted powder column.

This result led to a modification of our sample preparation technique whereby a known mass of powder is compacted to a preselected final length, thus precisely defining the mean sample density. This technique has been found to yield improved control over sample uniformity, as judged by the reproducibility of shear test results obtained by using samples prepared in this way.

Actually, this method of preparing test specimens is very similar to the proposed technique described in the last quarterly report<sup>2</sup>. At high compaction stresses, however, it was found that external support was required for the split tube within which the powder sample is confined during compaction. Another essential change was to roughen the inner surfaces of the split tube to prevent stretching of the rubber membrane during compaction.

The variation of density with axial distance from the loading piston for the modified sample preparation technique is shown in Figure 2.7. The drop in density near the high-density end of the sample appears to be caused by elastic relaxation effects. (See Figure 2.6 also.)

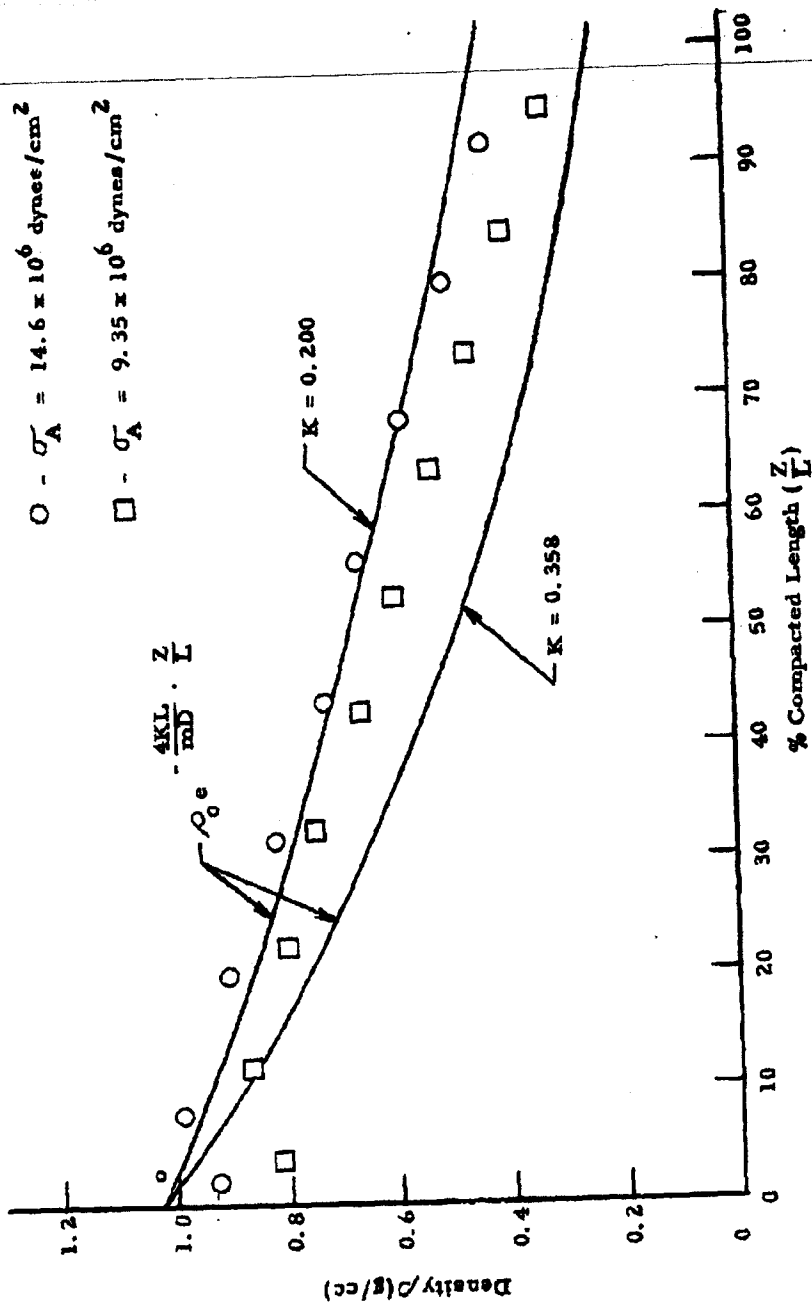


Figure 2.6 Density Variation in a Compacted Powder Column (Talc)

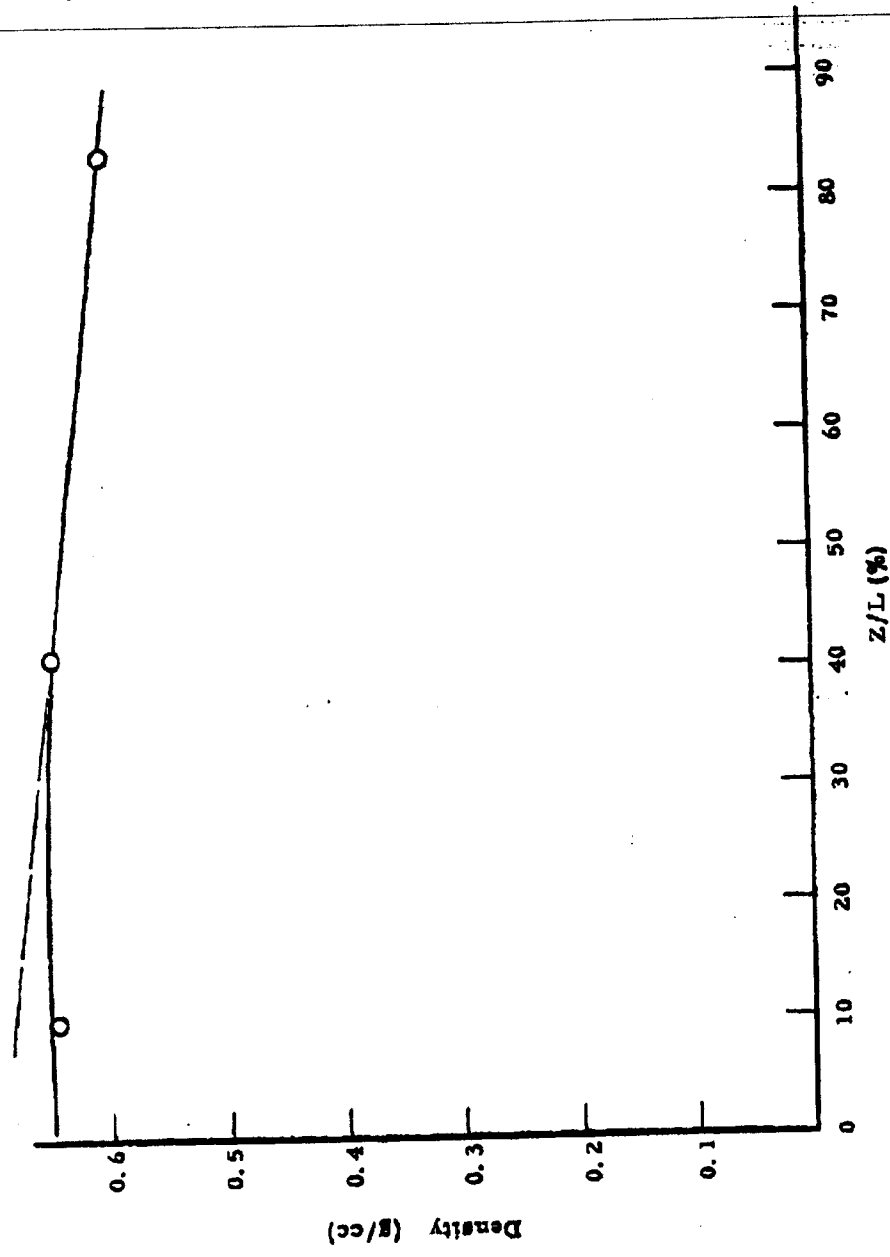


Figure 2.7 Test Specimen Density Distribution (Talc)

Page determined to be Unclassified  
 Reviewed Chief, RDD, WHS  
 IAW EO 13526, Section 3.5  
 Date: JUL 19 2013

### 2.2.2 Theoretical Density Variation

The density variation in a powder sample which has been compacted in a piston-cylinder device may be determined analytically by combining results from the piston-cylinder theory<sup>3</sup> with the empirical relationship between density and applied stress<sup>2, 3</sup>:

$$\sigma = C\rho^m \quad (2.1)$$

From the piston-cylinder theory, we have:

$$\sigma(Z) = \sigma(0) e^{-\frac{4KL}{D} \left(\frac{Z}{L}\right)} \quad (2.2)$$

Eliminating the axial stress  $\sigma(Z)$ , Equations (2.1) and (2.2) lead to the relationship:

$$\rho(Z) = \rho(0) e^{-\frac{4KL}{mD} \left(\frac{Z}{L}\right)} \quad (2.3)$$

In this equation the wall resistance parameter  $K$  depends on the shear angle  $\phi$  of the powder and the wall friction angle  $\theta$ , while  $m$  is an empirically determined powder parameter.

Computed values of  $\rho(Z)$  from Equation (2.3) are shown in Figure 2.6 for  $\sigma(0) = 14.6 \times 10^6$  dynes/cm<sup>2</sup>,  $m = 5.46$  (Reference 3) and for two values of the wall resistance parameter:  $K = 0.358$  and  $K = 0.200$ . The value  $K = 0.358$  (corresponding to the maximum theoretical value of the wall resistance parameter<sup>2</sup>) yields the maximum theoretical rate of decay of density. The smaller value of  $K = 0.200$  was obtained from Figure 2.1.3, Reference 2, for the experimental values:  $\phi = 40^\circ$  (calc),  $\theta = 35^\circ$  (calc on aluminum). The theoretical curve for  $K = 0.200$  agrees rather well with the experimental curve for  $\sigma(0) = 14.6 \times 10^6$  dynes/cm<sup>2</sup>.

### 2.2.3 Test Procedure and Typical Test Results

During initial work with the triaxial test technique, it was found that the stress at which yielding of the sample occurred was difficult to define. The principal reason for this appears to be the constraining effect of the rubber membrane, which prevents a sudden collapse of the powder when shear failure occurs. In an effort to increase the precision of the test and to secure a better indication of sample failure, the triaxial test apparatus was adapted for use with an available Instron test machine. Through use of the Instron, the following desirable features were achieved: 1) accurate force measurement through use of a sensitive load cell, 2) precise and adjustable rate of strain, and 3) accurate recording of applied axial load as a function of sample strain.

Figure 2.8 shows the triaxial test apparatus mounted in the Instron test machine. The test procedure is as follows:

- 1) The test specimen, prepared in the manner described above, is installed in the pressure chamber of the test apparatus and properly centered (locating pins are provided for this purpose in the sample end fittings).
- 2) The test chamber is sealed and pressured to the desired chamber pressure.
- 3) After checking to make sure there is no leakage to the sample interior, the machine is started and run until shear failure occurs.

In these tests, shear failure is evidenced by a sudden change in the slope of the load-strain curve. This is illustrated by Figure 2.9 showing a series of load-strain curves for a mean sample density of 0.650 g/cc and a chamber pressure of 1 psi. The appearance of the test specimens after failure is shown in Figure 2.10. It is apparent from the photograph that failure occurs by the formation of cracks in the compacted powder, although the rubber membrane prevents collapse of the sample.



JUL 19 2013



Figure 2.8 Triaxial Test Apparatus

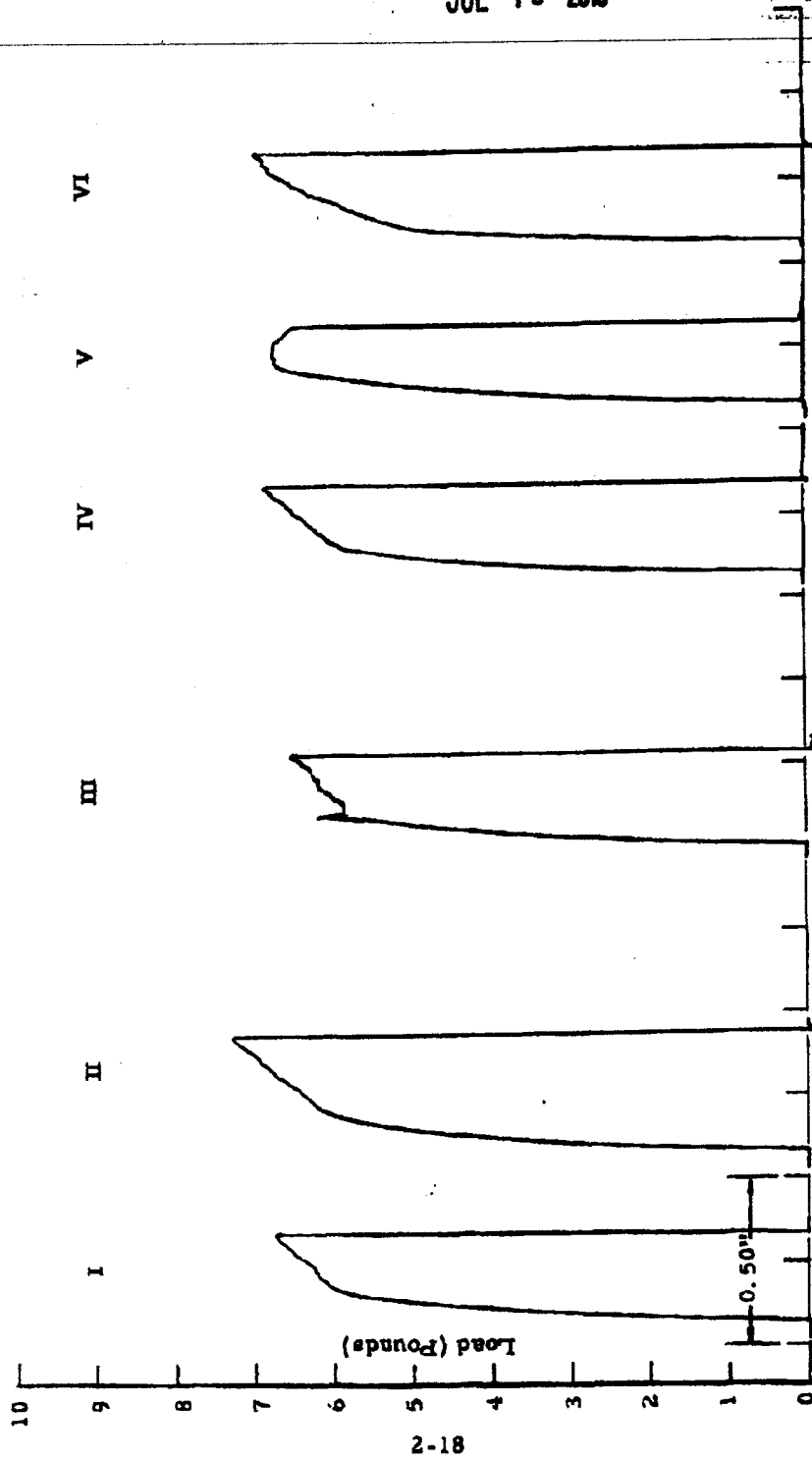


Figure 2.9 Typical Load-Strain Curves for Talc ( $\rho = 0.65$ ;  $P = 1$  psi)

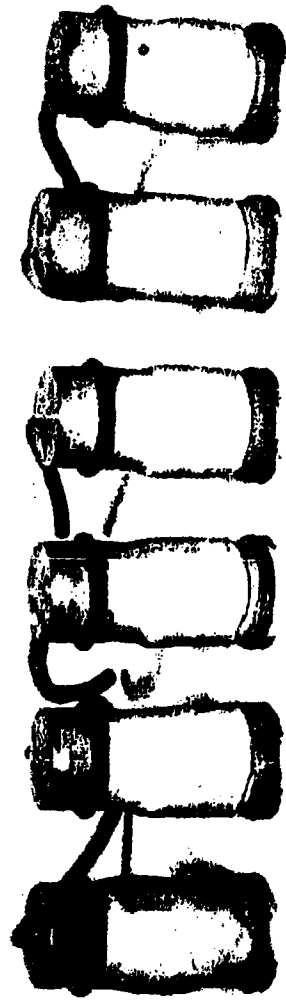


Figure 2.10 Test Specimens Illustrating Shear Failure ( $\phi = 0.65$ ;  $p = 1$  psi)

Date: JUL 19 2013

The results shown in Figures 2.9 and 2.10 are typical of runs carried out for pressures in the range 0 to 2 psi. At higher pressures, however, it was impossible to detect sample failure since the sample merely bulged outward without a break in the load-strain curve. This behavior is illustrated by Figures 2.11 and 2.12. It is suspected that this behavior may be caused by additional compaction during the test since the applied loads are comparable to the loads used in preparing the sample. Of course, the effect of the membrane in this case is to stabilize the powder as bulging occurs. There is little reason to doubt that the high loads shown in Figure 2.11 for a chamber pressure of 6 psi are attainable only because of the stabilizing effect of the membrane.

The yield locus established from tests carried out at pressures of 0, 0.24, 0.50 and 2.0 psi is plotted in Figure 2.13. The slope of the yield locus is about 35 degrees, which agrees quite well with the shear angle determined from sliding disk measurements<sup>2</sup> ( $\theta = 40$  degrees).

The experiments and test results reported herein have been primarily concerned with the development of techniques for application of the triaxial test to compactable powders. Additional tests are planned for future work in which powders other than talc will be tested and the effects of such factors as moisture content will be investigated.

Our studies of the triaxial test have disclosed several limitations of this method of conducting shear tests. The most serious limitation is that the test technique is restricted to samples which have been compacted to high densities; also, no means have been found to produce samples of uniform density. Another serious problem is the constraining effect of the rubber membrane, which prevents a "natural" shear failure. It should be noted, however, that the membrane is not required for tests at zero pressure. A further difficulty with the triaxial technique is the difficulty of defining the shear locus for small compressive stresses. Thus the strength of the powder in pure shear cannot be obtained directly from this type of test.

JUL 19 2013

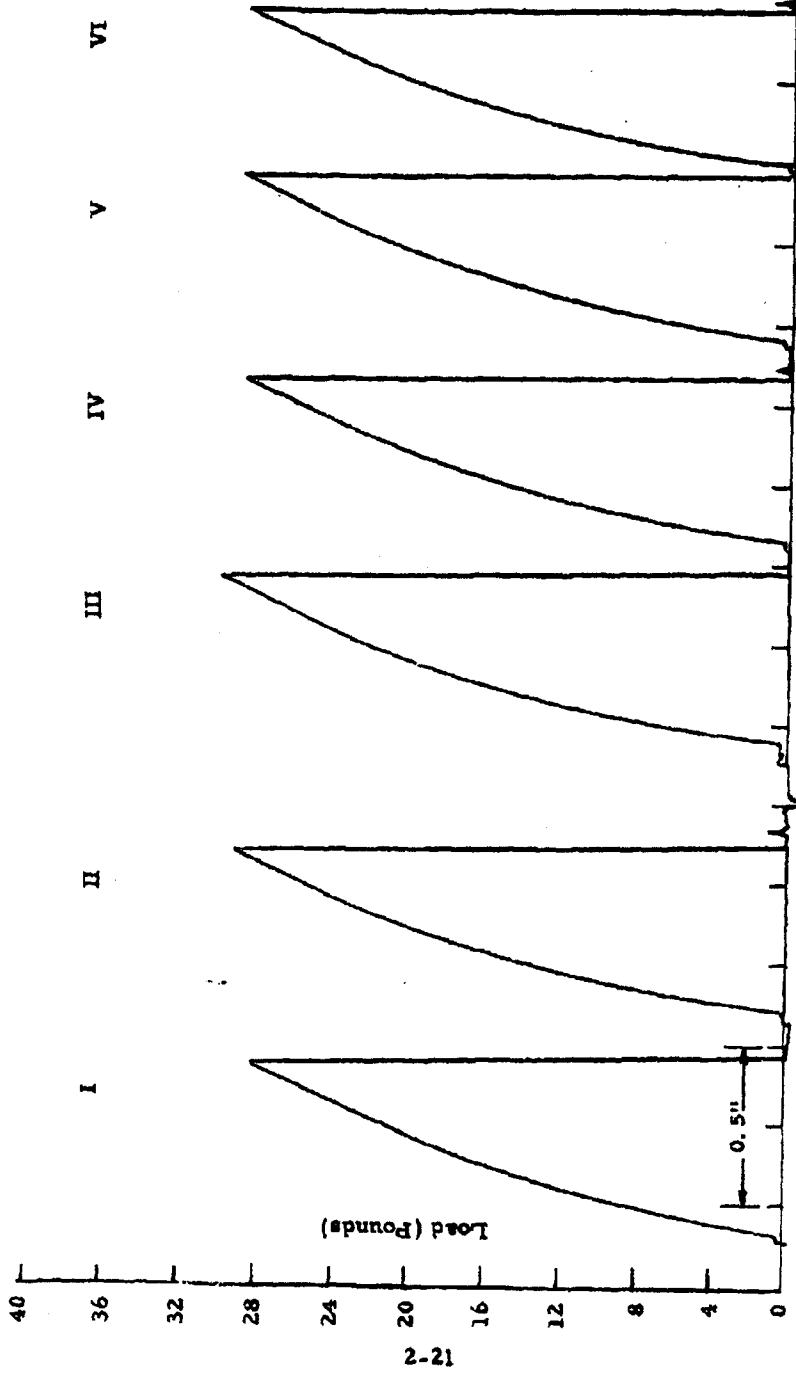


Figure 2.11 Load-Strain Curves for Talc ( $\rho = 0.65$ ;  $p = 6$  psi)

JUL 19 2019



2832

Figure 2.12 Test Specimens After High-Pressure Tests ( $\phi = 0.65$ ;  $p = 6$  psi)

2-23

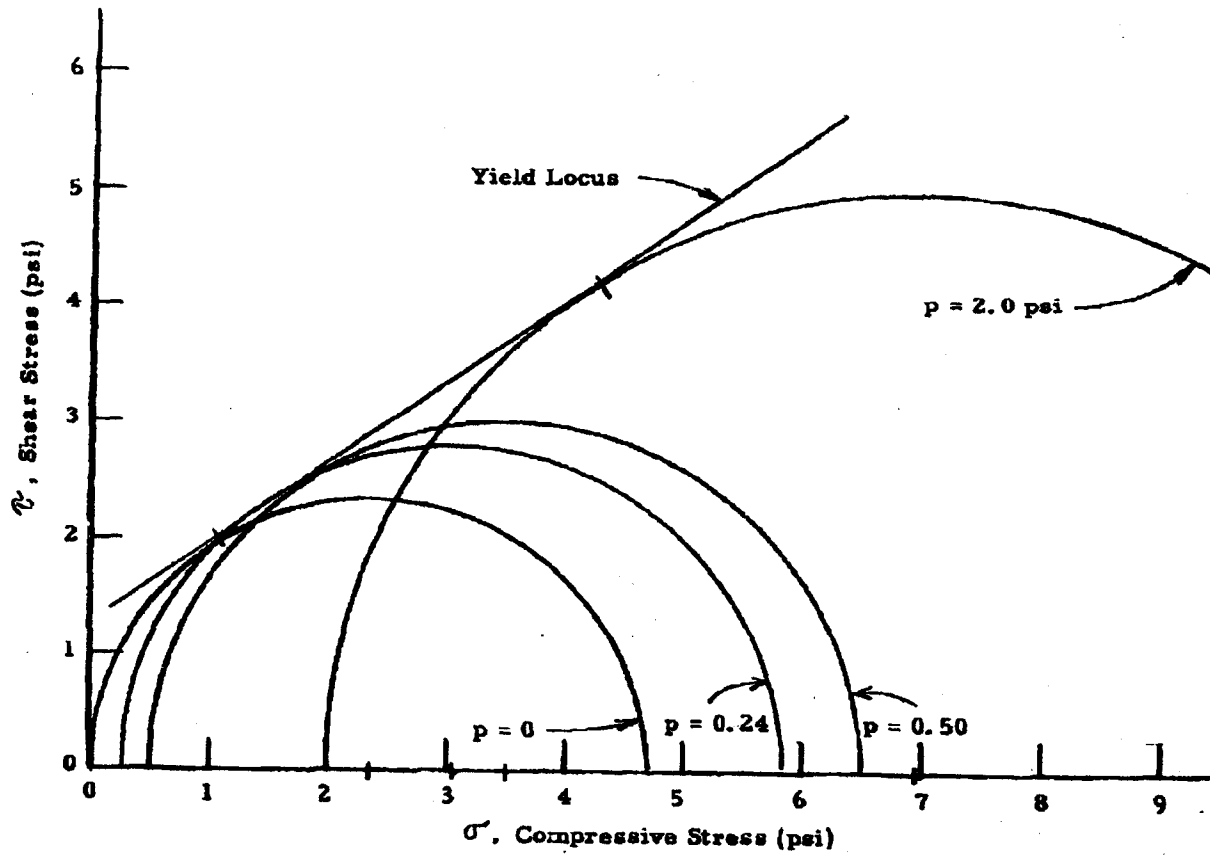


Figure 2.13 Triaxial Test Results for Talc at a Mean Sample Density,  $\rho = 0.65$

Page determined to be Unclassified  
Reviewed Chief, RDD, WHS  
IAW EO 13526, Section 3.6  
Date: JUL 19 2013

Date: JUL 19 2013

In spite of these deficiencies, the triaxial test provides much worthwhile information on the behavior of dry powders. Also, it is quite possible that some of the apparent limitations of the triaxial test can be removed through improvements in test techniques.

### 2.3 Bulk Tensile Strength of Compressed Powders

A new apparatus and technique for the measurement of bulk tensile strength of compressed powders was described in the last quarterly report<sup>2</sup>. Work in recent months has been devoted to an exhaustive study to refine techniques and to establish the most accurate and efficient method for a comparative measure of bulk tensile strength of various bulk powders.

According to theory<sup>2, 4</sup> the bulk tensile strength of a compressed powder is an exponential function of the distance from the compressive piston to the fracture plane:

$$\sigma = \sigma_0 e^{-kL} \quad (2.4)$$

where:

$\sigma$  = bulk tensile strength of a column of compressed powder at distance  $L$  from the piston

$\sigma_0$  = bulk tensile strength of the compressed powder immediately below the piston

$k$  = constant

$L$  = distance from piston to fracture plane.

The method employed involves the compression of bulk powder in a vertical segmented column. The design of the apparatus permits the powder to be fractured by a measured vertical force at several points down the column, permitting the bulk tensile strength to be measured as a function of: 1) bulk density, 2) distance from compressive force application to fracture plane, and 3) total column length.



Although the bulk tensile strength does vary with length of time of application of compressive load, our recent studies have led to the adoption of a 1-1/2 hour compression time. It is believed that this time period not only is adequate for good reproducibility but also allows the operator to make four efficient runs per working day. In addition to the adoption of 1-1/2 hours as a standard time of compression, three compressive loads ( $5.55 \times 10^5$ ,  $7.88 \times 10^5$ , and  $10.59 \times 10^5$  dynes/cm<sup>2</sup>) have been adopted as standard. Although this test as described does not exhaustively cover all possibilities, we believe that it does offer an acceptable method for a comparative study of a physical phenomena which is at best difficult to measure.

Figures 2.14, 2.15 and 2.16 represent typical plots for zinc cadmium sulfide at three compressive loads. The individual plots were made by the method of least squares. Individual points were omitted to afford greater ease of visual comparison of the various plots.

These data show as indicated in the last quarterly report<sup>2</sup> that  $\sigma_0$  is in fact a function of total plug length  $L_t$ . Figure 2.17 shows the relationship between  $\sigma_0$  and  $L_t$  at the three compressive loads. Since the values obtained for  $\sigma_0$  are for a fairly narrow range of values for  $L_t$  we must extend this range before making valid generalizations. The individual plots are however interestingly close to being linear.

In the near future we plan to obtain more data on the variation of  $\sigma_0$  with  $L_t$  for zinc cadmium sulfide and to utilize our standard method to study the bulk tensile strength characteristics of such powders as talc, powdered sugar, powdered milk, saccharin, and cornstarch.

#### 2.4 Frictional Forces Between Powders and Plated Metal Surfaces

A modification of a test method previously described<sup>5</sup> was used to study the frictional force between talc and samples of cold rolled steel that had been electroplated with nickel, cadmium or zinc. In principle the method

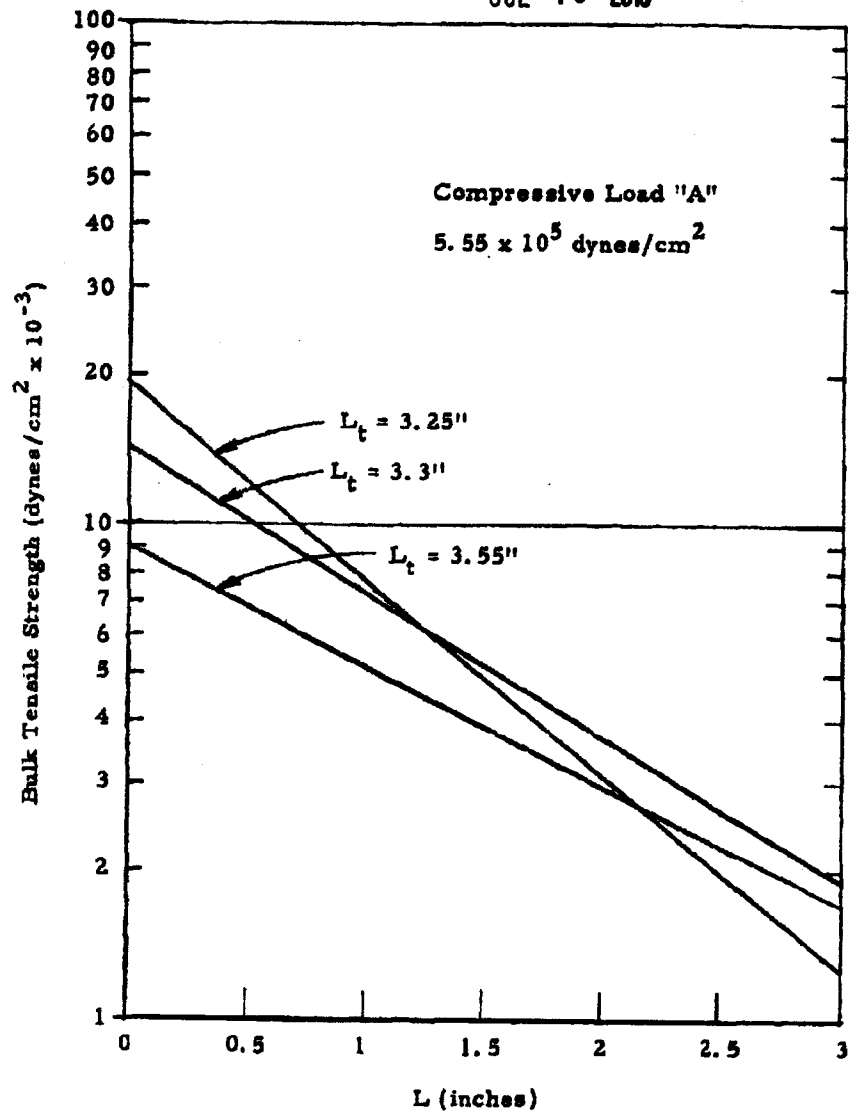


Figure 2.14 Bulk Tensile Strength for Zinc Cadmium Sulfide as a Function of Distance "L" from Compressive Force at Various Total Plug Lengths,  $L_t$

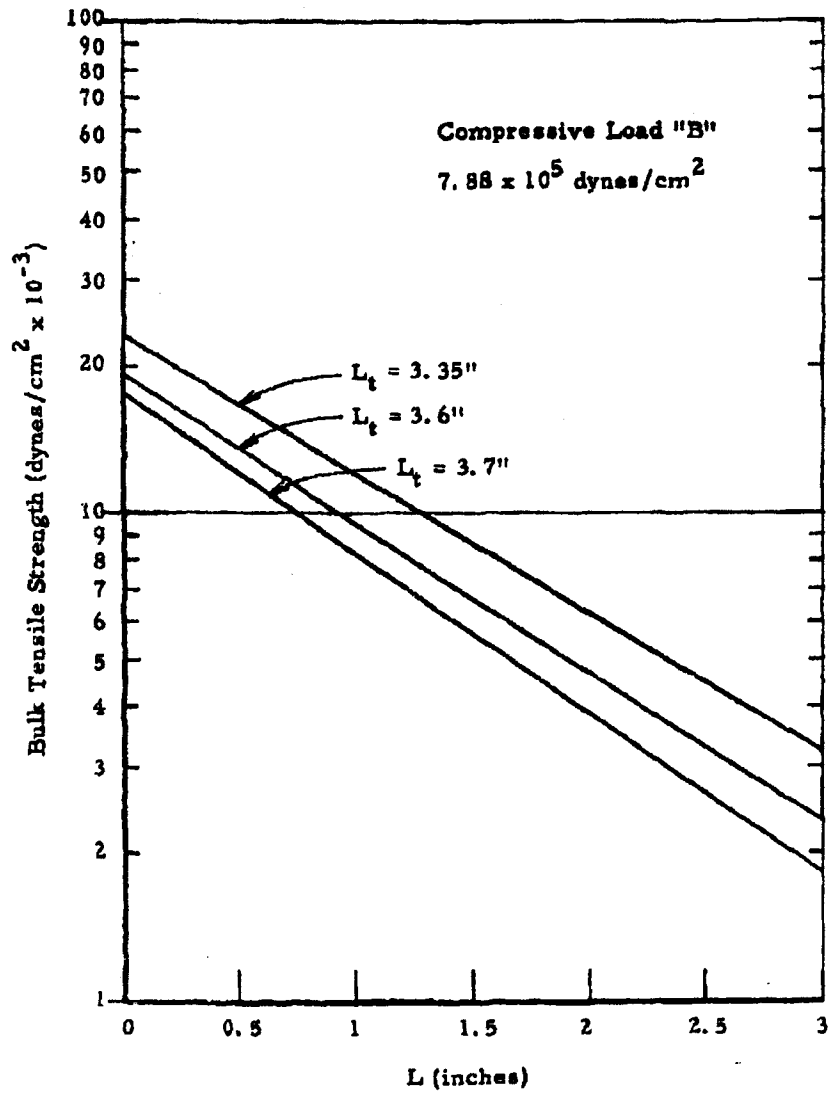


Figure 2.15 Bulk Tensile Strength for Zinc Cadmium Sulfide as a Function of Distance "L" from Compressive Force at Various Total Plug Lengths,  $L_t$

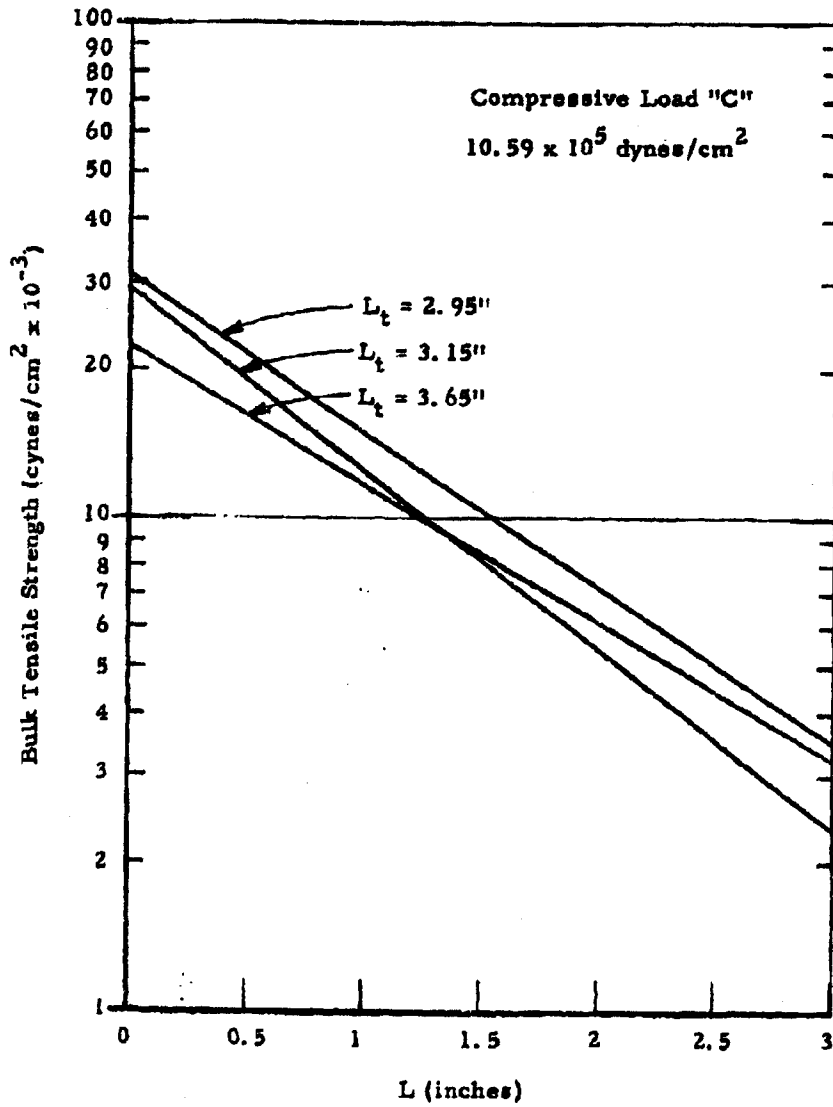


Figure 2.16 Bulk Tensile Strength for Zinc Cadmium Sulfide as a Function of Distance "L" from Compressive Force at Various Total Plug Lengths,  $L_t$

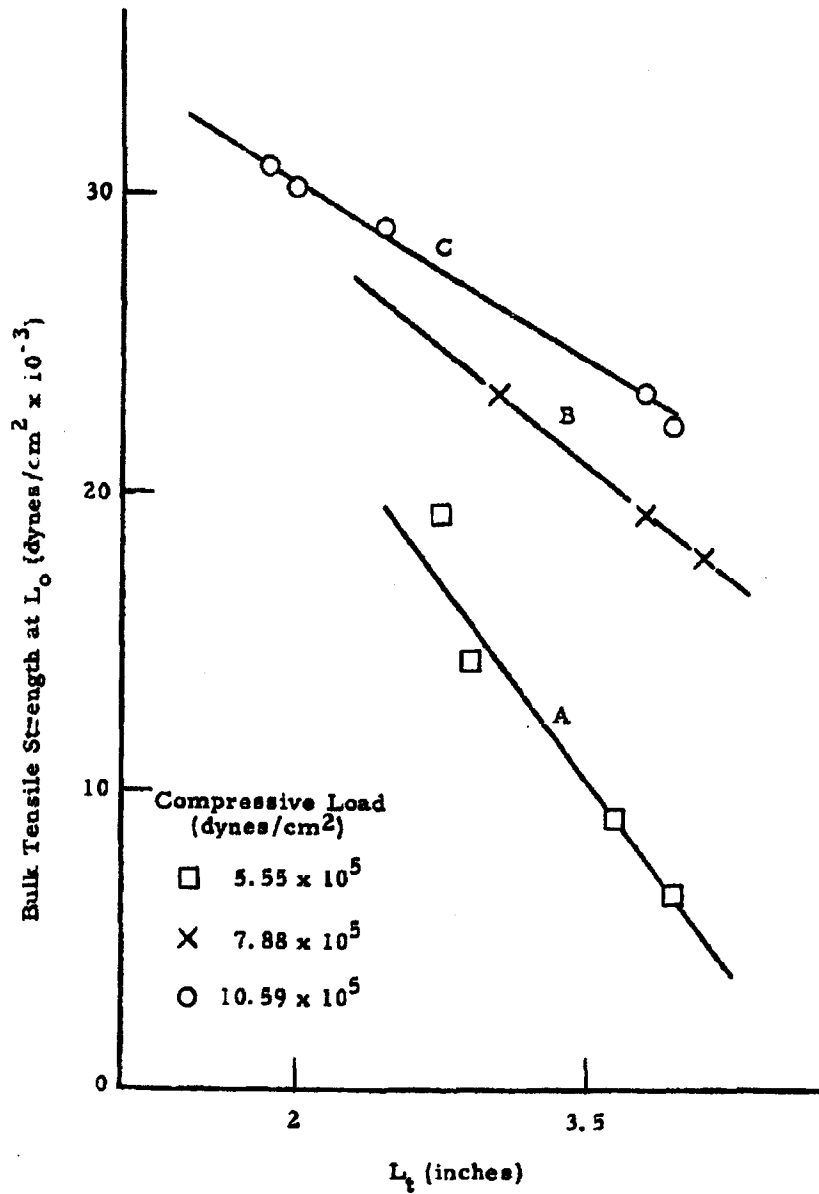


Figure 2.17 Bulk Tensile Strength at  $L_o$  for Zinc Cadmium Sulfide as a Function of Total Plug Length  $L_t$  at Various Compressive Loads

involves placing a powder on the metal surface and tilting the plate of metal slowly until the powder begins to slide. The slide angle is related to the coefficient of friction as follows:

$$\mu = \tan \theta$$

where:

$\mu$  = coefficient of friction

$\theta$  = angle of slide

To make a comprehensive study of this problem, the following three methods were used to place the talc upon the metal surface:

- 1) An aluminum ring of 3.5 cm ID was placed on a mechanical vibrator and filled with 1.5 g talc. After a standard 3-minute vibration to assure uniformity of packing, the sample was transferred to the plated metal surface on the tilting table.
- 2) The talc was processed identically to Part (1) except that prior to transfer to the plated surface, the talc was compacted into a plug by the use of a piston assembly with a 9-pound compressive load.
- 3) The talc was processed identically to Part (1) except that after transfer to the plated surface, the talc was compacted directly onto the plated surface by the 9-pound piston assembly.

The tests were performed in a controlled humidity environment (15 to 18 percent relative humidity). Upon analysis of these data, Method (3) was chosen for further study at a higher (> 60% RH) humidity. The following is a tabulation of values of angle of slide; each value reported is an average of at least five independent runs:

	Method	Plating			Unplated
		Nickel	Cadmium	Zinc	
Low Humidity (15-18% RH)	1	40.7	42.6	42.5	43.0
	2	36.0	37.6	37.8	39.7
	3	41.9	43.4	43.7	44.2
High Humidity (> 60% RH)	3	39.8	40.0	42.9	42.0

Although Method (2) tends to yield a lower slide angle than Methods (1) or (3), the data indicate only very minor differences in the frictional forces between the talc powder and the various electroplated surfaces. It is interesting to note, however, that regardless of the method utilized, the nickel plate gave consistently the lowest coefficient of friction and the unplated material consistently the highest. It should also be mentioned that in every case when the metal surface had been exposed for some time prior to test, the first test performed on each surface gave values 50 to 75 percent higher than the average. These values were not included in the tabulated data presented. Apparently either surface moisture and/or surface oxidation changes the frictional characteristics of the surface in a way that is removed by making a single test run.

Since there seems to be no obvious advantage in electroplating the metal surfaces of a disseminator in order to reduce frictional forces, no future work in this area is currently planned.

#### 2.5 Bulk Density of Compressed Powders

To expand our knowledge of the variation of bulk density in a column of compressed powder, a new apparatus (as shown in Figures 2.18, 2.19 and 2.20) has been designed and perfected. Saccharin has been used as a test powder in our initial series of experiments with the new apparatus.

JUL 19 2013



Figure 2.18 Bulk Density Apparatus Assembled for Filling



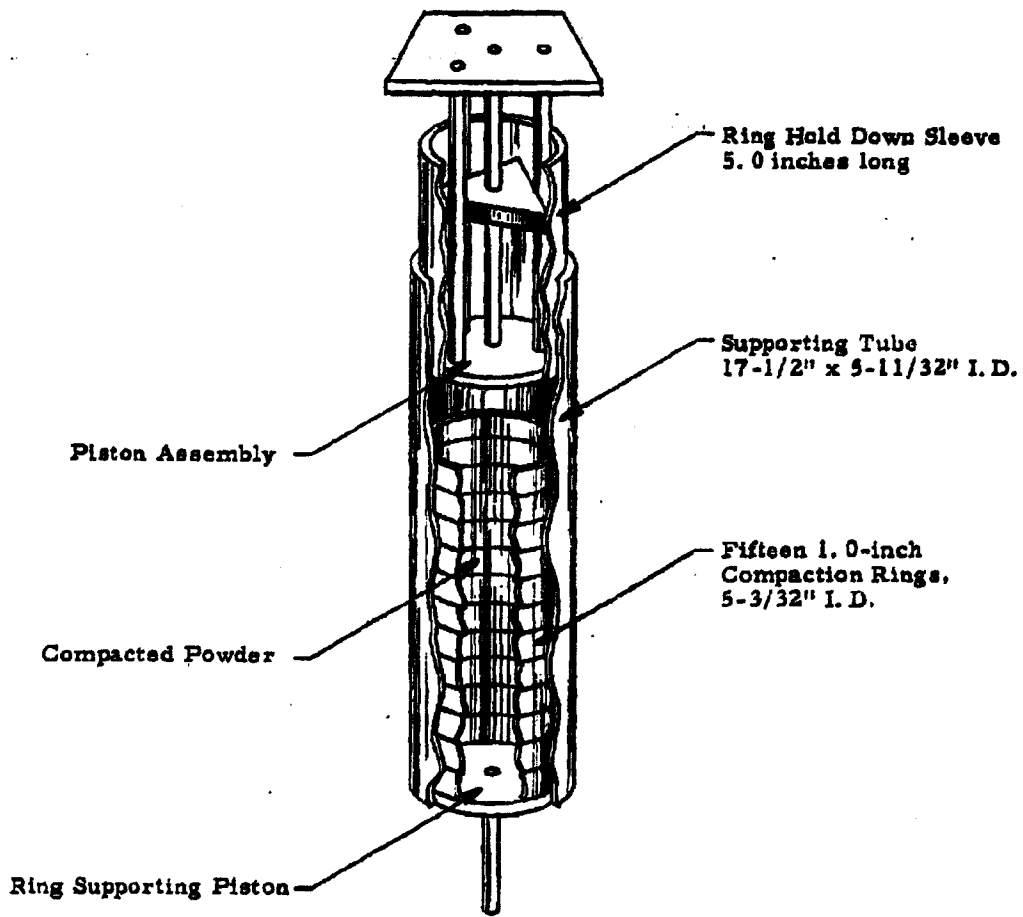


Figure 2.19 Bulk Density Apparatus Assembled for Compaction of Bulk Powders

JUL 19 2019

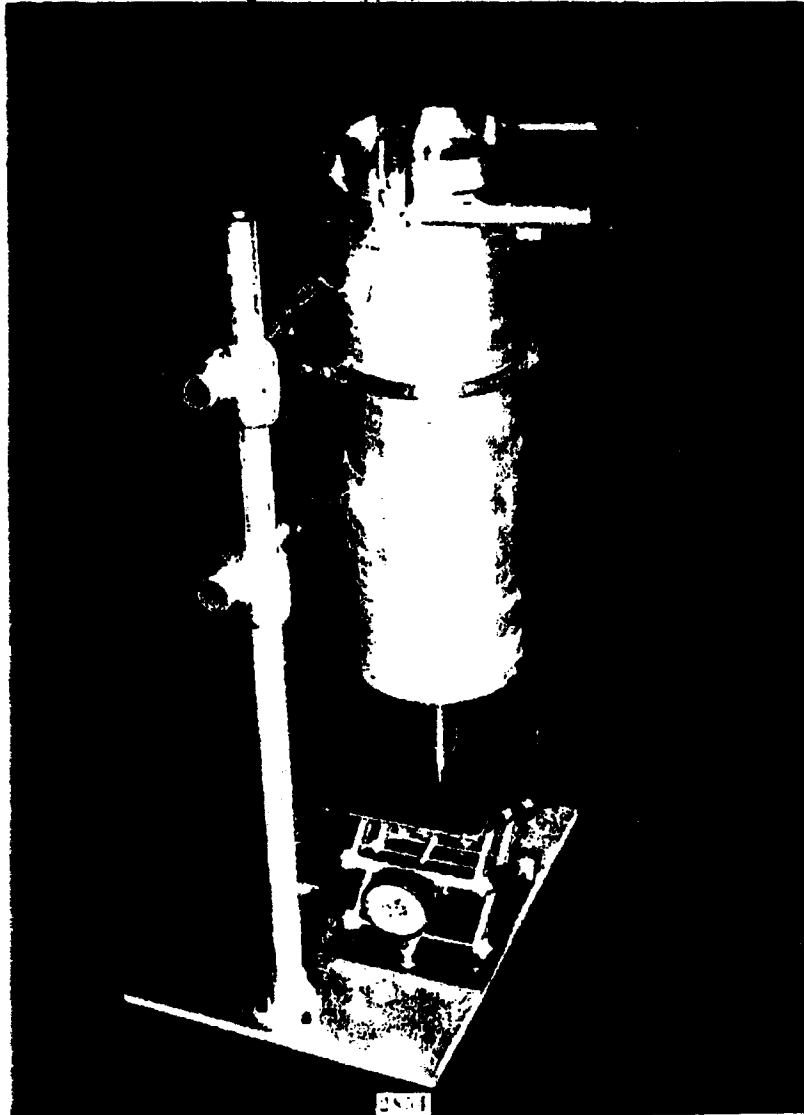


Figure 2. 20 Bulk Density Apparatus Assembled for Cutting of Individual Powder Segments

### 2.5.1 Apparatus and Technique

In an actual experiment the apparatus is assembled as shown in Figure 2.19 but with the sifter replacing the piston assembly (Figure 2.18). The sifter with a mechanical, doorbell-type vibrator attached is intended to aid in uniformity of packing. The powder under study is added slowly through the sifter until the column is filled to the top of the hold-down sleeve. The piston assembly is then put into place and the compressive load applied for a period of one-half hour. The compressive load, piston assembly, and hold-down sleeve are then removed. The entire column of compacted powder plus the compaction rings are moved upward with the aid of the lab jack and ring-supporting piston, exposing the metal rings containing the compacted powder.

The cutting assembly (Figure 2.20) is then used to divide the plug of compressed powder into one-inch segments of known cross-sectional area. By obtaining the weight of these segments, the bulk density may then be calculated. To obtain further information a "cookie-cutter" assembly is then used to remove a circular portion, representing one-half the cross-sectional area, from the center of each segment. This affords a gross comparison of the variation of bulk density along the radius of the column of compressed powder.

### 2.5.2 Discussion of Data

The results of an experiment using saccharin as a test powder are shown in Figure 2.21. The compactions were made in order of increasing compressive load with no special attention given to using virgin saccharin each time. To study the possible effects of previous history of compaction of a powder upon bulk density, the 18.9 lb test was repeated using the saccharin that had been used throughout several tests including the 354 lb compression.

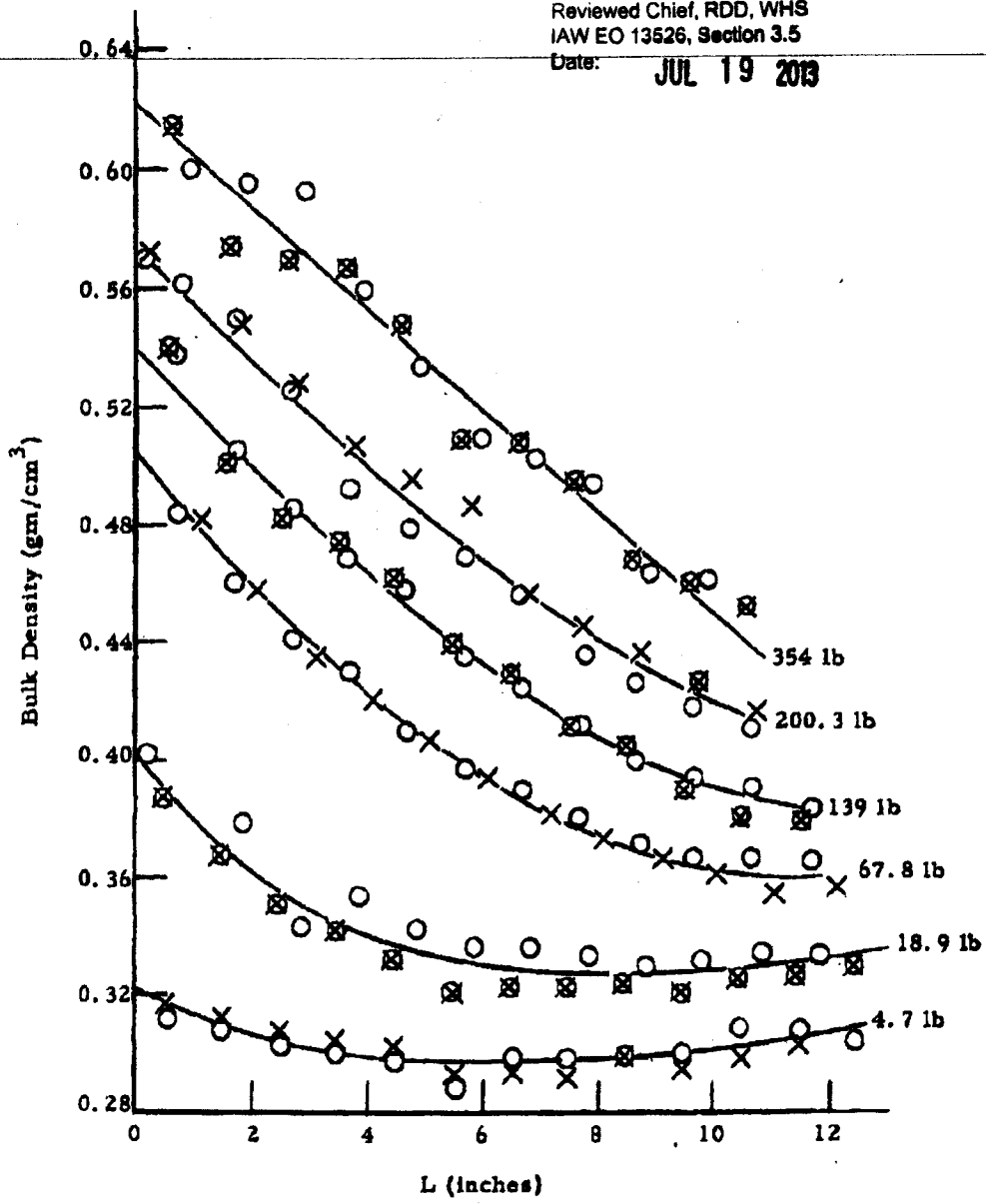


Figure 2.21 Bulk Density of Precompactated Saccharin as a Function of Distance from Piston at Various Compressive Loads

The two curves are shown for comparative purposes in Figure 2.22. It is interesting to note that the general shapes of the plots are nearly identical. The bulk density of the virgin powder for the first 18.9 lb test was  $0.293 \text{ gm/cm}^3$  compared with  $0.332 \text{ gm/cm}^3$  for the previously compacted saccharin used in the last 18.9 lb test. These experiments accentuate the dependence of bulk density upon the previous compaction history of the sample and the need for the use of virgin materials for each test in order to obtain reliable comparative results. With this background of experience the experiment was then repeated using virgin saccharin for each run. The results shown in Figure 2.23 indicate a linear relationship between the bulk density and distance from compressive piston. The deviation from linearity at greater distances from the piston will be included in the discussion of Figure 2.25.

As stated earlier in this report, data were obtained concerning the variation in bulk density along the radius of the plug. Since this variation was so uniform throughout each test, the data shown in Figure 2.24 are presented as typical of the variation found. In order to determine whether or not the radial variation in bulk density is due to the effects of the applied compressive load or to the method of filling the apparatus, an experiment was just completed at the writing of this report in which the bulk density apparatus was filled with saccharin in a manner identical to previous experiments and the bulk density measured without the application of a compressive load. The results are shown in Figure 2.25. Although the apparatus permitted accurate measurement of the average bulk density of the segments, only near the bottom of the column was the powder plug rigid enough to obtain data on the inner and outer segments. It is very interesting to note, however, that radial variation in bulk density of the order of magnitude observed with the compacted powder is also in evidence here. The radial variation is thus affected to a considerable extent by the method of filling the column. It is believed, however, that the vertical variation of bulk density should be relatively unaffected by this phenomena.

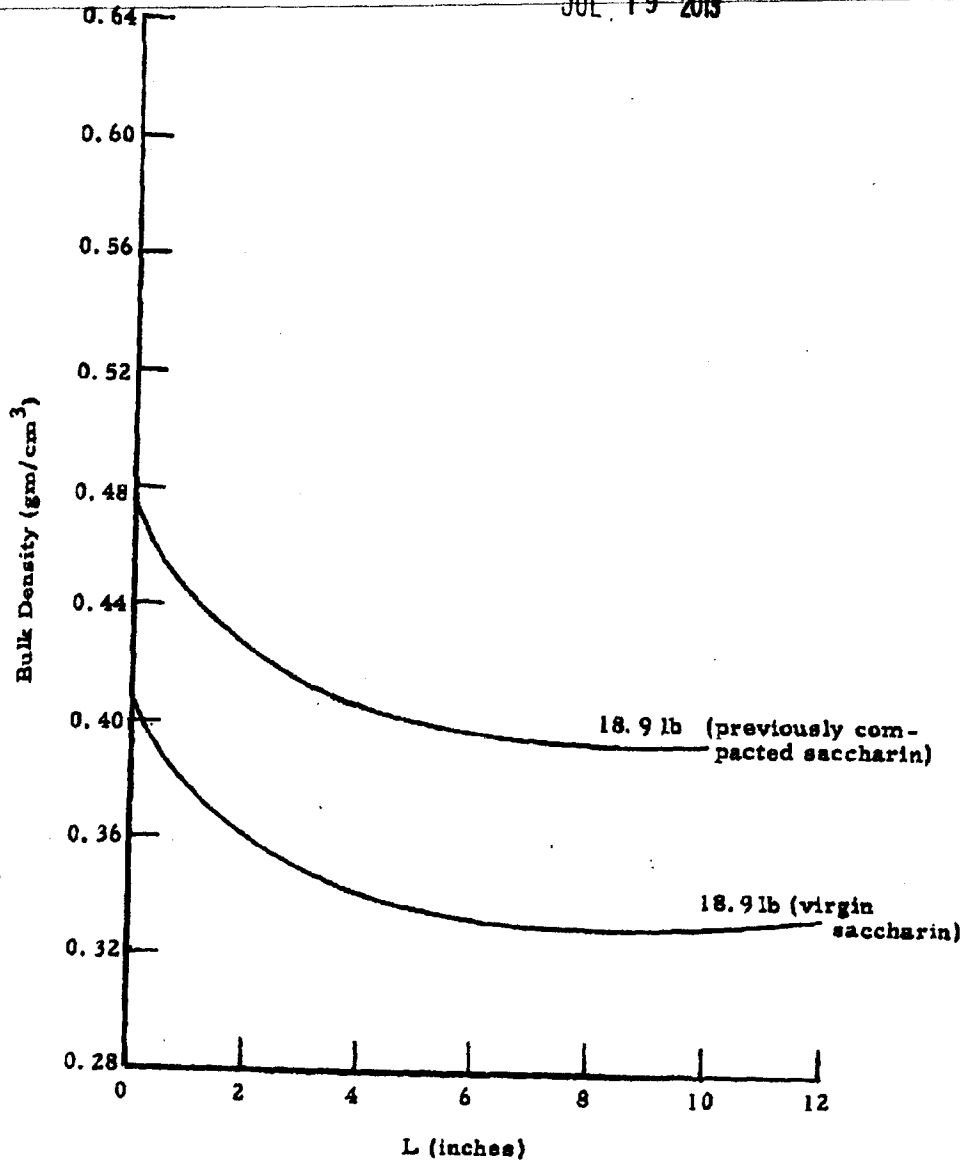


Figure 2.22 Bulk Density of Saccharin as a Function of Distance from Piston (A comparison of virgin saccharin with previously compacted saccharin.)

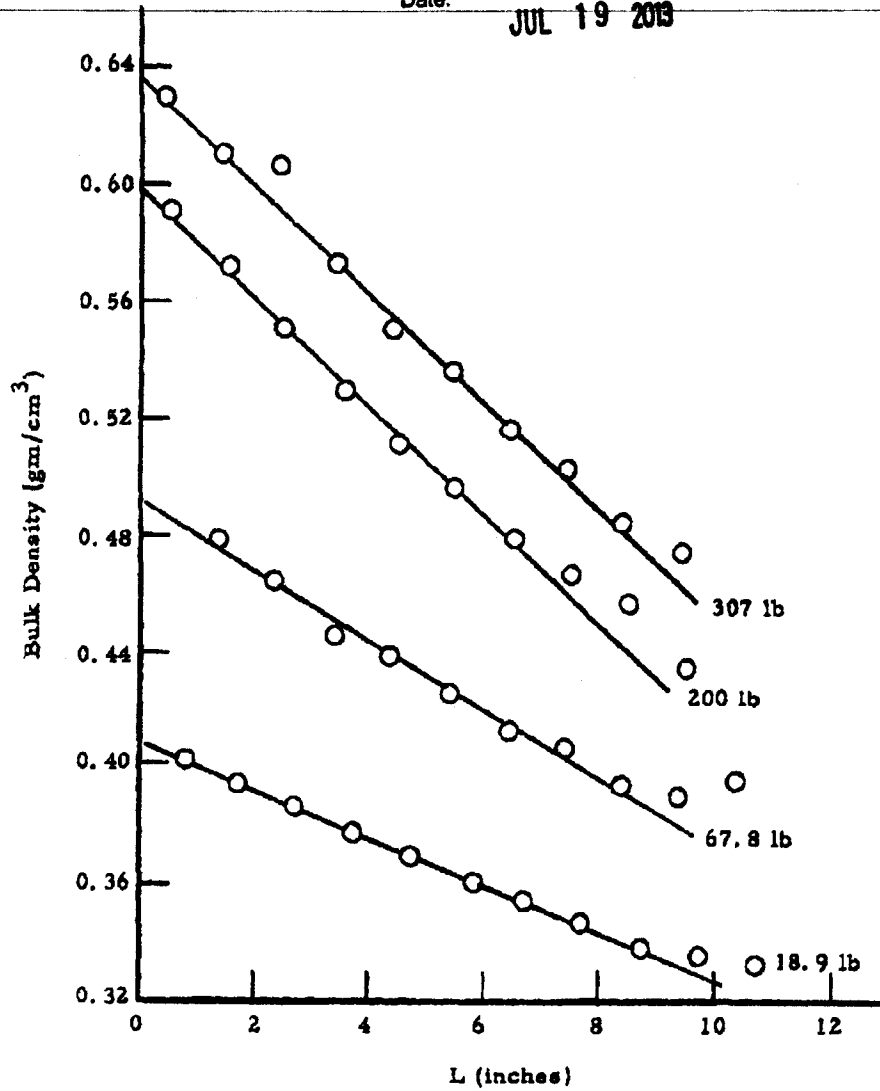


Figure 2.23 Bulk Density of Virgin Saccharin as a Function of Distance from Piston at Various Compressive Loads

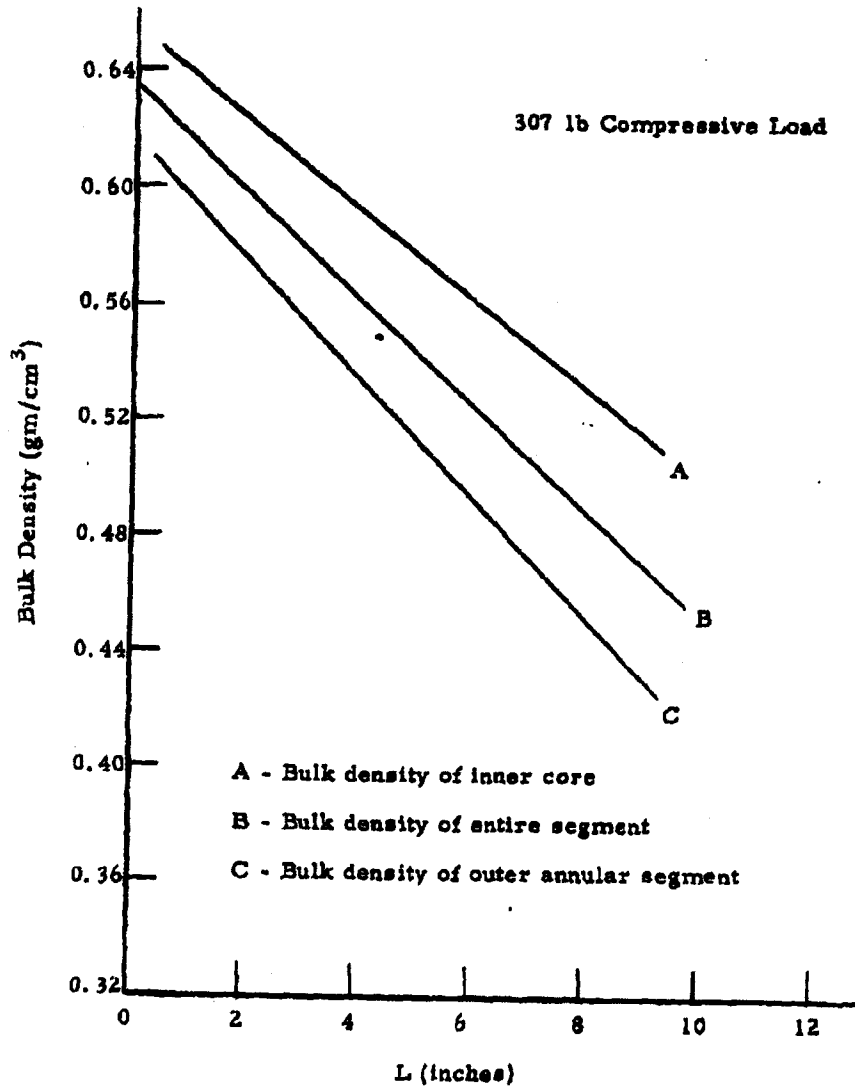


Figure 2.24 Variation in Bulk Density of Compacted Saccharin along the Radius of the Plug



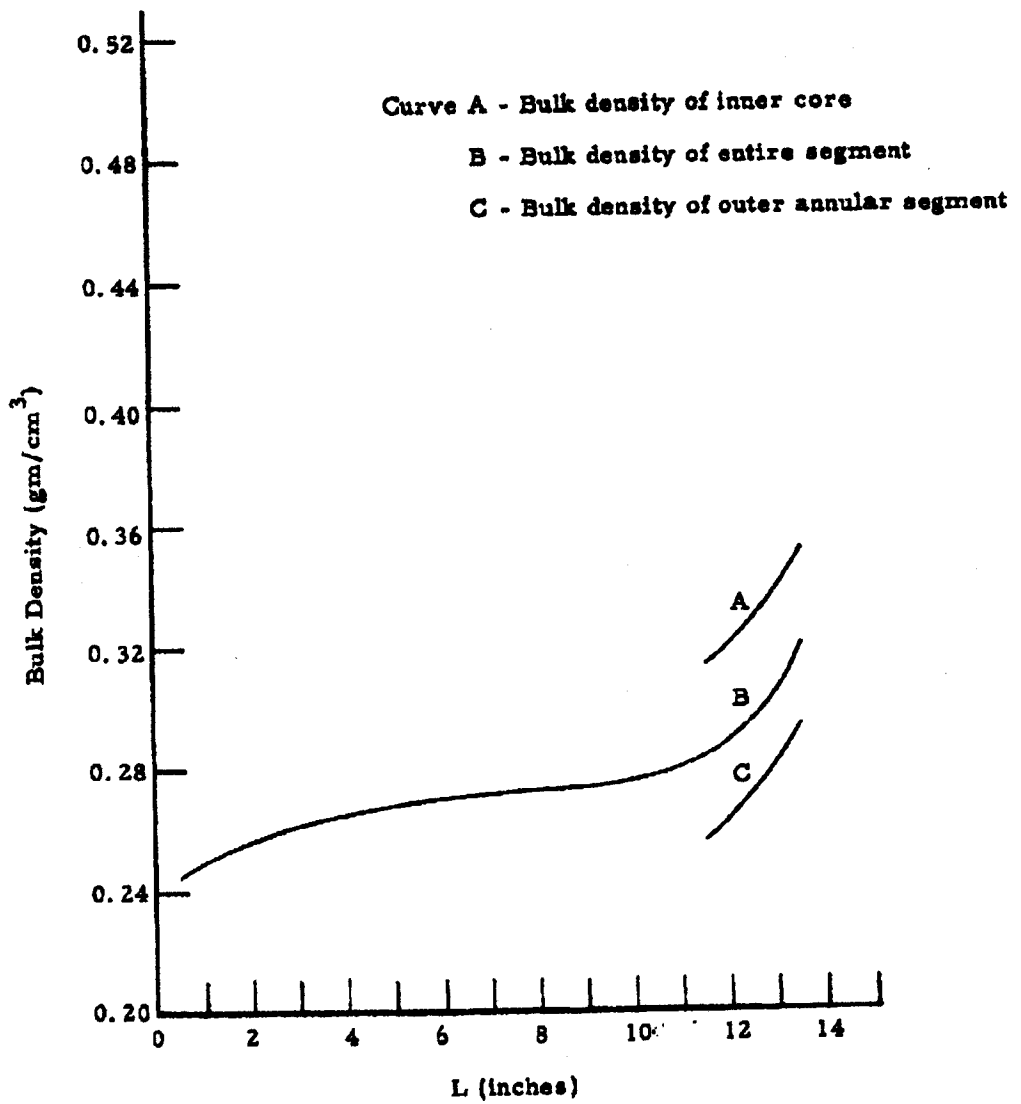


Figure 2.25 Variation in Bulk Density of Uncompacted Saccharin along the Radius of the Plug

Further examination of Figure 2. 25 shows a sharp rise in bulk density near the bottom of the column of uncompacted powder. The deviation from linearity in the plots shown in Figure 2. 23 could be explained on this basis.

In attempting to explain the increased bulk density near the center of the compressed plug, one might suspect that during the filling process the powder tends to "pile up" in the center. Visual observations made during the filling process indicate that this is probably not the case. The phenomenon that is observed is a buildup of powder, apparently due to electrostatic charge on the particles, along the walls of the apparatus as shown in Figure 2. 26. Not only could this lead to partial segregation according to particle size, but the powder along the walls is probably of lower bulk density since it is not supporting a mass of overlaying powder as is the material at the bottom of the cylinder. A sketch of this concept, involving a dense core surrounded by less dense material, is presented in Figure 2. 26.

Future work will certainly include continued investigation in this area of proper packing of the column. We also plan to extend our studies to other powders such as talc, cornstarch, and powdered milk. There is, of course, a limitation in our selection of powders for study because of the relatively large volumes of powder required if virgin powders are used for each test.

#### 2. 6 Shear Strength of Powders by Sliding Disk Method

During the present quarter our studies of the variation of shear strength of powders with compressive stress at various humidities have been extended to powdered sugar and powdered milk.

The techniques of measurement used were identical to those described in a previous report<sup>1</sup> in which the powder, after exposure for at least 48 hours to a controlled humidity environment, is caused to shear while under the influence of a compressive stress by applying a shearing force normal to the compressive stress.

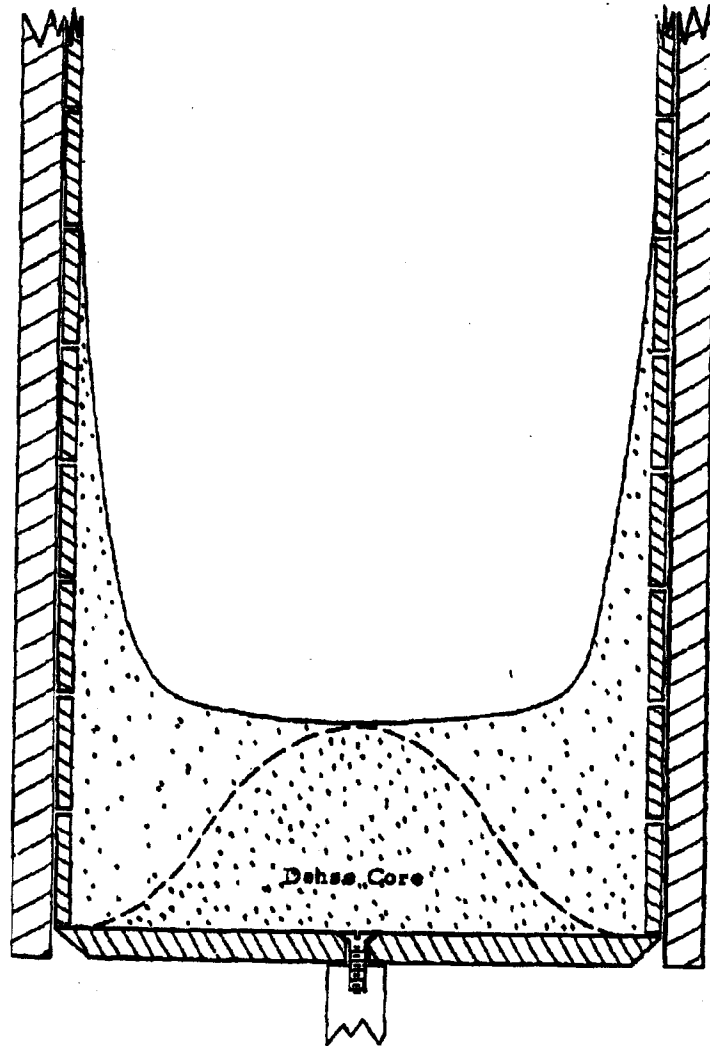


Figure 2.26 Sketch of a Probable Filling Mechanism  
in the Bulk Density Apparatus

The results are tabulated in Figures 2.27 through 2.31. It should be noted from the graphs that the relationship between shear strength and compressive stress remains relatively unchanged for both powders during the increase in relative humidity from 2 to 32 percent. However at 46 percent relative humidity and more noticeably at 69 percent relative humidity there is a marked increase in shear strength with compressive stress. Also, the relationship between shear strength and compressive stress is no longer linear for powdered milk.

Future work will include studies of powdered sugar and powdered milk at higher compressive stresses. In particular it will be interesting to determine if the shear strength is in fact reaching a maximum value for powdered milk at 69 percent relative humidity as indicated by the plot in Figure 2.31. We also plan to extend our studies to other powders such as cornstarch, talc, and saccharin.

## 2.7 Future Areas for Study on the Characteristics of Powders

The emphasis in our work has been devoted to the development of reliable test methods based upon a sound theoretical background. In the future we will concentrate upon coordination of information on specific powders in order to completely characterize the powder, and to determine which test or tests yield the most reliable information concerning the compactibility and dispersability of a powder. New areas of study which will be initiated include:

### 2.7.1 Bulk Density of Loose Powders

An apparatus is being constructed in which powders will be allowed to fall a fixed distance through vibrating screens into a unit cube. It is believed that this will afford a simple, rapid, and accurate method for measurement of the bulk density of a variety of loose powders.

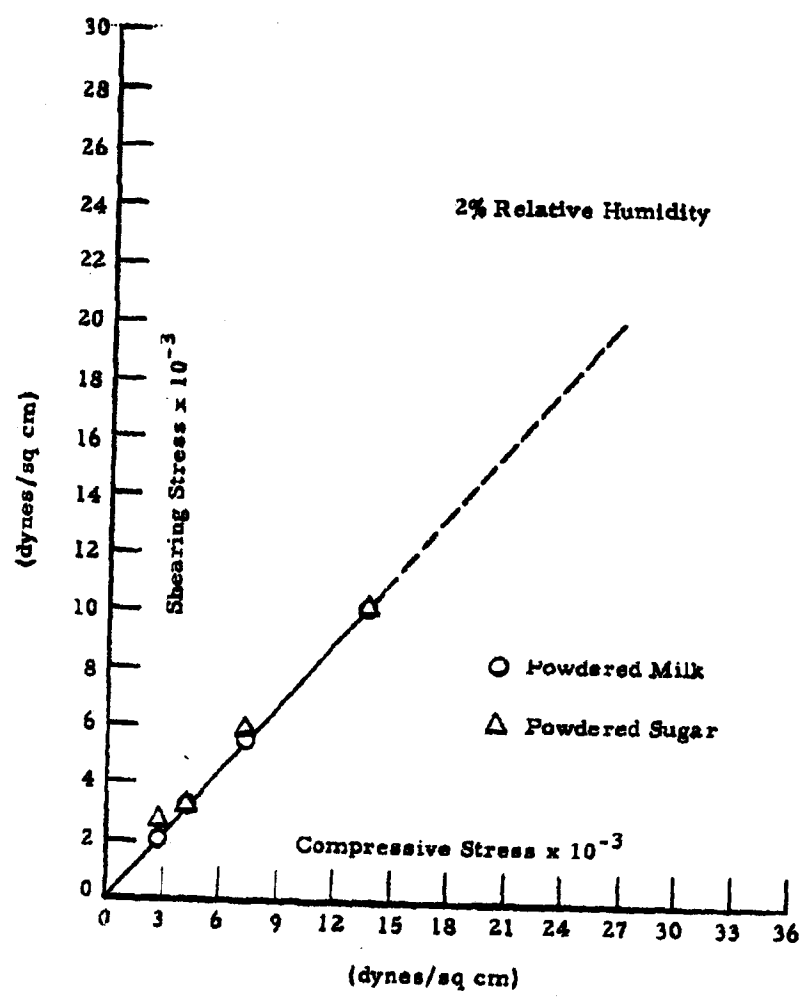


Figure 2.27 Variation of Shear Strength with Compressive Stress at 2 Percent Relative Humidity

Date: JUL 19 2013

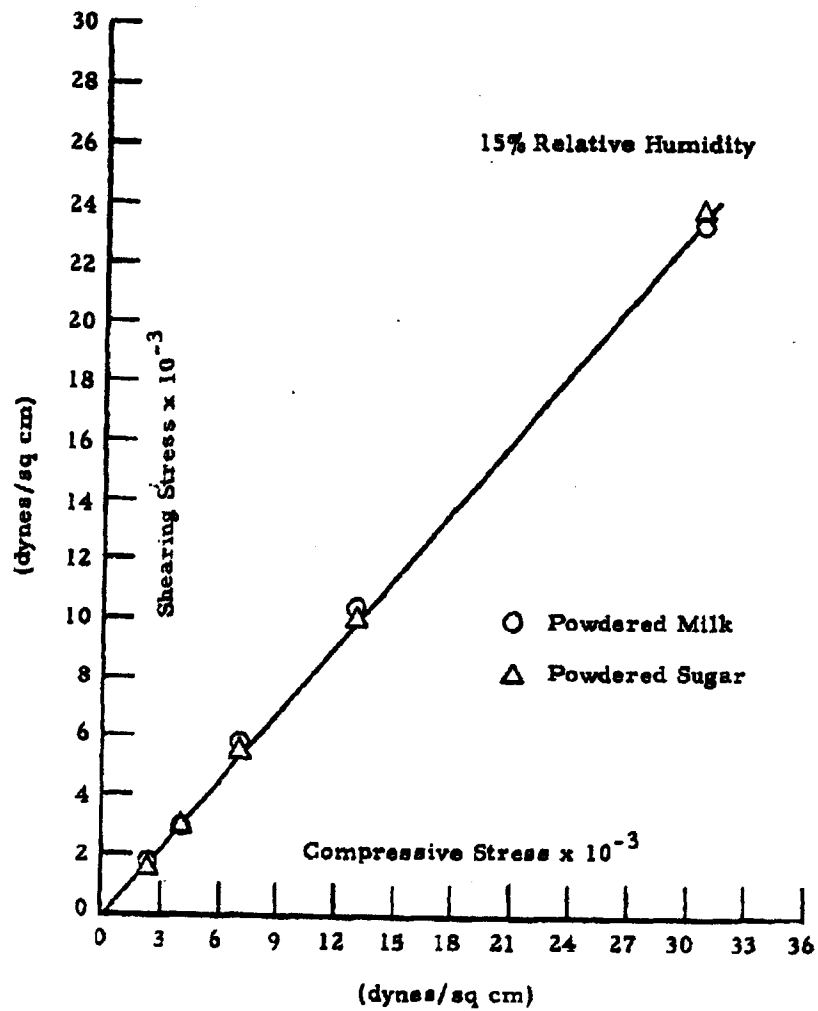


Figure 2. 28 Variation of Shear Strength with Compressive Stress at 15 Percent Relative Humidity

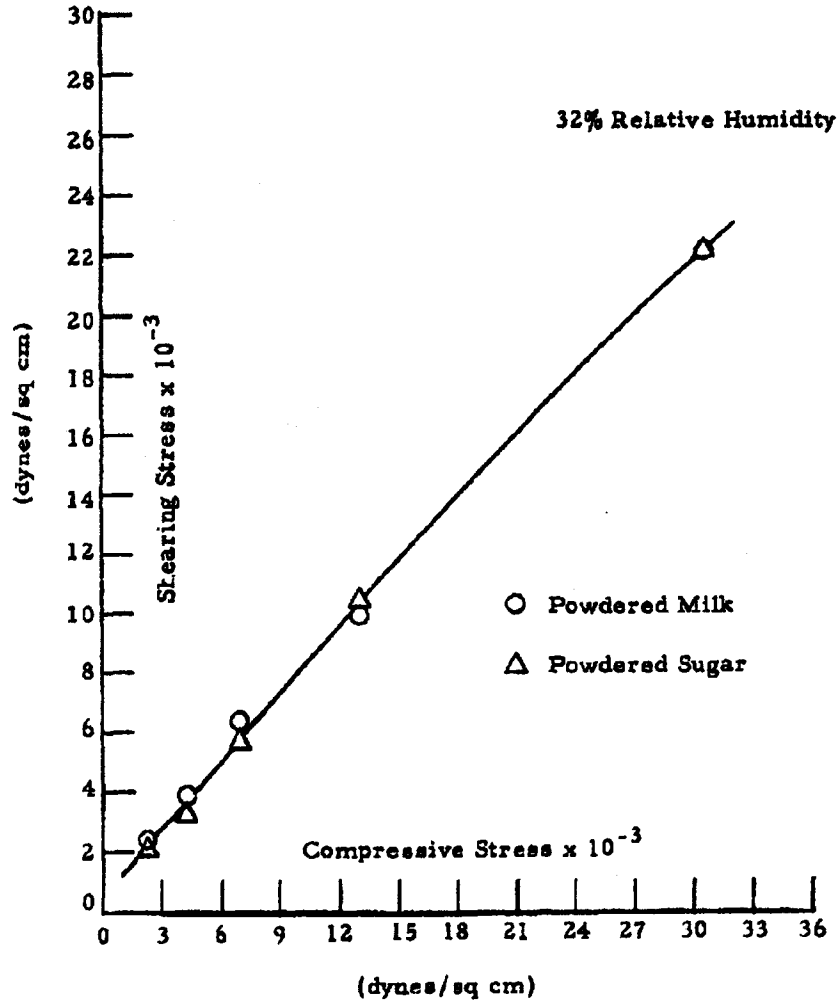


Figure 2.29 Variation of Shear Strength with Compressive Stress at 32 Percent Relative Humidity

Date: JUL 19 2013

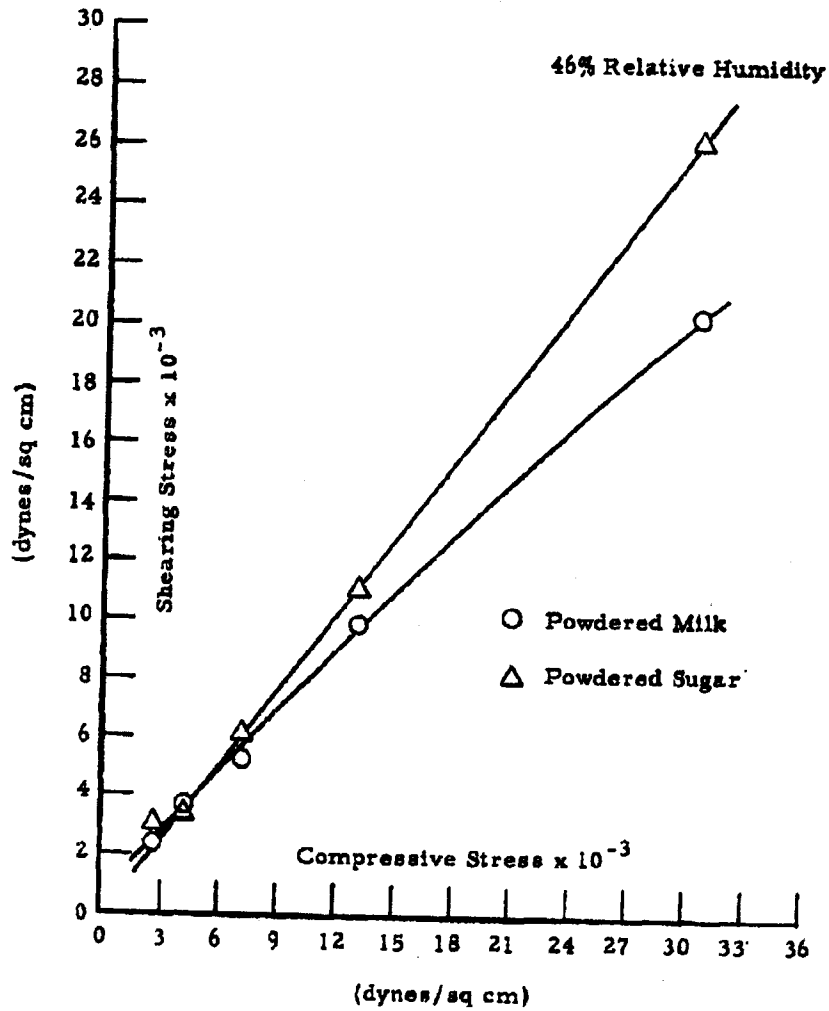


Figure 2.30 Variation of Shear Strength with Compressive Shear at 46 Percent Relative Humidity



Date: JUL 19 2013

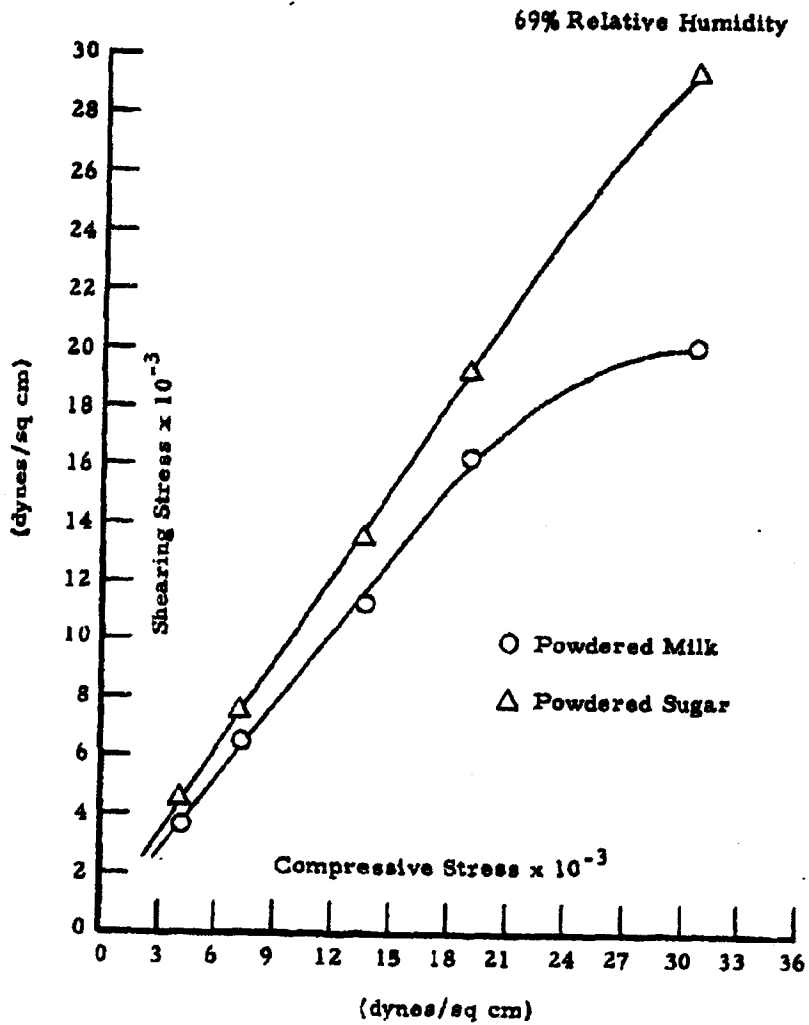


Figure 2.31 Variation of Shear Strength with Compressive Stress at 69 Percent Relative Humidity

### 2.7.2 Measurement of Static Charge of Particulate Materials

A study will be made of various methods of generating and removing static charges, and of methods for qualitative and quantitative measure of static charge.

### 2.7.3 Particle Size and Shape

One of the most important characteristics determining the behavior of powders in the 5-micron range is the magnitude and the character of the total surface of the individual particle. A characteristic which can be called "surface roughness" should be of fundamental importance in predicting the ease with which a powder can be compacted and redispersed. This characteristic can be evaluated by a summation of information obtained from particle size distribution, particle shape, and total surface area. Particle size distributions are now being determined via the Whitby centrifuge. Photomicrographs are now being utilized to study particle shape. This study will be extended to the use of electron micrographs.

### 2.7.4 Total Surface Area

Measurement of total surface area of powders in conjunction with the particle size and shape analysis should yield a clearer picture of the total "surface roughness."

There are several methods for measuring the specific surface area of powders<sup>6</sup>. Of these, the two most frequently used are the gas-adsorption (usually nitrogen) and air permeability methods.

In the gas adsorption method, the quantity of gas necessary to form a monomolecular layer on the surface is determined. By assuming a value for the area occupied by a single molecule, the area of surface covered by the

adsorbed gas molecules is then calculated. The area measured by this method depends on the size of the molecules adsorbed and the degree to which they are able to penetrate into any cracks or pores in the solid.

The air permeability method is essentially a rheological method in which the flow of a fluid (liquid or vapor) through a powder in a compacted bed is related to the surface area of a continuous solid. It is assumed in this method that the bed of powder behaves as a bundle of capillaries. In consequence, only the surface of the continuous paths through the material will contribute to the measured specific surface area. This area is not the same as that measured by adsorbing a gas on the surface of the powder, because in the latter method all the surface accessible to gas molecules of the type used will contribute. In general, the area measured by the adsorption of a gas will be larger than that obtained by a permeability method. This difference may be accentuated if the powder has appreciable "internal" surface due to cracks, internal pores, and other irregularities. In addition, the permeability method may not measure the full "external" surface of the powder because of the formation of blind pores during compaction of the bed.

With very fine powders a further complication arises since it is very difficult to compact a fine powder to give a bed of low-voids fraction; and with a porous type of bed there may be a serious lack of uniformity throughout the compacted bed. From these considerations it would appear that the logical method to be used for powders currently under study would be the gas adsorption method.

JUL 19 2013

### 3. AEROSOL STUDIES

The objective of this experimental program has been to perform a study of the properties of aerosols, both intrinsic and extrinsic, which have an effect on the aerosol's over-all stability. The degree of stability can be measured by observing the net rate of disappearance of the particles from the aerosol. Several factors, besides concentration, conceivably have an effect on aerosol stability. These factors are:

- 1) Particle size and shape
- 2) Particle type
- 3) Charge characteristics of particles and environment
- 4) Water content of particles
- 5) Absolute humidity of environment
- 6) Type of settling (turbulent or tranquil)

The instability of aerosols is obviously to be understood in terms of only two distinct processes:

- 1) Particles may be removed from the aerosol by settling on and adhering to the various surfaces to which the aerosol is exposed.
- 2) Particles may be removed from the aerosol by colliding with and adhering to other particles within the same aerosol resulting in a net decrease of independent particles (coagulation).

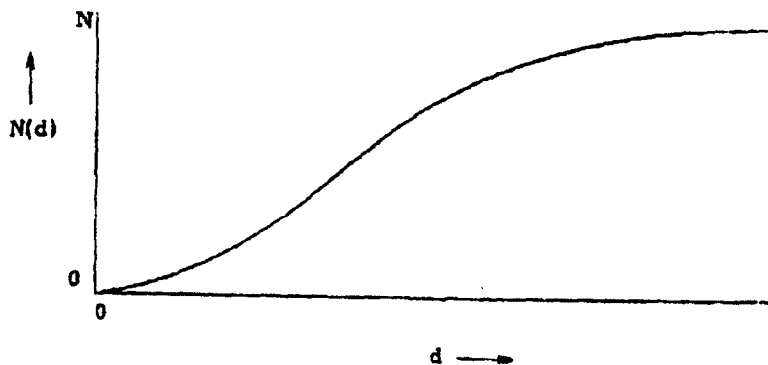
Since the rates of these two processes completely specify the stability of an aerosol, the fruitfulness of any experimental method is to be judged primarily on its capability for supplying actual numerical values for these rates. Much of our work during this period has been directed at this type of evaluation of our light-instrumented aerosol chamber.

### 3.1 Terminology and Definitions

A perusal of the literature of aerosols reveals a certain degree of independence among the various authors in regard to terminology. It is necessary, therefore, to define those terms used in this section which would conceivably conflict with the literature.

The number of particles per unit volume will be termed the concentration of the aerosol. The term concentration will often be specialized to mean the number of particles of a particular species, e. g., those with dimension in the range  $(d, d + \delta d)$  per unit aerosol volume.

The classification of aerosol particles according to species warrants some comment. Since the most important particle property with respect to its behavior in an aerosol is particle size, the primary classification should be made accordingly. In dealing with solid particles, however, it is often not obvious how this classification should be put into practice because the particles are often very irregularly shaped. In our work we shall generally suppose that the particles may be considered spherical and characterize particle size by means of the diameter  $d$ . Thus if  $N$  denotes the total number of particles under consideration, we denote the number of particles with diameter less than  $d$  by  $N(d)$ . Clearly  $N(0) = 0$  and  $N(d)$  approaches  $N$  as  $d$  becomes infinite, so that a plot of  $N(d)$  against  $d$  is qualitatively as shown in the sketch below.



The value  $d_m$  of  $d$  for which  $N(d_m) = 1/2 N$  is, of course, the median diameter. The terms monodisperse and polydisperse are widely used in reference to the variety of particle sizes present in a sample, a practice that we shall follow by saying that the dispersity is measured by the slope of the  $N(d)$  curve.

It is often convenient to speak of the fractional number of particles in a particular sample which have diameters less than  $d$ . Denoting this fraction by  $n(d)$  we have as its defining relation  $Nn(d) = N(d)$ .

The derivative of  $N(d)$  has significance. The number of particles having diameters in the small interval  $(d, d + \delta d)$  is  $N(d + \delta d) - N(d) = \frac{N(d)}{\delta d} \delta d = N'(d) \delta d$ . Here the prime denotes the derivative.  $n'(d)$  is similarly defined.  $N'(d)$  is commonly called the particle size distribution while  $N(d)$  is often called the cumulative particle size distribution.

There are several explicit formulae for the particle size distribution, each of which approximates a wide variety of distributions actually encountered in practice. Each of these formulae contain two or more parameters which are supposedly capable of accounting for practical variations. Inasmuch as it is often convenient to have such a formula available for discussion, we have chosen one for that purpose. Since it is felt that the data in most cases are not precise enough to form a basis for choice of formula, we simply take the most common such formula which is compatible with the conditions  $n(0)$  and  $n(\infty) = 1$ , namely, the logarithmic-normal distribution:

$$n(d) = \text{erf} \left( \frac{\log (d/d_g)}{\log \sigma_g} \right)$$

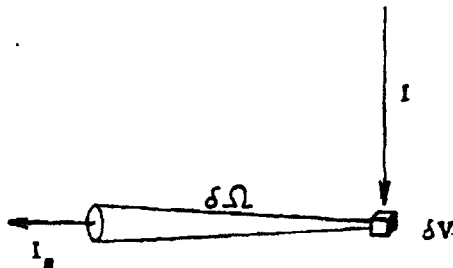
$$n'(d) \delta d = \frac{1}{(2\pi)^{1/2} \log \sigma_g} \exp \left\{ -1/2 \left( \frac{\log (d/d_g)}{\log \sigma_g} \right)^2 \right\} \delta (\log d)$$

Simple considerations show that  $d_g$  (the geometric mean diameter) in the above formula is also the median diameter mentioned earlier. The term  $\sigma_g$  (the geometric standard deviation) is a measure of the dispersity.

### 3.2 A Theoretical Calculation for Non-Agglomerative Aerosol Decay

It is expected that the information provided by scattered light will be rather subtly related to the fundamental processes of aerosol decay. For this reason it will be useful to have a simple, yet pertinent, relation between these processes and the aerosol light-scattering behavior. Such a relation is proposed in this section.

The light-scattering problem for an aerosol may be formulated as follows: Consider a small element of volume  $\delta V$  in the aerosol, this volume being irradiated from above by a monochromatic light beam of intensity  $I$ .



The amount of light scattered into a cone of solid angle  $\delta\Omega$  located at 90 degrees by a single particle of diameter  $d$  in  $\delta V$  is proportional to  $I$  and to  $\delta\Omega$ :

$$I_{\text{one particle}} = \sigma(d) \cdot I \cdot \delta\Omega$$

Date: JUL 19 2013

The constant of proportionality  $\sigma$  is called the differential scattering cross-section. Since the number of such particles in  $\delta V$  is  $C(d) \cdot \delta V$ , the total light scattered by particles of diameter  $d$  is:

$$\sigma(d) \cdot C(d) \cdot I \cdot \delta V \cdot \delta \Omega$$

The light scattered by all particles is

$$I_s = I \cdot \delta V \cdot \int_{\text{all } d} \sigma(d) \cdot C(d) \delta d \delta \Omega$$

This integral is to be evaluated under various conditions.

Let us first consider  $C(d)$ . As has been explained in Section 3.1, the particle size distribution will be assumed logarithmic - normal. We further assume that at some initial time  $t = 0$  the concentration is uniform throughout the chamber. Thus:

$$C(d, t = 0) = \frac{N'(d)}{V}$$

where  $V$  is the volume of the chamber.

This initial concentration may be modified with passing time. We consider two idealized modes in which the modification may come about.

First, suppose that the atmosphere in the chamber is "tranquil", i. e., sufficiently free of currents so that all particles settle vertically downward. In this case all particles of diameter  $d$  will fall as a unit, with the result that after time  $t$ , no particles of size  $d$  (or larger) will be present above a certain horizontal plane. This plane lies a distance  $h$  from the top of the chamber,  $h$  being given by:

$$h = t \cdot v(d) = t \cdot \frac{9gd^2}{18\eta}$$



where  $v(d)$  is the Stokes' settling velocity of a particle of diameter  $d$ ,  $\rho$  is the particle density,  $g$  is the gravitational constant, and  $\eta$  is the air viscosity. The concentration as a function of time is therefore

$$C(d, h, t) = \begin{cases} C(d, t = 0) & \text{for } h > t \cdot v(d) \\ 0 & \text{for } h < t \cdot v(d) \end{cases}$$

that is,  $C(d, t = 0)$  is to be multiplied by a function which has value 1 for  $0 < d < \sqrt{\frac{18 h \eta}{\rho g t}}$  and value zero for larger  $d$ .

As an alternate mode of decay, suppose that the air in the chamber is so turbulent that the particles move in an essentially random manner. For this case it has been stated by various authors<sup>7, 8</sup> that concentration remains uniform throughout the chamber, but that after time  $t$  the number of particles of size  $d$  is reduced by the factor

$$e^{-\frac{v(d)}{H} t}$$

where  $H$  is the total height of the chamber. Thus

$$C(d, t) = C(d, 0) \cdot e^{-\frac{v(d)}{H} t}$$

The remaining factor in the scattering integral, the differential scattering cross-section  $\sigma(d)$ , is in general a very complicated function of  $d$  as well as of the light wavelength and the index of refraction. However, the ratio of particle diameter to light wavelength to be encountered in the present experiment is probably large enough so that a simple approximation from classical optics may suffice<sup>9</sup>. This approximation is:

$$\sigma(d) = \frac{d^2}{6\pi}$$

The light-scattering problem thus leads to the two integrals:

For the tranquil case:

$$\frac{1}{6\pi} \cdot \frac{NI \delta V \delta \Omega}{V \sqrt{2\pi \ln \sigma_g}} \int_0^{d_{\max}} d^2 e^{-\frac{1}{2} \left( \frac{\ln d/d_g}{\ln \sigma_g} \right)^2} \delta(\ln d)$$

with  $d_{\max} = \sqrt{\frac{18 h \eta}{\rho g t}}$ ;

For the turbulent case:

$$\frac{NI \delta \Omega \delta V}{6 \pi V} \cdot \frac{1}{\sqrt{2\pi \ln \sigma_g}} \int_0^{\infty} d^2 e^{-\frac{v(d)t}{H}} e^{-\frac{1}{2} \left( \frac{\ln d/d_g}{\ln \sigma_g} \right)^2} \delta(\ln d)$$

It is to be noted that the present considerations take no account of agglomeration. Another inadequacy, which may be partially corrected, is that the turbulent decay expression:

$$e^{-\frac{v(d)t}{H}}$$

takes into account only "gravitational impingement" on the floor and neglects "inertial impingement" on other surfaces of the chamber. The effect of aerosol decay by inertial impingement may be seen qualitatively by the following considerations.

As a current of air approaches a wall it is turned back, with an attendant centrifuging action. Thus, the particles experience an equivalent gravitational force, and inertial impingement is actually quite similar to gravitational impingement. The effect on the decay rate is to add an apparent gravitational constant  $g'$  to the  $g$  which appears in the exponent of  $e^{-\frac{v(d)}{H}t}$ . For further details on this process, see Reference 8.

The integral for the tranquil settling case may be solved analytically. The result is:

$$d_g^2 e^{2 \ln^2 \sigma_g} \left\{ 1 - \operatorname{erf} \left( \frac{\ln \frac{v(d_g) \cdot t}{h} + 4 \ln^2 \sigma_g}{2 \ln \sigma_g} \right) \right\}$$

$$= d_g^2 e^{2 \ln^2 \sigma_g} \left\{ 1 - \operatorname{erf} \frac{\ln \frac{v(d_g) t}{h}}{2 \ln \sigma_g} \right\}$$

where:

$$d_s = d_g e^{2 \ln^2 \sigma_g}$$

is the surface median diameter. This function is linear if plotted in logarithmic-normal form with  $\log t$  as abscissa. The 84, 50 and 16 percent points come at

$$t = \frac{h}{v(d_g) \sigma_g^2}, \quad \frac{h}{v(d_g)}, \quad \frac{h \sigma_g^2}{v(d_g)}$$

respectively.

The turbulent settling integral may be considered qualitatively by comparison to the tranquil expression. The two integrals differ in the modulating factor in the integrand. Where the tranquil integrand has a factor which drops from 1 to 0 sharply at  $\sqrt{d = \frac{18 h \eta}{\rho g t}}$ , the turbulent integrand has a factor  $(e^{-\frac{v(d)}{H} t})$  which drops from 1 to 0 gradually, reaching 60.6 percent (the inflection point) at:

$$\frac{v(d)}{H} t = \frac{1}{2}; \quad d = \sqrt{\frac{18 \eta}{\rho g t} \cdot \frac{H}{2}}$$

Thus if  $N'(d)$  changes sufficiently slowly with  $d$  (the aerosol is sufficiently polydisperse) the turbulent settling curve should be very similar to the tranquil expression if, in the latter,  $h$  is taken equal to  $\frac{H}{2}$ .

As a check on the reasoning of the above paragraph, the turbulent settling integral was submitted to the computer group for numerical integration. A few curves, thus obtained, are shown in Figure 3.1.  $\rho d_g^2 t$ , with  $\rho$  in  $\text{gm/cm}^3$ ,  $d_g$  in microns and  $t$  in minutes, is used as the variable. It may be seen that the plots have considerable curvature for small values of  $\sigma_g$ , but approach linearity for larger values. The dashed line in Figure 3.1 is the plot of

$$e^{-\frac{v(d_g)}{H} t}$$

which is the solution of the turbulent settling integral as  $\sigma_g \rightarrow 1$ . It will be noted that latter nearly coincides with the curve for  $\sigma_g = 1.2$ . All the curves of Figure 3.1 cross 50 percent in the neighborhood of  $\rho d_g^2 t = 370$ , which may be compared with the value 286 obtained from

$$v(d_g) \cdot t = h \approx \frac{H}{2} \text{ at } 50\%$$

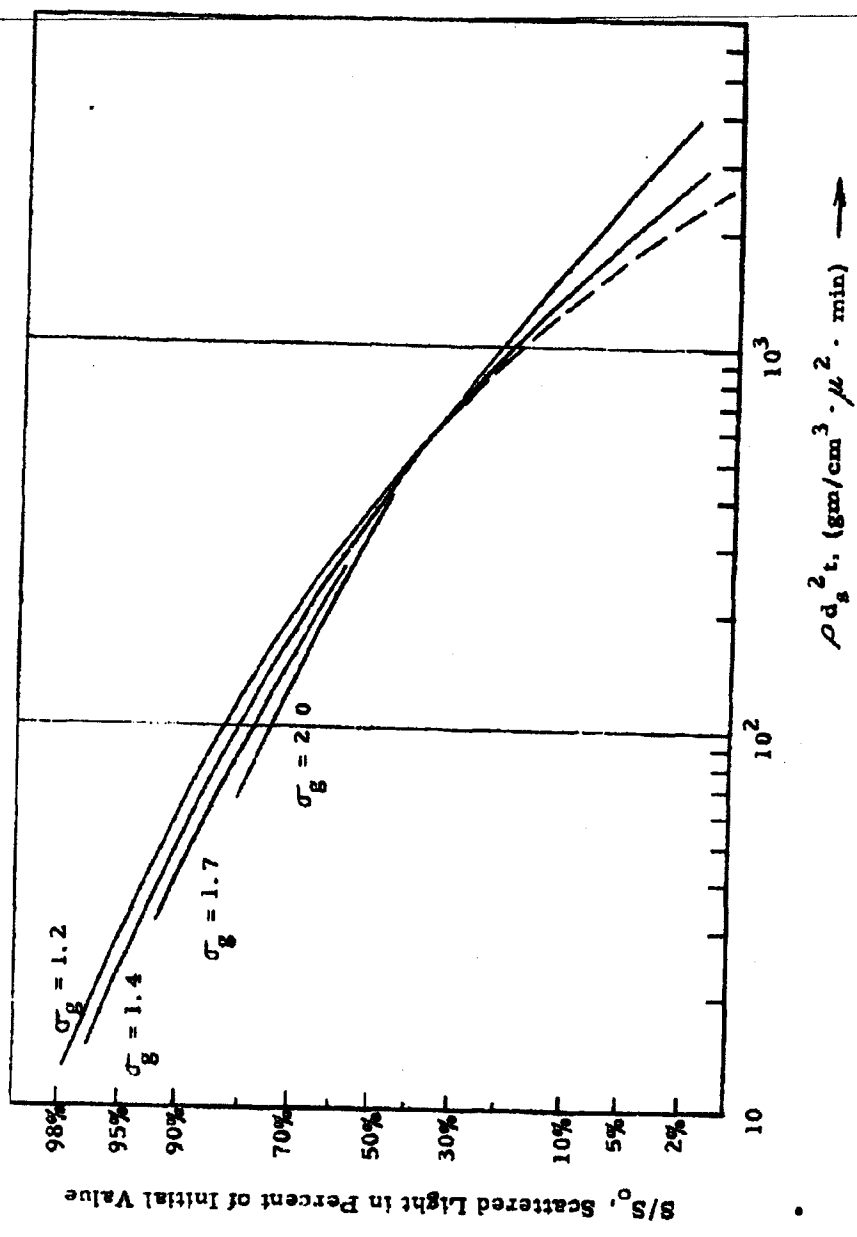


Figure 3.1 Theoretical Curves for Turbulent Settling

### 3.3 Experimental Work

The experimental objectives, somewhat idealized, of this program were stated earlier. As mentioned before, most of the work of the present quarter was carried out with a view to seeing how nearly these objectives could be accomplished in practice. Other areas of work were experimental techniques and determination of operating parameters.

Originally, it was considered desirable to restrict the scope of the experiment to the stability properties of aerosols; that is, to the behavior of aerosols subsequent to formation. This, however, requires the existence of a well-defined initial condition of the aerosol, a situation which is difficult to achieve in practice. Thus, while most of the runs to be discussed are concerned with aerosol decay (for which runs the dispersing process was assumed to be reasonably efficient), some work was directed at evaluation of dispersing efficiency.

The powder dispersing system was described in an earlier report. Briefly, it consists of a small chamber, containing the powder sample, which is pressurized with dry nitrogen gas. A diaphragm ruptures, due either to the pressure differential or to mechanical puncturing, suddenly releasing the pressure. A dispersing action is attendant. It was found that a 2-mil film of "phenoxy 8" plastic made a suitable diaphragm material, rupturing at 125 psi in our configuration. This material was used almost exclusively.

There were, broadly speaking, three series of runs:

- 1) Runs in which the fan was not used at all; these were intended for the study of the dispersing process.
- 2) Runs for which the fan was used only for a short initial period, intended for study of aerosol behavior under "tranquil" conditions.
- 3) Runs for which the fan was left on throughout the entire run, intended for study of aerosol behavior under "turbulent" conditions.

It was found that stirring (Series (3) above) has a decided regularizing influence on the aerosol. In the "fan on" situation the two light-scattering signals were brought into coincidence almost instantaneously and stayed in coincidence, both decreasing smoothly, throughout the entire run. The Series (2) runs, on the other hand, often led to irregular (nonmonotonic) decreasing light signals subsequent to the turning off of the fan. The Series (3) runs will be discussed first.

Representative runs from Series (3) are shown plotted in logarithmic-normal form in Figures 3.2, 3.3 and 3.4. Note that these plots are at least approximately linear. For purposes of discussion, we identify three abscissae,  $t'$ ,  $t^*$ ,  $t''$ , on this line (see Figure 3.2). These are the intercepts of the line with 84, 50 and 15 percent scattered light intensity, respectively\*.

Table 3.1 presents a summary of the "fan on" runs. Note that  $t''/t'$ , which according to Section 3.2 measures aerosol dispersity, is sensibly constant for a given powder while  $t^*$ , which is an inverse measure of the aerosol mean particle diameter, decreases with both amount of powder dispersed and with stirring. It may also be significant that the curves for the lower fan speeds differ more from linearity than the other figures. This point bears further checking.

The last two columns of the table show values of  $\rho d_s^2$  and  $\sigma_g$ , where  $\rho$  is particle density in gm/cm<sup>3</sup>,  $d_s$  is the surface median diameter in microns and  $\sigma_g$  is the geometric standard deviation, computed from  $t^*$  and  $t''/t'$ . The relations used are:

\* According to the tranquil settling expression of Section 3.2, the ratio  $t''/t'$ , which measures the slope, has the value  $(\sigma_g)^4$ . This should remain approximately true for turbulent settling. An approximate relation for  $t^*$ , as discussed in Section 3.2, is

$$H = 2 \cdot v(d_s) t^* ; \rho d_s^2 t^* = 286$$

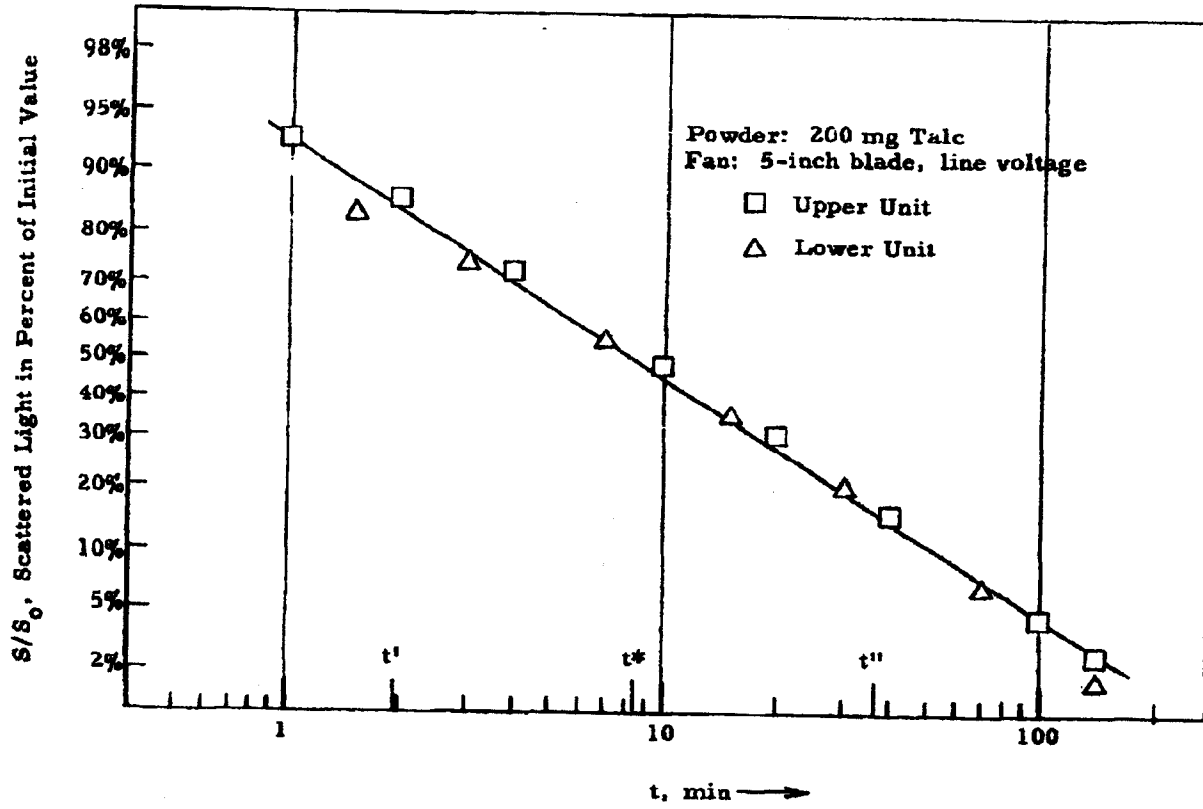


Figure 3.2 Experimental Curve for Light Scattered from Talc Aerosol



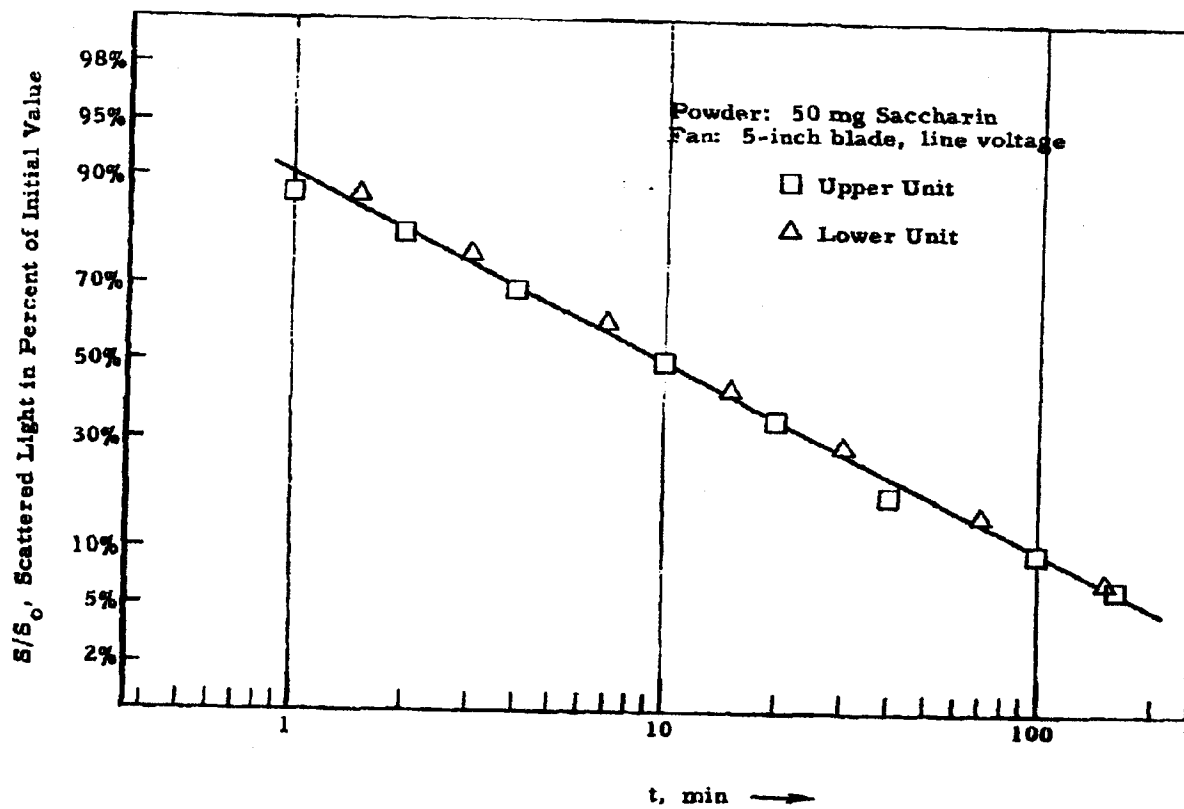


Figure 3.3 Experimental Curve for Scattered Light from Saccharin Aerosol

JUL 19 2013

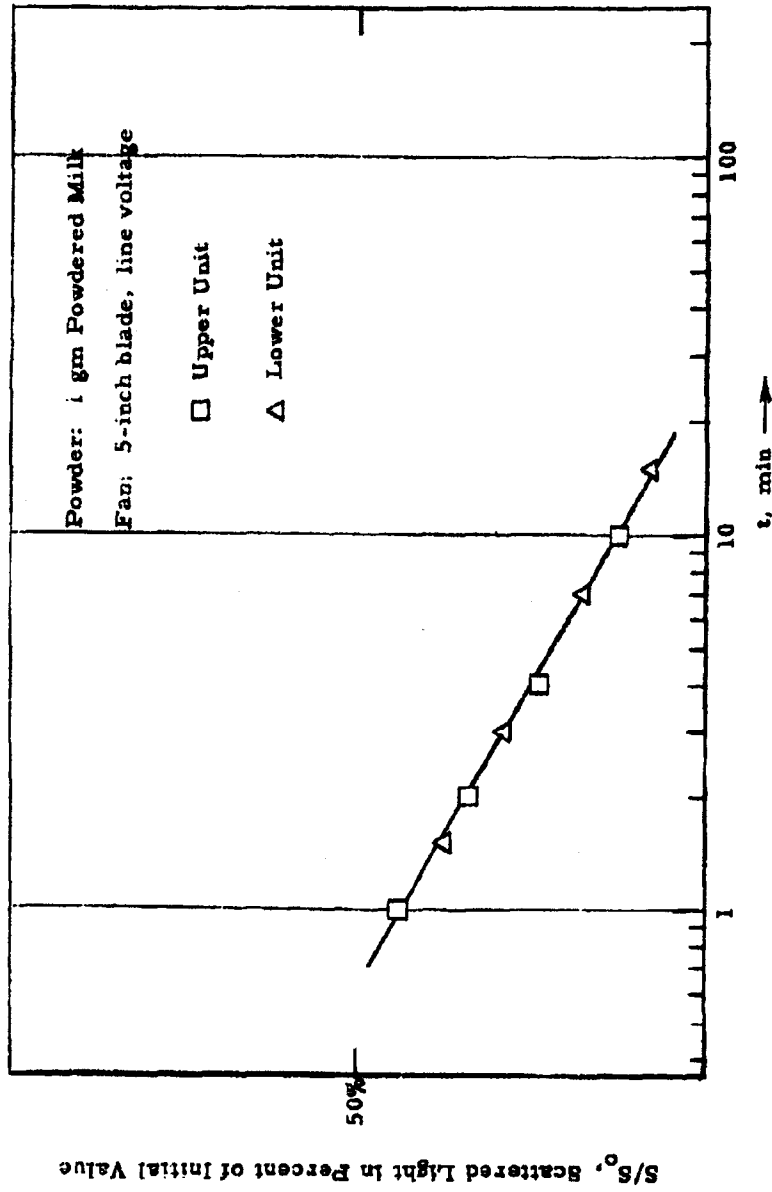


Figure 3.4 Experimental Curve for Scattered Light from Powdered Milk Aerosol

JUL 19 2013

$$\rho d_p^2 = \frac{370}{t^*}$$

$$\sigma_g = \sqrt[4]{t''/t'}$$

The values of  $\rho d_p^2$ , especially, may be viewed with suspicion since no effort has been made to take inertial impingement into quantitative account. Since our purpose is not aerosol assay as such, we do not intend to make the correction.

Table 3.1 Experimental Data for "Fan On" Runs

Powder Dispersed	Fan Condition	t* (min)	t''/t'	$\rho d_p^2$	$\sigma_g$
200 mg talc	Large blade, line voltage	8.2	17.5	45.1	2.04
50 mg talc	Large blade, line voltage	12.2	21.5	30.3	2.15
20 mg talc	Large blade, line voltage	19.0	20.7	19.5	2.13
50 mg talc	Large blade, line voltage	10.0	35.3	37.0	2.44
1 gram pwd. milk	Large blade, line voltage	0:59	28.6	62.7	2.31
56 mg talc	Small blade, 50 volts	20.5	20.4	18.1	2.13
56 mg talc	Small blade, 35 volts	18.0	32.8	20.5	2.39

Other "fan on" runs, conducted with yet a different powder, turned up an appreciably different type of light-scattering signal. The powder used here was "K ferric oxide"\* , a very nearly monodispersed material of reasonably spherical particles. Particle diameter is approximately 2 microns. For this powder the scattered light decreased exponentially, as may be seen in Figure 3.5. This behavior is in accordance with the hypothesis of Section 3.2. Further, the experimental decay constant 0.035 compares favorably with the expected value of

$$\frac{v(d_p)}{H} = 0.037 .$$

With regard to Figure 3.5, however, a question may be raised concerning the larger value of the slope during the first 5 or 10 minutes of each run. It is believed that there are several possible explanations for this rather minor deviation, none of which contradict the hypothesis advanced in Section 3.2.

Interpretive remarks, in terms of the relative roles played by agglomeration and by settling on surfaces, must remain rather hypothetical at this time. It has been stated that the light-scattering data for polydisperse powders are fairly well represented by a straight line on a logarithmic-normal plot. This would say that either the aerosols observed so far have log-normal particle distributions and decay without agglomeration (as in the model of Section 3.2), or that agglomerative effects balance out the deviations from log-normality. It is also conceivable that the agglomeration has the simple effect of tilting or displacing the line on the log-normal plot, a behavior which was indeed observed. On the other hand, the line position

---

\*K ferric oxide was at one time produced and marketed as a pigment under the trade name "KROX" by Minnesota Mining and Manufacturing Co., St. Paul, Minnesota.

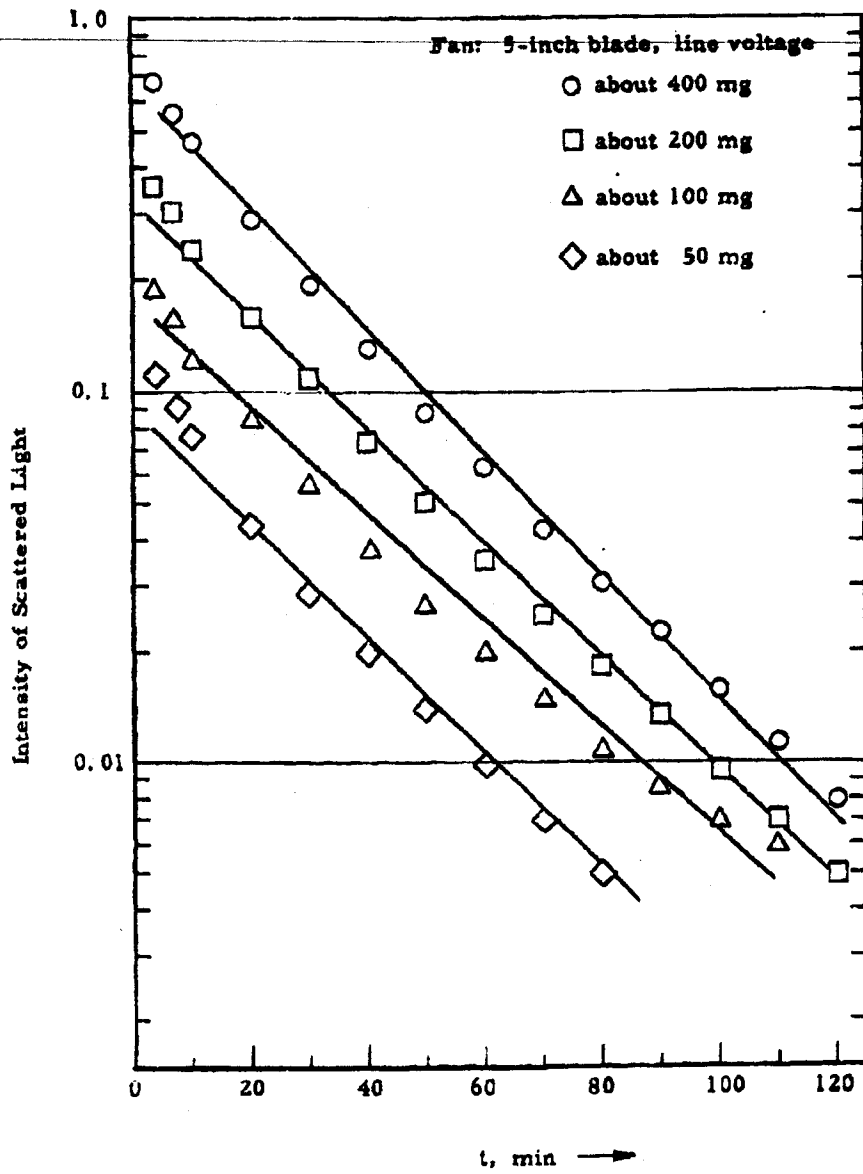


Figure 3.5 Experimental Curves for Light Scattered from K-Ferric Oxide Aerosol

and slope may also depend on the efficiency of the dispersing process. All these possibilities will have to be studied further before more definite statements as to the relative roles of agglomeration and settling may be made.

Several runs have been made under "tranquil" conditions (Series (2) above). In view of the sometimes very erratic behavior of these aerosols, it would be misleading to list quantitative results; rather, some significant qualitative statements may be advanced.

The "tranquil" decay runs were made with the fan in operation from several minutes before to a few minutes (usually 3 or 6) after the firing of the powder charge. In general, the behavior was that the two light signals were equal and decreased smoothly until the fan was shut off. At this point the rate of decrease of scattered light changed markedly to smaller values and the two signals became unequal (the lower usually, but not always, exceeding the upper), both decreasing in a nonmonotonic way. Signal excursions of 20 to 30 percent above and below the median line, lasting several minutes, were common.

The implication of the erratic behavior is clear: "clouds" form in the aerosol and drift at random through the light-scattering area. The significant point is that these clouds form spontaneously, since the light signals decrease smoothly during the time the fan is on, indicating a uniform concentration throughout the chamber. These effects were particularly severe for the larger powder charges (above 100 mg). There may be a "threshold concentration", above which an aerosol is unstable and tends to form clouds.

One may speculate as to the mechanism of formation of the clouds. Perhaps in the absence of stirring, soft eddy currents, which tend to trap aerosol particles, are set up by convection effects. Another possibility is that a highly charged particle attracts others which, however, do not actually collapse on this nucleus to form an agglomerate.

JUL 19 2013

Another significant result of the "tranquil" runs is the lack of separation of the two light signals. According to Section 3.2 the lower signal should lag the upper by a factor of two in time. This was not observed, although in most cases the aerosols "tried" to follow the rule for the first half hour or so. Evidently there exist convection currents in the chamber which impose a turbulent condition on the aerosol, at least late in the life of the aerosol when the larger particles have settled out.

Finally, some remarks on the dispersing system are in order. A general feature of all runs to date has been the presence of a "spike" on the light-scattering record at the instant of firing. These spikes\*, which varied from 2 to 4 times the equilibrium value at  $t = 0$ , were at first considered unimportant, arising perhaps from the mechanical shock of firing. During the course of the work, however, the speculation arose that spikes were due to a dense cloud passing the light-scattering region at high velocity. These high velocities, if present, are undesirable since it is likely that the powder is carried across the chamber and impacted on the floor opposite the dispersing gun.

Several runs were made without the fan (Series (1) above), incorporating various nozzles and other devices in an effort to slow down the dispersing gas stream. These runs generally tended to confirm the suspicion of a high velocity cloud since the relative amplitudes of the signals indicated that the aerosol was at first concentrated near the bottom of the chamber and "billowed up" from there during the course of the next half hour. None of the measures tried gave a really satisfactory improvement of the situation.

---

\* This behavior has been noticed in connection with other instruments - see Final Report, Vol. 4, Material Evaluation, GMI Contract No. DA-18-064-CM-2336, p. 26.

### 3.4 Conclusions and Plans for Immediate Future Work

The work accomplished thus far has served to establish operating conditions and to test our understanding of the aerosol decay process. In regard to the latter, it has been seen that the theoretical expressions set down in Section 3.2 have a considerable degree of validity, and they have been found very useful in interpreting the light-scattering data. Their usefulness would, however, be enhanced if the effect of agglomeration in the aerosol decay were known. Efforts will be made to take account, at least qualitatively, of agglomeration.

The work of the past quarter has also turned up some unexpected possibilities. For example the "jitter" or "noise" on the fan-on traces appears to depend on the type of powder dispersed and in any case seems too large to be accounted for by electronic noise. Thus, the possibility arises that statistical fluctuations in the number of particles involved in scattering are being observed. It is conceivable that statistical methods may be applied to extract certain information from the "jitter" values, namely, actual numbers of particles involved in scattering. This possibility will be explored during the next quarter.

The experimental program of the next quarter will also be concerned with systematic studies of humidity effects in aerosol decay. As a first step several runs are planned under the two extreme humidity conditions, both of which should be relatively easy to establish. In these runs, as in others planned, we shall generally use stirring throughout the run, with the fan operating at speed sufficient to overcome convection currents\*.

The powder dispersing system will be kept under review. While this system does not work as planned, it is probably satisfactory for dispersing small charges of powder.

\*The same procedure was adopted by Tanner et al., Biological Laboratories Interim Report 36, "Design, Construction and Operation of the Aerophilometer" Special Operations Division, Camp Detrick, June 1953, p. 6.



#### 4. VIABILITY STUDIES

##### 4.1 Presence of Bg Contaminants in Sm Powder

The results of several trials designed to measure the degree of heat inactivation of Sm powder aerosols were invariably heavily contaminated with Bg colonies. Careful examination of our equipment and techniques eliminated these sources as potential causes. Hypothetical reasoning led to the conclusion that the Sm powder itself contained Bg contaminants in the ratio of  $1:10^6$  to  $1:10^7$ . This level of contamination would not be evident during routine platings of the Sm powder which had a viable count of  $1 \times 10^{11}$ /gm. When dilutions were made of this powder to yield countable plates (30 to 300 colonies), the plates would show only pure cultures of Sm. On the other hand, analyses of samples in which 99.9999% of the vegetative Sm was destroyed by heat would yield plates in which Bg predominated.

This hypothesis was verified by preparing a liquid suspension of Sm powder in tryptose-phosphate broth which was immersed in a water bath at 75°C. Aliquots were removed at 5-minute intervals and plated in the appropriate dilutions to yield countable plates. The results showed a steady diminution in Sm counts relative to exposure intensity, and a constant level of Bg "contamination". At the end of 30 minutes the predominant organism on the plate was Bg.

This observation is significant only when considering circumstances where a given treatment would have different influences on vegetative cells compared to spores.

##### 4.2 Effect of Agitation and Compaction on Viability of Sm Powder

A series of trials were performed to determine the effect of compaction on Sm powder viability, with and without the addition of Cab-O-Sil. The additive was incorporated into the powder either by mechanical stirring

or in a fluid energy mill. Immediately after compaction, plate counts were run both on the original bulk samples and on pellets disintegrated in a tissue homogenizer. These results are shown in Table 4.1.

Table 4.1 Effect of Agitation and Compaction upon Viable Count of Sm Powders

Agitation	Additive	Viable Count/gram x 10 <sup>10</sup>		
		Bulk Powder	Compacted Pellet	Pellet Density
Untreated	none	4.11	2.84	0.617
Mechanical Stirring	none	3.01	2.15	0.624
	1% Cab-O-Sil	2.72	2.69	0.629
Fluid Energy Mill	none	3.13	3.39	0.625
	1% Cab-O-Sil	3.07	2.68	0.616

It is evident that neither coating with Cab-O-Sil nor compaction to 0.62 grams per cc density had any significant or deleterious immediate effects on Sm viability.

~~CONFIDENTIAL~~

DECLASSIFIED IN FULL  
Authority: EO 13526  
Chief, Records & Declass Div, WHS  
Date: JUL 19 2013

## 5. DISSEMINATION AND DEAGGLOMERATION STUDIES

### 5.1 General

During this period major emphasis was placed on wind tunnel experiments at Fort Detrick employing the 40-foot diameter test sphere. The objective of this program was to evaluate the General Mills GMI-3 fixture with Sm and P. tularensis, under environmental operational conditions which simulate actual operation of the prototype unit for dissemination of dry BW agents. In the evaluation such parameters as recovery factor, source strength, decay rate, VMMD, slopes with 95 percent confidence limits, LD<sub>50</sub>, probit slope and its 95 percent confidence limits will be determined. The Sm test series was conducted on April 4, 5, 6 and 9, 1962, while the P. tularensis series was conducted on May 4, 7, 8, 9, 10 and 11, 1962\*.

In preparation for the above activity, effort was also devoted during the period to developing the test fixture in our laboratory.

### 5.2 Evaluation of the General Mills, Inc. Test Fixture Disseminating Dry Sm and Dried Pasteurella Tularensis

At the present time statistical analyses of the results of the Fort Detrick test program are not available. However, the procedure and general results will be given in this report.

The over-all program was designed to test six operational treatments with dried Sm and dried P. tularensis. These included the two wind tunnel Mach numbers, 0.5 and 0.8, and three bulk densities: normal, approximately 0.43 grams per cc and 0.53 grams per cc. In the Sm test four

\* Technical Evaluation Division Test No. 62-TE-1602; MD Division No. 1927.

~~CONFIDENTIAL~~

~~CONFIDENTIAL~~

DECLASSIFIED IN FULL  
Authority: EO 13526  
Chief, Records & Declass Div, WHS  
Date: JUL 19 2013

replicates were obtained per treatment, while in the P. tularensis series six replicates were determined per treatment. In all of the tests, each treatment was run daily.

Apparatus for these tests included, in addition to the GMI-3 fixture, related equipment used for compacting powders to the required bulk densities and mechanically breaking down the resulting slugs into fine agglomerates on the order of 2000 microns and less and basic particles. Approximately 0.8 grams of these samples were placed in the GMI-3 fixture and disseminated at a feed rate of 30 lb/min. These apparatus are further discussed in our previous report<sup>10</sup>.

A blowdown wind tunnel and auxiliary equipment such as air storage tanks and pumps were erected for these experiments adjacent to the test sphere. The test section into which the organisms were disseminated, shown in Figure 5.1, has a 2-inch by 4-1/2-inch cross-section. Actual ejection of the material into the air stream was achieved during a four-millisecond period.

Environmental conditions inside the sphere during these tests were maintained at 75 degrees Fahrenheit temperature, essentially atmospheric pressure and 35 percent relative humidity.

Samples of the generated aerosols were obtained with ABP-30 samplers\* filled with 20 milliliters of tryptose saline during Sm trials and 20 milliliters of gelatine peptone phosphate during P. tularensis runs. One minute samples were taken at the midpoints of 4, 18, and 32-minute time periods at a flow rate of 12.5 liters per minute. Four sampling stations were operated concurrently.

Single stage impactors (SSIs) with cutoffs of 3, 5, 7, and 9 microns and a GP-20 total collector were used with 25 milliliters of sampling fluid. This group of samplers were operated only at the 4-minute time period.

\*All-glass impinger preceded by a British pre-impinger.

~~CONFIDENTIAL~~

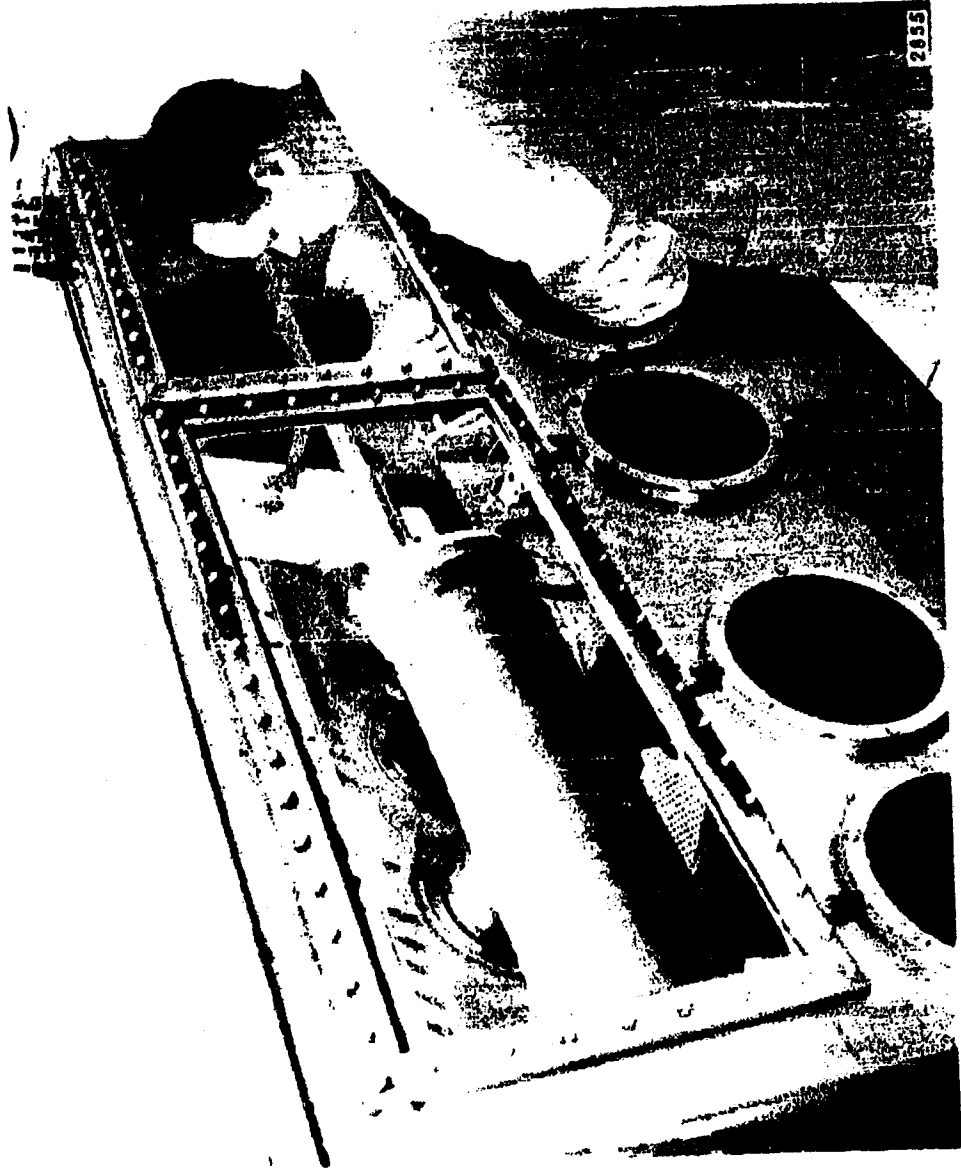


Figure 5.1 Wind Tunnel Test Section Located in Glove Box  
of Spherical Test Chamber at Fort Detrick

~~CONFIDENTIAL~~

DECLASSIFIED IN FULL  
Authority: EO 13526  
Chief, Records & Declass Div, WHS  
Date: JUL 19 2013

The four ABP-30 samples taken during each time interval were pooled while the SSIs and GP-20s were assayed separately.

In the original P. turlarensis test program, it was planned that eight Hartley strain guinea pigs in the weight range, 250 to 370 grams, would be exposed at each of three time periods for each trial after the first day. However, because of the high recovery factors during the initial experiments, a new test plan for the animals was required. As a result they were only exposed on the final three days.

### 5.3 Preliminary Results

#### 5.3.1 Sm Tests

In addition to determining the viability of generated aerosols in the sphere, control samples of the normal and compacted materials were taken and assayed. By this method data were obtained on the effects of two factors which enter into this evaluation program, 1) the compaction of the particulate material to densities up to 0.53 grams per cc, and 2) the aerodynamic breakup process during dissemination. Each factor can be analyzed separately or the two can be combined to demonstrate the over-all performance for any one treatment.

In studying the mean values of the control counts, there appears to be little, if any, effect on viability due to compaction of Sm. Count values ranging from  $123.98 \times 10^9$  to  $127.35 \times 10^9$  organisms per gram were obtained at bulk densities 0.53 grams per cc and 0.43 grams per cc, respectively. At normal bulk density a value between these was obtained.

Mean values of the recovery factors at the 4-minute time period varied randomly in a range from 2.52 to 3.36 percent for the six treatments, while for the AP #10 fixture the value was 3.50 percent. At the two wind tunnel Mach numbers studied, there appears to be little difference in the viability of the generated aerosol.

~~CONFIDENTIAL~~

**CONFIDENTIAL**

DECLASSIFIED IN FULL  
Authority: EO 13526  
Chief, Records & Declass Div, WHS  
Date: JUL 19 2013

At first glance these recovery factors may be deceiving and therefore may appear quite low. Thus, it is necessary to explain that the recovery factor is directly proportional to the quantity of fill which has a particle size less than 5 microns. In this case the particle size distribution, based on a Whitby centrifuge analysis, showed that only 6.5 percent by mass of the material consisted of particles less than 5 microns in size. In addition, the mass median diameter and geometric standard deviation of the material was 16.6 microns and 1.95, respectively.

### 5.3.2 P. Tularensis Tests

Preliminary data similar to that presented above are also available for the trials with P. tularensis. In the case of the control samples, the mean values at each bulk density, based on five replicates, range from  $13.52 \times 10^{10}$  to  $20.11 \times 10^{10}$  organisms per gram for bulk densities ranging from the normal condition to 0.53 grams per cc, respectively. The results show an increase in organism count with increase in compaction, an effect which is unexplained at this time.

Mean recovery factors for this series of tests based on six replicates range from 28.59 to 35.77 percent. There is an indication that recovery decreases at the higher bulk density due to aerodynamic breakup; however, for the combined effects of compaction and breakup, increasing recovery factors were obtained with increasing bulk density. Again in this case, wind tunnel Mach number appears to have no relative effect on recovery.

The mean recovery factor obtained with the AP #10 reference fixture was 28.44 percent.

The mass median diameter of the sample material was 4.3 microns while the geometric standard deviation was 1.38. Approximately 70 percent by mass of the material was less than 5 microns in size.

**CONFIDENTIAL**

**CONFIDENTIAL**

DECLASSIFIED IN FULL  
Authority: EO 13526  
Chief, Records & Declass Div, WHS  
Date: JUL 19 2013

In spite of the fact that the particle size distribution was fairly fine, the recovery factor obtained in these tests is considered to be quite high and exceeded our expectations.

A more complete presentation of the results from both the S<sub>m</sub> and P. tularensis tests will be made at a later date when the complete statistical analyses have been finished. At that time it should be possible to make definite conclusions as to the operational characteristics and effectiveness of the GMI-3 fixture and wind tunnel combination.

**CONFIDENTIAL**



~~CONFIDENTIAL~~

DECLASSIFIED IN FULL  
Authority: EO 13526  
Chief, Records & Declass Div, WHS  
Date:

JUL 19 2013

## 6. CONTINUATION OF EXPERIMENTS WITH THE FULL-SCALE FEEDER FOR COMPACTED DRY AGENT SIMULANT MATERIALS

### 6.1 Introduction

Experimental work with the full-scale feeder continued during this reporting period. The information obtained substantiates previously reported<sup>11</sup> conclusions that the design concept under study is quite feasible. Performance was evaluated at powder flow rates ranging from 20 lb/min up to 49 lb/min. Air flow rates from three to nine scfm were investigated. Particular attention was devoted to performance during the starting period and various operating procedures were tried in an effort to minimize the delay in reaching full feeding rates.

In general, the procedures employed in conducting these test runs are the same as described in the Seventh Quarterly Progress Report<sup>12</sup>. A few modifications were made to the unit and an improved arrangement for collecting the discharged material was devised.

### 6.2 Equipment Modifications

The original plan was to try three diameters for the discharge opening - 0.375, 0.500 and 0.750 inches. The smallest diameter of 0.375 inch was soon determined to be too small. The 0.500 and 0.750 diameters were both satisfactory but it was found that the gas pressure within the unit using the 0.750 diameter opening was significantly lower. Consequently, a decision was made to use the latter opening in all of the test runs being reported herein and to tentatively establish this diameter as the one to use in the airborne disseminator.

For the tests reported in the Seventh Quarterly Progress Report<sup>13</sup> the motivating gas was admitted directly into the disaggregator section of the unit through a hole near the top of the cylinder. For the tests reported herein, the unit was modified in that an aerating ring was installed in the

~~CONFIDENTIAL~~

center of the cylinder as shown in Figure 6.1. This ring contains 32 orifices each 0.040 inch in diameter which are positioned uniformly around the ring on both sides. Four additional orifices are mounted 1.75 inches directly above the powder discharge opening. The objective in using the aerating ring is to obtain better mixing of gas and powder. To accommodate this aerating ring it was necessary to remove the wire wall scrapers and the 6-inch baffles which were mounted between the disaggregator disks. The scrapers were eliminated but the four long baffles were replaced by eight 1.25 x 2-inch baffles, four being mounted on each disk.

The initial arrangement for collecting powder for weighing was to use a short length (approximately 24 inches) of 1.25-inch inside diameter tubing between the discharge on the unit and the top of the 50-gallon drum. The top of the drum was covered with a sheet of muslin to allow the gas to pass out of the drum without carrying out the powder. Since this technique could conceivably affect the powder flow at the point of discharge from the disseminator, a new technique was devised in which the tubing was omitted and the powder allowed to flow directly into a stand pipe six inches in diameter mounted on the collection drum as shown in Figure 6.2. The end of the stand pipe is placed four inches below the discharge tube on the disseminator. The cover of the drum is well ventilated by many holes and the muslin filter cloth is placed on top of this cover. A chamber is formed above the cover by means of plastic sheeting so that the gas can be withdrawn from between the plastic and the filter cloth using a vacuum cleaner. With this technique the powder has been observed to flow freely into the collection drum in a well-defined stream or jet.

### 6.3 Test Results

The results obtained with the full-scale feeder during this reporting period are summarized below. This summary is followed by a more detailed discussion of the data.

~~CONFIDENTIAL~~

DECLASSIFIED IN FULL  
Authority: EO 13526  
Chief, Records & Declass Div, WHS  
Date: JUL 19 2013

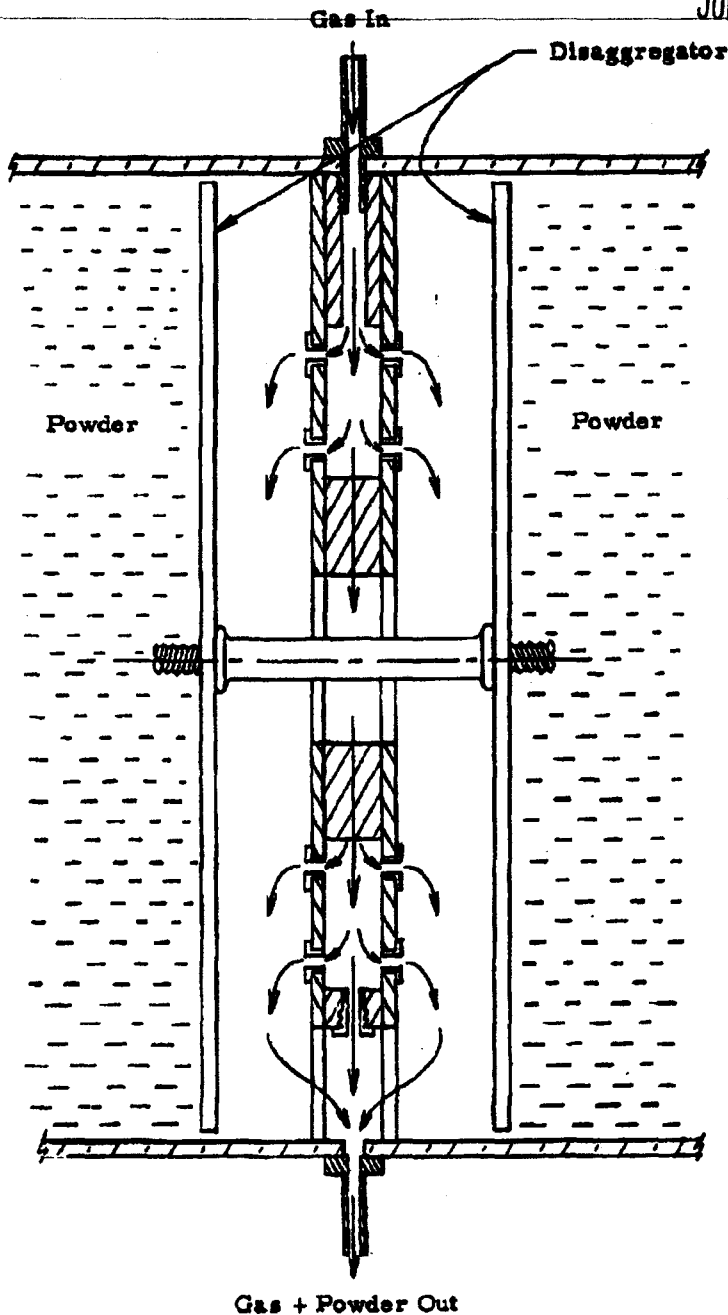


Figure 6.1 Aerating Ring Installed in Center Section of Full-Scale Experimental Feeder

~~CONFIDENTIAL~~

JUL 19 2013

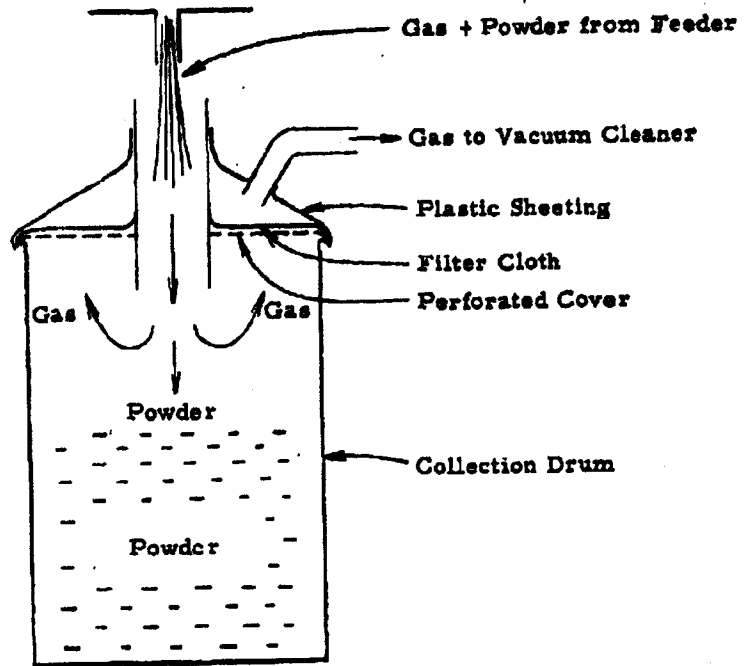


Figure 6.2 Arrangement for Collecting Powder without Direct Connection between Collection Drum and Discharge Tube

DECLASSIFIED IN FULL  
Authority: EO 13526  
Chief, Records & Declass Div, WHS  
Date:

JUL 19 2013

- 1) A total quantity of approximately 2,600 pounds of talc were successfully loaded into and discharged from the feeder under a variety of operation conditions.
- 2) The torque and power required to drive the feeder were found to be well within the initial objectives. The torque was usually less than 100 ft-lbs and the power less than 0.5 hp.
- 3) A discharge opening of 0.75 inch in diameter gives good performance over the feed rates investigated.
- 4) Powder was discharged successfully with gas flow rates ranging from three to nine scfm.
- 5) A gas flow rate of at least six scfm was found to be necessary in order to minimize the delay in attaining full powder discharge rate.
- 6) The delay in attaining full powder discharge rate was also minimized by pre-pressurizing; i. e., the operating pressure was established in the cylinder before starting to feed powder.
- 7) The gas requirements were found to be compatible with the space which will be available for storing gas within the airborne disseminator.
- 8) No significant difference in performance was observed for operation where the gas flow was started before feeding the powder as compared with operation where gas and powder were started simultaneously.
- 9) The feeder operated satisfactorily for powder flow rates ranging from 20 to 49 lb/min.
- 10) The gas pressure measured within the cylinder was found to vary from approximately 0.3 to 1.1 psig depending upon the powder and gas flow rates used.

The experimental feeder was operated successfully under various conditions of powder and gas flow rates. The range of operating conditions covered is shown in Figure 6.3 by plotting each run as a point on a family of curves showing air-to-powder ratios (by weight) for various powder and gas flow rates. The highest powder feed rate obtained was 49 lb/min.

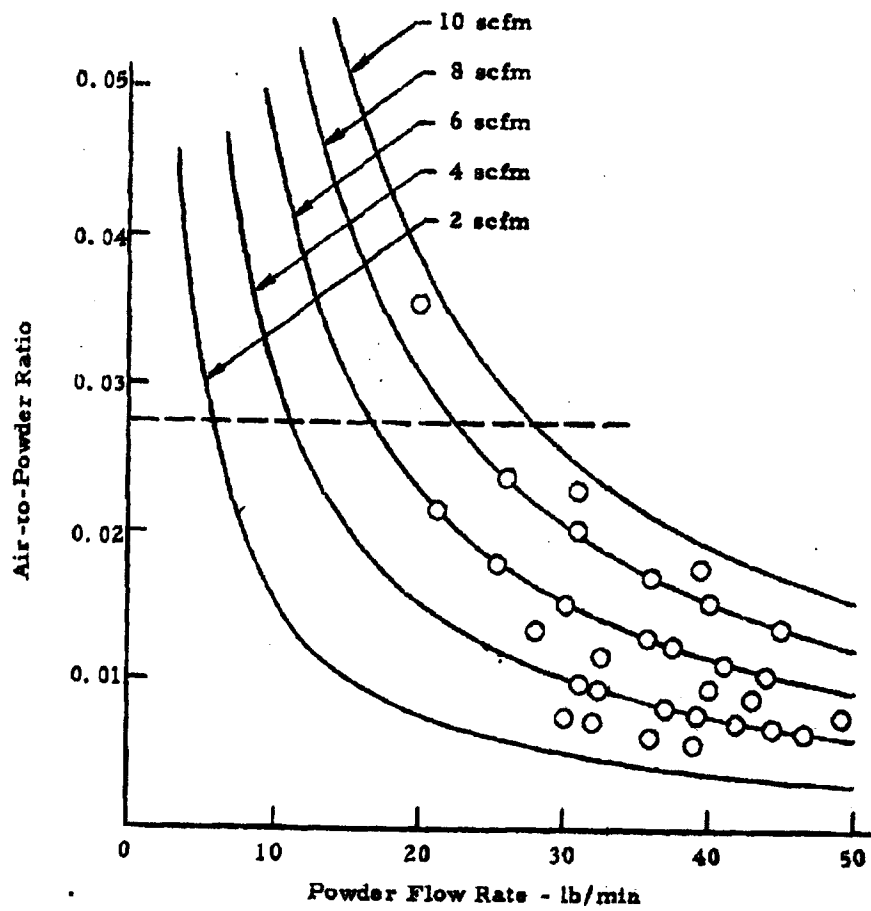


Figure 6.3 Air-to-Powder Ratios for Various Feeder Operating Conditions (actual test runs with talc are plotted)

~~CONFIDENTIAL~~

DECLASSIFIED IN FULL  
Authority: EO 13526  
Chief, Records & Declass Div, WHS  
Date: JUL 19 2013

This is not the maximum capacity of the feeder but it is the highest rate attainable with the present variable speed drive when the feeder is loaded with material at a density of approximately 0.48 g/cc. Operation up to rates as high as 60 lb/min are planned by compacting to higher density during loading.

Typical powder flow rate curves are presented in Figure 6.4. The plotted data were obtained by recording the time at which a certain amount of powder had accumulated in the collection drum. In most cases time was noted for each 5-lb increment. The curves were selected from many such curves which have been drawn to illustrate typical performance for a variety of operating conditions. The data for any given run produce a well-defined straight line indicating that the flow from the feeder is very uniform.

The driving torque and speed were observed for all test runs so that the input power requirement could be determined. The torque was observed to vary over a range from 15 to 100 ft-lb with one exception where the torque rose to 240 ft-lb. This excessive torque prompted an investigation which revealed that the thread clean-out feature which removes powder from the feed screw was plugged. This deficiency was corrected and there was no re-occurrence of an excessively high torque value.

The maximum driving speed used on any test was 24 rpm. The horsepower requirement based upon 24 rpm and 100 ft-lb is 0.46 hp.

One series of test runs was conducted using nitrogen rather than air as the motivating gas. As was expected, there was no observable difference in performance of the feeder when using nitrogen as compared to air.

The curves in Figure 6.3 can be used to show how the motivating gas flow employed in laboratory tests compares with the allowable flow when the gas supply is limited as it will be in the airborne disseminator. The design study has shown that it will be feasible to carry a gas storage bottle capable of supplying 113 standard cubic feet of nitrogen. When based on the maximum payload capacity of 350 lb, this gives a ratio of 2.75 percent by weight

~~CONFIDENTIAL~~

Material: "Mistron Vapor" Talc

Compaction Density: 0.45 to 0.48 gm/cc

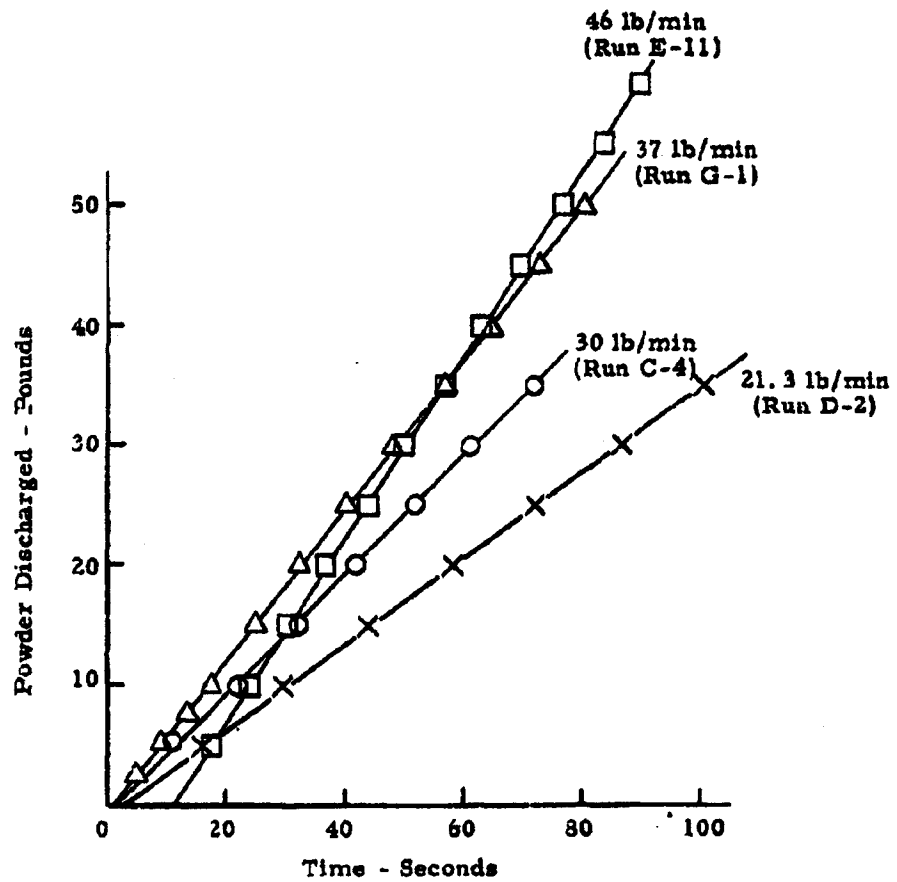


Figure 6.4 Powder Discharge Rate



of nitrogen-to-agent payload. The horizontal dashed line in Figure 6.3 for this ratio is well above the conditions at which the feeder has been demonstrated to operate satisfactorily.

The gas is used most efficiently when the gas flow rate is reduced as the powder feed rate is decreased. However, it is possible to operate the feeder over a wide range of powder flow rates with a fixed gas flow rate without exceeding the 2.75 percent ratio. For example, if the gas flow were set at six scfm the powder feed could range from 17 lb/min up to 50 lb/min or more. In order to stay within allowable limits, the gas flow rate must be quite low when the powder feed rate reaches 10 lb/min. Anticipating a problem, the feeder performance was tested at the low gas flow rates.

In switching to the lower gas flow rates (three and four scfm) it was observed that there was a delay in reaching the full powder flow rate at which the unit was being operated. To obtain a measure of this delay, the flow rate curve is drawn as a straight line extended back to intersect the time-axis as shown in Figures 6.4 and 6.5 where time is measured from the instant at which the unit is started. It is desirable to obtain performance such that full flow rate is established in the shortest possible time.

Up to this point the operating procedure was to establish the desired gas flow before starting the drive system which feeds the powder. When operating in this manner the pressure within the feeder is essentially equal to atmospheric pressure before the powder starts feeding. When feeding starts the pressure increases to a value which depends upon both the powder flow rate and the gas flow rate. If the approximate operating pressure exists in the cylinder before starting the powder feeding, the delay in reaching full powder flow rate should be a minimum. Therefore, tests were made in which this internal pressure was established prior to feeding powder by restricting the air flow just below the discharge opening of the feeder. The restriction was removed at the same time that the powder feeding drive was turned on.

Material: "Mistron Vapor" Talc  
Compaction Density: 0.48 gm/cc  
Cylindrical Pressure: 6.4 cm Hg  
Air Flow: 4 scfm  
Powder Flow: 43 lb/min

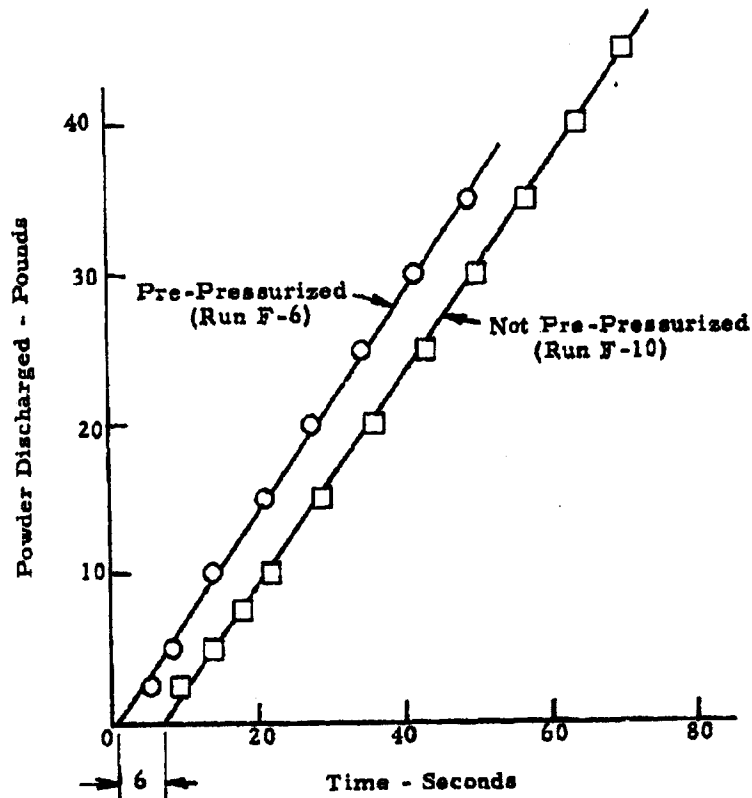


Figure 6.5 The Effect of Pre-Pressurizing on the Time Required to Establish Uniform Flow

**CONFIDENTIAL**

DECLASSIFIED IN FULL  
Authority: EO 13526  
Chief, Records & Declass Div, WHS  
Date: JUL 19 2013

The pre-pressurizing technique proved effective as shown in Figure 6.5. These flow rate curves were obtained with four scfm air flow and 43 lb/min powder flow for both cases. The vertical separation of the two curves represents approximately five pounds of material. This indicates that without pre-pressurizing about five pounds more talc was stored in the disaggregator section of the feeder during the initial seven or eight seconds of operation for the test where pre-pressurizing was not used.

When operating the feeder for a series of runs in which the same powder feed rate was used for each run while the gas flow rate was varied, it was observed that the delay in attaining full powder flow rate, as determined from plotted flow rate curves, tends to be longer for the low gas flow rates than for the high. During these runs the following data were obtained:

- 1) Time from starting feeder drive to the instant when powder began to flow from discharge opening.
- 2) Time from stopping feeder drive to termination of powder flow.
- 3) Amount of powder discharged after feeder drive was stopped.

The results of these observations are presented in Figures 6.6 and 6.7 only to illustrate trends in performance characteristics; the amount of data involved is insufficient to justify using these curves to obtain lag-times or post powder-flow quantities for application in any related studies.

The time-lag data are presented in Figure 6.6. The lower curve shows how the observed time from start of feeder to start of powder flow was almost independent of the rate of gas flow used. The delay was approximately one second. The delay in stopping, however, increased significantly as the gas flow decreased below five scfm. The delay observed for eight scfm was approximately 2.25 seconds. It increased slightly to approximately 2.75 seconds at five scfm, but rose sharply to about eight seconds at three scfm.

**CONFIDENTIAL**

**CONFIDENTIAL**

DECLASSIFIED IN FULL  
Authority: EO 13526  
Chief, Records & Declass Div, WHS  
Date: JUL 19 2013

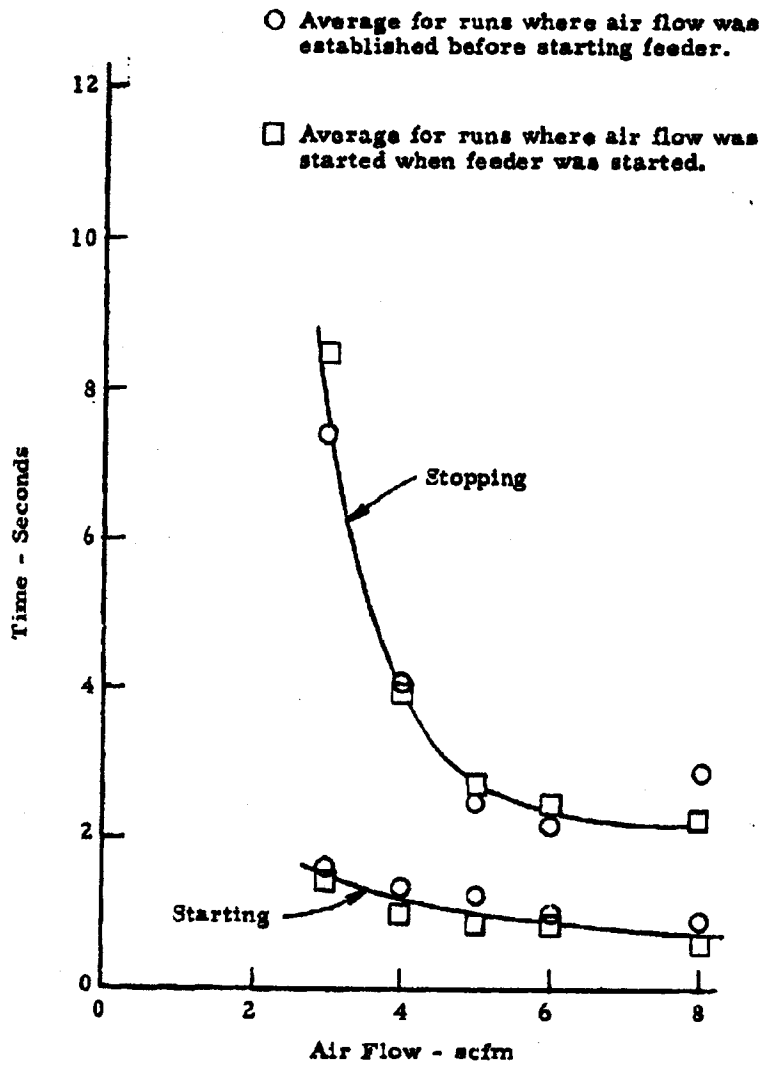


Figure 6.6 Time Lag in Powder Flow

**CONFIDENTIAL**

- Average for runs where air flow was established before starting feeder
- Average for runs where air flow was started when feeder was started

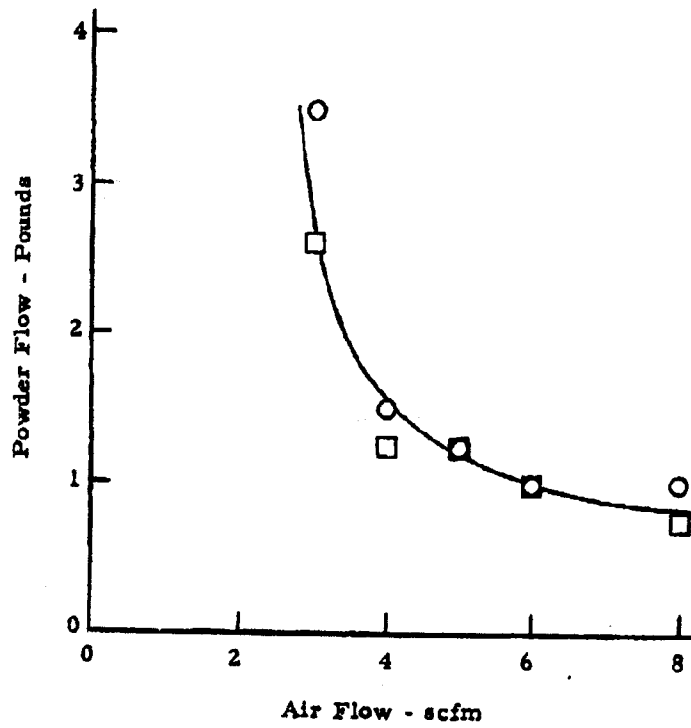


Figure 6.7 Powder Flow After Stopping Feeder Drive

Figure 6.7 shows the amount of powder collected after stopping the feeder as measured for various gas flow rates. The curve shows that the air flow rate must be above five scfm if the amount of powder is to be minimized.

Another factor which could conceivably influence the initial delay is the relative timing of the start of gas and powder flow. This aspect of the problem was studied by making two types of runs, the first with the gas flow established prior to feeding powder, and the second with gas and powder flow started simultaneously. Data from both types of runs were used in plotting the curves in Figures 6.6 and 6.7. The data show that there was no significant difference in performance for the two methods of operation. This was also true when performance was evaluated on the basis of flow rate curves drawn for the runs.

#### 6.4 Plans for Future Work

All of the experimental feeding experiments with the full-scale unit have been conducted with talc compacted to a density of approximately 0.45 g/cc. A hydraulic press is now being fabricated which will make it possible to compact to higher densities when filling the feeder. Tests will be performed at a density of 0.6 g/cc or higher when the press is available. This density will result in a powder flow rate of at least 60 lb/min when the feeder drive is set for maximum speed.

A supply of powdered sugar has been obtained and plans are to run the feeder with powdered sugar to determine if performance varies with the material being handled. Since powdered sugar is more hygroscopic, these tests will not be conducted until the air dryer for humidity control is installed and operating. The dryer installation has been delayed because the vendor failed to meet his quoted delivery date.

██████████

DECLASSIFIED IN FULL  
Authority: EO 13526  
Chief, Records & Declass Div, WHS  
Date: JUL 19 2013

Some of the future feeding experiments will be performed with the laboratory model of the disseminator which the Engineering Department is now fabricating. This unit is to be a full-scale prototype of the inner tank assembly of the airborne disseminator and will operate on the same basic principles employed in the unit which has been thus far used to demonstrate the feasibility of feeding compacted dry powder materials.

## 7. DESIGN STUDIES ON A DRY AGENT DISSEMINATING STORE

The design concept of an external aircraft store for disseminating dry agent material from a compacted state was described in our Fifth Quarterly Progress Report<sup>14</sup>. Section 6 of this current report contains a discussion of the experimental evaluation of the basic concept using a full-scale model. This experimental program has demonstrated that the proposed concept is feasible. Some of the principal components of an airborne disseminator based on this concept were described in the Seventh Quarterly Progress Report<sup>15</sup>. During this eighth reporting period progress was made toward integrating these components into a well-designed disseminating store as described in the following paragraphs.

### 7.1 General Arrangement for the Airborne Dry Agent Disseminating Store

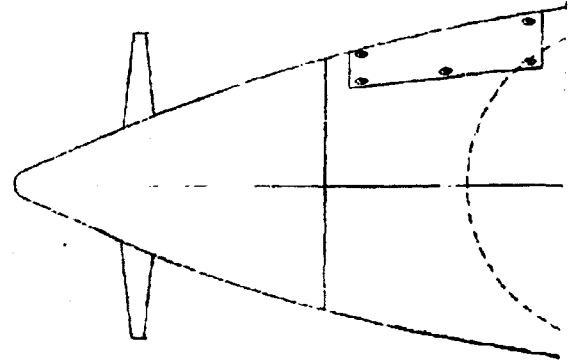
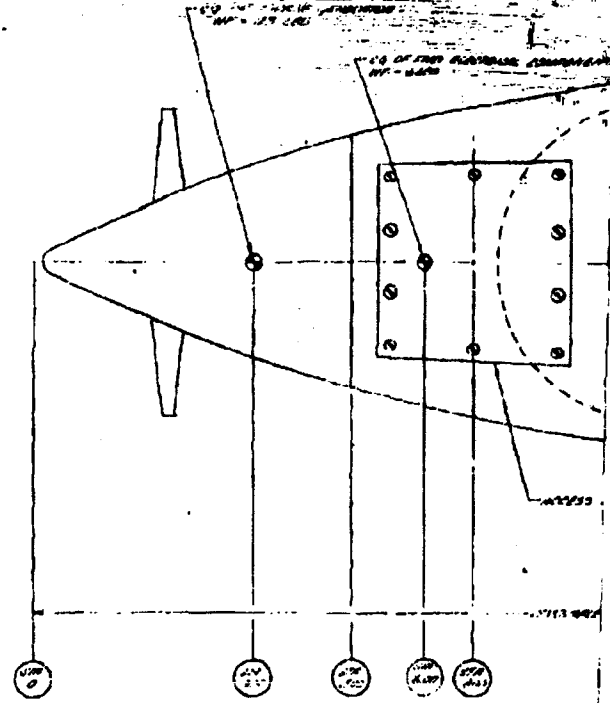
A preliminary general arrangement for the airborne dry agent disseminating store is shown in Figure 7.1 (GMI Dwg SK-29100-612). The basic structure is an aluminum shell that provides a mounting skeleton for the inner tank assembly, the gas supply system, the turbine generator, the actuator and the necessary control apparatus.

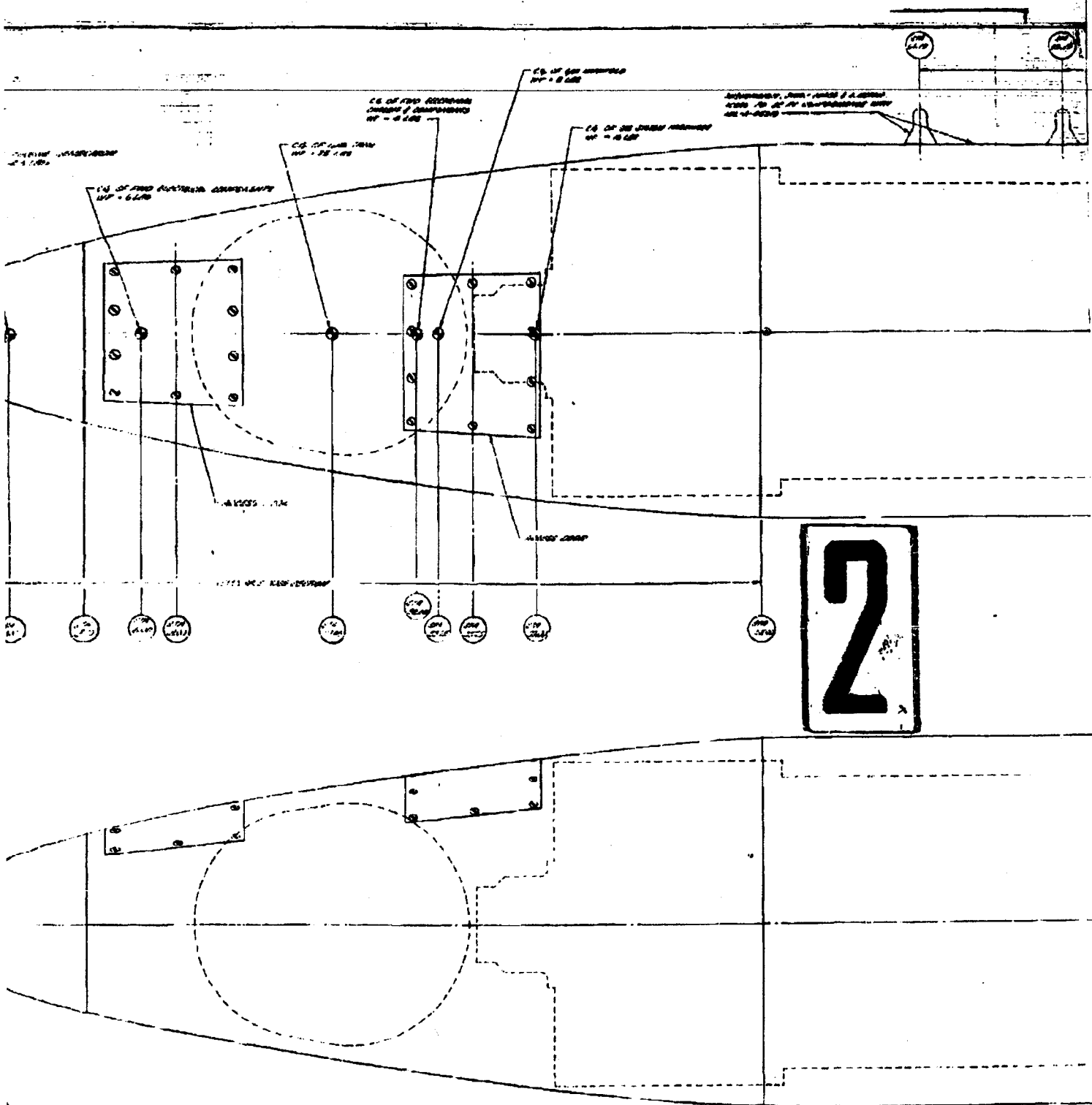
The external skin is a 180-inch long aerodynamically shaped tank that has the same dimensions as defined for the 150-gallon Fletcher Aviation Co. Store No. 21-150-6024. This is a store that utilizes both 14- and 30-inch lug spacing for aircraft mounting. Two horizontal fins are mounted on the aft section to augment tank stability during flight.

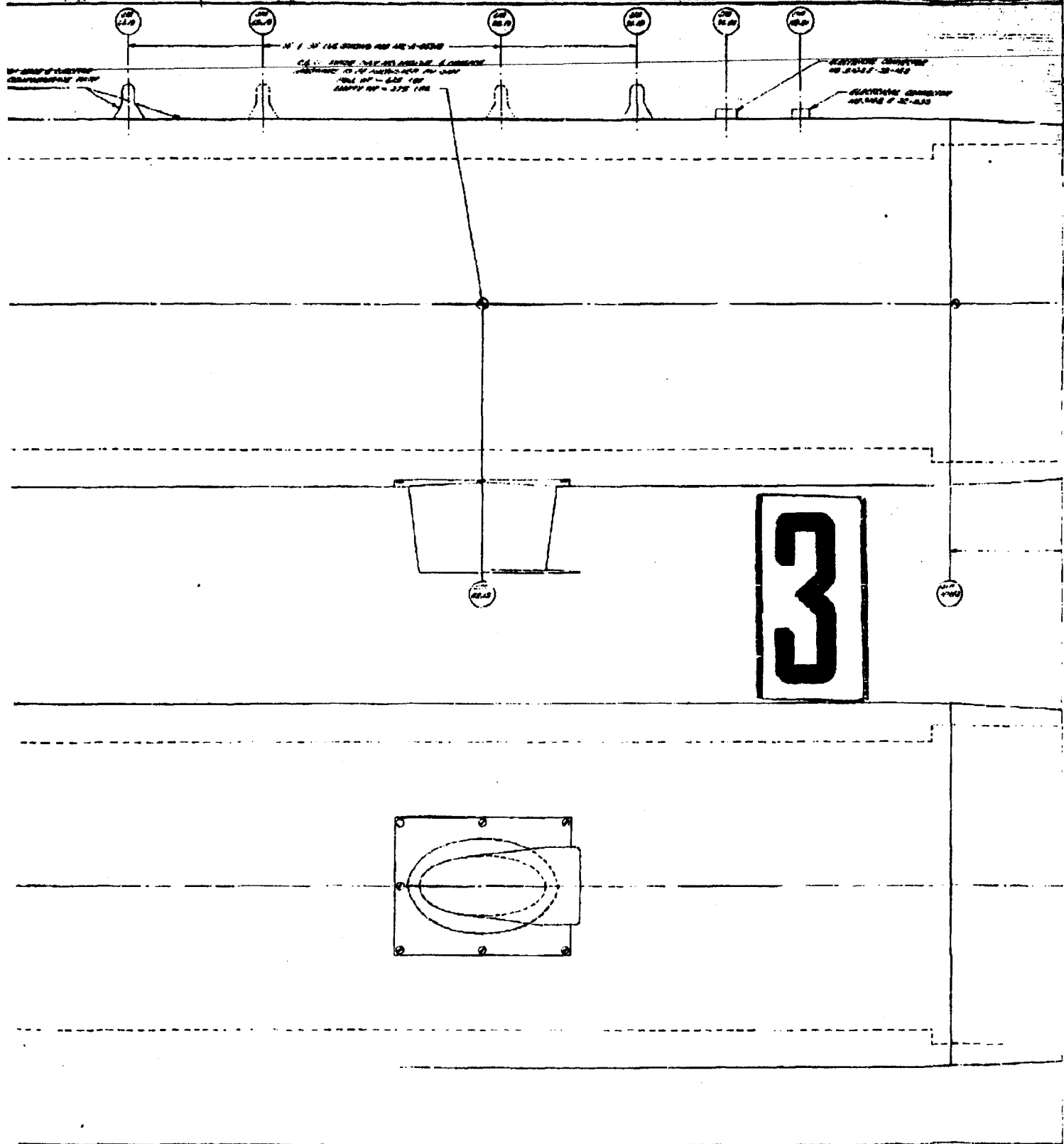
The store (exclusive of turbine generator assembly) consists of the forward, the center and the aft sections which extend from stations 13.0 to 52.0, stations 52.0 to 109.62, and stations 109.62 to 180, respectively. This particular sectioning of the tank was required to provide access to both ends of the inner tank for charging with the compacted dry agent. To minimize assembly time, the joints at stations 52.0 and 109.62 will be



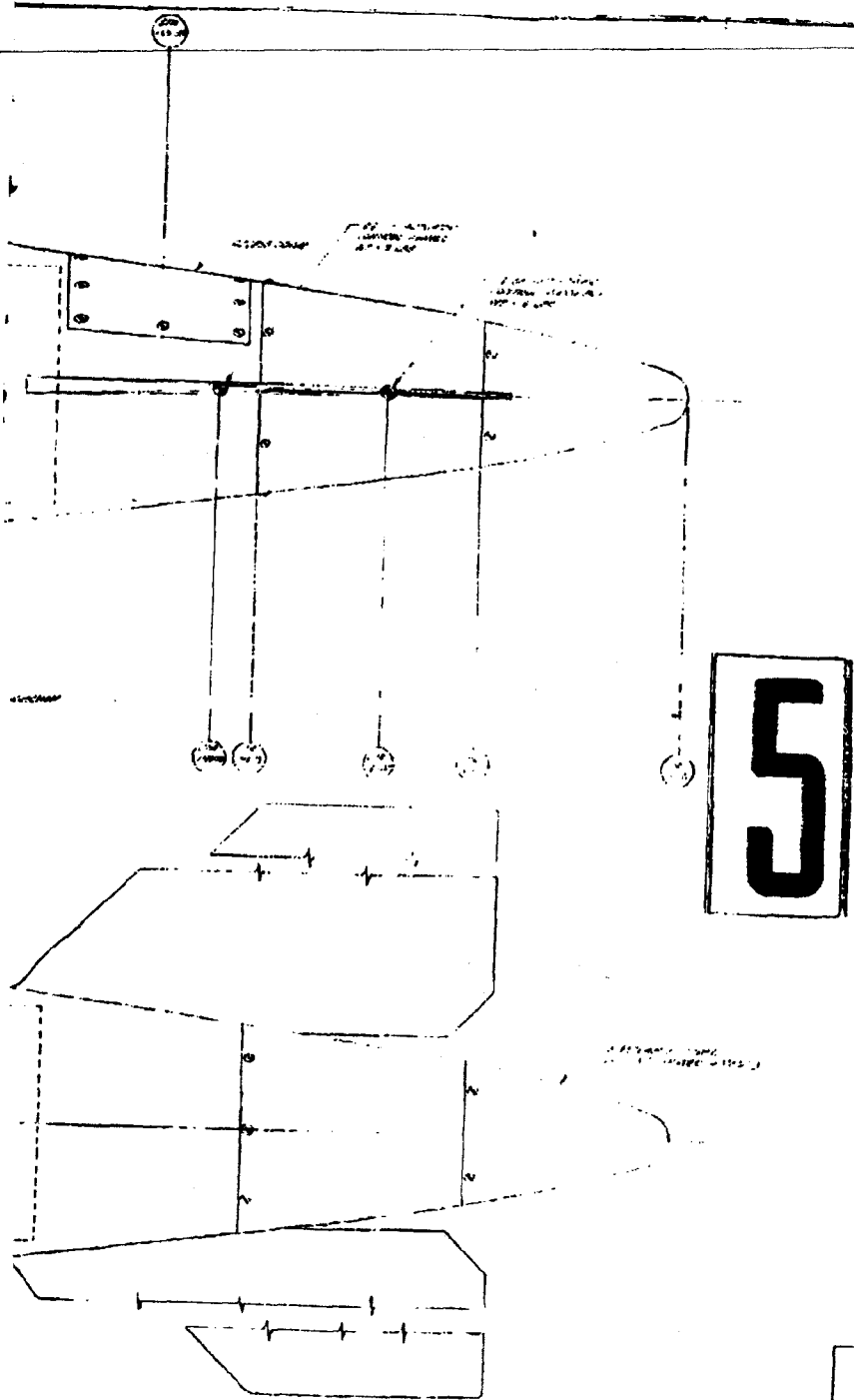
Page determined to be Unclassified  
Reviewed Chief, RDD, WHS  
IAW EO 13526, Section 3.5  
Date: JUL 19 2013











			(19)
		175	175
		175	175
		175	175

equipped with a bayonet-type joining feature. In separating or joining the tank sections all that will be required is the loosening of a locking screw and rotating the end section approximately 22.5 degrees. Gas line and cable disconnects will be provided on the fore and aft sections from the center section. Access doors are located in the nose and tail sections at positions determined on the basis of necessity and ease of manipulation of the various system components and controls. Locations of various system components were evaluated during this period on the basis of available space, system operation and over-all effect on the store center of gravity.

The forward section from stations 13.0 to 52.0 contains the primary gas system hardware and the necessary electrical components for power distribution. The ram air turbine generator is mounted at station 13.0.

The center section, with section joints at stations 52.0 and 109.62, will provide the primary support structure and will house the inner tank assembly which contains the agent payload and the feeding mechanism.

The aft section from stations 109.62 to 180 contains the rotary actuator assembly, the actuator control electronics (including a control panel), and the ground and generator power distribution system electronics. Gas system control electronics are also included in this section. A special coupling is required between the actuator and the drive screw for easy separation when the aft section is removed for the dry agent loading operation.

#### 7.1.1 Ram Air Turbine Generator

The ram air turbine generator is the same 4.5 kva, 115/200 volt, 400 cps, 3-phase generator made by General Motors, Allison Division, which is used on the GMI liquid agent disseminating store. However, it will be necessary to modify the exterior of the generator housing to make it conform to the shape of the dry agent disseminator. The generator is thoroughly described in GMI Specification GMS-29100-020, a copy of which was appended

JUL 19 2013

to our Fifth Quarterly Progress Report<sup>16</sup>. A new specification, GMS-29100-611 has been issued for the generator to go into the dry agent disseminator because of the modified exterior.

### 7.1.2 Dry Nitrogen System

Dry nitrogen is used in the disseminator to fluidize the disaggregated powder and transport it out of the store through the discharge tube into the slip stream. The nitrogen system schematic drawing is presented in Figure 7.2. The system consists of a high-pressure storage vessel, manual and solenoid shut-off valves, a pressure regulator, a critical flow orifice, a manifold check valve and a manifold with high velocity jets. These basic components are supplemented by pressure gauges, relief valves, pressure switches, etc. required for safe control of the system. Following is a description of the system as it will function in the disseminator.

Dry nitrogen is introduced into the pressure vessel through the charging valve and stored at 3000 psi pressure. The manual shut-off valve is closed during charging and storage to insure that no leakage will occur. During pre-flight preparation of the disseminator the manual valve is opened and the solenoid valve is used to stop and start the flow of nitrogen during operation of the disseminator.

The rate of flow of nitrogen to be used during operation is determined by adjusting the pressure regulator to be predetermined pressure before take-off. This controlled pressure in conjunction with the critical flow orifice will give a constant rate of mass flow which is independent of the downstream pressure.

The pressure regulator is adjusted while nitrogen is flowing. A supply of nitrogen is introduced into the checkout valve from an external supply, passes through the pressure regulator, and is exhausted to the atmosphere through the ground checkout discharge. This method of adjustment does not bleed nitrogen out of the system's pressure vessel and will not build up pressure in the inner tank assembly.





When the nitrogen is released from the pressure vessel, isentropic expansion will cause significant cooling. Under certain conceivable conditions this temperature drop could cause variations of mass flow rate of from 10 to 20 percent. If this problem should arise it can be corrected by adding heat to the gas. For these reasons a heater jacket, laced to the pressure vessel, has been added to the system. If actual test experience shows that the heater is unnecessary it can easily be removed from the system.

A flow indication pressure switch is mounted in the manifold upstream of the critical flow orifice to show whether or not the solenoid valve is open and sufficient pressure is available for proper flow.

The cylinder pressure switches operate when the cylinder pressure exceeds the normal operating level. This would happen if the orifice which discharges the mixture of powder and nitrogen became plugged. The switches will actuate a relay to shut off the gas solenoid valve.

The line pressure switch is used as a safety back-up for the cylinder pressure switches. Its actuation point will be set below the relief valve setting.

The manifold check valve allows free flow of nitrogen into the cylinder but prevents back flow so that the nitrogen system will not become contaminated by agent entering through the manifold.

The pressure equalizing lines allow flow from the mixing chamber to the spaces behind the pistons so that the pistons will not work against a gas pressure differential.

The nitrogen flows through the manifold and out into the mixing chamber via the high velocity jets. The jets will give a velocity of from 150 to 350 ft/sec depending on the flows and the size of the jets used. This velocity will cause swirls in the mixing chamber and will tend to cause good mixing of powder and gas as the powder comes off the disaggregator cutters.

The nitrogen pressure vessel can store a total of 12.65 pounds or 175 scf of nitrogen at 3000 psi and 70°F. The amount available for mixing with the powder is 9.62 pounds (or 2.75 percent of the 350-pound powder capacity) because of allowances which must be made for changes of flow rate with temperature change, errors in pressure measurement and regulation, and a requirement for a residual pressure to be maintained in the vessel.

With the regulated pressure range of 30 to 100 psig on the fixed orifice, the available range of flow rates is 5.7 scfm minimum to 14.6 scfm maximum. Figure 7.3 shows how this range of nitrogen flow rate combines with the powder feed rate to give various ratios of nitrogen to powder flow. The ratio can be kept at 2.75 percent up to powder feed rates of 38 lb/min by increasing the gas flow as the powder flow is increased. At feed rates above 38 lb/min the maximum flow rate of 14.6 scfm governs. The ratio then decreases until the minimum percent is 1.76 at a feed rate of 60 lb/min.

If the gas-to-powder ratio is allowed to vary from 2.75 down to one percent, only two nitrogen flow rates are needed, 5.7 and 14.6 scfm.

A preliminary study of the standard practices employed in charging high-pressure vessels indicates that there are two practical methods of charging the pressure vessel with dry nitrogen for this application. One is to compress the gas from standard 2200 psi bottles directly into the pressure vessel with a portable compressor. The second method is to order 6000 psi bottles and use these to top off the vessel after filling part way with the readily attainable 2200 psi bottles.

The relative merits of these methods are now being investigated and the necessary facilities will be made available for laboratory and field operation of the nitrogen system.

7-8

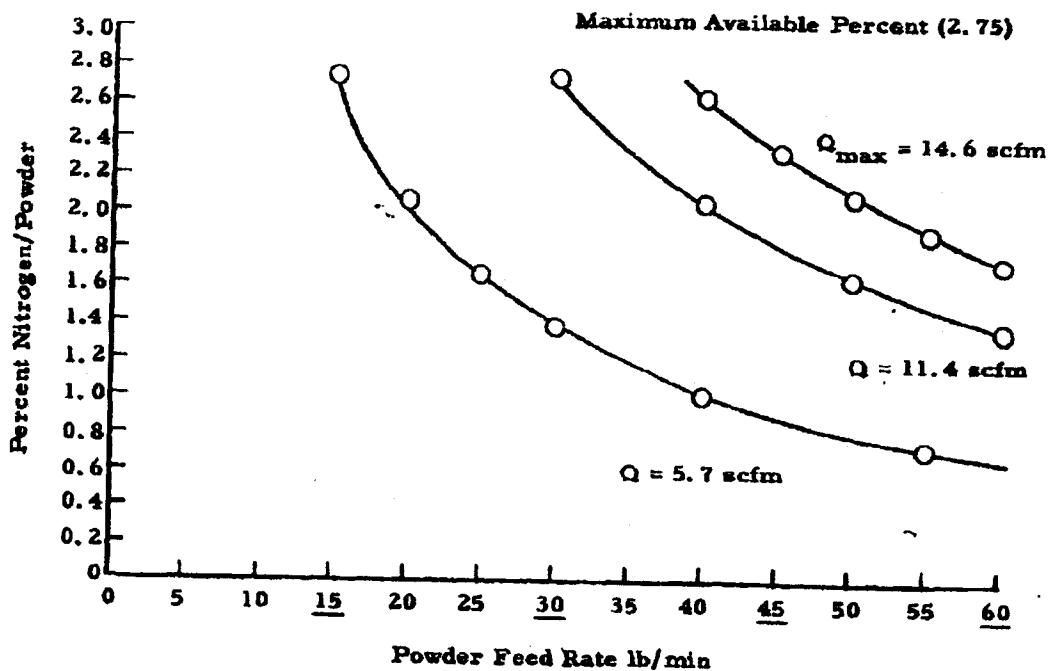


Figure 7.3 Ratio of Nitrogen-to-Powder Flow Rates Obtained from Powder Feed Rate versus Available Nitrogen Flow Rates ( $Q$ )

DECLASSIFIED IN FULL  
Authority: EO 13526  
Chief, Records & Declass. Div., WHS  
Date: JUL 19 2013

### 7.1.3 Center Section

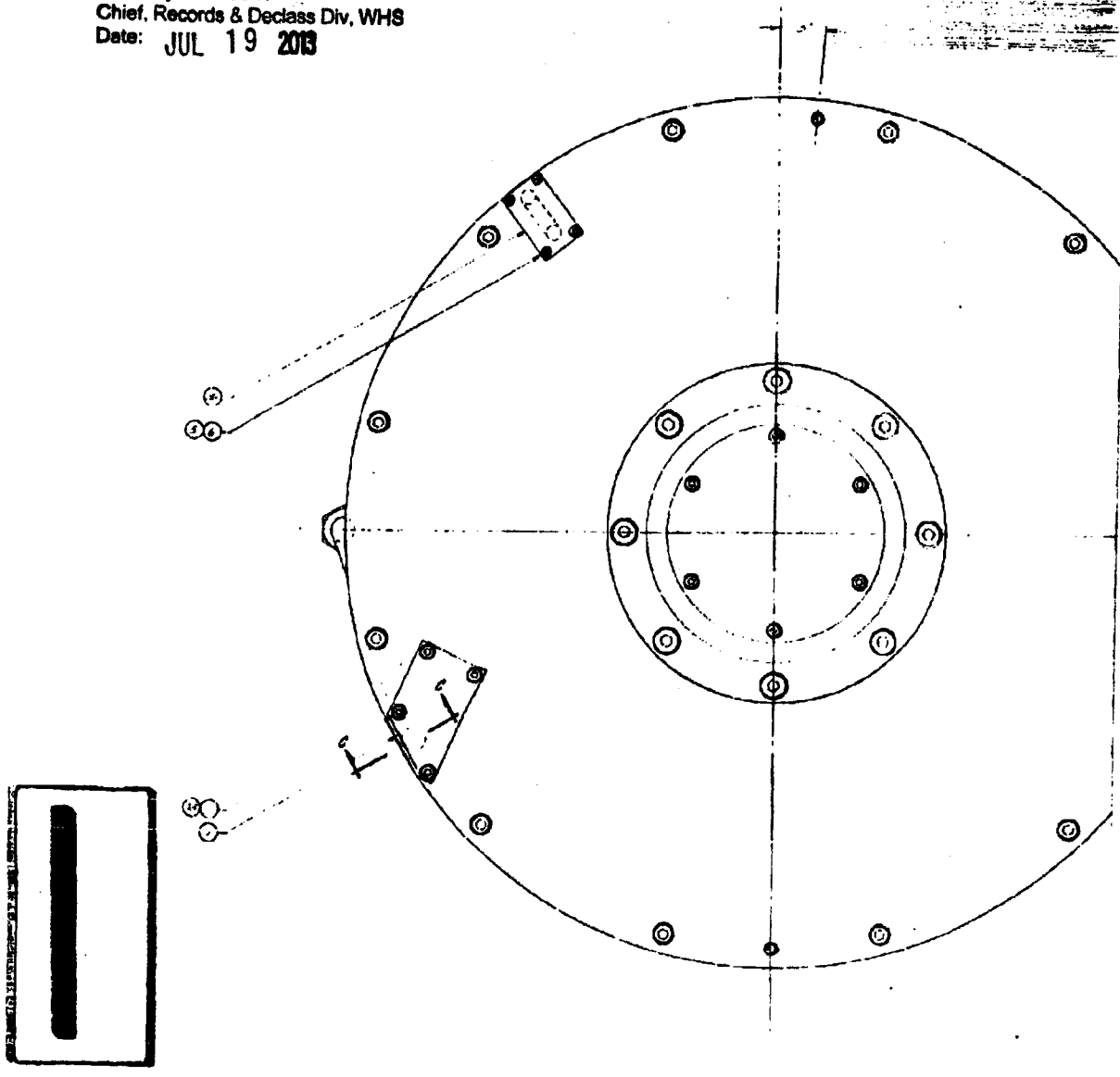
The center section of the store is the basic disseminator. It extends from station 35.5 to station 131.75. It is actually somewhat longer than the length arrived at by subtracting the nose and tail sections from the overall length because the ends of the inner tank assembly extend beyond the stations where the nose and tail joints are made. The construction of this center section will be similar to the liquid agent disseminating store in that the space between the inner cylinder and the external shell will be filled with a foamed-in-place rigid plastic. A strong-back and stiffening rings will be used to satisfy structural requirements. Nitrogen lines and electrical conduits will be placed between the inner and outer shells.

The inner tank assembly consists of a cylinder with removable end plates, a drive screw running the length of the cylinder, two pistons with threaded hubs riding the drive screw, and a disaggregator with cutters in disks keyed to the drive screw at the center. The design of this assembly will be similar to the second experimental model shown in Figure 7.4 and described in Section 7.2. The essential differences in the airborne model as now envisioned will be that a one-piece cylinder with a removable gas manifold will be used to eliminate the center joint shown in the experimental unit, and double O-ring seals will be used on the end plates and all other attachments to the cylinder.

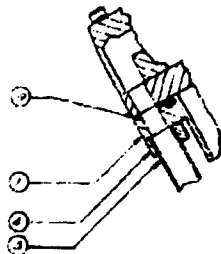
The inner cylinder is 83.25 inches long and 16.5 inches inside diameter. A volume of 9.1 cubic feet is available within the cylinder for containing compacted dry agent material.

The fluidized powder will be discharged through a short tube extending from the bottom of the center section. An NACA study<sup>17</sup> of discharge tubes of this type showed that in order to obtain good separation of the discharge flow from the boundary layer of the store, the tube should be housed by an air foil capped with an air-flow control plate. In the case of the disseminator it is necessary that the tube shroud be large enough to house the valve mechanism and, consequently, a tapered elliptical shroud is considered to be the best compromise design. Such a shroud is shown in Figure 7.1.

DECLASSIFIED IN FULL  
 Authority: EO 13526  
 Chief, Records & Declass Div, WHS  
 Date: JUL 19 2013

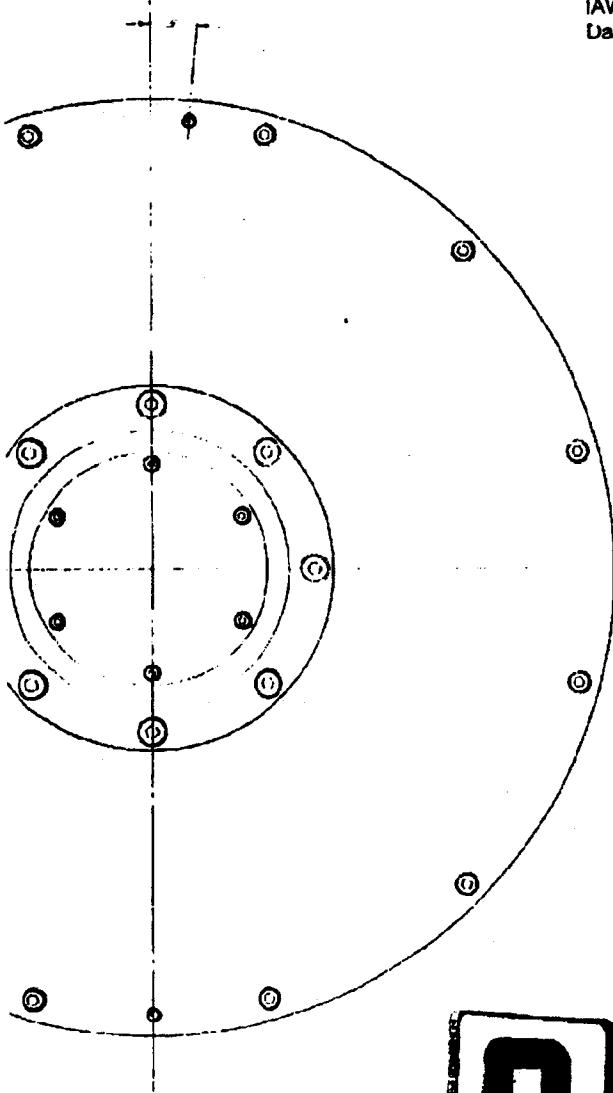


- ▽ 1. 1/2" DIA. HOLE LOCATED 1/2" FROM CENTER
- ▽ 2. 1/4" DIA. HOLE LOCATED 1/2" FROM CENTER
- ▽ 3. 1/8" DIA. HOLE LOCATED 1/2" FROM CENTER
- ▽ 4. 1/4" DIA. HOLE LOCATED 1/2" FROM CENTER
- ▽ 5. 1/8" DIA. HOLE LOCATED 1/2" FROM CENTER

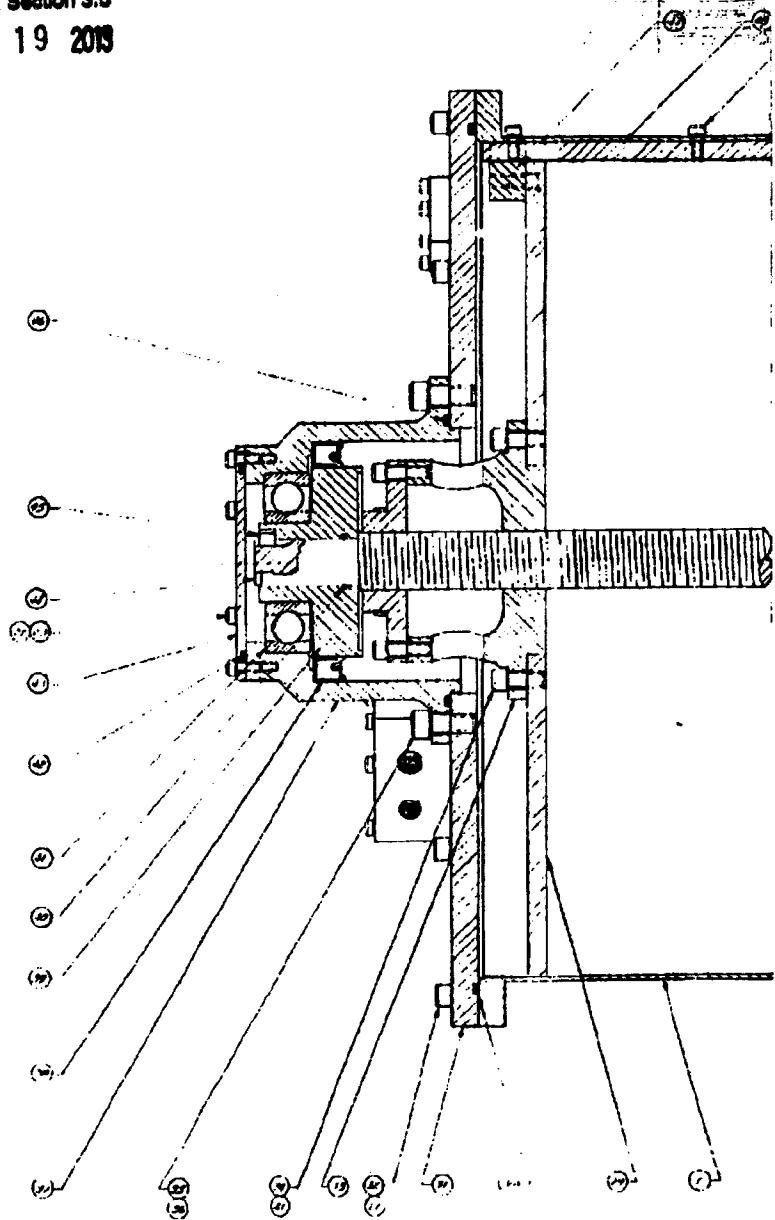


CONFIDENTIAL

Page determined to be Unclassified  
Reviewed Chief, RDD, WHS  
IAW EO 13526, Section 3.5  
Date: JUL 19 2013

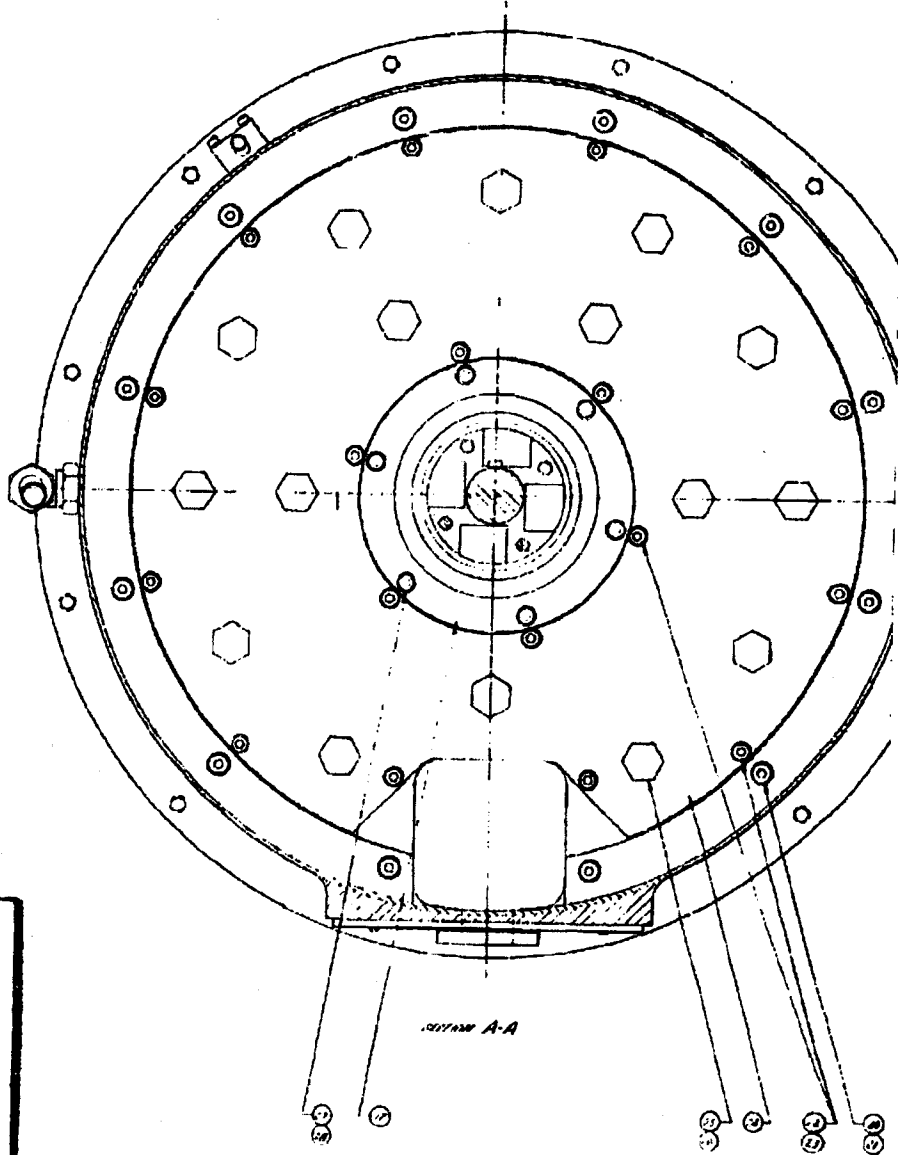
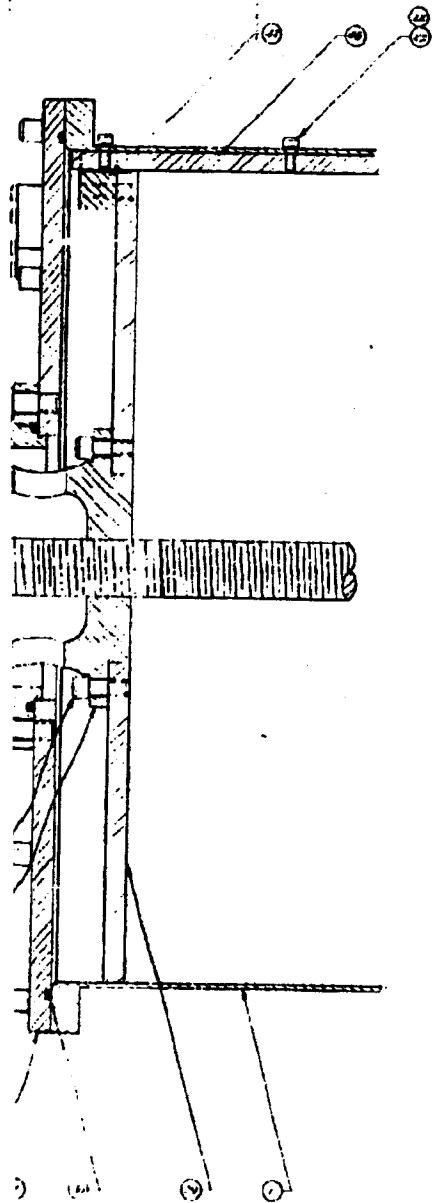


2



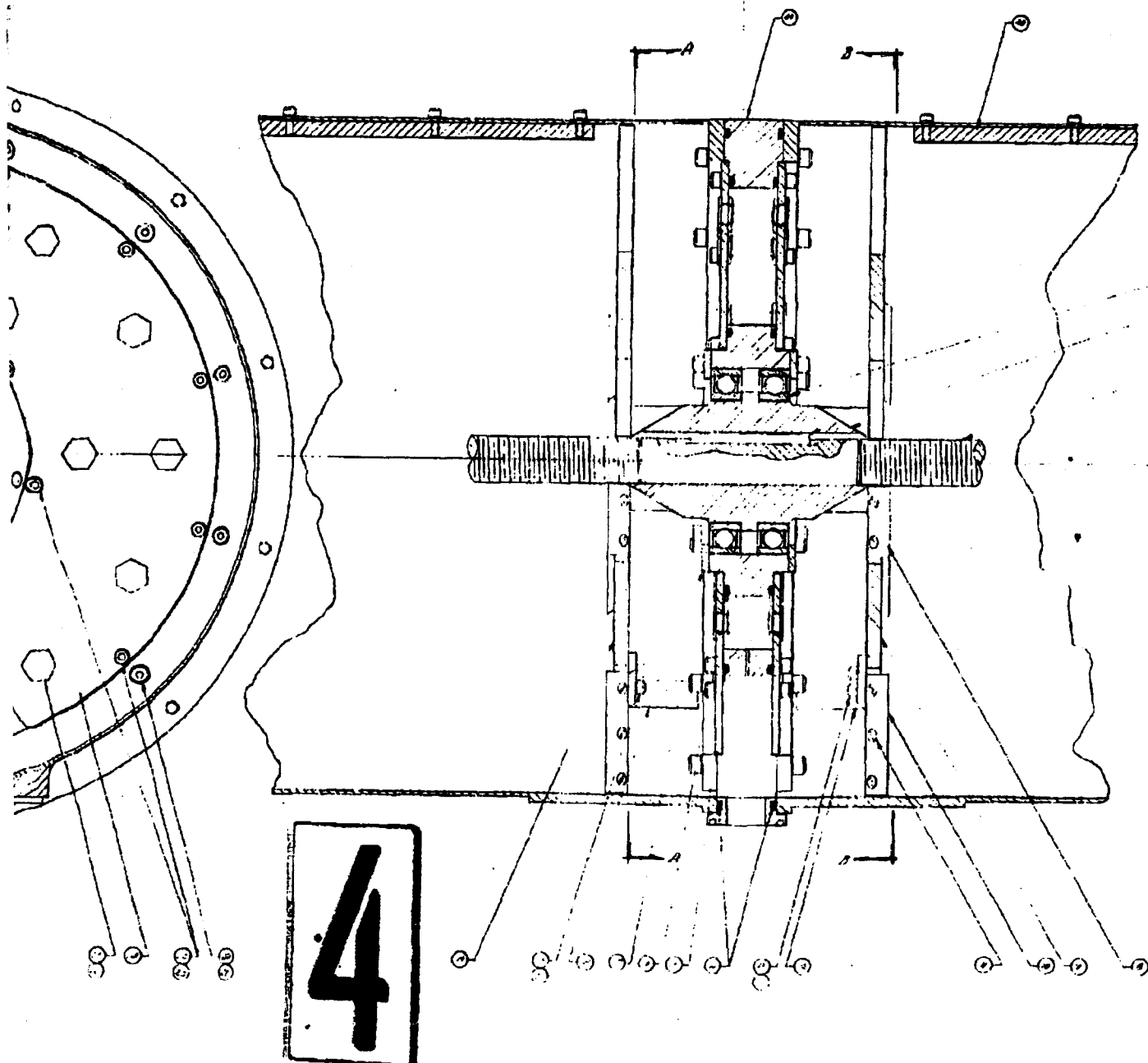
Page determined to be Unclassified  
Reviewed Chief, RDD, WHS  
IAW EO 13526, Section 3.5  
Date:

JUL 19 2013



3

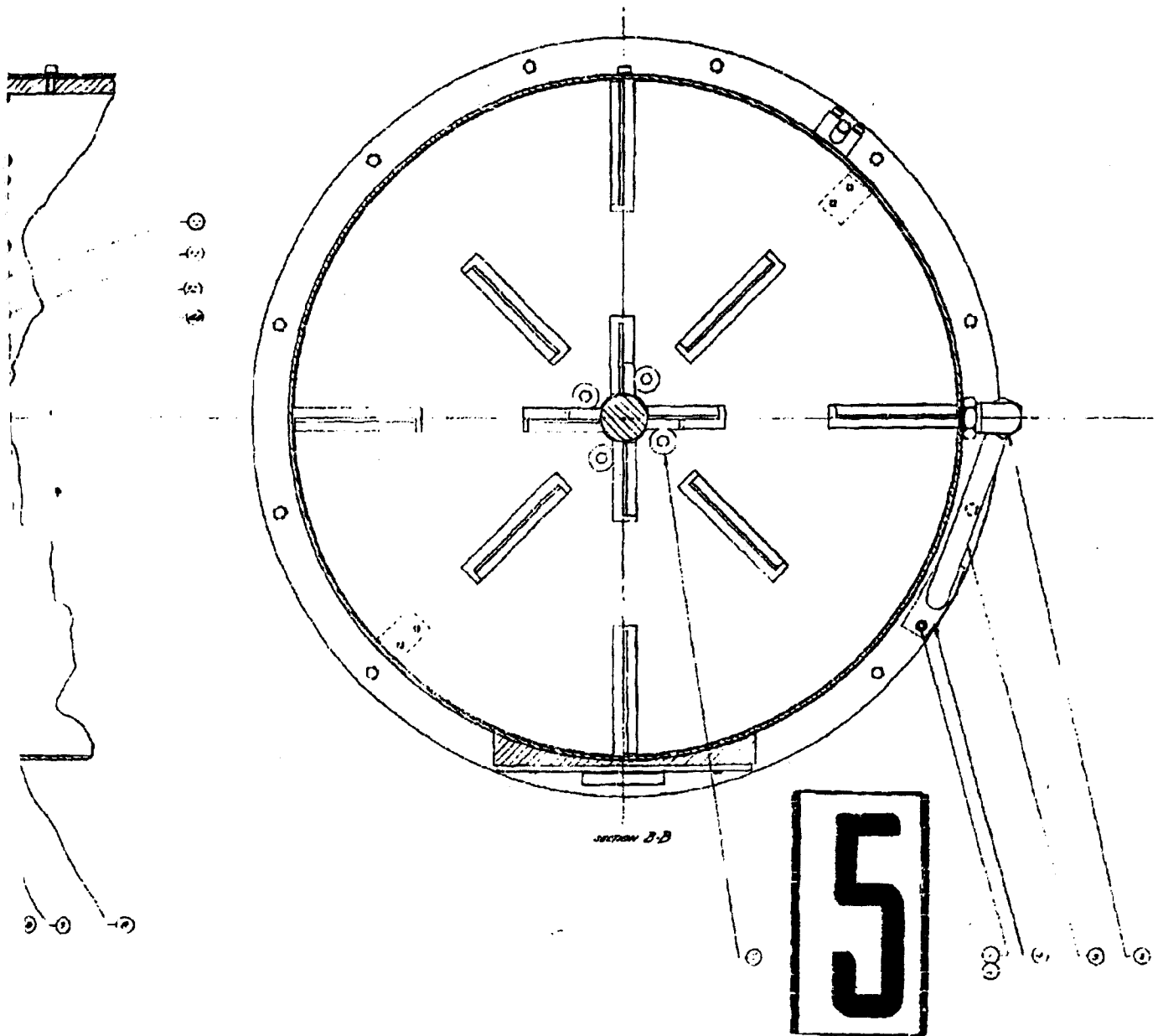
Page determined to be Unclassified  
Reviewed Chief, RDD, WHS  
IAW EO 13526, Section 3.5  
Date: JUL 19 2013



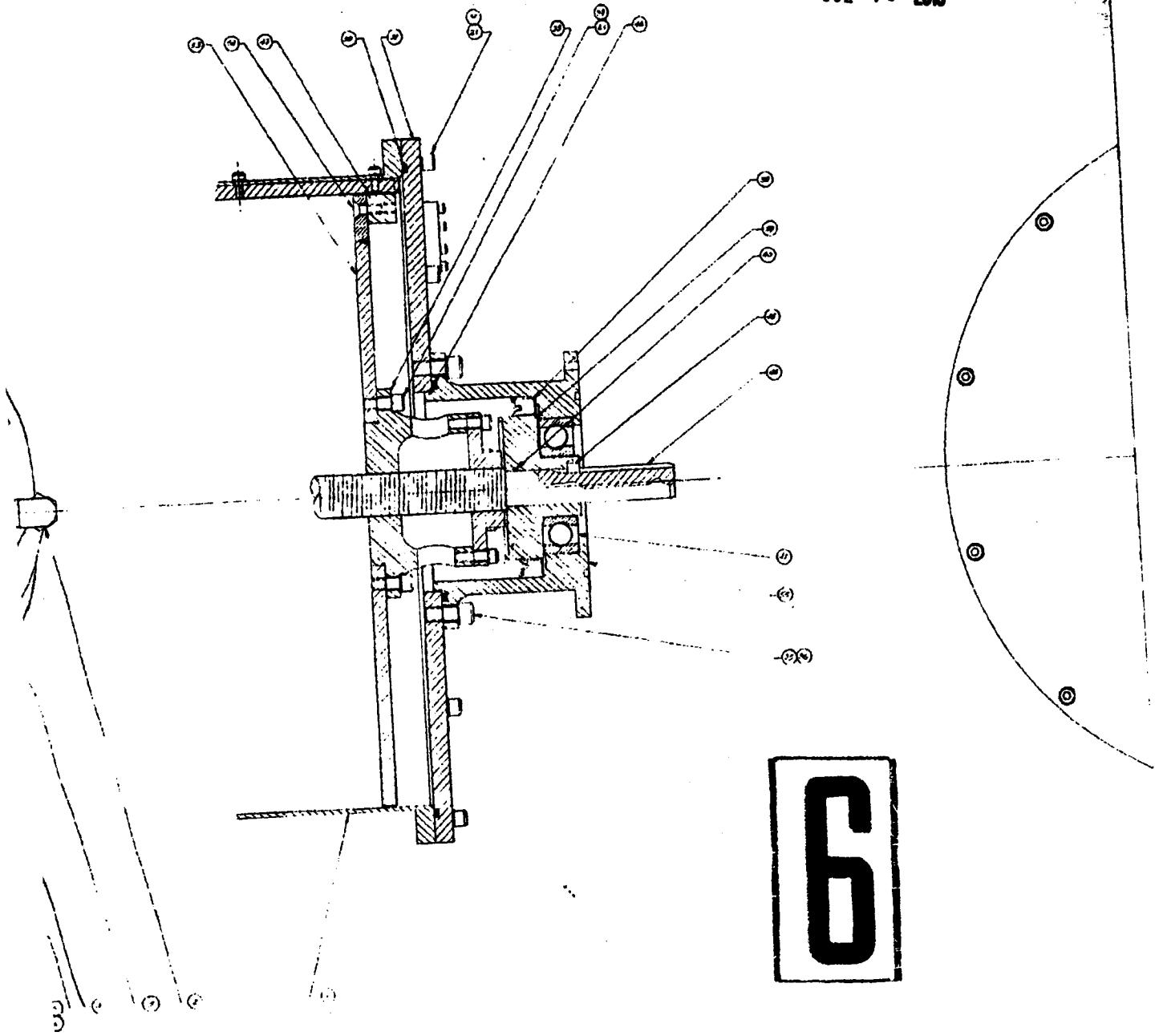


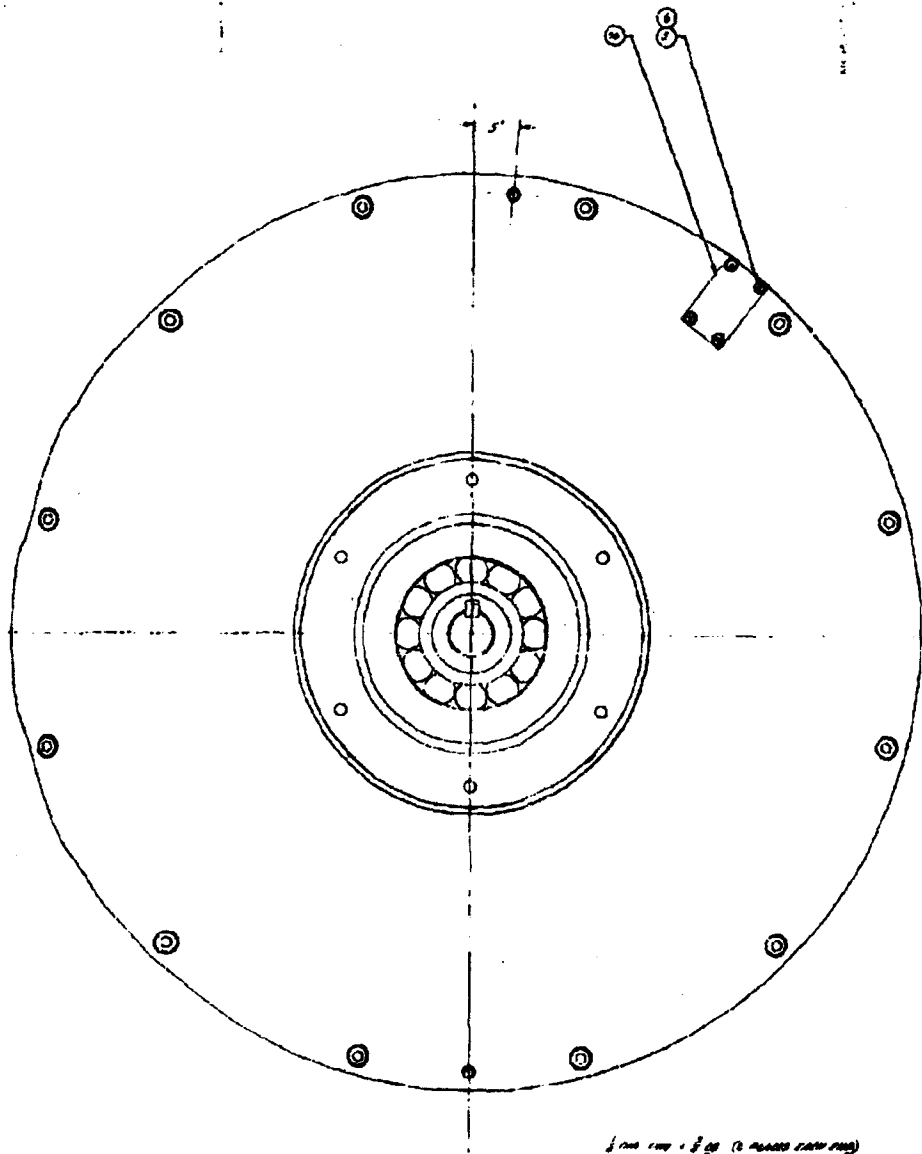
CONFIDENTIAL

DECLASSIFIED IN FULL  
Authority: EO 13526  
Chief, Records & Declass Div, WHS  
Date: JUL 19 2013



DECLASSIFIED IN FULL  
Authority: EO 13526  
Chief, Records & Declass Div, WHS  
Date: JUL 19 2013





DECLASSIFIED IN FULL  
Authority: EO 13526  
Chief, Records & Declass Div, WHS  
Date: JUL 19 2013

7

*1/2" DIA. x 1/8" THK. (12 BOLTS EACH SIDE)  
MATERIAL: ALUMINUM 6061-T6  
FINISH: ANODIZED*



~~CONFIDENTIAL~~

DECLASSIFIED IN FULL

Authority: EO 13526

Chief, Records & Declass Div, WHS

Date:

JUL 19 2013

#### 7. 1. 4 Rotary Actuator Assembly

The requirements of the rotary actuator for driving the feeding mechanism, as outlined in the Seventh Quarterly Progress Report<sup>18</sup> and repeated below, were submitted to a number of potential vendors but none could furnish a satisfactory item without resorting to a design and development program. Since General Mills, Inc. has had considerable experience in developing equipment of this type, a decision was made to have our personnel proceed with the design and fabrication of the actuator.

The requirements of the actuator are:

- 1) Output Speeds. - 12, 18, 24, 36 and 48 rpm in either direction. (These speeds are changed from those given in the referenced report.)
- 2) Output Torque. - 2500 pound-inches in either direction at the above speeds.
- 3) Maximum Allowable Overhung Shaft Load. - 1500 pounds.
- 4) Maximum Allowable Inward Thrust Load on Shaft. - 2000 pounds.
- 5) Maximum Allowable Outward Thrust Load on Shaft. - 2000 pounds.
- 6) Duty Cycle. - Continuous for periods up to 1/2 hour.
- 7) Life. - 200 hours.
- 8) Operating Temperature. - 160°F to -65°F.
- 9) Operating Altitude. - Sea level to 15,000 feet.
- 10) Acceleration. - 10 g's in any direction.
- 11) Vibration. - 5 to 500 cps at 0.036-inch double amplitude or  $\pm 10$  g whichever is the lower value.
- 12) Input Electrical Characteristics. - 400 cycle, 200 volt, 3 phase, ac.
- 13) Connectors. - Water-tight connector at cable entrance to actuator housing.

~~CONFIDENTIAL~~

~~CONFIDENTIAL~~

DECLASSIFIED IN FULL  
Authority: EO 13526  
Chief, Records & Declass Div, WHS  
Date:

JUL 19 2013

During this reporting period the design was essentially completed and all major items were released for fabrication or procurement. As the design progressed, it was necessary to modify some of the characteristics so that they now differ from the description presented in the Seventh Quarterly Progress Report<sup>18</sup>.

The electric motor which has been ordered from the Westinghouse Electric Corporation is a 400 cps, 3-phase, 200-volt, 5600-rpm motor with a rated torque capacity of 22 pound-inches. The speed-selector portion of the actuator will still provide for five driving speeds as given in Item (1) above. At all but the highest speed the speed-changing gearing will all provide some speed reduction. The highest ratio is actually a step-up to about 117 percent of input speed.

The major speed reduction still occurs in the fixed-ratio speed-reducing part of the actuator which is a series three-stage planetary gear unit. The reduction ratio of the first and second stages is 4.75 to 1 each, and that of the third stage is 6 to 1, giving an over-all reduction ratio of 135.375 to 1. The input in each stage is at the sun gear and the output at the planet carrier or its extension. The incoming torque is received through a safety clutch which is designed to slip when the force exceeds a given amount.

The approximate size of the actuator package is now 12 inches maximum diameter and 21 inches length. Slightly more than half of the unit has a diameter of about 5 inches. The weight has been calculated at 65 pounds. The actuator assembly will have two mounting flanges for securing the unit in the tail section of the store. The principal mounting of the actuator is at the forward bulkhead of the motor housing and the secondary mounting is the flange portion of the housing at the forward or output end of the planetary speed-reducing unit.

~~CONFIDENTIAL~~

~~CONFIDENTIAL~~

DECLASSIFIED IN FULL

Authority: EO 13526

Chief, Records & Declass Div, WHS

Date: JUL 19 2013

## 7.2 Fabrication of the Second Experimental Unit

The design for the airborne dry agent disseminating store which is evolving from design studies and laboratory experiments will differ in some respects from the full-scale feeder which has been used thus far in this phase of the program. The same basic concepts will be employed, but; in general, the experimental feeder design is not directly applicable to the airborne store. Therefore, a second experimental model is being fabricated to test the design to be employed in the airborne store. This new experimental unit is shown in Figure 7.4 (GMI Dwg SK-29100-778). The more important changes in this model as compared with the first experimental feeder are discussed below.

- 1) The cylinder dimensions are reduced to 83.25 inches long by 16.5 inches inside diameter. These dimensions are those of the inner tank to be incorporated in the airborne version. Stainless steel, type 304 ATSI, is utilized rather than aluminum as in the first generation model.
- 2) The drive screw is machined as one piece rather than two as on the first generation model. This eliminates the problem of joining the two screws together when assembling the unit. The disaggregator is keyed to the drive screw to permit easy removal of the screw for cleaning and maintenance.
- 3) Ball bearings for radial and thrust support are again used at the ends of the screw but additional bearings are mounted at the center of the cylinder to support the disaggregator and reduce friction at this point. The center support structure has been incorporated in the aerating ring structure to obtain a compact arrangement.
- 4) The orifice plates forming the sides of the aerating ring or manifold have removable nozzles for directing the gas which mixes with the powder and causes it to flow out of the unit.
- 5) The piston hubs are elongated to provide better support on the drive screw.
- 6) The experimental unit is designed for loading from the ends, using a special loading tube, as is planned for the airborne version.

~~CONFIDENTIAL~~

~~CONFIDENTIAL~~

DECLASSIFIED IN FULL  
Authority: EO 13526  
Chief, Records & Declass Div, WHS  
Date: JUL 19 2013

Controls for the gas system are not shown in Figure 7.4 but the following items will be installed on the experimental unit to test for performance:

- 1) Pressure switches to indicate abnormally high pressure within the cylinder at the center and at the ends behind the pistons.
- 2) A check valve at the entrance to the aerating ring to prevent back flow.
- 3) A pressure switch to indicate abnormally high pressure in the gas line entering the aerating ring.
- 4) A pressure relief valve in this line.
- 5) A fixed critical flow orifice ahead of the pressure relief valve.
- 6) A pressure regulator in the gas supply line.

This experimental unit will be tested with the same facilities which have been used to obtain data with the first experimental unit.

### 7.3 Fabrication of Loading Equipment for Use With the Second Experimental Unit

Loading of the disseminator with compacted dry agent will require auxiliary equipment to compress the finely-divided bulk solids into cylindrical packages of the required length, diameter and density. Special equipment may also be necessary to transfer the compacted powder from the press to the disseminator. In order to study this aspect of the program, a hydraulic press and a loading fixture have been designed for use with the second experimental unit. Fabrication of this equipment was started during this reporting period.

~~CONFIDENTIAL~~



~~CONFIDENTIAL~~

DECLASSIFIED IN FULL  
Authority: EO 13526  
Chief, Records & Declass Div, WHS  
Date: JUL 19 2013

### 7.3.1 Hydraulic Press

The hand press employed in loading the full-scale feeder with compacted powder is not suitable for producing densities greater than approximately 0.45 grams per cc. Since the objective is to investigate disseminator performance with compaction densities up to 0.6 grams per cc, it will be necessary to have a press capable of producing the total force associated with this density. Consequently, a simple hydraulic press is being fabricated which will be capable of exerting a force of 8300 pounds. The compaction ram will be attached to a hydraulic cylinder having a 38-inch stroke. Hydraulic controls will be provided to enable the operator to vary the rate of piston travel and to adjust the piston force.

### 7.3.2 Loading Fixture

A loading fixture is being fabricated which consists of a loading tube and a manual lift truck. The loading tube will be positioned in the hydraulic press for filling and compacting of the powder. The lift truck will be used to raise the filled loading tube and rotating it to a horizontal position in line with the disseminator. The loading tube will then be attached to the end of the inner tank of the disseminator and the compacted material will be pushed into the disseminator using air pressure to operate the loading tube. The loading fixture will then be removed and the piston and end plate of the disseminator will be installed.

~~CONFIDENTIAL~~

~~CONFIDENTIAL~~

DECLASSIFIED IN FULL  
Authority: EO 13526  
Chief, Records & Declass Div, WHS  
Date: JUL 19 2013

## 8. TESTING OF THE LIQUID AGENT DISSEMINATING STORE

The liquid agent disseminating store, which was described in the Seventh Quarterly Progress Report<sup>19</sup>, has been subjected to a series of structural and functional tests in the laboratory and in the field. Laboratory structural tests were conducted at Fletcher Aviation Company, El Monte, California using two test units which were fabricated for that purpose. The third unit, which is a complete developmental model, was tested in the laboratory at General Mills, Inc. and, subsequently, flight tested on an A4D-1 airplane at the Naval Air Test Center, Patuxent River, Maryland. The disseminator has met the requirements of the various tests with a very high degree of success. An assembly drawing showing the complete unit is included as Appendix A of this report.

A report (see Appendix B) of the structural test program is included with this progress report and is discussed briefly below. The results of the test work conducted at General Mills, Inc. will be presented in a final engineering report which is being prepared. The Naval Air Test Center is submitting an official report on the flight tests. A short description of the flight test project is presented in paragraph 8.2 following.

### 8.1 Structural Testing at Fletcher Aviation Company, El Monte, California

Appendix B is Fletcher Aviation Company Report No. 43.286, "Qualification Tests, General Mills Tank Assembly" covering the structural testing conducted by Fletcher on two units fabricated for this purpose. The test models were structurally similar to the delivered unit with the exception that components such as the turbine, pump, actuator, etc., were simulated by means of dummy units having the same weight, center of gravity, and attachment provisions.

The tests were conducted in general accordance with Specification MIL-7378A, "Tanks, Fuel, Aircraft, External, Auxiliary, Removable." Following is a list of the test performed:

~~CONFIDENTIAL~~

~~CONFIDENTIAL~~

DECLASSIFIED IN FULL  
Authority: EO 13526  
Chief, Records & Declass Div, WHS  
Date: JUL 19 2013

- 1) Examination of product for conformance with drawings and for quality of workmanship.
- 2) Determination of weight and center of gravity locations.
- 3) Determination of tank capacity.
- 4) Slosh-and-vibration test.
- 5) Leakage test.
- 6) Ground ejection test.
- 7) Static structural test.

The disseminator successfully met the requirements of the various tests. In order to pass the slosh-and-vibration test it was necessary to stop the test after it had been in progress for 17-1/2 hours and repair a crack in the skin and add reinforcement strips as described in pages 4.7 through 4.12 of Appendix B. After this modification the tank successfully withstood an additional 25 hours of slosh-and-vibration testing.

During the repair, the inner tank was inspected. It was discovered that the buna rubber lining of the inner Fiberglas tank had separated from the tank and was torn in several places (see page 4.11 of Appendix A). In addition, the two anti-slosh baffles were intact but had broken free and were lying on the bottom of the tank. The lining and the bulkheads were removed before the test was repeated.

When this Fiberglas tank was delivered to Fletcher for incorporation into the assembly, it was known that the bond between the liner and the tank proper was inferior. The liner was already separated from the tank in places. Since this liner was used to facilitate release of the tank from the mold during fabrication and is not required for structural or leakage purposes, this fault was not considered to be important.

~~CONFIDENTIAL~~

~~CONFIDENTIAL~~

DECLASSIFIED IN FULL  
Authority: EO 13526  
Chief, Records & Declass Div. WHS  
Date: JUL 19 2013

**8.2 Flight Tests of Liquid Agent Disseminating Store at NATC,  
Patuxent River, Maryland**

Through arrangements with the Bureau of Naval Weapons it became possible to conduct flight tests with the liquid agent disseminator using an A4D airplane. The unit was shipped to the Naval Air Test Center, Patuxent River, Maryland where a series of flight tests were conducted by the Weapon Systems Test Division on 16, 17, 18 May, 1962. The WST Division was directed to prepare a final report covering these tests. The following remarks concerning the flight tests are based on observations made by General Mills, Inc. personnel who participated in the tests and on preliminary verbal reports made by Lt. H. Turk, the test pilot.

The following "detailed Requirements" were listed in Weptask No. RMMO-33-015/201-1/F008-10-005 issued by the Bureau of Naval Weapons for the flight test project. The unit successfully passed all phases of this testing program.

- 1) Perform fit tests with the spray tank suspended from the Aero 7A Bomb Rack of the A4D-1 aircraft.
- 2) Provision for appropriate electrical connectors in the aircraft pylon, if required.
- 3) Perform static functional spray tests using water.
- 4) Perform flight tests to the maximum safe speeds not to exceed the limits of normal flying as set forth in BUWEPS Instruction 3710.0 of 19 October 1960.
- 5) Pilot to observe and report unfavorable conditions during taxiing, take-offs, landings, and maneuverability tests (high and low altitude, high and low speed).
- 6) Perform high altitude, low temperature soak followed by functional test with dyed water. Upon landing make a visual check of aircraft and report areas covered with dye. Report temperature and duration of cold soak.
- 7) Perform low altitude (300 to 500 feet) high-speed functional test with dyed water. Upon landing make a visual check of the aircraft and report areas covered with dye.

~~CONFIDENTIAL~~

~~CONFIDENTIAL~~

DECLASSIFIED IN FULL  
Authority: EO 13526  
Chief, Records & Declass Div, WHS  
Date: JUL 19 2013

- 8) Provide for camera coverage of functional test items (3), (6) and (7) above.
- 9) Furnish twelve photographic copies of the GMI spray tank and aircraft installation to BUWEPS (Code RMMO-334).

The photographs in Figures 8.1 and 8.2 show the disseminator mounted on the Aero 7A bomb rack on the fuselage centerline station of the A4D-1 airplane. Electrical connections to the store were easily made by installing a cable running from the pylon to a junction box in the fuselage just forward of the pylon. The cockpit control panel was installed in a position used for such auxiliary equipment and required no airplane modifications.

The static functional spray tests were conducted with the unit mounted on a bomb rack hanging from a steel frame provided by the Navy. A ground power source was used to operate the disseminator. Figure 8.3 shows water spraying from the booms during this test.

The flight tests were conducted in three flights. The pilot reported no unfavorable conditions due to the disseminator during these flights and found the control panel to be entirely satisfactory. The unit functioned properly at all times.

The high-altitude, low-temperature test was conducted on the second flight in which two auxiliary 300-gallon fuel tanks were installed at the wing stations to obtain the desired flight duration. Two minimum-maximum thermometers mounted in the aft section of the disseminator for this test indicated a temperature range from 73°F to 80°F.

Maneuvers resulting in 5 "g" loading were performed on the third flight. Following these maneuvers, several low-altitude dissemination runs were made within sight of an observation tower so that motion pictures could be made with a telephoto lens. The dissemination process was visible to the naked eye and the aerosol was observed to trail out from the booms of the disseminator in a clearly defined band that did not diffuse until it was well aft of the airplane.

~~CONFIDENTIAL~~

~~CONFIDENTIAL~~

DECLASSIFIED IN FULL  
Authority: EO 13526  
Chief, Records & Declass Div, WHS  
Date:

JUL 19 2013



Figure 8.1 GMI Liquid Agent Disseminating Store Mounted on Aero 7A Bomb Rack on A4D-1 Airplane - Side View

~~CONFIDENTIAL~~

~~CONFIDENTIAL~~

DECLASSIFIED IN FULL  
Authority: EO 13526  
Chief, Records & Declass Div, WHS  
Date: JUL 19 2013

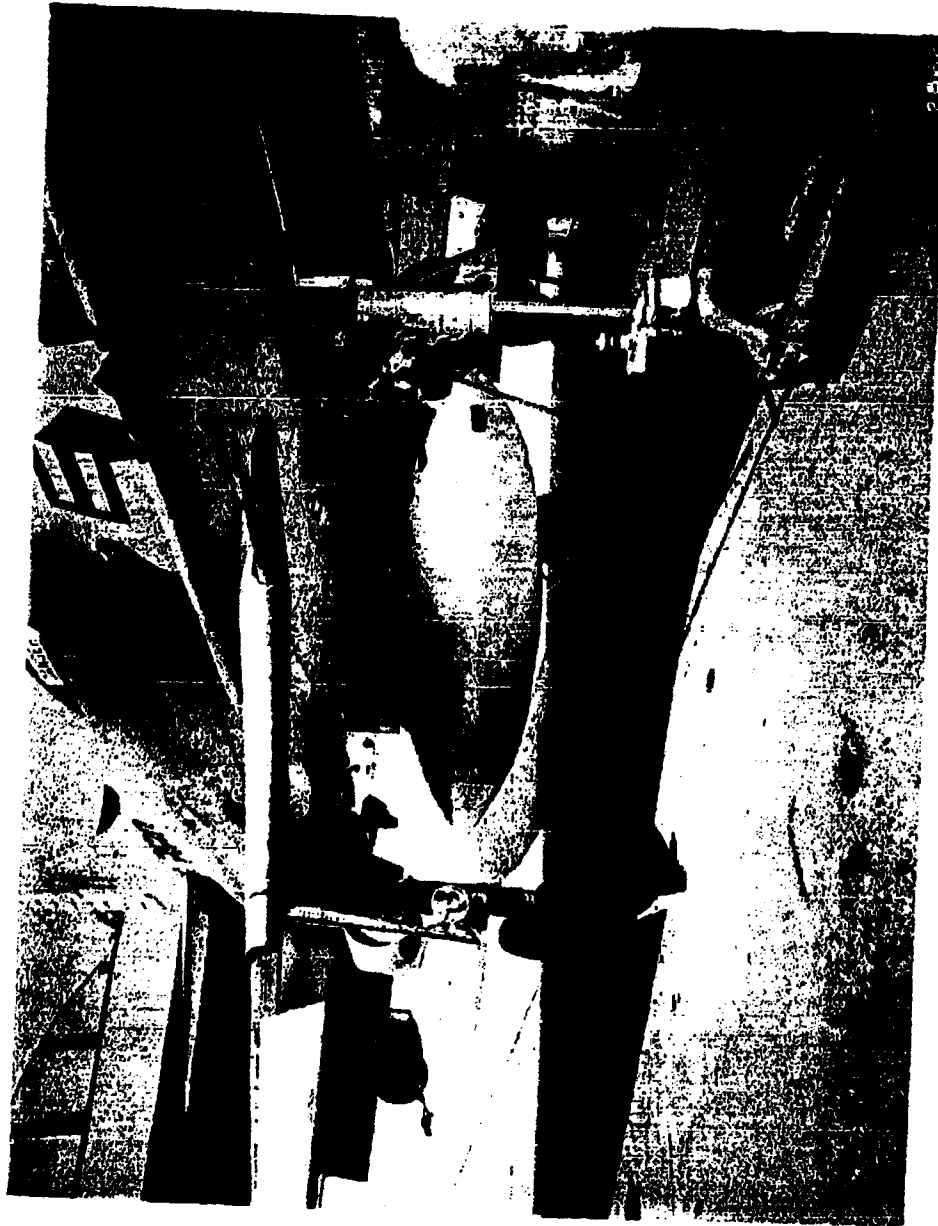


Figure 8.2 GMI Liquid Agent Disseminating Store Mounted on  
Aero 7A Bomb Rack on A4D-1 Airplane - Front View

~~CONFIDENTIAL~~

DECLASSIFIED IN FULL  
Authority: EO 13526  
Chief, Records & Declass Div, WHS  
Date:

~~CONFIDENTIAL~~

JUL 19 2013



Figure 8.3 GMI Liquid Agent Disseminating Store Spraying  
Water During Static Functional Test

~~CONFIDENTIAL~~



~~CONFIDENTIAL~~

DECLASSIFIED IN FULL

Authority: EO 13526

Chief, Records & Declass Div, WHS

Date:

JUL 19 2013

For each of the three flights the disseminator was filled with dyed water to aid in photography and to provide a tracer for studying contamination of the aircraft. Both methylene blue and uranine (sodium fluorescein) were used at a concentration of approximately 0.25 percent each. The methylene blue was planned to produce evidence of contamination visible under normal light and the uranine under ultraviolet. A very careful examination of the airplane was made after each flight and no evidence of contamination was found. In fact, the only areas on the store itself which were contaminated were the booms, the boom wells, and the exterior surfaces immediately adjacent to the boom wells.

~~CONFIDENTIAL~~

~~CONFIDENTIAL~~

DECLASSIFIED IN FULL  
Authority: EO 13526  
Chief, Records & Declass Div, WHS  
Date: JUL 19 2013

## 9. SUMMARY AND CONCLUSIONS

During this reporting period, significant work was accomplished in our research and development program on the dissemination of solid and liquid BW agents. Progress in each of seven areas of effort is summarized below with the pertinent section of this report indicated at the end of the paragraph.

Data obtained with an improved piston-cylinder compaction apparatus have resulted in an empirical formula of the form  $\sigma = K \left(\frac{1}{\rho}\right)^r$  relating stress,  $\sigma$ , and density,  $\rho$ , of a compacted powder. Values for K and r were determined for talc, saccharin, powdered sugar, powdered milk and cornstarch. Tests with the hydrostatic compaction apparatus yielded results in agreement with the improved piston-cylinder compaction apparatus, but the hydrostatic apparatus proved to be difficult to use. Measurements at high stress levels with the above powders indicate that considerably less elastic energy is stored in a compacted powder bed than was first assumed. It has been found that very little elastic recovery occurs as stress is reduced at high stress levels. The triaxial shear tests have thus far proven successful only with relatively highly compacted samples and low (2 psi or less) radial pressures. Additional data were obtained using the bulk tensile strength apparatus with zinc cadmium sulfide which indicates that total sample length and length of time of application of compressive load when preparing the sample are important considerations. Bulk density investigations have produced data showing a decrease in density with increased radial distance from the axis of a sample compacted in a cylinder. Using the sliding disk method to measure shear strength as a function of compressive stress it has been observed that the relationship remains unchanged as humidity is increased from 2 to 32 percent but marked changes were observed at 46 and 69 percent (Section 2).

The aerophilometer has been operated while studying experimental techniques and determining operating parameters essential to carrying out the program on stability properties of aerosols. A mathematical analysis has produced theoretical expressions which, as shown by experiments,

~~CONFIDENTIAL~~

~~CONFIDENTIAL~~

DECLASSIFIED IN FULL  
Authority: EO 13526  
Chief, Records & Declass Div. WHS  
Date:

JUL 19 2013

have a considerable degree of validity and have proven very useful in interpreting the light-scattering data. The decrease in scattered light with time has been recorded for aerosols of talc, saccharin, powdered milk and K-ferric oxide using the fan to produce turbulence. Erratic behavior was observed when tranquil conditions were employed. Apparently, "clouds" form in the aerosol and drift randomly through the light-scattering area (Section 3).

An experiment has shown that Sm powder being used in trials designed to measure the degree of heat inactivation were invariably contaminated with Bg colonies. A series of trials have demonstrated that neither coating with Cab-O-Sil nor compaction to 0.62 grams per cc density has any significant or deleterious immediate effects on viability of Sm (Section 4).

A program was conducted at Fort Detrick under Technical Evaluation Division Test No. 62-TE-1602; MD Division No. 1927, using the 40-foot diameter test sphere to evaluate the General Mills GMI-3 fixture and wind tunnel when used for generating aerosols of dry Sm and dry P. tularensis. When the Technical Evaluation Division furnishes the statistical analysis of data, it will be possible to report on the effects of compaction and subsequent aerodynamic breakup during dissemination on the viability of dry agents. Preliminary examination of the data indicates that good recovery factors were obtained (Section 5).

The full-scale experimental feeder for use with compacted dry agent simulants has been operated successfully over material flow rates ranging from 20 to 49 lb/min. It has been demonstrated that reasonably low gas flows are sufficient to fluidize the powder and carry it out through a discharge tube. Although the feeder has been operated satisfactorily with gas flow as low as 3 scfm, tests have shown that best performance has resulted when the rate was approximately 6 scfm. Torque and power required to drive the feeder have both been well below the limits established in the design studies for an airborne disseminator based on the basic principles employed in the full-scale feeder (Section 6).

~~CONFIDENTIAL~~

~~CONFIDENTIAL~~

DECLASSIFIED IN FULL  
Authority: EO 13526  
Chief, Records & Declass Div, WHS  
Date:

JUL 19 2013

The design studies on a dry BW agent disseminating store have progressed to the stage where major components are now well defined and a preliminary general arrangement has been prepared. The store will have the same external shell as a standard 150-gallon auxiliary fuel tank and will have provisions for both 14- and 30-inch spacing of the mounting lugs. The agent will be contained within a tank assembly forming an integral part of the center section of the store. The air turbine generator and the gas supply vessel will be housed in the nose section, and the rotary actuator in the tail. Both nose and tail sections will be attached to the center section with bayonet-type joints. The dry agent will be discharged through a tube projecting below the store sufficiently far so that the material is injected into the slipstream beyond the boundary layer. An experimental version of the inner tank assembly is being fabricated for use in laboratory tests of the engineering design (Section 7).

The liquid agent disseminating store was flight tested on an A4D-1 airplane by the Weapons System Test Division at the Naval Air Test Center, Patuxent River, Maryland. Dyed water was successfully disseminated under various conditions and no trace of dye could be found on the airplane after it returned to the ground. The pilot reported no unfavorable conditions of flight and there was no damage to the store during maneuvers resulting in 5 "g" loading and speeds up to the maximum safe limits of normal flying for the A4D-1 airplane (Section 8).

~~CONFIDENTIAL~~

Date: JUL 19 2013

## X. REFERENCES

- 1) General Mills, Inc. Electronics Div. Report No. 2249. Dissemination of solid and liquid BW agents (U), by G. R. Whitnah et al. Contract DA-18-064-CML-2745. Fifth Quarterly Progress Report (November 30, 1960). Confidential.
- 2) ----. Report No. 2300. Dissemination of solid and liquid BW agents (U), by G. R. Whitnah et al. Contract DA-18-064-CML-2745. Seventh Quarterly Progress Report (June 22, 1962). Confidential.
- 3) ----. Report No. 2125. Dissemination of solid and liquid BW agents (U), by G. R. Whitnah. Contract DA-18-064-CML-2745. First Quarterly Progress Report (October 13, 1960). Secret.
- 4) ----. Report No. 2112. Fundamental studies of the dispersibility of powdered materials, by J. H. Nash et al. Contract DA-18-108-405-CML-824. First Quarterly Progress Report (September 26, 1960). (AD 243, 607); Report No. 2148. Second Quarterly Progress Report (December 31, 1960). (AD 249, 913).
- 5) ----. Report No. 2216. Dissemination of solid and liquid BW agents (U), by G. R. Whitnah et al. Contract DA-18-064-CML-2745. Fourth Quarterly Progress Report (August 10, 1961). (AD 325, 247). p. 18. Confidential.
- 6) Mathews, D. H. Measurement of the specific surface area of fine powders. A comparison of the gas adsorption and air permeability methods. J. Appl. Chem. (London) 7: 610-13 (1957).
- 7) U. S. Atomic Energy Commission. Handbook of aerosols. Washington, D. C., Gov't. Print. Off., 1950. (PB 125, 198). Chap. 5, p. 66.
- 8) Fuks, N. A. Mechanics of aerosols (Translation). U. S. Army Chemical Warfare Laboratories. Special Publication 4-12 (1955). (AD 227, 876). p. 282.
- 9) Hulst, H. C. van de. Light scattering by small particles. N. Y., Wiley, 1957.
- 10) General Mills, Inc. Report No. 2300, op. cit., p. 5-5.
- 11) Ibid. pp. 6-1 and 6-2.
- 12) Ibid. pp. 6-2 thru 6-7.

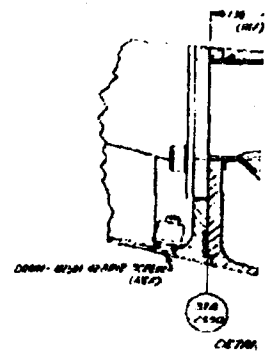
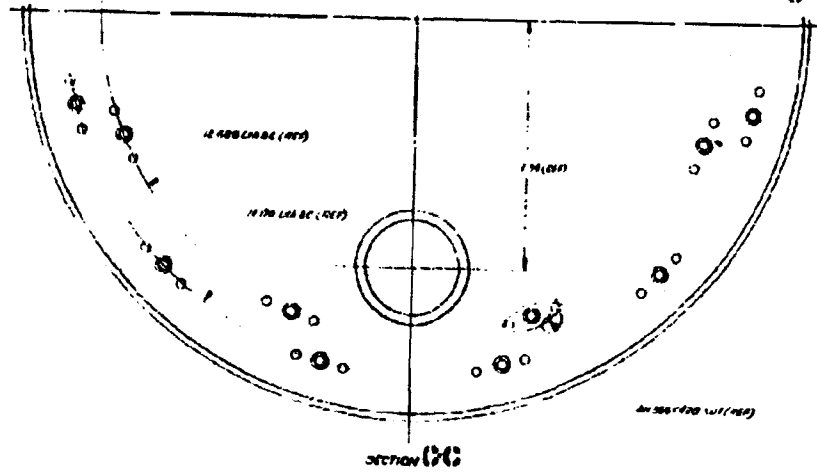
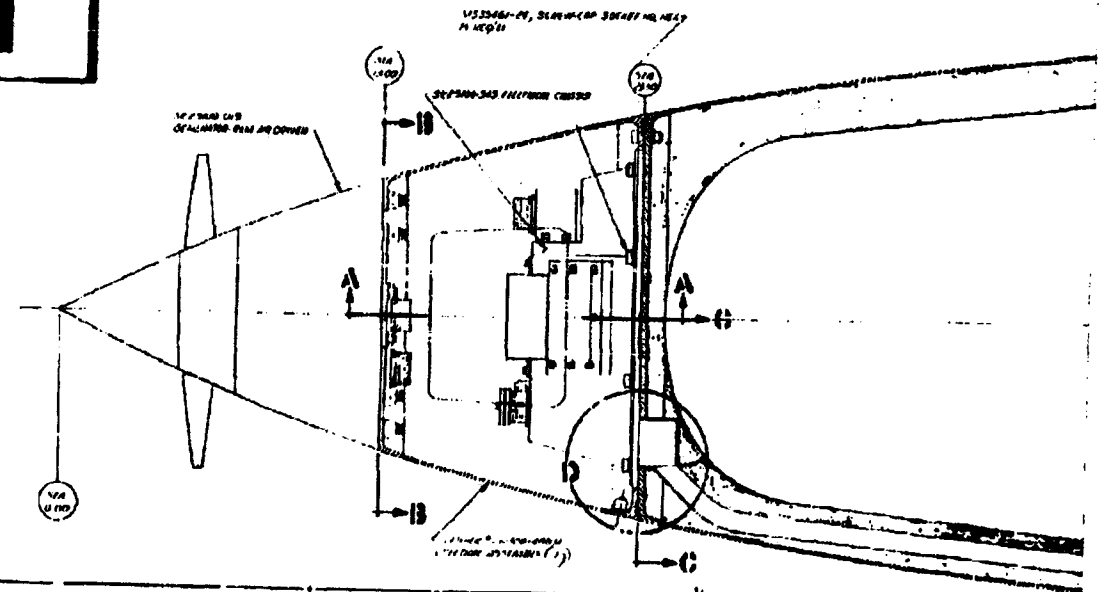
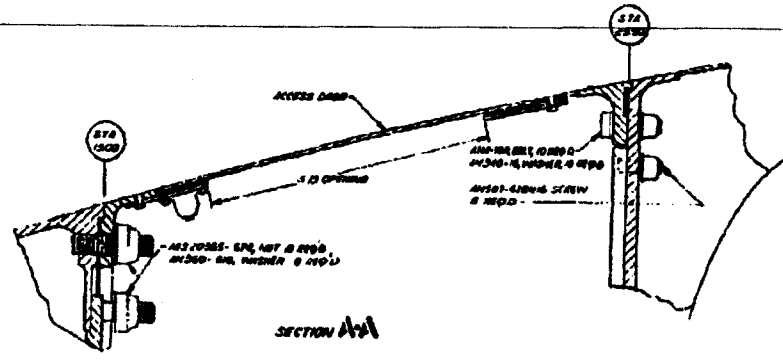
Page determined to be Unclassified  
Reviewed Chief, RDD, WHS  
IAW EO 13526, Section 3.5  
Date: JUL 19 2013

- 13) Ibid. pp. 6-1 thru 6-12.
- 14) General Mills, Inc. Report No. 2249, op. cit., pp. 33-46.
- 15) ----. Report No. 2300, op. cit., pp. 8-1 to 8-5.
- 16) ----. Report No. 2249, op. cit., Appendix C.
- 17) National Advisory Committee for Aeronautics. TN 3359. An investigation of drains discharging liquid into subsonic and transonic streams, by A. R. Vick and F. V. Silhan (1955).
- 18) General Mills, Inc. Report No. 2300, op. cit., pp. 8-2 and 8-3.
- 19) Ibid. pp. 10-1 thru 10-14.

Page determined to be Unclassified  
Reviewed Chief, RDD, WHS  
IAW EO 13526, Section 3.5  
Date: JUL 19 2013

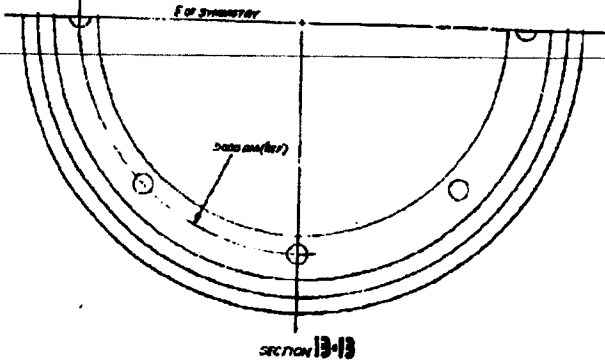
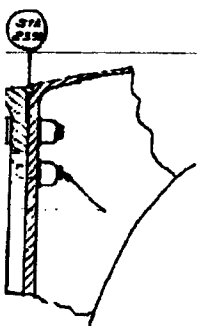
APPENDIX A  
ASSEMBLY DRAWING  
LIQUID AGENT DISSEMINATOR

**CONFIDENTIAL**

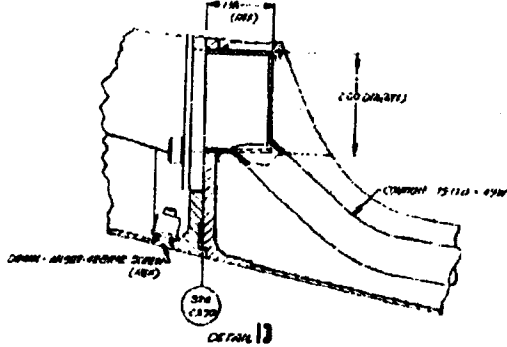
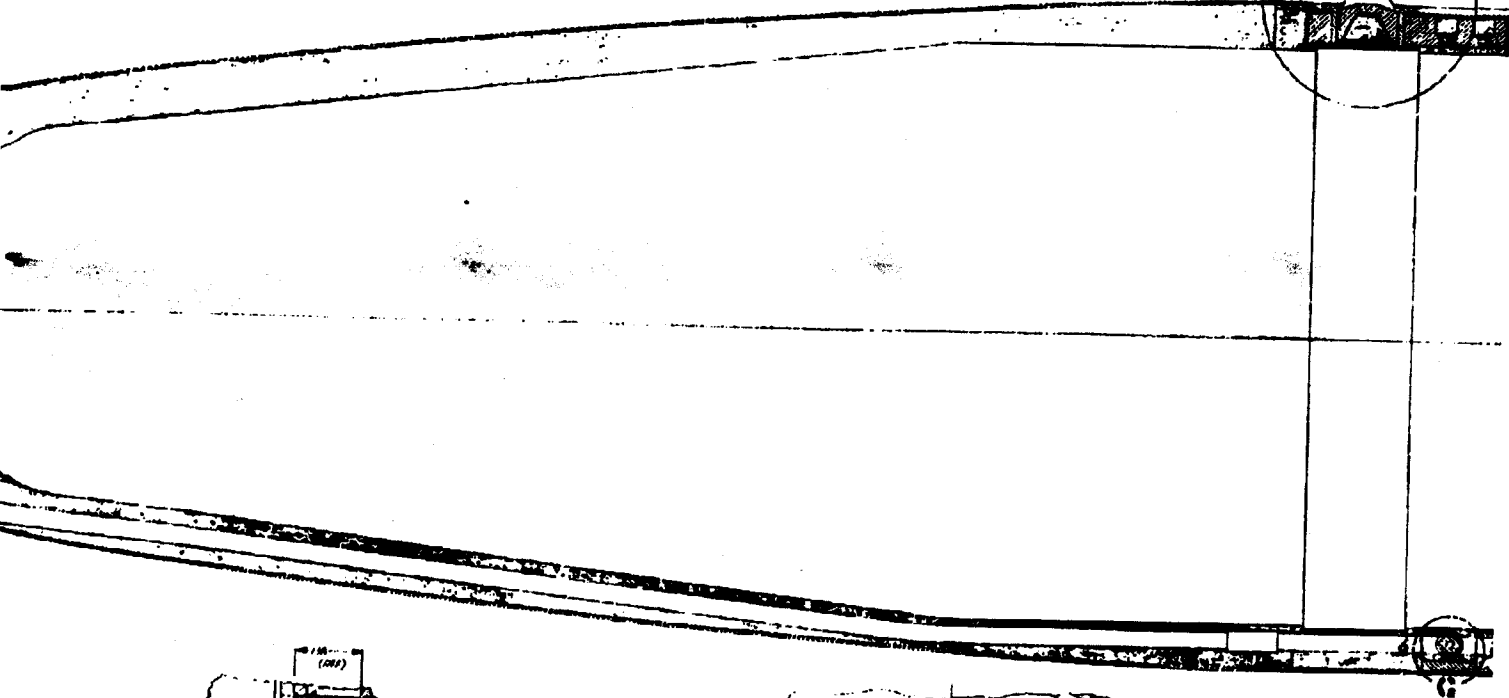
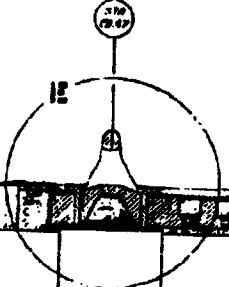


**CONFIDENTIAL**

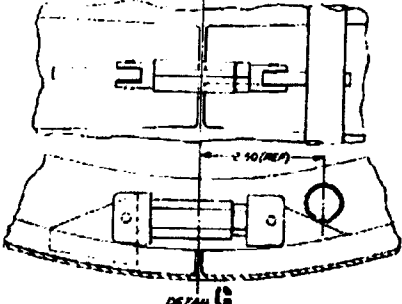




SECTION 13-13

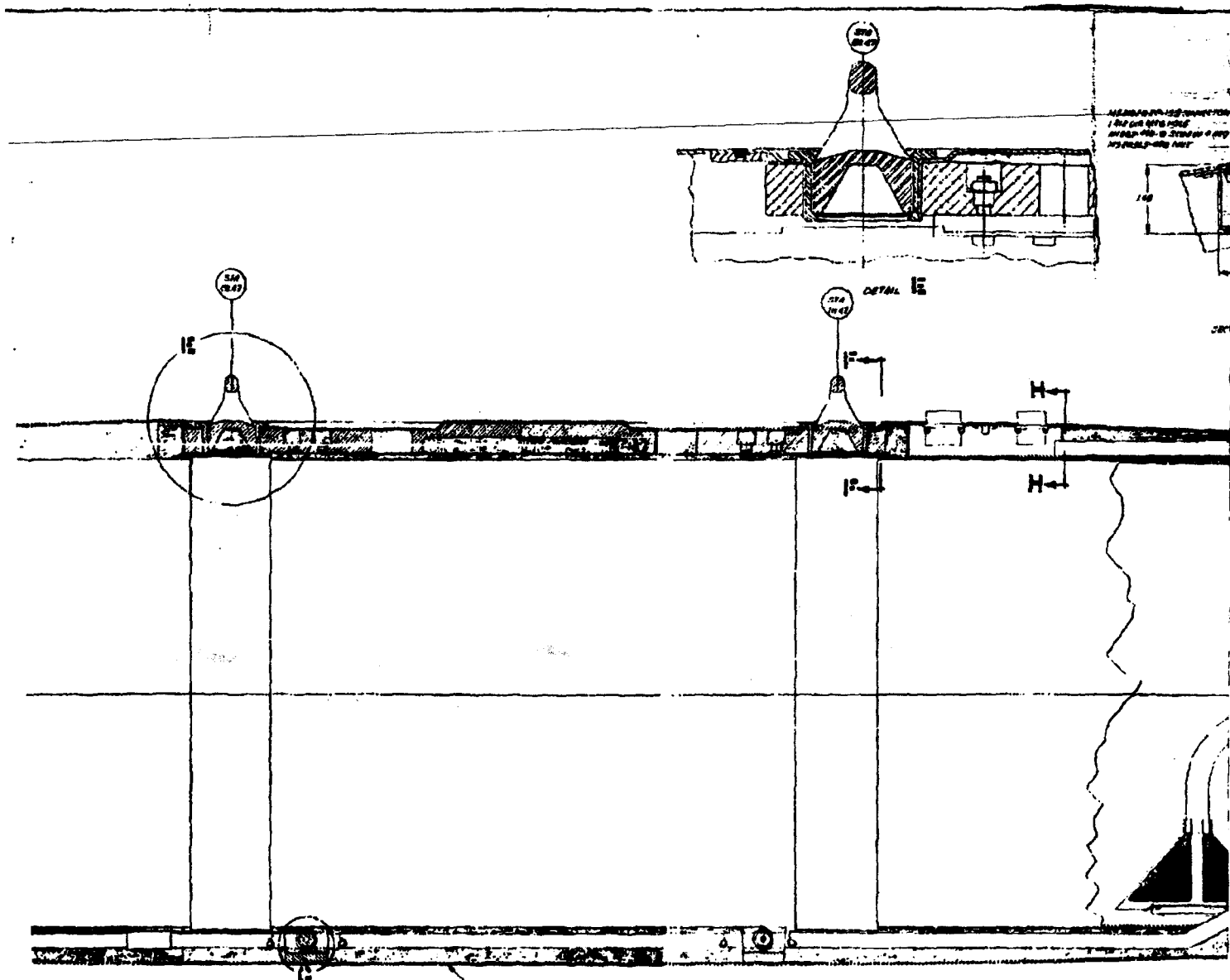


DETAIL 13



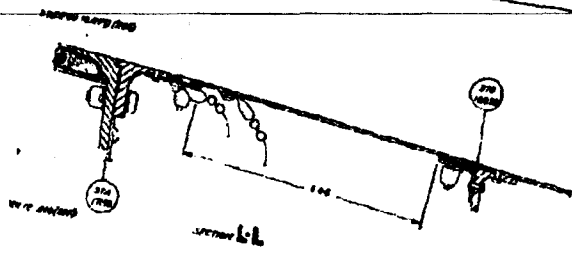
DETAIL 6



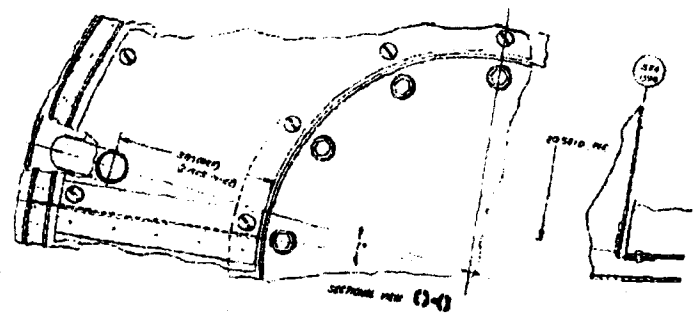
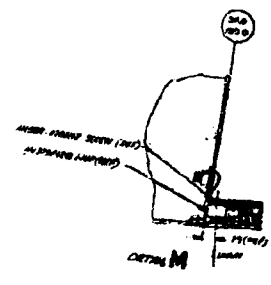
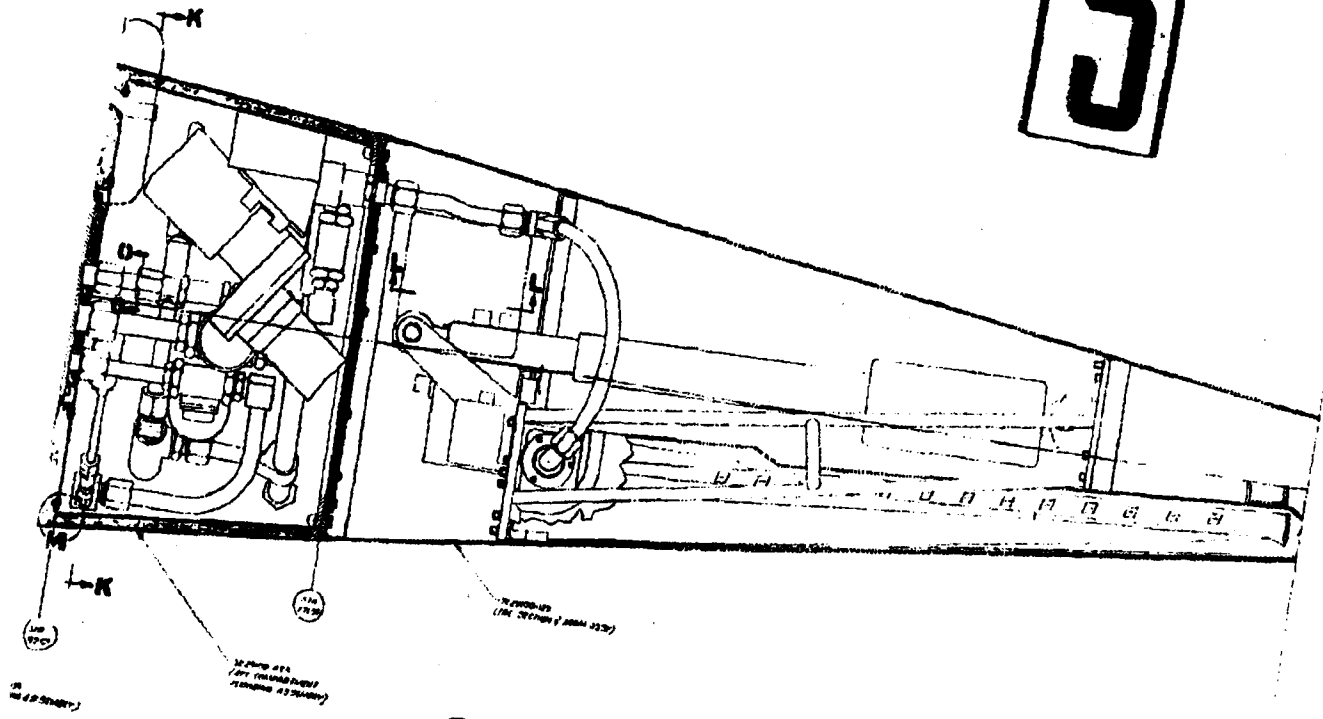


3



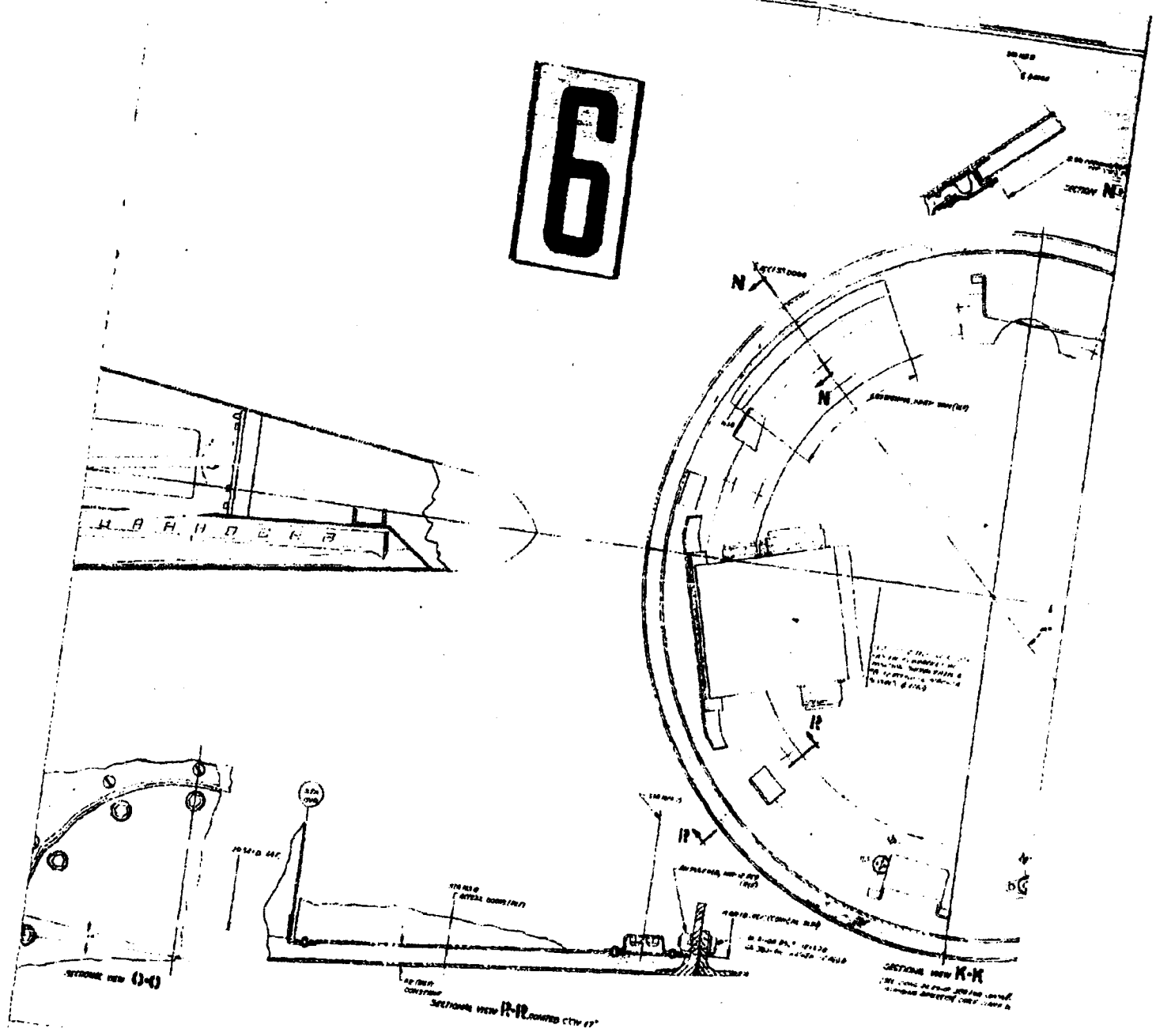


5



JUL 19 2013

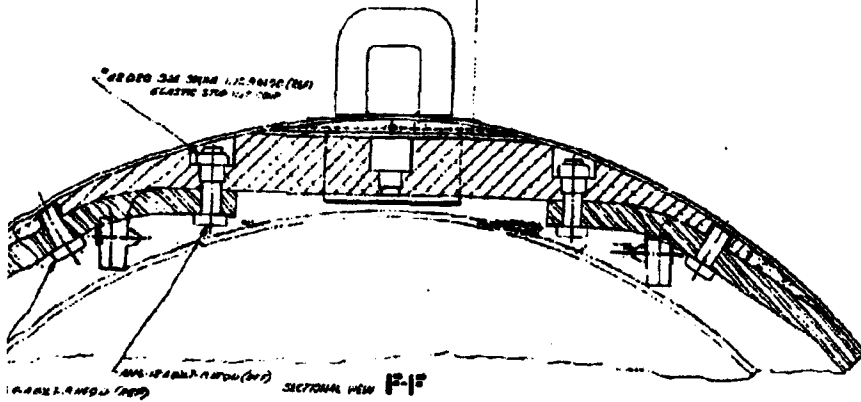
6





JUL 19 2013

~~CONFIDENTIAL~~



- NOTE:  
SEE DRAWING 3700 107 1000 FOR THIS ASSEMBLY
- 370000-017 CABLE #1 - INTERNAL CONTROL
  - 370000-018 CABLE #2 - INTERNAL CONTROL POWER
  - 370000-019 CABLE #3 - SECTION POWER
  - 370000-020 CABLE #4 - FLOW CONTROL
  - 370000-021 CABLE #5 - SIGNAL CONTROL
  - 370000-022 CABLE #6 - TAIL CONTROL
  - 370000-023 CABLE #7 - SECTION POWER
  - 370000-024 CABLE #8 - DISPERSED LINE
  - 370000-025 CABLE #9 - TAIL CONTROL
  - 370000-026 CABLE #10 - TAIL CONTROL
  - 370000-027 CABLE #11 - TAIL CONTROL
  - 370000-028 CABLE #12 - TAIL CONTROL
  - 370000-029 CABLE #13 - TAIL CONTROL
  - 370000-030 CABLE #14 - TAIL CONTROL
  - 370000-031 CABLE #15 - TAIL CONTROL
  - 370000-032 CABLE #16 - TAIL CONTROL
  - 370000-033 CABLE #17 - TAIL CONTROL
  - 370000-034 CABLE #18 - TAIL CONTROL
  - 370000-035 CABLE #19 - TAIL CONTROL
  - 370000-036 CABLE #20 - TAIL CONTROL
  - 370000-037 CABLE #21 - TAIL CONTROL
  - 370000-038 CABLE #22 - TAIL CONTROL
  - 370000-039 CABLE #23 - TAIL CONTROL
  - 370000-040 CABLE #24 - TAIL CONTROL
  - 370000-041 CABLE #25 - TAIL CONTROL
  - 370000-042 CABLE #26 - TAIL CONTROL
  - 370000-043 CABLE #27 - TAIL CONTROL
  - 370000-044 CABLE #28 - TAIL CONTROL
  - 370000-045 CABLE #29 - TAIL CONTROL
  - 370000-046 CABLE #30 - TAIL CONTROL
  - 370000-047 CABLE #31 - TAIL CONTROL
  - 370000-048 CABLE #32 - TAIL CONTROL
  - 370000-049 CABLE #33 - TAIL CONTROL
  - 370000-050 CABLE #34 - TAIL CONTROL
  - 370000-051 CABLE #35 - TAIL CONTROL
  - 370000-052 CABLE #36 - TAIL CONTROL
  - 370000-053 CABLE #37 - TAIL CONTROL
  - 370000-054 CABLE #38 - TAIL CONTROL
  - 370000-055 CABLE #39 - TAIL CONTROL
  - 370000-056 CABLE #40 - TAIL CONTROL
  - 370000-057 CABLE #41 - TAIL CONTROL
  - 370000-058 CABLE #42 - TAIL CONTROL
  - 370000-059 CABLE #43 - TAIL CONTROL
  - 370000-060 CABLE #44 - TAIL CONTROL
  - 370000-061 CABLE #45 - TAIL CONTROL
  - 370000-062 CABLE #46 - TAIL CONTROL
  - 370000-063 CABLE #47 - TAIL CONTROL
  - 370000-064 CABLE #48 - TAIL CONTROL
  - 370000-065 CABLE #49 - TAIL CONTROL
  - 370000-066 CABLE #50 - TAIL CONTROL
  - 370000-067 CABLE #51 - TAIL CONTROL
  - 370000-068 CABLE #52 - TAIL CONTROL
  - 370000-069 CABLE #53 - TAIL CONTROL
  - 370000-070 CABLE #54 - TAIL CONTROL
  - 370000-071 CABLE #55 - TAIL CONTROL
  - 370000-072 CABLE #56 - TAIL CONTROL
  - 370000-073 CABLE #57 - TAIL CONTROL
  - 370000-074 CABLE #58 - TAIL CONTROL
  - 370000-075 CABLE #59 - TAIL CONTROL
  - 370000-076 CABLE #60 - TAIL CONTROL
  - 370000-077 CABLE #61 - TAIL CONTROL
  - 370000-078 CABLE #62 - TAIL CONTROL
  - 370000-079 CABLE #63 - TAIL CONTROL
  - 370000-080 CABLE #64 - TAIL CONTROL
  - 370000-081 CABLE #65 - TAIL CONTROL
  - 370000-082 CABLE #66 - TAIL CONTROL
  - 370000-083 CABLE #67 - TAIL CONTROL
  - 370000-084 CABLE #68 - TAIL CONTROL
  - 370000-085 CABLE #69 - TAIL CONTROL
  - 370000-086 CABLE #70 - TAIL CONTROL
  - 370000-087 CABLE #71 - TAIL CONTROL
  - 370000-088 CABLE #72 - TAIL CONTROL
  - 370000-089 CABLE #73 - TAIL CONTROL
  - 370000-090 CABLE #74 - TAIL CONTROL
  - 370000-091 CABLE #75 - TAIL CONTROL
  - 370000-092 CABLE #76 - TAIL CONTROL
  - 370000-093 CABLE #77 - TAIL CONTROL
  - 370000-094 CABLE #78 - TAIL CONTROL
  - 370000-095 CABLE #79 - TAIL CONTROL
  - 370000-096 CABLE #80 - TAIL CONTROL
  - 370000-097 CABLE #81 - TAIL CONTROL
  - 370000-098 CABLE #82 - TAIL CONTROL
  - 370000-099 CABLE #83 - TAIL CONTROL
  - 370000-100 CABLE #84 - TAIL CONTROL
  - 370000-101 CABLE #85 - TAIL CONTROL
  - 370000-102 CABLE #86 - TAIL CONTROL
  - 370000-103 CABLE #87 - TAIL CONTROL
  - 370000-104 CABLE #88 - TAIL CONTROL
  - 370000-105 CABLE #89 - TAIL CONTROL
  - 370000-106 CABLE #90 - TAIL CONTROL
  - 370000-107 CABLE #91 - TAIL CONTROL
  - 370000-108 CABLE #92 - TAIL CONTROL
  - 370000-109 CABLE #93 - TAIL CONTROL
  - 370000-110 CABLE #94 - TAIL CONTROL
  - 370000-111 CABLE #95 - TAIL CONTROL
  - 370000-112 CABLE #96 - TAIL CONTROL
  - 370000-113 CABLE #97 - TAIL CONTROL
  - 370000-114 CABLE #98 - TAIL CONTROL
  - 370000-115 CABLE #99 - TAIL CONTROL
  - 370000-116 CABLE #100 - TAIL CONTROL

8

This document is down-graded to  
*Confidential* when separated from  
other classified documents.

~~CONFIDENTIAL~~

ASSEMBLY DRAWING	GROUP 301 SHOWN IN POSITION (SEE DRAWING 3700 107 1000)
370000-070	370000-070

Page determined to be Unclassified  
Reviewed Chief, RDD, WHS  
IAW EO 13526, Section 3.5  
Date: JUL 19 2013

**APPENDIX B**

**FLETCHER AVIATION COMPANY  
REPORT NO. 43.286**

**"QUALIFICATION TESTS,  
GENERAL MILLS TANK ASSEMBLY"**



REPORT NO. 43.286

DATED 1/8/62

Page determined to be Unclassified  
Reviewed Chief, RDD, WHS  
IAW EO 13526, Section 3.5  
Date: JUL 19 2013

**FLETCHER aviation corporation**

SUBSIDIARY OF A. J. INDUSTRIES, INC.  
1200 WEST FLORIS DRIVE • EL MONTE, CALIFORNIA • CUNBERLAND 2-3111 • BRIDGE 2-6881



QUALIFICATION TESTS  
GENERAL MILLS TANK ASSY

APPROVED

*Wayne Callahan*  
Test Engineer

*[Signature]*  
Chief Engineer

*Harold W. Marine*  
Project Engineer

MODEL 26-300

COPY NO.

REFERENCE

ISSUED

PREPARED	NAME W. Callahan	DATE 1-8-62	FLETCHER AVIATION COMPANY	PAGE	TEMP.	FORM A
CHECKED			TITLE QUALIFICATION TESTS GENERAL MILLS TANK ASSEMBLY	MODEL	26-300	
APPROVED				REPORT No.	43.286	

① ②

INTRODUCTION

This report covers a portion of the qualification tests conducted on General Mills (G.M.I.) special tank assembly, Part No. SK29100-026. The test assemblies are identical to the final assembly except that operational components such as the ram air turbine, generator, pump, valves actuator, etc., were models having the same weights and center of gravity locations. Further qualification testing will be conducted by G.M.I. to substantiate the operational capabilities of the complete assembly.

This document presents the qualification testing conducted in accordance with the requirements of specification MIL-T-7378A.

Qualification tests described herein were conducted at the Fletcher Aviation Company test facility.

REFERENCES:

- |                                    |   |   |
|------------------------------------|---|---|
| Specification MIL-T-7378A          | - | Tanks, Fuel Aircraft, External Auxiliary, Removable       |
| G.M.I. Specification Drawing       | - | SK29100-026   |
| G.M.I. Specification GMS-29100-026 | - | External Removable Tank Assy for G.M.I. Electronics Group |
| F.A.C. Drawing 26-300-48031        | - | Tank Assembly, G.M.I. Specification                       |

Page determined to be Unclassified  
Reviewed Chief, RDD, WHS  
IAW EO 13526, Section 3.5  
Date: JUL 19 2013

PREPARED	NAME W. Callahan	DATE 1-8-62	FLETCHER AVIATION COMPANY		PAGE	TEMP.	PERM.
CHECKED	TITLE QUALIFICATION TESTS GENERAL MILLS TANK ASSY			MODEL	26-300		
APPROVED				REPORT No.	43.286		

TABLE OF CONTENTS

	<u>Page No.</u>
INTRODUCTION . . . . .	A
TABLE OF CONTENTS . . . . .	B
REVISIONS . . . . .	C
Examination of Product . . . . .	1.0
Weight Test . . . . .	2.0
Capacity Test . . . . .	3.0
Slosh & Vibration Test . . . . .	4.0
Leakage Test . . . . .	5.0
Ground Ejection Test . . . . .	6.0
Structural Test . . . . .	7.0

Page determined to be Unclassified  
Reviewed Chief, RDD, WHS  
IAW EO 13526, Section 3.5  
Date: JUL 19 2013

PREPARED	NAME <b>W. Callahan</b>	DATE <b>1-8-62</b>	<b>FLETCHER AVIATION COMPANY</b>	PAGE	TEMP.	SIZE <b>C</b>
CHECKED	<i>[Signature]</i>	<i>[Signature]</i>	TITLE <b>QUALIFICATION TESTS GENERAL MILLS TANK ASSY</b>	MODEL <b>26-300</b> <b>43.286</b> REPORT No.		
APPROVED:						

**REVISIONS**

<u>SYMBOL</u>	<u>REVISED PAGES</u>	<u>DATE</u>
<u>1</u>	A, 2.1, 2.2, 4.1, 4.2, 4.3, 7.1, 7.8, 7.9, 7.10, 7.11	1-17-62
	<u>ADDED PAGES</u> 7.8.1, 7.8.2, 7.9.1, 7.9.2, 7.1.1	
		APPROVED: <i>[Signature]</i>

<u>2</u>	<u>REVISED PAGES</u> A, 2.1, 2.2	1-22-62
		APPROVED: <i>[Signature]</i>

<u>3</u>	<u>REVISED PAGES</u> 1.0, 1.2, 2.0, 2.2, 3.0, 3.2, 4.0, 4.4, 4.5, 4.6, 5.0, 5.2, 6.0, 6.3, 7.0, 7.10 7.11.	
	<u>ADDED PAGES</u> 2.3, 3.3, 4.7, 4.7.1, 4.8, 4.9, 4.10, 4.11, 4.12, 4.13, 4.14, 4.15, 5.3, 6.4, 6.5, 7.12, 7.13, 7.14, 7.15	
		APPROVED: <i>[Signature]</i>

<u>4</u>	<u>REVISED PAGES</u> 1.0, 2.2, 4.5, 4.6, 4.8, 4.9, 7.1, 4.12	
	<u>ADDED PAGES</u> 2.2.1, 6.3.1.	
		APPROVED: <i>[Signature]</i>

Page determined to be Unclassified  
Reviewed Chief, RDD, WHS  
IAW EO 13526, Section 3.5  
Date: **JUL 19 2013**

PREPARED:	NAME	DATE	FLETCHER AVIATION CORPORATION	PAGE	REV.	FORM
	W. Callahan	1-9-62				1.0
CHECKED:			TITLE	MODEL		
			EXAMINATION OF PRODUCT	26-300		
APPROVED:			GENERAL MILLS TANK ASSY	43.286		
				REPORT NO.		

(4) (3)

ADMINISTRATIVE DATA

PURPOSE OF TEST:

To determine that the assembly conforms to the applicable drawings.

MANUFACTURER:

Fletcher Aviation Company

MANUFACTURER'S MODEL NO:

26-300

ASSEMBLY DRAWING:

26-300-48011

QUANTITY OF ITEMS:

One

SECURITY CLASSIFICATION:

None

TEST DATE:

1-30-62

TEST CONDUCTED BY:

Wayne Callahan

DISPOSITION OF SPECIMEN:

Use for Weight Test

ABSTRACT:

The assembly successfully met all of the requirements of the test. Rubber liner of inner tank was not tight in several areas.

JUL 19 2013

PREPARED	NAME H. MEIN	DATE 1-9-62	FLETCHER AVIATION COMPANY	PAGE	TEMP	PERM
CHECKED			TITLE EXAMINATION OF PRODUCT GENERAL MILLS TANK ASSEMBLY	Model 26-300		1-1
APPROVED				43.286		
				REPORT No.		

FACTUAL DATA

REQUIREMENTS:

1. That the assembly and accessible components thereof conform to their applicable engineering drawings.
2. That the assembly and all components conform to aircraft quality standards for workmanship.

TEST EQUIPMENT:

1. Standard inspection tools; linear scales, micro-meters, calipers.

TEST PROCEDURE:

1. Inspect the complete assembly for general conformance to F.A.C. drawing no. 26-300-48031.
2. Remove access doors and inspect all compartments for metal chips, filings, or other foreign material.
3. Inspect all mating components and access doors for fit, sealing capabilities and general workmanship.
4. Inspect tank and inner compartment surfaces for evidence of damage or undue abrasion.
5. Inspect for loose bolts, rivets, or other fastening devices.
6. Inspect for parts not treated for corrosion resistance.
7. Inspect for misalignment of mating components.
8. Remove inner tank cover plate and inspect inner tank for general cleanliness, workmanship, and conformance to G.M.I. requirements.
9. Generally inspect simulated components (G.M.I. furnished) for fit and security of installation.
10. Install doors and inspect entire tank contour for surface irregularities.

NAME	DATE	FLETCHER AVIATION CORPORATION	PAGE	TEMP	FEES
PREPARED: W. Callahan	1-5-62				1.2
CHECKED:		TITLE: EXAMINATION OF PRODUCT GENERAL MILLS TANK ASSY	MODEL 24-100		43-286
APPROVED:			REPORT NO.		
③					
<b>RESULTS OF TEST:</b> Satisfactory					
<b>RECOMMENDATIONS:</b>					
PAC ENG'R <u>William Callahan</u>					
QUAL CONTROL. _____					
CUSTOMER _____					

NAME	DATE	FLETCHER AVIATION CORPORATION	PAGE	TERM.	PRICED
PREPARED W. Callahan	1-4-62				2.0
CHECKED		TITLE		MODEL	
		WEIGHT TEST		26-300	
APPROVED:		GENERAL MILLS TANK ASSY		43.286	
				REPORT NO.	

③

ADMINISTRATIVE DATA

PURPOSE OF TEST:  
To determine the weight and location of the center of gravity.

MANUFACTURER:  
Fletcher Aviation company

MANUFACTURER'S MODEL NO:  
26-300

ASSEMBLY DRAWING:  
26-300-48031

QUANTITY OF ITEMS:  
One (1)

SECURITY CLASSIFICATION:  
None

TEST DATE:  
2-1-62

TEST CONDUCTED BY:  
Wayne Callahan

DISPOSITION OF SPECIMEN:  
Use for Capacity Test

ABSTRACT:  
The assembly successfully met all of the requirements of the test.



PREPARED	NAME W. Callahan	DATE 1-5-62	FLETCHER AVIATION COMPANY	PAGE	FORM	DESK.
CHECKED			TITLE WEIGHT TEST			2.1
APPROVED			GENERAL MILLS TANK ASSY		MODEL 26-300	
					43.286	
					REPORT No.	

(1) (2)  
FACTUAL DATA

REQUIREMENT:

1. To determine the total weight of the empty assembly.
2. To determine the center of gravity locations to the requirements of the detail specifications for the tank.

TEST EQUIPMENT:

1. Two platform scales.
2. Tank cradle.
3. Rocker bar.
4. Water meter.

TEST PROCEDURE:

1. The cradle is weighed.
2. The tank and cradle are weighed and the cradle weight is deducted from the total weight.
3. The cradle is balanced on the rocker bar.
4. The tank is placed on the cradle in the "balance" position. The c.g. station is recorded.
5. Water is metered into the tank to 1/4 of the rated capacity.
6. The force and moment arm required to balance the tank at a range of tank attitudes from 5° nose down up to and including 30° nose up.
7. Items 5 and 6 are repeated for the 1/2, 3/4 and full capacity.
8. The c.g. for each condition is determined from the total weight and the balancing force.

JUL 19 2013

PREPARED	NAME <b>N. Callahan</b>	DATE	<b>FLETCHER AVIATION COMPANY</b>	PAGE	TEMP.	PERM.
CHECKED			TITLE			<b>2.2</b>
APPROVED			<b>WEIGHT TEST GENERAL MILLS TANK ASSY</b>		<b>MODEL 26-300</b>	
					<b>43.286</b>	
					<b>REPORT NO.</b>	

**TEST RESULTS**

① ② ③ ④

<u>TANK ATTITUDE</u>	<u>WATER CONTENTS</u>	<u>C.G.</u>
Level	Empty	T.S. 112.0
Level	1/4 Full	105.6
5°N.D.	" "	95.7
5°N.U.	" "	113.9
10°N.U.	" "	118.9
30°N.U.	" "	123.6
Level	1/2 Full	102.3
5°N.D.	" "	98.2
5°N.U.	" "	110.1
10°N.U.	" "	116.2
30°N.U.	" "	120.2
Level	3/4 Full	100.2
5°N.D.	" "	99.1
5°N.U.	" "	105.7
10°N.U.	" "	109.1
30°N.U.	" "	110.1
Level	Full	99.9
5°N.D.	" "	100.1
5°N.U.	" "	99.8
10°N.U.	" "	99.9
30°N.U.	" "	99.4

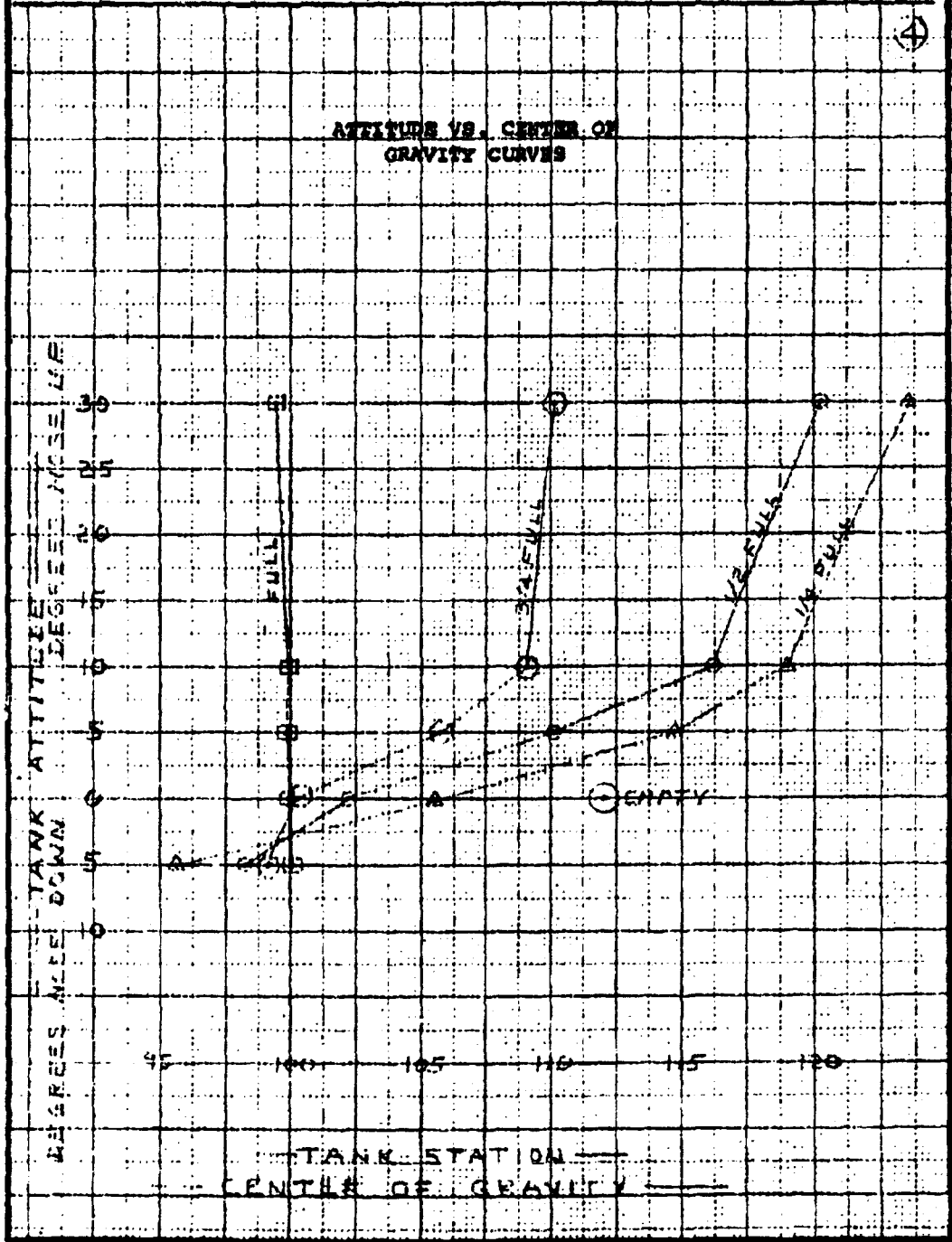
Weight of Empty assembly 568 lbs.

F.A.C. ENGR. Wayne Callahan

F.A.C. QUALITY CONTROL [Signature]

CUSTOMER [Signature]

Engineer <b>W. Callahan</b>	Date <b>4-9-62</b>	Company <b>FLETCHER AVIATION CORP.</b>	Page <b>2/2</b>
Created		Model <b>26-300</b>	Report No. <b>43.286</b>
Approved			



PREPARED	NAME	DATE	FLETCHER AVIATION CORP.	PAGE	TEMP.	PERM
	G. FORD		TITLE			
CHECKED			W. ELLIOTT			
APPROVED						
				REPORT NO.		

PREPARED	NAME	DATE	FLETCHER AVIATION CORPORATION	PAGE	TAMP.	PENL.
	W. Callahan	1-5-62				3.0
CHECKED			TITLE			
			CAPACITY TEST			
APPROVED			GENERAL MILLS TANK ASSY	MODEL	26-300	
					43.286	
				REPORT No.		

ADMINISTRATIVE DATA (3)

PURPOSE OF TEST:

To demonstrate the capacity of the assembly

MANUFACTURER:

Fletcher Aviation Company

MANUFACTURER'S MODEL NO:

26-300

ASSEMBLY DRAWING:

26-300-48031

QUANTITY OF ITEMS:

One (1)

SECURITY CLASSIFICATION:

None

TEST DATE:

1-31-62

TEST CONDUCTED BY:

Wayne Callahan

DISPOSITION OF SPECIMEN:

Use for Leakage Test

ABSTRACT:

The assembly successfully met all of the requirements of the test.

PREPARED	NAME M. Callahan	DATE 1-5-62	FLETCHER AVIATION COMPANY	PAGE	TEMP.	TEAM 3.1
CHECKED			TITLE CAPACITY TEST GENERAL MILLS TANK ASSY	MODEL	26-300 43.286	
APPROVED				REPORT NO.		

**FACTUAL DATA**

**TEST REQUIREMENTS:**

To determine total volume of the foamed in place inner tank assembly.

**TEST EQUIPMENT:**

1. Bowser Exactometer.
2. Suitable graduated container.

**TEST PROCEDURE:**

1. The tank shall be supported at 90° to normal ground attitude with the inner tank opening in the uppermost position.
2. The tank shall be filled to the top and the volume recorded.

PREPARED	NAME W. Callahan	DATE 1-5-62	FLETCHER AVIATION COMPANY	PAGE	TEMP.	PERM. 3.2
CHECKED	TITLE CAPACITY TEST GENERAL MILLS TANK ASSY			MODEL	26-300	
APPROVED				REPORT NO.	43,286	

**TEST RESULTS:**

③

The total tank volume is 191.0 gallons.

F.A.C. ENGR.:

W. Callahan

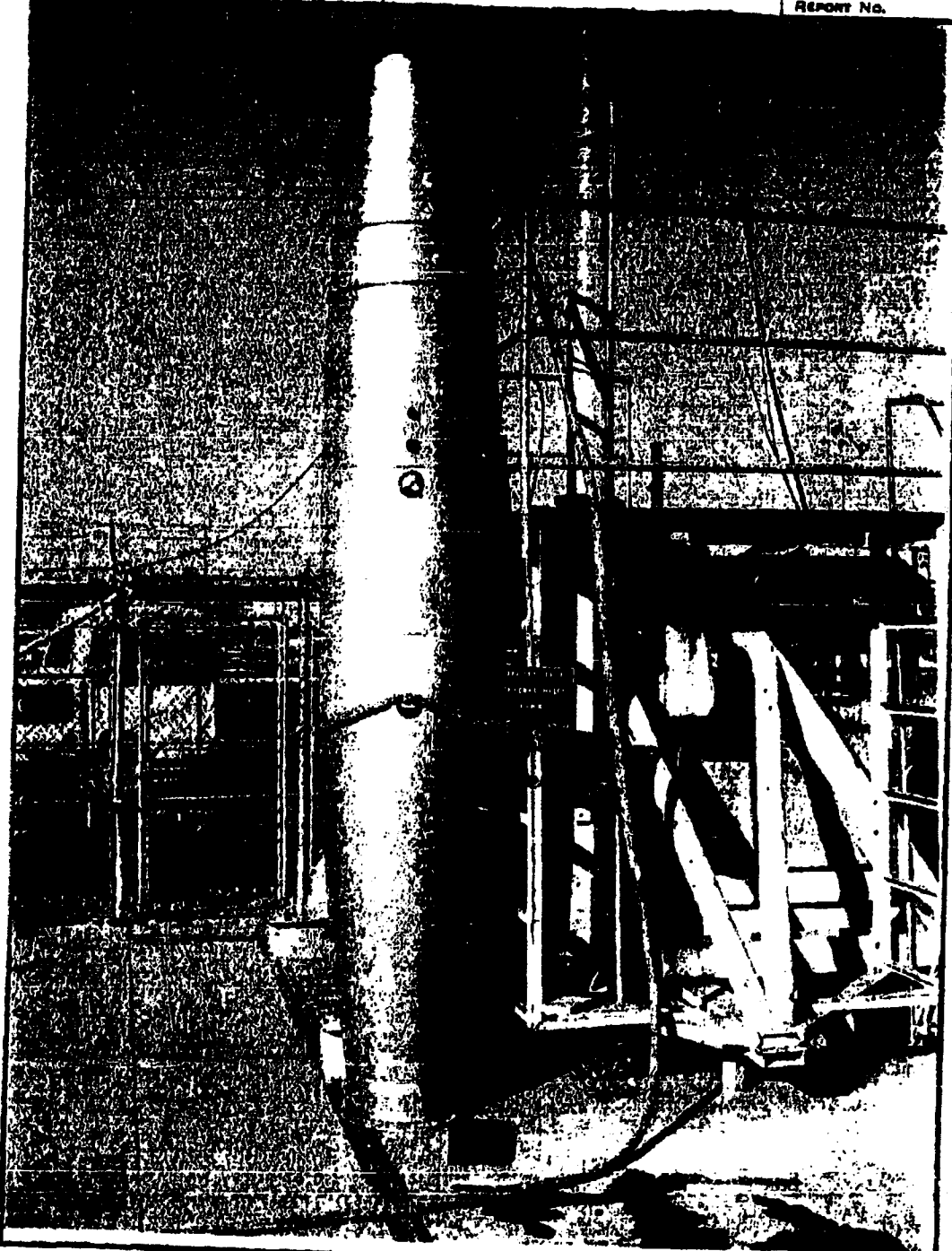
F.A.C. QUALITY CONTROL:

[Signature]

CUSTOMER:

[Signature]

PREPARED	NAME <b>G. FORD</b>	DATE	FLETCHER AVIATION CORP.			PAGE	TEMP.	PERM
CHECKED			TITLE <b>CAPACITY TEST</b>					
APPROVED						MODEL		
						REPORT NO.		





PREPARED	NAME W. Callahan	DATE 1-3-62	FLETCHER AVIATION COMPANY	PAGE	TEMP.	PERM. 4.0
CHECKED			TITLE SLOSH/VIBRATION TEST GENERAL MILLS TANK ASSY	Model	26-300	
APPROVED				REPORT No.	43.286	

ADMINISTRATIVE DATA (3)

PURPOSE OF TEST:

To demonstrate the tank will withstand vibration and pitching forces encountered in service.

MANUFACTURER:

Fletcher Aviation Company

MANUFACTURER'S MODEL NO.:

26-300

ASSEMBLY DRAWING:

26-300-480J1

QUANTITY OF ITEMS:

One (1)

SECURITY CLASSIFICATION:

None

TEST DATE:

2-5-62

TEST CONDUCTED BY:

Wayne Callahan

DISPOSITION OF SPECIMEN:

Use for Leakage Test

ABSTRACT:

The assembly successfully met all of the requirements of the test.

PREPARED	NAME W. Callahan	DATE 1-6-62	FLETCHER AVIATION COMPANY	PAGE	TEMP.	PERM. 4.1
CHECKED			TITLE SLOSH/VIBRATION TEST GENERAL MILLS TANK ASSY	Model	26-300	
APPROVED				REPORT No.	43.286	

FACTUAL DATA

REQUIREMENTS:

1. The complete test specimen is mounted in the support fixture on the slosh and vibration machine. The centerline of the tank, so mounted, is a minimum of twenty inches above the slosh axis. The tank booms are in the retracted position.

The test specimen is filled two thirds full with water at ambient temperature and is simultaneously slosh and vibration tested in accordance with the following conditions.

- A. The vibration displacement is a minimum double amplitude of 0.032 average between the top and bottom of the tank and at the supporting rings. The average peak value, at the point of measurement during a thirty second interval, is the value recorded.
  - B. The vibration frequency is 2000  $\begin{matrix} +0 \\ -60 \end{matrix}$  C.P.M.
  - C. The tank is mounted with the major horizontal axis at 90° to the axis of the shaft of the rocker platform.
  - D. The slosh angle is 30° total, approximately 15° on either side of the horizontal position.
  - E. The tank is pressurized to 15 P.S.I.G.
  - F. The tank is slosh-vibrated for 25 hours at 16 to 20 slosh C.P.M.
2. Following the slosh and vibration test, the tank booms are extended with the tank two-thirds full with water at ambient temperature and is simultaneously slosh and vibration tested in accordance with the following conditions:
    - A. Repeat steps "A" through "E" of the previous test.

PREPARED	NAME W. Callahan	DATE 1-6-62	FLETCHER AVIATION COMPANY	PAGE	TEMP.	PERK.
CHECKED			TITLE SLOSH/VIBRATION TEST GENERAL MILLS TANK ASSY	Model	26-300	4.
APPROVED				Report No.	43.286	

FACTUAL DATA ①

REQUIREMENTS (contd)

2. The tank is slosh-vibrated for 15 minutes at 16 to 20 slosh CPM.
3. The tank is filled with water and vibrated for 10 minutes at vibration displacement specified in "A" of the previous test.

TEST EQUIPMENT:

1. Slosh and vibration machine.
2. Tank support fixture.
3. Water meter.
4. Strobotac or equivalent.
5. Vibration meter.
6. Vibration pickup.
7. Pressure gage.

TEST PROCEDURE:

1. The test assembly is mounted on the slosh and vibration machine by means of a support fixture. The centerline of the assembly is a minimum of 20 inches above the slosh axis.
2. The tank is filled with water in the amount corresponding to 2/3 of the rated capacity of the tank in gallons.
3. The tank is pressurized to 15 P.S.I.G.

PREPARED	NAME W. Callahan	DATE 1-6-62	FLETCHER AVIATION COMPANY	PAGE	TEMP.	DESK 473
CHECKED			TITLE SLOSH/VIBRATION TEST GENERAL MILLS TANK ASSY	Model	26-300 43.286	
APPROVED				REPORT No.		

FACTUAL DATA

TEST PROCEDURE: (contd)

4. The slosh and vibration machine is put into cyclic pitching of the longitudinal axis from 15° nose up to 15° nose down.
5. The motor drive for the eccentric weights, producing vibration is activated and brought up to 2000  $\begin{smallmatrix} +0 \\ -60 \end{smallmatrix}$  CFM.
6. Vibration readings are taken and the eccentric weights adjusted to produce the required values of vibration displacement.
7. The slosh rate is checked to be 17 per min.
8. The rotation speed of the eccentric weights is measured to be 2000  $\begin{smallmatrix} +0 \\ -60 \end{smallmatrix}$  R.P.M.
9. The air pressure is checked and adjusted if necessary, to 15 P.S.I.G.
10. Simultaneous slosh and vibration is continued for 25 hours.
11. The tank booms are extended and the tank is simultaneous slosh vibrated for 15 minutes in the configuration described in steps 1 through 9.
12. Note the resonant vibration behavior of the booms.
13. The tank is then depressurized, filled with water, the booms retracted, and again pressurized to 15 P.S.I.G.
14. The vibration mechanism is started and readings taken. Adjustments are made as necessary to produce the required vibration.
15. Rotation speed of the eccentric weights is adjusted to 2000  $\begin{smallmatrix} +0 \\ -60 \end{smallmatrix}$
16. Vibration is stopped at the end of 10 minutes and the tank is depressurized and drained.

PREPARED	NAME W. Callahan	DATE 1-6-62	FLETCHER AVIATION CORPORATION	PAGE	TEMP.	FORM 4.4
CHECKED			TITLE BLOSH/VIBRATION TEST		MODEL	26-300
APPROVED			GENERAL MILLS TANK ASSY			43.286
					REPORT No.	

**TEST RESULTS:**

③

See page 4.7

**RECOMMENDATIONS:**

F.A.C. ENG'R.:

*W. Callahan*

QUALITY CONTROL:

\_\_\_\_\_

CUSTOMER:

*W. Callahan*

PREPARED	NAME <u>W. Callahan</u>	DATE <u>1-6-62</u>	FLETCHER AVIATION CORPORATION	PAGE	TOTAL PAGES <u>4:5</u>
CHECKED			TITLE <u>SLOSH-VIBRATION TEST</u> <u>GENERAL MILLS TANK ASSY</u>	MODEL	<u>26-300</u>
APPROVED				REPORT NO.	<u>43,286</u>

TANK NO. \_\_\_\_\_ MODEL 26-300 (4) (3)

TEST CONDUCTED BY: Wayne Callahan DATE: 2-5-62

VIBRATION

TANK CAPACITY: 191 GALS. TEST: 127 GALS.

OPERATING PRESSURE: 15 P.S.I.G. TEST PRESSURE: 15 P.S.I.G.

TANK AT 90° TO SLOSH AXIS

ECC. WT. SETTING			SLOSH RATE	VIBRATION MEASUREMENT/IN.					
In./Overlap		Speed		At Lugs	Fwd. Ring		Aft. Ring		
Fwd.	Aft.	R.P.M.	C.P.M.		Fwd	Aft	Upper	Lower	Upper
1.25	1.25	1985	17	.015	.015	.020	.023	.018	.019
1.75	1.75	1985	17	.017	.017	.022	.023	.020	.021
2.25	2.25	1985	17	.018	.018	.025	.025	.025	.029
2.75	2.75	1985	17	.021	.023	.033	.035	.037	.030

START OF RUN: DATE: 2-5-62 TIME: 2:45 p.m.

LOG: Crack developed in outer skin. See page 4.7, 4.8 & 4.9

END OF RUN: DATE: 2-6-62 TIME: 8:20 a.m.

REASON: Crack developed

JUL 19 2013

PREPARED	NAME <u>M. Callahan</u>	DATE <u>1-5-62</u>	FLETCHER AVIATION CORPORATION	PAGE	TEMP.	FEED. <u>4.6</u>
CHECKED			TITLE <u>SLOSH-VIBRATION TEST</u>	Model	<u>26-300</u>	
APPROVED			<u>GENERAL MILLS TANK ASSY</u>		<u>43.286</u>	
				REPORT No.		

TANK NO. \_\_\_\_\_ MODEL 26-300

TEST CONDUCTED BY: Wayne Callahan DATE: 2-8-62

VIBRATION

TANK CAPACITY: 191.0 GALS. TEST: 127.0 GALS.

OPERATING PRESSURE: 15 P.S.I.G. TEST PRESSURE: 15 P.S.I.G.

TANK AT 90° TO SLOSH AXIS

ECC. WT. SETTING			SLOSH RATE	VIBRATION MEASUREMENT/IN.					
In./Overlap		Speed		At Lugs		Fwd. Ring		Aft. Ring	
Fwd.	Aft.	R.P.M.	C.P.M.	Fwd	Aft	Upper	Lower	Upper	Lower
2.5	2.5	1990	17	.027	.028	.025	.045	.029	.041
2.25	2.25	1990	17	.021	.023	.023	.038	.025	.037

START OF RUN: \_\_\_\_\_ DATE: 2-8-62 TIME: 1:50 P.M.

LOG: R.P.M. and amplitude checked every 1/2 hour

END OF RUN: \_\_\_\_\_ DATE: 2-9-62 TIME: 2:50 p.m.

REASON: End of 25 hour test

PREPARED	NAME W. Callahan	DATE 2-8-62	FLETCHER AVIATION COMPANY	PAGE	TOTAL PAGES 4:7
CHECKED			TITLE SLOSH & VIBRATION TEST GENERAL MILLS TANK ASSY	MODEL	26-300 43.286
APPROVED				REPORT No.	

RESULTS OF TEST

After 17-1/2 hours of simultaneous slosh and vibration a crack in the outer skin located immediately aft of the aft hook was noted. The test was discontinued at this point and the test assembly was removed from the fixture. Close examination revealed the crack to be approximately 18 inches in circumferential length, 15° in both directions from the top centerline of the assembly. The crack appeared to have started in the smallest radius of the bend adjacent to the "flat" for the aft mounting hook. (Ref. photo on page 4.10 of this report)

When the tank was disassembled and the inner fiberglass tank inspected, the following discrepancies were noted:

1. Inner rubber liner loose from tank, torn in several places.
2. Several layers of apparently non-impregnated fiberglass strands adhering to the loose rubber liner, also hanging loose in the tank.
3. Slosh baffle bulkheads integral but loose and lying on bottom of tank.
4. Circumferential ring to hold bulkheads still intact.
5. Small partial ring segments to retain bulkheads entirely loose.
6. The exposed inside surfaces of the inner tank appeared to be smooth.

The photograph on page 4.11 shows the condition of the inner tank immediately after removal from test fixture.

The outer skin of the tank was repaired in accordance with the sketch on page 4.12. The slosh baffles and rubber liner were removed from the inner tank, and the assembly was again subjected to the complete test. The tank then successfully completed the test in accordance with the procedure previously outlined.



PREPARED	NAME W. Callahan	DATE 2-8-62	FLETCHER AVIATION COMPANY	PAGE	471
CHECKED			TITLE SLOSH & VIBRATION TEST GENERAL MILLS TANK ASSY	MODEL	26-300
APPROVED				REPORT No	43.286

RESULTS OF TEST (contd)

A displacement of .038 inches double amplitude at the tips of the booms were noted during the 15 minutes of slosh-vibration with the booms extended. At the conclusion of the test the booms were again extended and a scan for resonance was made with the following results:

1. Resonant frequency of booms - 1650 C.P.M.
2. Displacement at resonant frequency - .35 inch double amplitude at tips.

JUL 19 2013

PREPARED	NAME <u>W. Callahan</u>	DATE <u>2-5-62</u>	FLETCHER AVIATION CORPORATION	PAGE	<u>48</u>
CHECKED			TITLE <u>SLOSH-VIBRATION TEST</u>	MODEL	<u>26-300</u>
APPROVED			<u>BOOMS EXTENDED</u>		<u>43.286</u>
			<u>GENERAL MILLS TANK ASSY</u>	REPORT NO.	

TANK NO. \_\_\_\_\_ MODEL 26-300 ④

TEST CONDUCTED BY: Wynne Callahan DATE: 2-9-62

VIBRATION

TANK CAPACITY: 191 GALS. TEST: 127 GALS.

OPERATING PRESSURE: 15 P.S.I.G. TEST PRESSURE: 15 P.S.I.G.

TANK AT 90° TO SLOSH AXIS

ECC. WT. SETTING			SLOSH RATE	VIBRATION MEASUREMENT/IN.					
In./Overlap		Speed		At Lug	Fwd. Ring		Aft. Ring		
Fwd.	Aft.	R.P.M.	C.P.M.		Fwd	Aft	Upper	Lower	Upper
2.25	2.25	1990	17	.028	.026	.025	.037	.030	.035

START OF RUN: \_\_\_\_\_ DATE: 2-9-62 TIME: 3:00 p.m.

LOG: \_\_\_\_\_

END OF RUN: \_\_\_\_\_ DATE: 2-9-62 TIME: 3:15 p.m.

REASON: End of 15 minute test

PREPARED	NAME N. Callahan	DATE 1-6-62	FLETCHER AVIATION CORPORATION	PAGE	TOT. PAGES 4.9
CHECKED	TITLE VIBRATION TEST GENERAL MILLS TANK ASSY.			MODEL	26-300
APPROVED					43.286
					REPORT No.

TANK NO. \_\_\_\_\_ MODEL 26-300 (4)

TEST CONDUCTED BY: Wayne Callahan DATE: 2-9-62

VIBRATION

TANK CAPACITY: 191 GALS. TEST: 191 GALS.

OPERATING PRESSURE: 15 P.S.I.G. TEST PRESSURE: 15 P.S.I.G.

TANK AT 90° TO SLOSH AXIS

ECC. WT. SETTING			VIBRATION MEASUREMENT/IN.					
In/Overlap		Speed	At Lugs		Fwd. Ring		Aft. Ring	
Fwd	Aft	R.P.M	Fwd	Aft	Upper	Lower	Upper	Lower
3.00	3.00	1990			.023	.033	.022	.031
3.50	3.50	1990			.029	.038	.029	.033

START OF RUN: \_\_\_\_\_ DATE: 2-9-62 TIME: 3:50 P.M.

LOG: \_\_\_\_\_

\_\_\_\_\_

\_\_\_\_\_

END OF RUN: \_\_\_\_\_ DATE: 2-9-62 TIME: 4:00 P.M.

REASON: End of 10 minute run

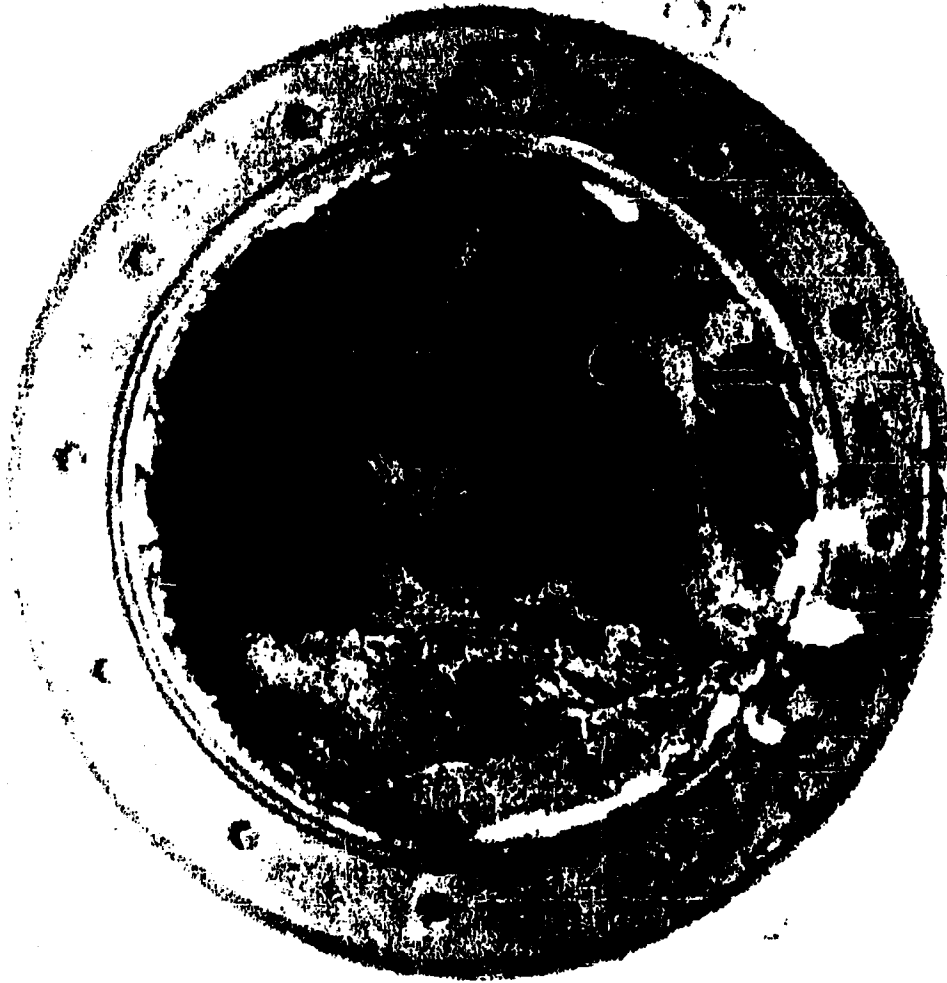
JUL 19 2013

G. FORD		FLETCHER AVIATION CORP.		TEMP	PERM
				PAGE	
APPROV. VEC				REPORT NO.	

**SLOSH & VIBRATION**  
**GENERAL MILLS**  
**TANK**  
**FAC FEB-62**



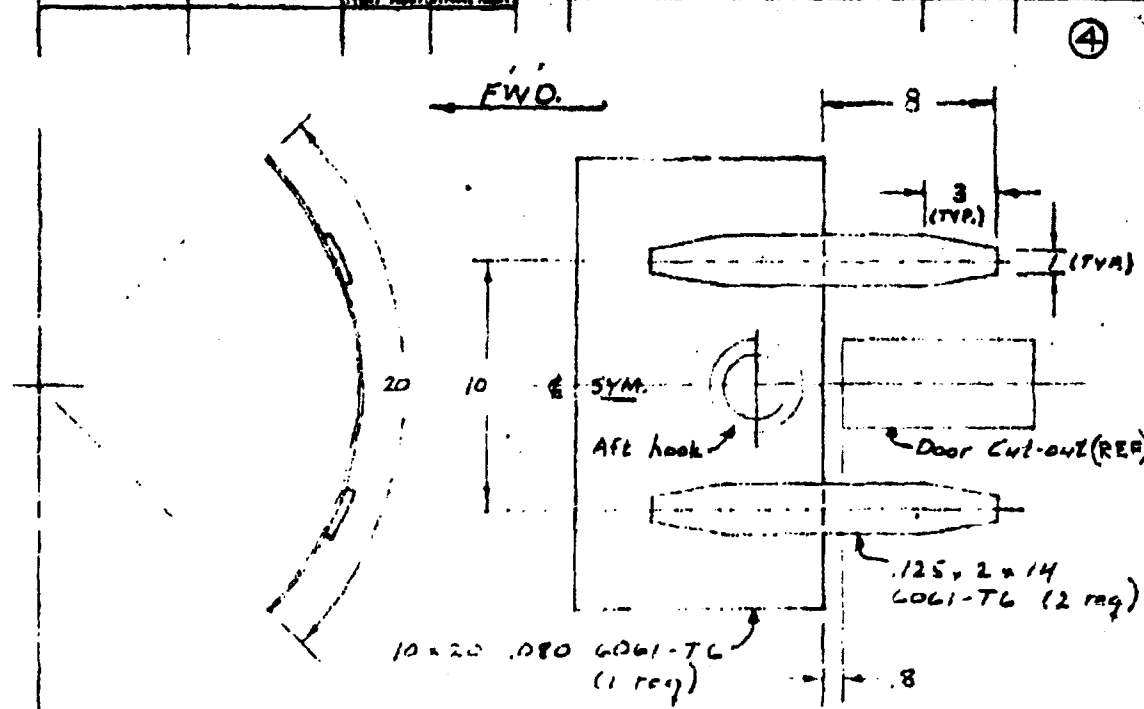
PREPARED	NAME G. FORD	DATE	FLETCHER AVIATION CORP.	PAGE	TEMP.	PERM.
CHECKED			TITLE SLOSH VIBRATION TEST	4	4	
APPROVED				MODEL 26-300	43-286	REPORT NO.



REPORT 42306 PAIR 4

THIS REPRODUCTION IS A PROPRIETARY DESIGN AND CONFIDENTIAL DISCLOSURE OF THE PATENT RIGHTS OF FLETCHER AVIATION CORPORATION. IT IS HEREBY FORWARDED TO YOU UNDER THE PROVISIONS OF THE PATENT AND TRADE SECRET ACTS, 35 U.S.C. 431 AND 18 U.S.C. 1905, AND IS LOANED SUBJECT TO THE CONDITIONS THAT IT IS NOT TO BE USED FOR REPRODUCTION OR IN ANY OTHER WAY PERMISSIBLE TO THE PATENT AND TRADE SECRET ACTS, 35 U.S.C. 431 AND 18 U.S.C. 1905, AND IS NOT TO BE REPRODUCED NOR COPIED IN WHOLE OR IN PART, AND IS NOT TO BE RETURNED TO THE PATENT AND TRADE SECRET ACTS, 35 U.S.C. 431 AND 18 U.S.C. 1905.

APPLICATION				REVISIONS			
NEXT ASSY.	USED ON	REVISION	SYM.	DESCRIPTION	DATE	APP.	

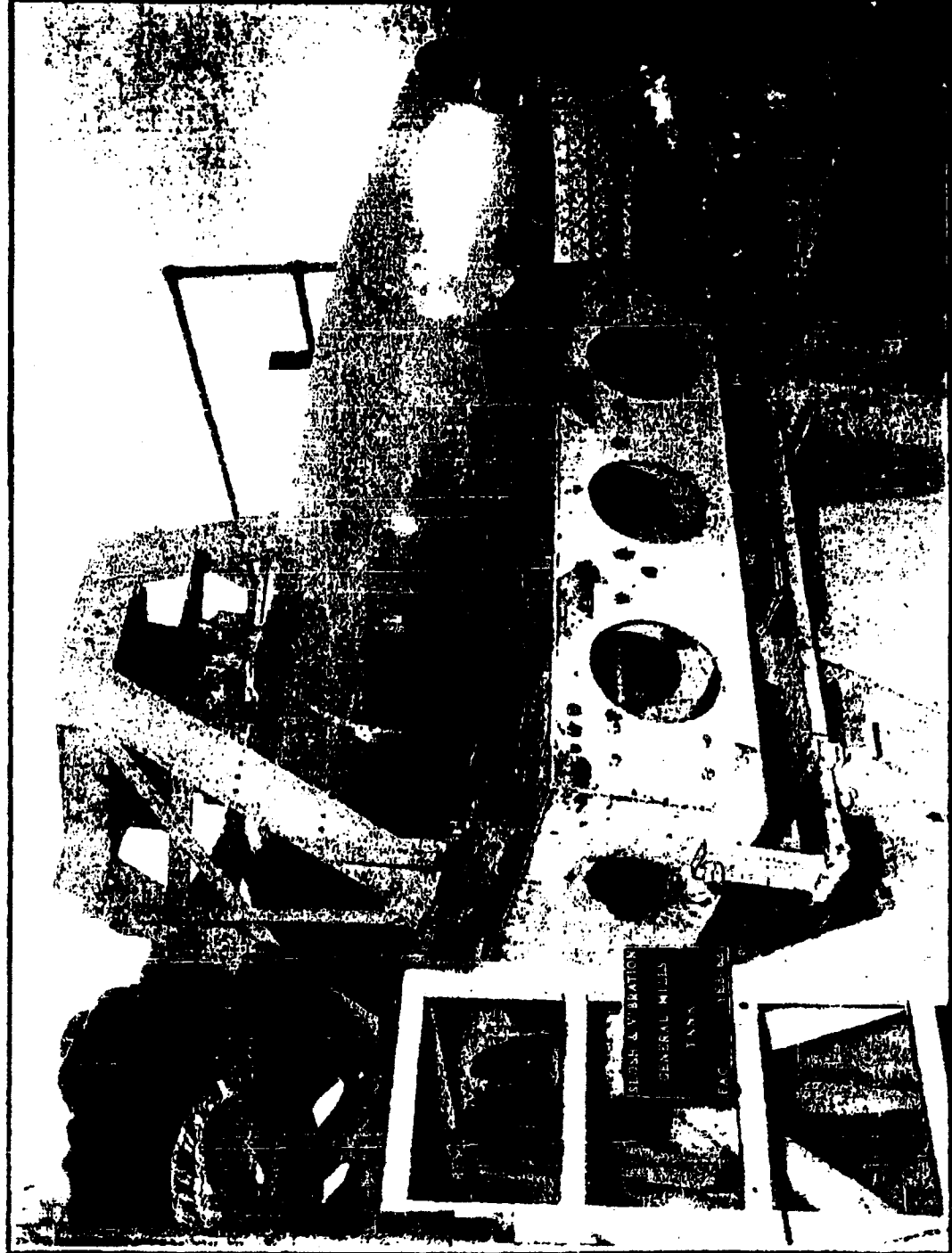


- 1- Cut out 10x20 area to match patch.
- 2- Clean out foam to 2' from edge of hole.
- 3- Butt weld patch into place, & add reinf. strips.  
All weld 100%
- 4- Foam fill void bet. inner tank & outer shell

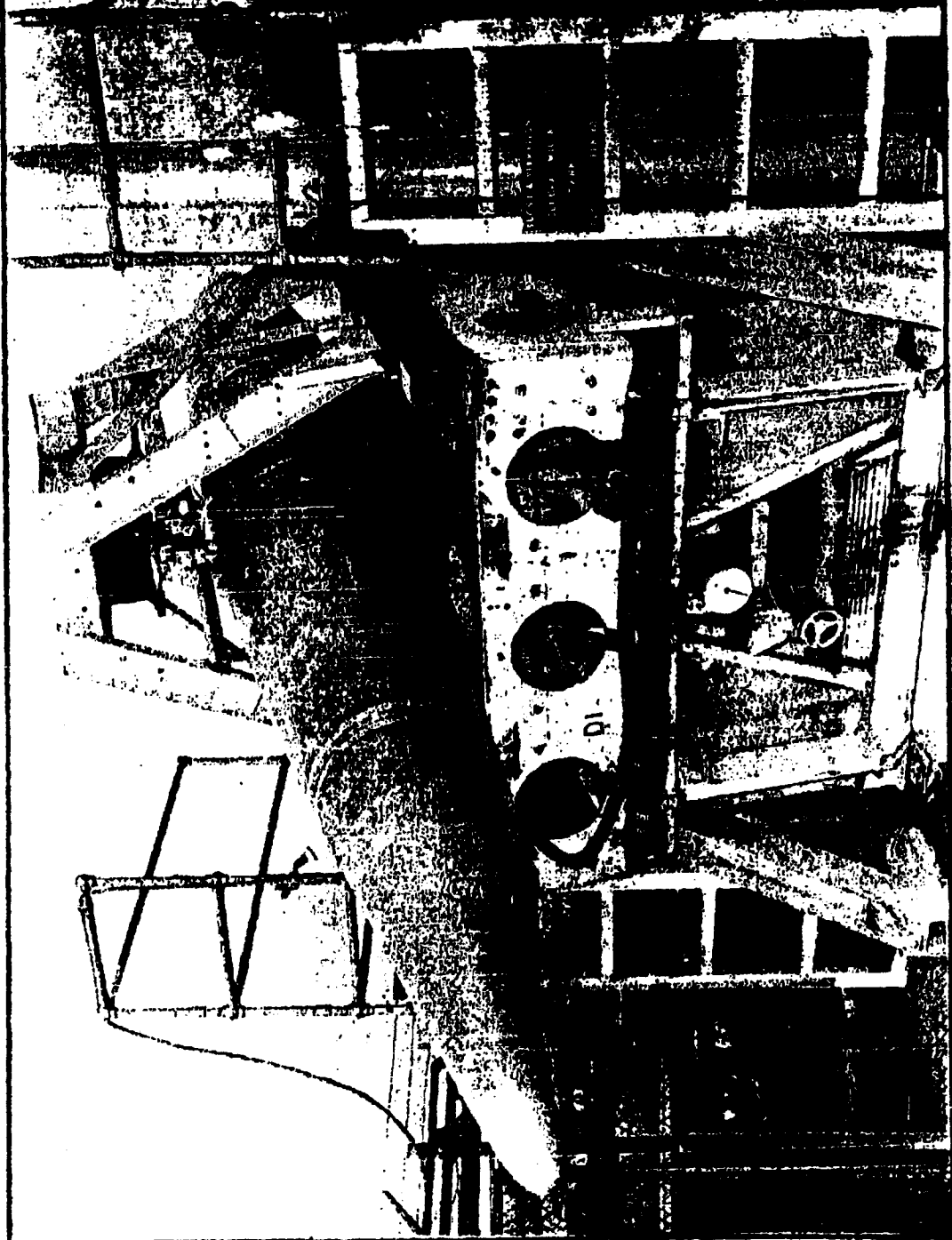
LN.	QTY.	PART NO.	DESCRIPTION	TYPE	SIZE	SPECIFICATION
-----	------	----------	-------------	------	------	---------------

UNLESS OTHERWISE SPECIFIED		NAME		DATE		<b>FLAIR AVIATION COMPANY</b> <small>FORMERLY</small> <b>FLETCHER AVIATION CORPORATION</b> FLETCHER AIRPORT ROSEMEAD, CALIFORNIA
DIM. IN INCHES - TOLERANCES ON DECIMALS		DRAWN	R W Hill	2-7	REPAIR SKETCH	
.015		STRESS	R W Hill	2-7	GENL MILLS TANK	
.030		CHECK				
.010		PR. ENG.	R W Hill	2-7		
V SURFACE TOUGHNESS PER MIL-STD-10		REC. ENG.			CODE IDENT. NO. 72429	
BREAK SHARP CORNERS		CHK. ENG.			SCALE: 1/8 Size	26-300-6064
REMOVE DIMENSIONS BEFORE PLATING					WEIGHT: —	ENT. 1 OF 1
HEAT TREAT						
None						

PREPARED	NAME <b>G. FORD</b>	DATE	<b>FLETCHER AVIATION CORP.</b>	PAGE	TEMP.	PERM.
CHECKED			TITLE	28-50		3
APPROVED				MODEL		
				4223		
				REPORT No.		

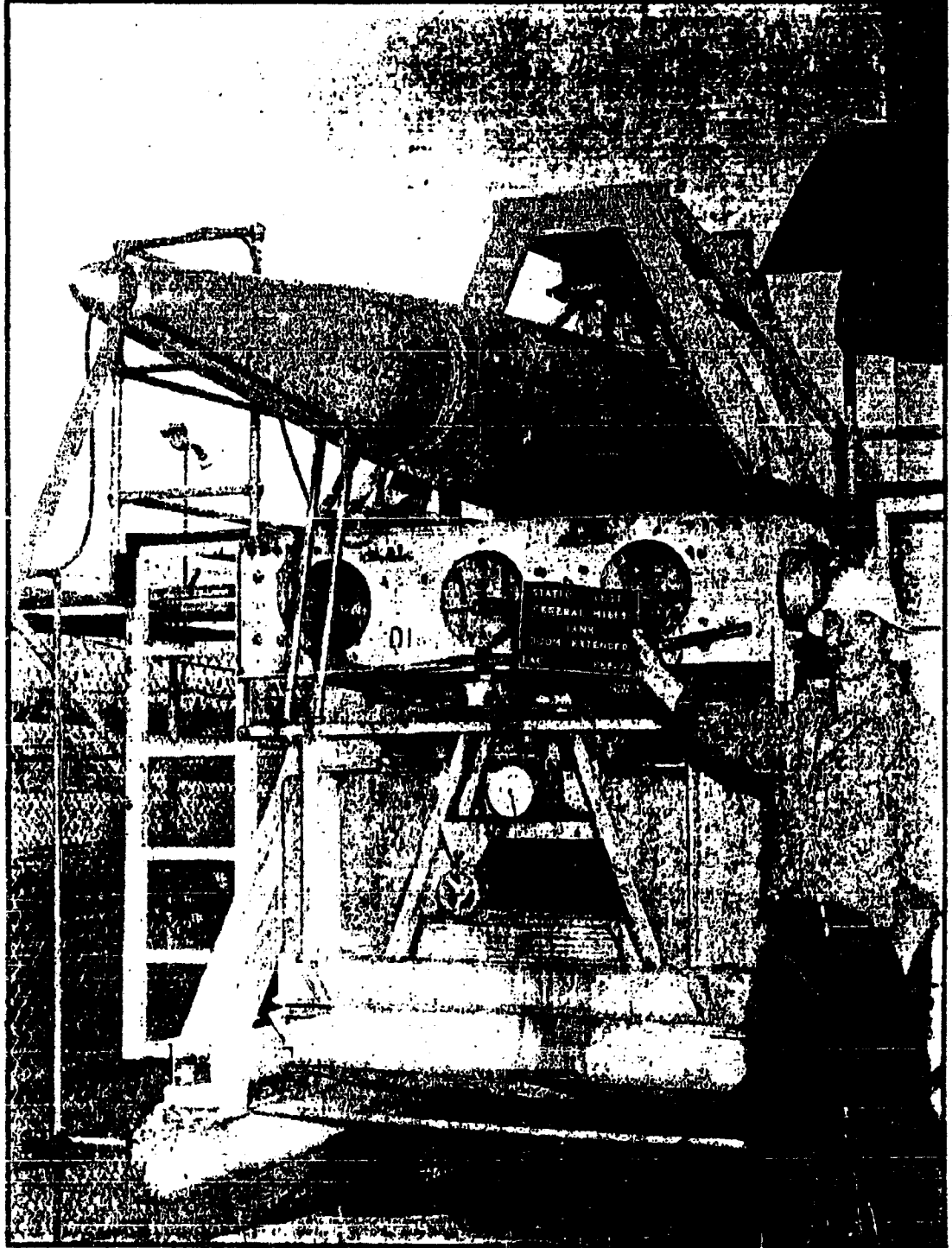


PREPARED	NAME <b>G. FORD</b>	DATE	<b>FLETCHER AVIATION CORP.</b>	PAGE	TEMP.	PERM.
CHECKED			TITLE <b>VIBRATION</b>	<b>20</b>		<b>500</b>
APPROVED			<b>TEST</b>	MODEL	<b>40-28</b>	REPORT NO.





PREPARED	NAME G. FORD	DATE	FLETCHER AVIATION CORP.	PAGE	TEMP.	PERM
CHECKED			TITLE BURNING OPERATION TEST			
APPROVED			300A18 EXTENDED			
						REPORT NO.



PREPARED	NAME W. Callahan	DATE 1-5-62	FLETCHER AVIATION COMPANY	PAGE	TEMP.	FEED.
CHECKED			TITLE LEAKAGE TEST GENERAL MILLS TANK ASSY	MODEL	26-300	43.285
APPROVED				REPORT NO.		

ADMINISTRATIVE DATA (3)

PURPOSE OF TEST:

To demonstrate that the tank will withstand the required internal pressure without leakage.

MANUFACTURER:

Fletcher Aviation Company

MANUFACTURER'S MODEL NO.:

26-300

ASSEMBLY DRAWING

26-300-48031

QUANTITY OF ITEMS:

One (1)

SECURITY CLASSIFICATION:

None

TEST DATE:

2-12-62

TEST CONDUCTED BY:

Wayne Callahan

DISPOSITION OF SPECIMEN:

Use for ejection test.

ABSTRACT:

The assembly successfully met all of the requirements of the test.

PREPARED	NAME W. Callahan	DATE 1-5-62	FLETCHER AVIATION COMPANY	PAGE	TEMP.	FORM 5.1
CHECKED			TITLE LEAKAGE TEST GENERAL MILLS TANK ASSY	MODEL	26-300 43.286	
APPROVED				REPORT NO.		

FACTUAL DATA

REQUIREMENTS:

1. The inner fiberglass tank with all openings sealed is subjected to an internal pressure of 20 P.S.I.G. using Freon 12. The tank is then checked for leakage using a General Electric H-1 tester.

TEST EQUIPMENT:

1. Tank Support
2. Pressure Gage
3. Freon 12 container with regulator.
4. General Electric H-1 tester.

PROCEDURE:

1. With the tank supported, a regulated Freon 12 supply line is connected to the assembly.
2. A pressure gage is connected to the assembly.
3. Freon 12 pressure is admitted into the assembly until the pressure gage indicates 20 P.S.I.G.
4. External surfaces of the assembly are checked for leakage using the General Electric H-1 tester at a sniffing rate of 1/2 inch per second.
5. Inspect the tank visually for evidence of failure such as damage to the bulkheads or liner of the inner tank or structural damage to the inner or outer tank.

PREPARED	NAME W. Callahan	DATE 1-5-62	FLETCHER AVIATION COMPANY		PAGE	FORM	PERM.
CHECKED			TITLE LEAKAGE TEST GENERAL MILLS TANK ASSY		MODEL	26-300 43.286	
APPROVED					REPORT NO.		

③

**TEST RESULTS:**

During the leakage test it was determined that the foaming process used to install the foam between the inner tank and outer shell contained halogen gas. Since the General Electric tester used in probing for leaks is sensitive to this gas, there was a constant leakage indication during the test.

The sensitivity of the instrument was adjusted so that it would not indicate leakage from the presence of gas in the foam. It was then determined that it would indicate leakage if any of the stronger mixture from the inner tank escaped to atmosphere.

The test was concluded with the instrument adjusted per the preceding paragraph, and the test conducted per the outlined procedure on page 5.1. There was no evidence of leakage. No evidence of leakage when pressurized to 20 p.s.i.g.

F.A.C. ENGR.

Wayne Callahan

F.A.C. QUALITY CONTROL:

\_\_\_\_\_

CUSTOMER:

W. J. [Signature]

PREPARED BY	NAME G FORD	DATE	FLETCHER AVIATION CORP.	PAGE	TEMP	PERM
REVIEWED			TITLE			
APPROVED				WHEEL		
				REPORT NO.		

PREPARED	NAME W. Callahan	DATE 1-8-62	FLETCHER AVIATION COMPANY	PAGE	TEMP.	PERM. 6:0
CHECKED			TITLE GROUND EJECTION TEST GENERAL MILLS TANK ASSY	Model	26-300 43.206	
APPROVED				Report No.		

③

ADMINISTRATIVE DATA

PURPOSE OF TEST

To determine ejection characteristics.

MANUFACTURER

Fletcher Aviation Company

MANUFACTURER'S MODEL NO.

26-300

ASSEMBLY DRAWING

26-300-48031

QUANTITY OF ITEMS

One (1)

SECURITY CLASSIFICATION

None

DATE TEST COMPLETED

2-16-62

TEST CONDUCTED BY

Wayne Callahan

DISPOSITION OF SPECIMEN

Hold at Fletcher Aviation Company for sixty (60)  
days for G.M.I. disposition.

ABSTRACT

The assembly successfully met all of the requirements  
of the test.

PREPARED	NAME W. Callahan	DATE 1-8-62	FLETCHER AVIATION COMPANY	PAGE	TEMP.	FORM
CHECKED			TITLE GROUND EJECTION TEST GENERAL MILLS TANK ASSY			6.1
APPROVED						MODEL 26-300 43.286 REPORT NO.

### FACTUAL DATA

#### REQUIREMENTS

That one (1) or more ejection be made with a lightweight tank and one (1) or more ejection be made with heavy-weight tank so as to accurately determine the peak force, velocity, acceleration, and tank attitude at end of stroke. The peak ejection force shall not exceed 30,000 lbs.

#### TEST EQUIPMENT

1. Ejection frame
2. Suspension fixture
3. Pylon
4. Lightweight Store
5. Heavyweight Store
6. 28V D.C. power supply
7. 20,000 Ohm/Volt Multimeter
8. Midwestern Oscillograph
9. F.A.C. Force Transducer
10. Extensometer (Century Eng.)
11. Accelerometer
12. Amplifier (Miller)
13. High Speed Camera (Wollensak)
14. Goose Control

#### TEST PROCEDURE

1. Install suspension fixture on ejection frame.
2. Install pylon on suspension fixture.
3. Install lightweight store on pylon.
4. Apply 28V D.C. to the mechanism.
5. Measure voltage at firing pins.
6. Remove safety pin.
7. Measure voltage at firing pins.
8. Disconnect power supply and install safety pin.

PREPARED	NAME W. Callahan	DATE 1-8-62	FLETCHER AVIATION COMPANY	PAGE	TERR. PERM. 6.2
CHECKED			TITLE GROUND INJECTION TEST GENERAL HILLS TANK ASSY	Model	26-300 43.286
APPROVED				REPORT No.	

**FACTUAL DATA**

**TEST PROCEDURE** (contd)

11. Install extensometer.
12. Install camera.
13. Check instrument and camera circuit.
14. Install cartridges.
15. Remove safety pin.
16. Activate instrument and camera circuits.
17. Activate firing mechanics.
18. Clean pylon assembly and inspect.
19. Install heavyweight store on pylon.
20. Repeat steps 4 through 17.



PREPARED	NAME W. Callahan	DATE 1-8-62	FLETCHER AVIATION COMPANY	PAGE	TANK	FORM 6-3
CHECKED			TITLE GROUND EJECTION TEST	Moms. 26-100		
APPROVED			GENERAL MILLS TANK ASST	43,286		
				REPORT NO.		

TEST RESULTS

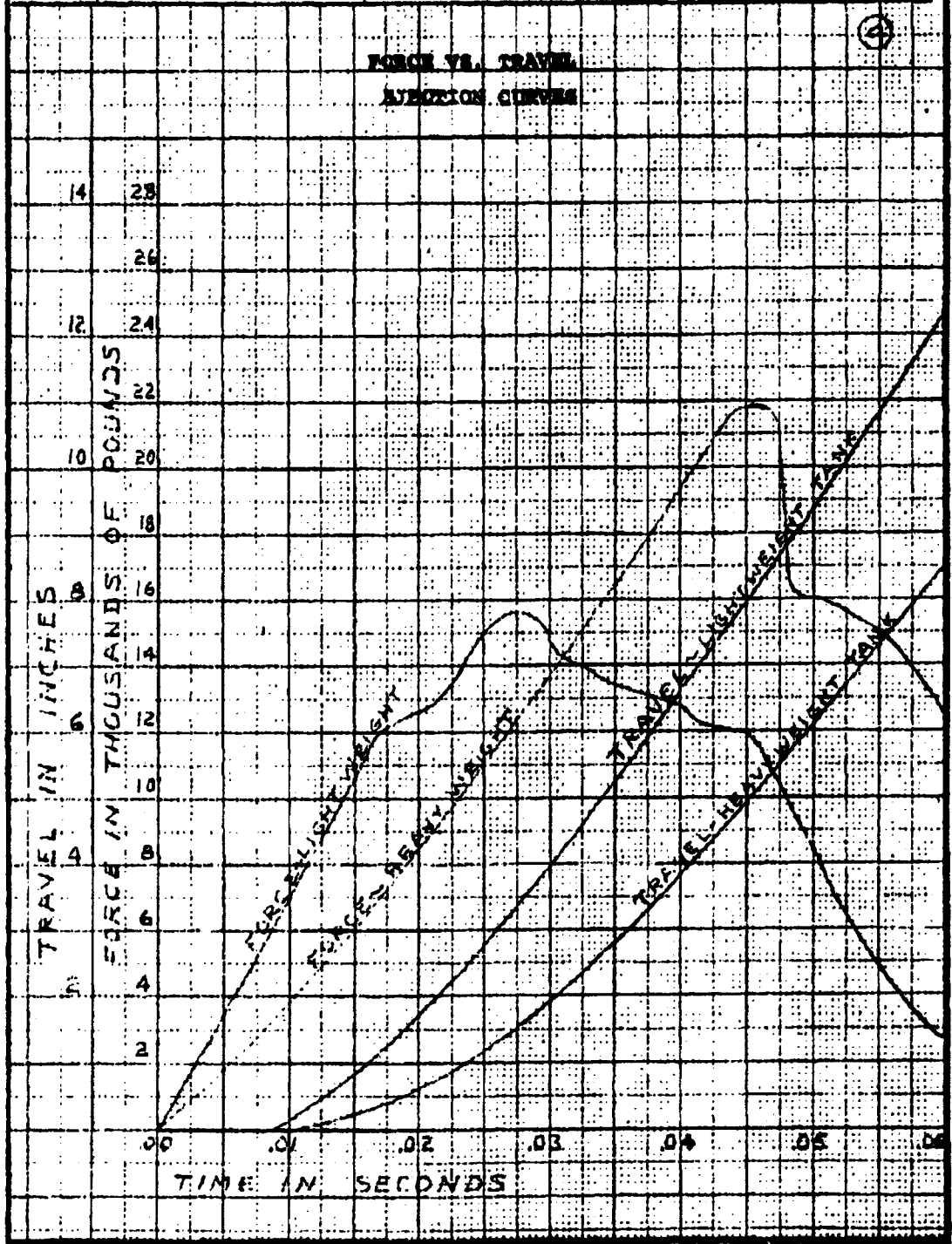
③

	<u>Lightweight Tank</u>	<u>Heavyweight Tank</u>
Peak Ejection Force	<u>15,600 lbs.</u>	<u>21,956 lbs.</u>
Peak Acceleration	<u>27.4 "G's"</u>	<u>37.1 "G's"</u>
Peak Velocity	<u>21.9 ft/sec.</u>	<u>17.8 ft/sec.</u>
Attitude at end of stroke	<u>Level</u>	<u>Level</u>

RECOMMENDATIONS: \_\_\_\_\_  
 \_\_\_\_\_  
 \_\_\_\_\_

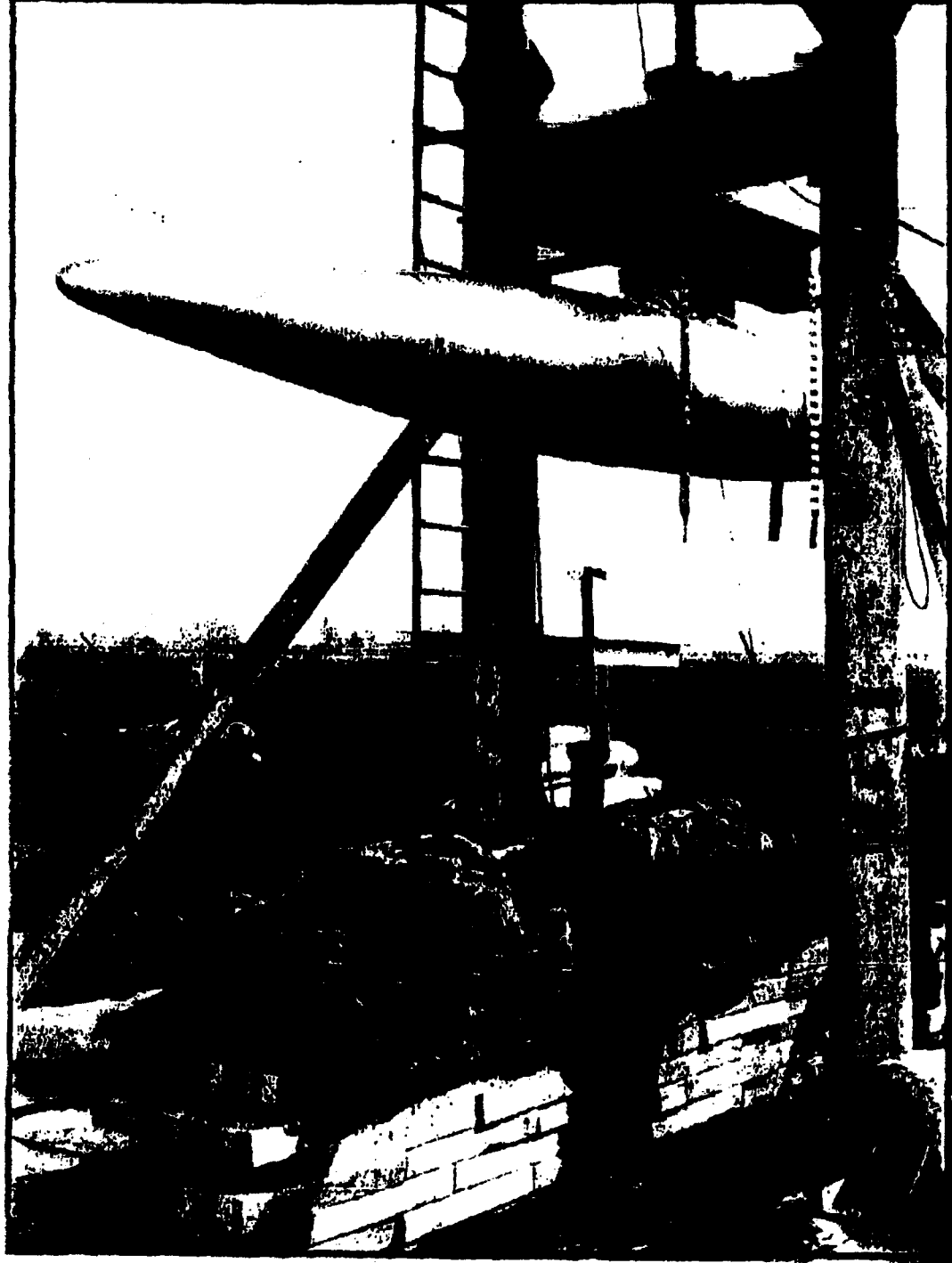
F.A.C. ENG'R: William Callahan  
 QUALITY CONTROL: \_\_\_\_\_  
 CUSTOMER: A. F. B...

Prepared	W. Callahan	4-9-62	FLETCHER AVIATION CORP.		Page	63.1
Checked	H. H.		GROUND EJECTION TEST GENERAL MILLS TANK ASSY		Model	25-300
Approved					Report No.	43.286



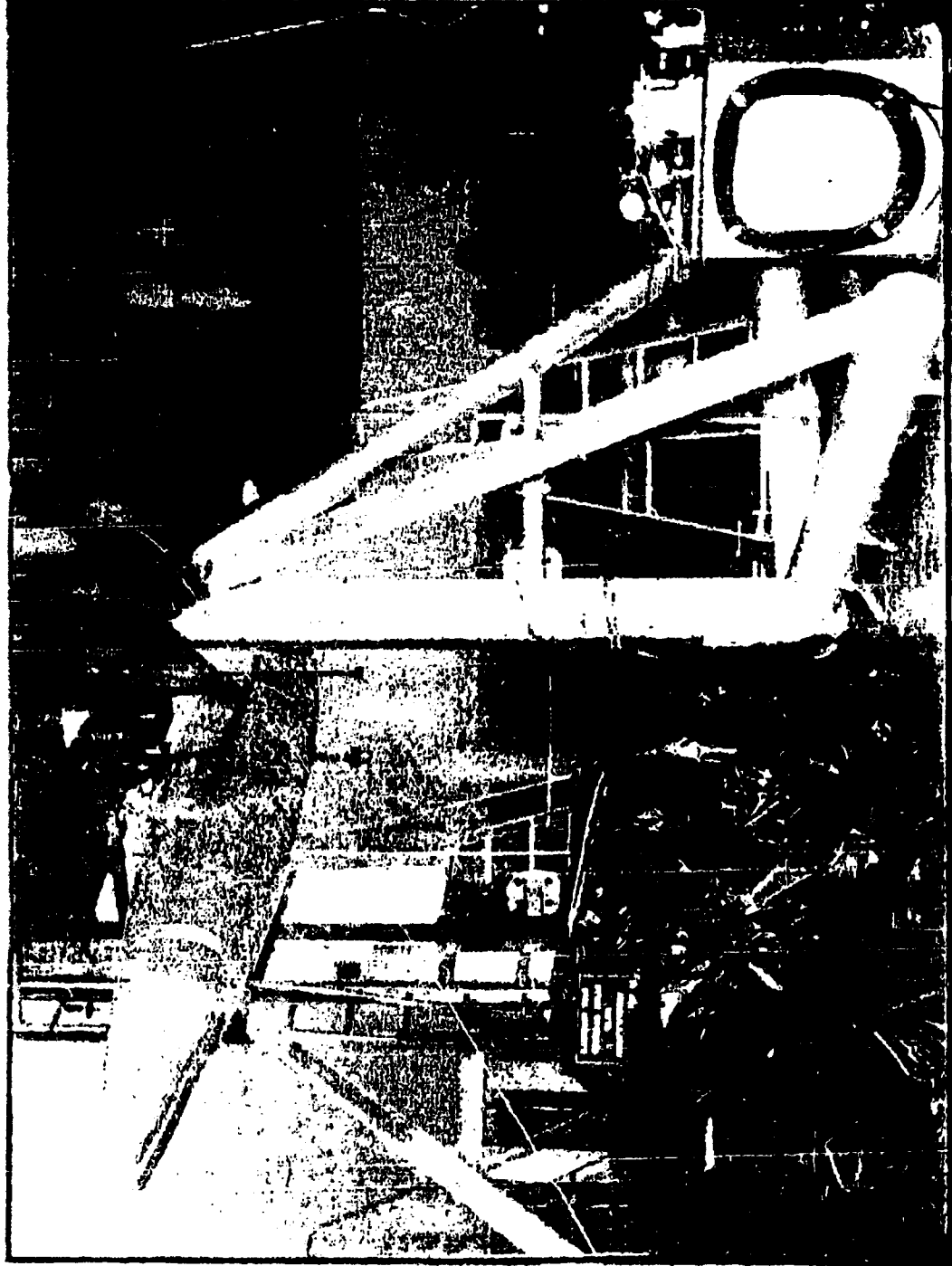
Page determined to be Unclassified  
Reviewed Chief, RDD, WHS  
IAW EO 13526, Section 3.5  
Date: JUL 19 2013

PREPARED	NAME <b>G. FORD</b>	DATE	<b>FLETCHER AVIATION CORP.</b>	PAGE	TEMP.	PERM.
CHECKED			TITLE <b>GROUND EJECTION TEST</b>	<b>6.4</b>	<b>26-300</b>	
APPROVED				MODEL	<b>43.286</b>	REPORT NO.



JUL 19 2013

PREPARED	NAME G. FORD	DATE	FLETCHER AVIATION CORP.	TEMP	PERM
REVIEWED			TITLE	PAGE	6.15
APPROVED			GROUND SUPPORT TEST	26300	
				MODEL	43072
				REPORT NO.	



JUL 19 2013

PREPARED	NAME N. Callahan	DATE 1-6-62	FLETCHER AVIATION COMPANY		PASS	7.0
CHECKED			TITLE STRUCTURAL TEST GENERAL MILLS TANK ASSY		MODEL	26-300 43.286
APPROVED					REPORT NO.	

ADMINISTRATIVE DATA (3)

PURPOSE OF TEST:

To demonstrate the structural integrity of the tank.

MANUFACTURER:

Fletcher Aviation Company

MANUFACTURER'S MODEL NO.

26-300

ASSEMBLY DRAWING:

26-300-

QUANTITY OF ITEMS:

One (1)

SECURITY CLASSIFICATION:

None

TEST DATE:

2-8-62 through 2-12-62

TEST CONDUCTED BY:

Wayne Callahan

DISPOSITION OF SPECIMEN:

Hold at F.A.C. for 60 days for G.M.I. disposition.

ABSTRACT:

The assembly successfully met all of the requirements of the test.

JUL 19 2013

PREPARED BY	NAME Callahan	DATE 1-6-62	FLETCHER AVIATION COMPANY	PAGE	7.1
CHECKED	<i>H. H. ...</i>	<i>1-11-62</i>	TITLE STRUCTURAL TEST GENERAL MILLS TANK ASSY	MODEL	25-100 43.286
APPROVED				REPORT NO.	

FACTUAL DATA

①④

TEST REQUIREMENT

The tank is subjected to the following test conditions and does support these conditions without failure.

A tank that has not been used for other tests shall be used for this test. The static test tank shall be a complete structure, less such non-structural elements as turbine generator, booms, actuator, boom support structure, fluid handling components, and electrical components. Also, the inner fiberglass tank shall be simulated by a suitable structure of the same size and configuration. The static test tank shall be of the same quality workmanship as the flight tank delivered on the contract and shall be, except for the inner tank, structurally identical to the flight tank as indicated in the reports and drawings submitted.

The test techniques of the tank is as follows:

The tank support jig shall be constructed to duplicate the attach point locations of the Aero 7A rack to produce the most critical hook and sway brace reactions.

Loads are introduced into the test tank by means of tension pads internal formers, and/or external straps. Of these methods, tension pads are preferable in that they allow a better load distribution and are less susceptible to local overloading difficulties. Care is taken to insure that the load application devices do not materially affect the strength of the test tank by introducing artificial stiffness, etc.

All applied test loads are suitably monitored by calibrated equipment (pressure gages, load dynamometers, etc.) so that acceptable test accuracy is obtained.

Internal pressure, where applicable, is applied pneumatically or hydraulically and the pressure suitably monitored with calibrated measuring devices.

JUL 19 2019

PREPARED	NAME W. Callahan	DATE 1-6-62	FLETCHER AVIATION COMPANY	PAGE	7 of 11
CHECKED			TITLE STRUCTURAL TEST GENERAL MILLS TANK ASSY	FORM	26-300
APPROVED				REPORT NO.	43.286

**FACTUAL DATA (contd)**

Tare weight of store and all load application devices is accounted for in all test loadings. Particular care is taken when dense fluids (water, etc.) are used for introducing internal pressure so that true incremental loads for all load components are obtained. Independent application of combined load components (that is vertical, side, and aft loads) are preferable over resultant load application to facilitate maintaining correct relationship of load components with each other for full range of load from zero to ultimate.

JUL 19 2013

PREPARED	NAME W. Callahan	DATE 1-6-62	FLETCHER AVIATION CORPORATION	PAGE	TOTAL PAGES 7.2
CHECKED			TITLE STRUCTURAL TEST GENERAL MILLS TANK ASSY	MODEL 26-100	43,286
APPROVED				REPORT NO.	

The test loads of the tank are as specified in contract.

TEST EQUIPMENT:

1. Static test frame.
2. Tank support fixture.
3. Loading pads, whiffle trees, etc., per applicable test conditions.
4. Hydraulic pumps.
5. Hydraulic cylinders (jacks) with net areas as listed on test data sheets.
6. Hydraulic test gages: as necessary
7. Four 24-inch Starrett steel engine marked scales reading to .010 inch.
8. Surveyor's level.

TEST PROCEDURE:

All test conditions are run with the test tank mounted in the horizontal position in the test jig. The test procedure is identical in each case and consists of the following steps:

1. The system of loading jacks and whiffle trees is installed, checked functionally, and inspected for proper location.
2. Readings of deflection at zero load is taken by means of a series of steel scales hung along the length of the tank, and a surveyor's level. Lateral deflections are measured from a wire stretched alongside of the tank.
3. The load is then applied in increments of 25% of limit load, and the deflection readings taken at 25, 50, 75, and 100%
4. The jack loads are then reduced to zero, and deflection readings taken to check possible permanent set.
5. Load is again applied in 25% increments up to 100% of limit load.



JUL 19 2013

PREPARED	NAME W. Callahan	DATE 1-6-62	RETCHER AVIATION CORPORATION	PAGE	7.3
CHECKED			TITLE STRUCTURAL TEST	MODEL	26-100
APPROVED			GENERAL MILLS TANK ASSY	REPORT NO.	43.286

TEST PROCEDURE: (CONT.)

6. The static load is increased to 125% of limit load.
7. Deflection readings are taken.
8. The static load is increased to 150% of limit load, and deflection readings are taken. (150% of limit load = 100% ultimate load.)
9. The jack loads are reduced to zero and deflection readings are taken.

PREPARED	NAME R.W. Hill	DATE 1-9-62	FLETCHER AVIATION COMPANY	PAGE	TEMP.	FORM
CHECKED			TITLE STRUCTURAL TESTS GENERAL MILLS TANK			7.4
APPROVED				MODEL	43.286	
				REPORT No.		

**STRUCTURAL STATIC TESTS**

A review of F.A.C. Report No. 43.284, "Loads and Stress Analysis, General Mills Tank", shows that there are three design conditions critical for the tank and its attaching structure. These are conditions #10, 25, and 29. Condition #29 is an ejection condition which will be adequately covered by the actual tank full and empty ejections. (Ref. pages 6.0 to 6.3 incl.) Test loads for Condition #10 and 25 are developed on the following pages.

As on page #2 of Report #43.284, the sign convention for the test loads is as follows:

- Z = Upward acting
  - Y = Acting to the left
  - X = Aft acting
- Positive moment vectors are in the same direction using the left-hand rule.

The unit loads shown on page 7.5 are revised to agree with the latest weight data in Appendix "A" of Report #43.284.

All load factors, loads and moments in this section, are on an ultimate basis. (1-1/2 x limit load) The tank itself will be tested empty and unpressurized.

PREPARED	NAME <i>R.W. Hill</i>	DATE <i>1-2-61</i>	FLETCHER AVIATION CORPORATION	PAGE	TOTAL PAGES <i>7.5</i>
CHECKED			TITLE	MODEL	
APPROVED			<i>Static Tests</i>	<i>43.286</i> REPORT NO.	

UNIT INERTIA LOAD DISTRIBUTION  
 (Revised per Appendix "A", report "43.284")

T.S.	Tank Full		1/2 Full, Aft CG.	
	$\frac{P}{\eta}$	$\frac{10^3 P}{M}$	$\frac{P}{\eta}$	$\frac{10^3 P}{M}$
15	73.1	1.547	59.9	2.743
35	164.4	2.653	38.0	1.403
55	260.7	2.896	37.6	1.056
75	341.9	2.078	68.3	1.312
95	353.0	+ .370	196.7	2.037
115	352.0	- 1.403	349.6	+ .523
135	309.8	- 2.793	307.8	- 2.268
155	187.0	- 2.627	187.0	- 3.035
175	50.8	- .969	50.8	- 1.275
195	53.0	- 1.278	53.0	- 1.799
215	16.3	- .474	16.3	- .697
$\Sigma$	2142.0	0	1365.0	0

PREPARED	NAME <i>R.W. Hill</i>	DATE <i>1-7-62</i>	FLETCHER AVIATION CORPORATION	PAGE	76
CHECKED			TITLE <i>Static Tests</i>	MODEL	<i>43.286</i>
APPROVED				REPORT NO.	

TEST LOADS - Cond 10 (Tank 1/2 full, aft CG)

$$\left. \begin{aligned} P_x &= -9.00 \\ P_y &= 4.50 \\ P_z &= -3.00 \\ W &= 9.00 \\ Y &= 0 \end{aligned} \right\} \text{(Pg. 9, Rep. 43.284)}$$

$$I_{yy} = I_{zz} = 4112.6 \text{ slug-ft}^2 \text{ (Pg. A-2, Rep. 43.284)}$$

$$M_{yy} = 12 \times 4112.6 \times 9.00 = 47800 \text{ in-lbs}$$

$$M_{zz} = 0$$

1	2	3	4	5
T.S.	$\frac{P}{W}$	$\frac{10^3 P}{M}$	$P_x$	$P_y$
	Previous page		-9.00 ② +478 ①	4.50 ②
15	59.9	2.743	-408	270
35	38.0	1.403	-275	171
55	37.6	1.056	-288	167
75	48.3	1.312	-552	307
15	196.7	2.037	-1673	895
115	349.6	1.523	-3121	1573
135	307.8	-2.268	-2879	1385
155	187.0	-3.035	-1828	842
175	50.8	-1.275	-518	229
175	53.0	-1.799	-563	238
215	16.3	-.697	-180	73
$\Sigma$	1365.0	0	-12285	6142

$$P_x = -3.00 \times 1365.0 = -4095$$

PREPARED	NAME <i>R W Hill</i>	DATE <i>1-1-62</i>	FLETCHER AVIATION CORPORATION	PAGE	7.7
CHECKED			TITLE	MODEL	
APPROVED			<u><i>Static Tests</i></u>	43.286	REPORT No.

Test Loads - Cond. #25 (Tank Full)

$$\left. \begin{aligned} n_z &= 1.50 \\ n_y &= 2.25 \\ n_x &= 11.25 \\ \bar{e} &= -18.00 \\ \bar{\psi} &= 7.00 \end{aligned} \right\} \text{(Pg. #11, Rep. #43.284)}$$

$$I_{yy} = I_{zz} = 772.6 \text{ slugs-ft}^2 \text{ (Pg. #A.2, rep. #43.284)}$$

$$M_{yy} = 12 \times 772.6 \times (-18.00) = -166,880 \text{ in-lbs}$$

$$M_{zz} = 12 \times 772.6 \times 7.00 = 83,440 \text{ in-lbs}$$

1	2	3	4	5
T.S.	$\frac{P}{n}$	$\frac{10P}{M}$	$P_z$	$P_y$
	Page #7.5		1.50 <sup>②</sup> -166.88 <sup>③</sup>	2.25 <sup>②</sup> -83.44 <sup>③</sup>
15	73.1	1.547	-148	35
35	164.4	2.653	-176	149
55	260.7	2.876	-92	345
75	341.9	2.078	+166	596
95	353.0	+ .370	468	763
115	352.0	-1.403	762	909
135	309.8	-2.793	931	930
155	197.0	-2.427	719	640
175	50.8	-.969	238	195
195	53.0	-1.278	293	226
215	16.3	-.474	104	76
	2162.0	0	3245	4863

$$P_x = 11.25 \times 2162 = 24320 *$$

JUL 19 2013

REPORT NO. R 21 4111 1-9-62 TITLE PAGE 7.8

CHECKED APPROVED Static Tests MODEL 43-286 REPORT NO.

**WIFFLE-TREE LOADING**

Load Condition ... 10. (Flight)  
 Reference Diagram Page

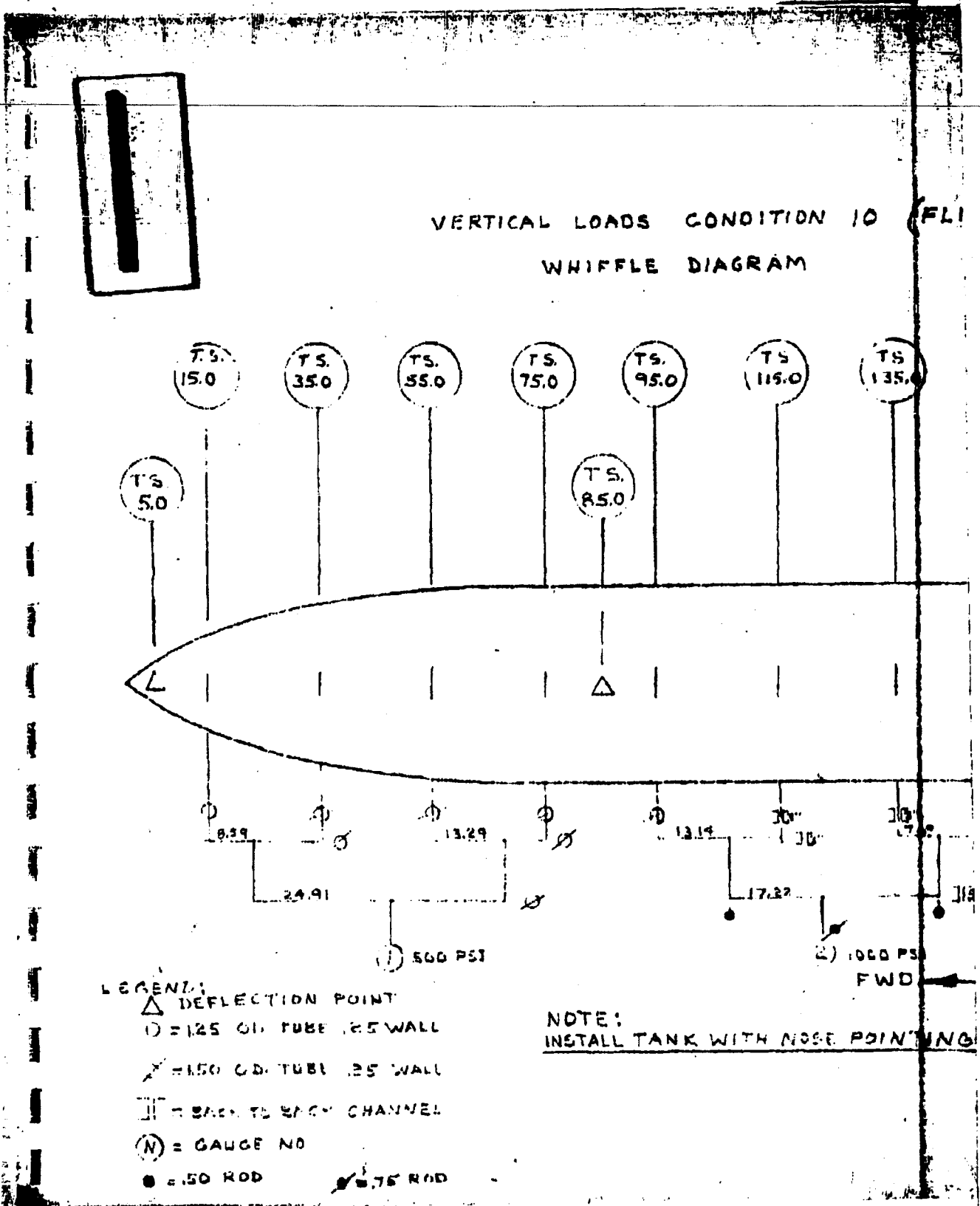
**VERTICAL LOADS**

Sta.	Ult. Id.	Dead Wt.	Tare	Net Id.	Comb.	Sta.	Comb.	Sta.
15	-409	73	15	-320	-561	23.59		①
35	-275	17		-241		-1267		48.50
55	-278	36		-237	-706	68.29		
75	-552	68		-469				
95	-1473	78		-1580	-4609	108.14		②
115	-3121	77		-3029		-9189		125.36
135	-2879	45		-2819	-4580	142.69		
155	-1828	52		-1761				
175	-518	51		-452	-947	185.45		③
175	-563	53		-475		-1096		187.47
215	-180	16	15	-147	-147	215.00		

**HORIZONTAL LOADS**

Sta.	Ult. Id.	Comb.	Sta.	Comb.	Sta.
15	331	502	21.81		④
35	171				
51	169	476	67.90		⑤
77	307				
97	885	2458	107.80		⑥
117	1573				
137	1385	2227	142.56		⑦
157	542				
177	229	467	185.19		⑧
197	238			-419	155.94
217	16	12	215.00		
205c Pull	4095				⑨

④ = Pump and gauge no.

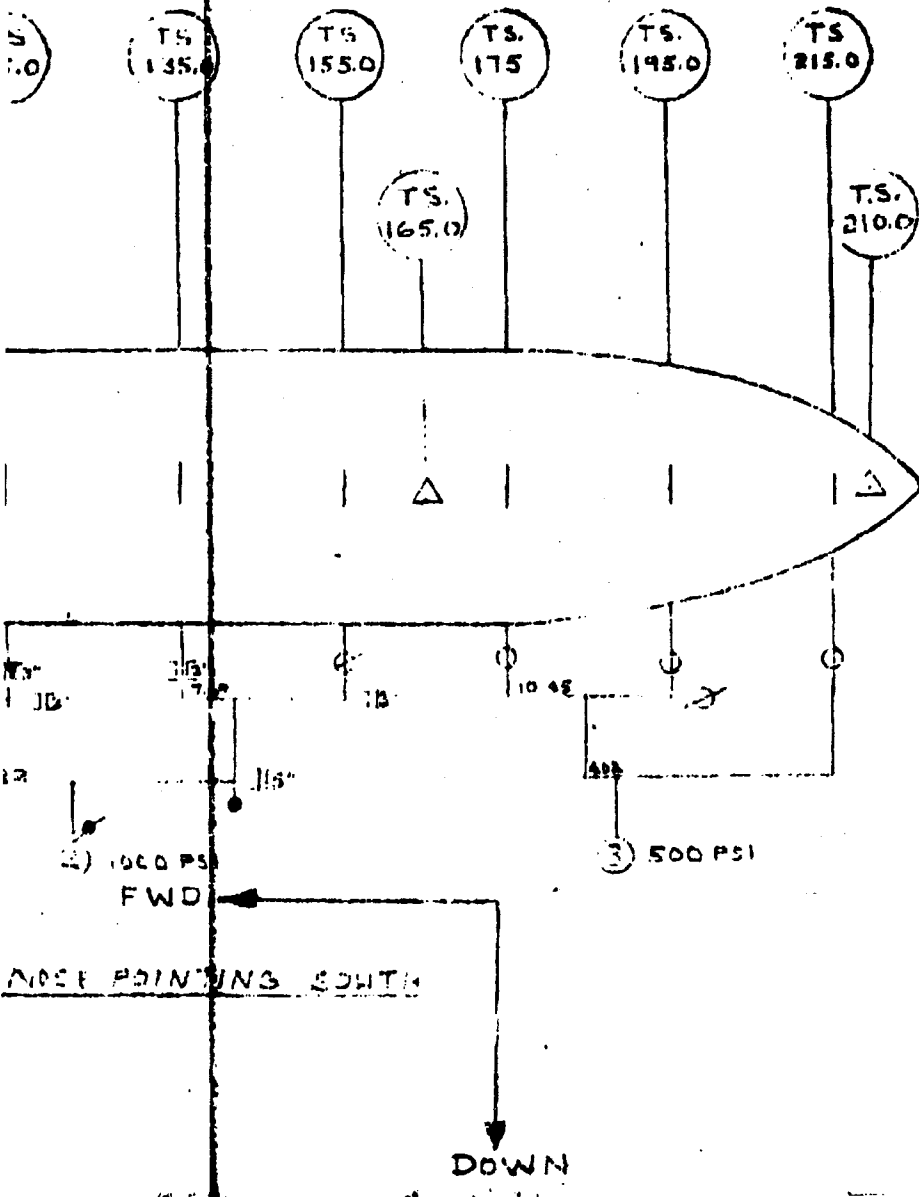


JUL 19 2009

PAGE 7.8  
REPORT NO. 43,286

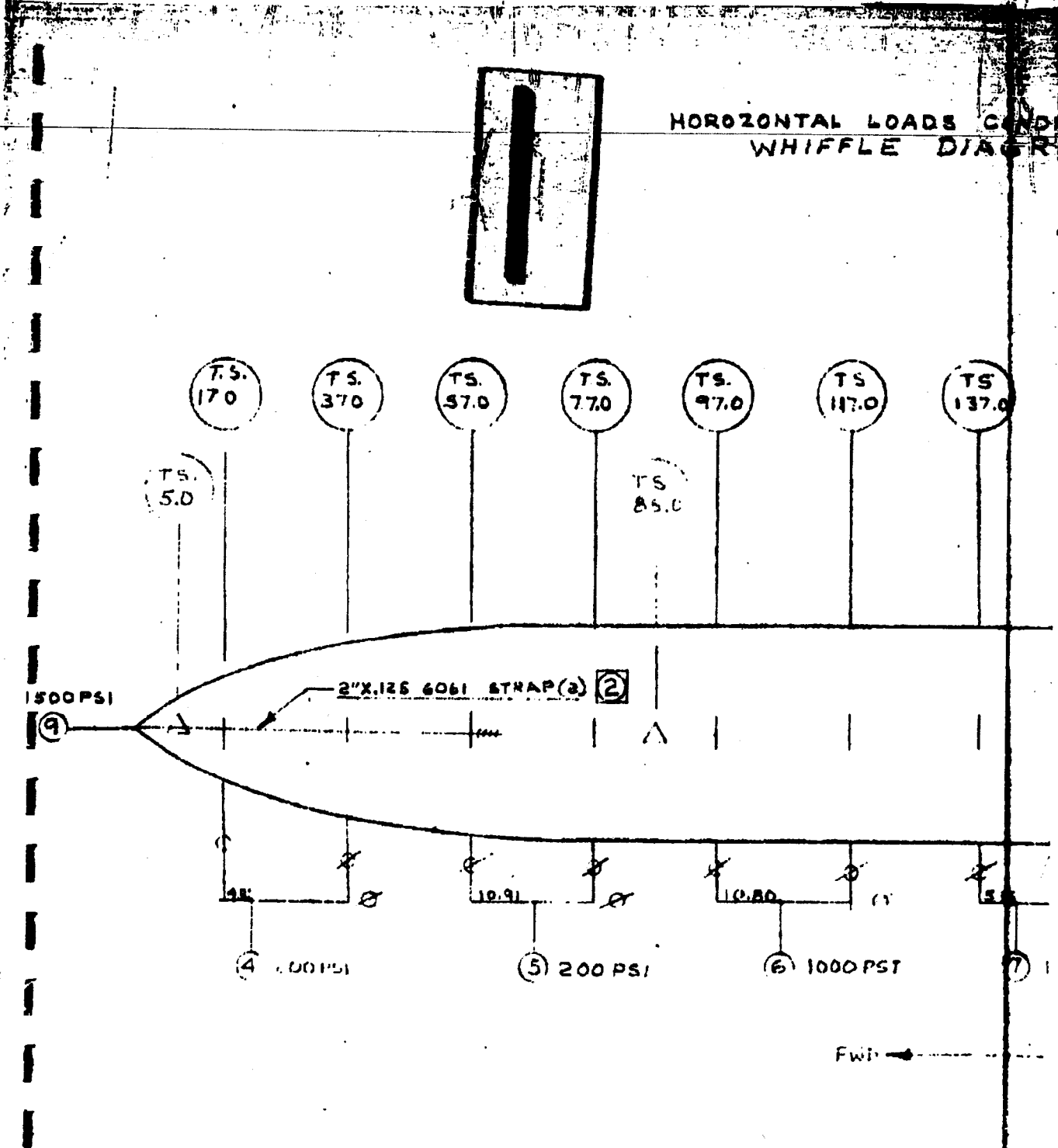
ION 10 (FLIGHT)

M





HORIZONTAL LOADS COND  
WHIFFLE DIAGR

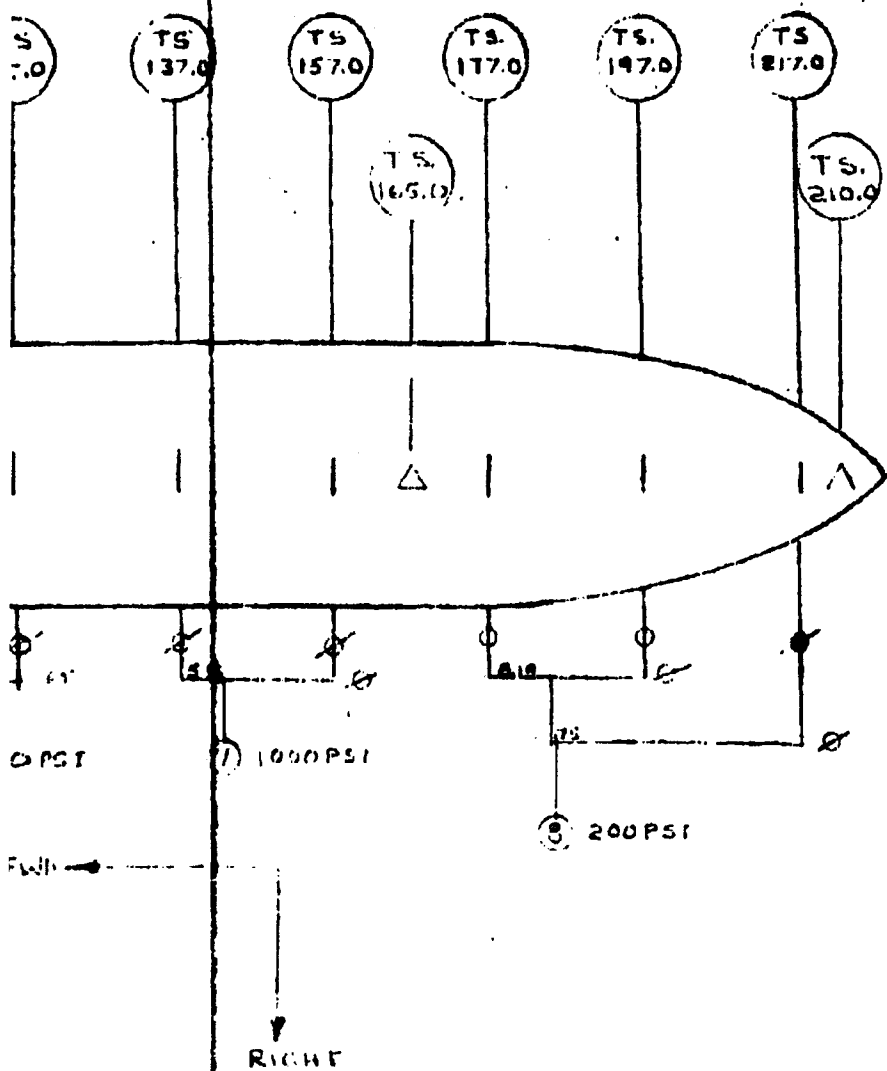


LEGEND: SEE PAGE 781

NOTE:

1. INSTALL TANK WITH NOSE POINTING FORWARD
2. INSTALL STRAPS ON HORIZONTAL C/L

LOADS CONDITION 10 (FLIGHT)  
LE DIAGRAM



Prepared: RW Hill 1-9-62 TITLE: WITCHER VIATION CORPORATION PAGE: 7-7  
 CHECKED: \_\_\_\_\_  
 APPROVED: \_\_\_\_\_ Static Tests 43.286  
 REPORT NO. \_\_\_\_\_

**WIFFLE-TREE LOADING** ①  
 Load Condition No. 25 (Cat Take-off)  
 Reference Diagram Pages \_\_\_\_\_

**VERTICAL LOADS**

Sta.	Ult. Ld.	Dead Wt.	Tare	Net Ld.	Comb.	Sta.	Comb.	Sta.
15	-148	73	15	-60	-222	29.59	-243	① 33.56
35	-196	19		-162				
55	-92	36		-41	-41	55.00		
75	+166	68		+249	810	88.85		
95	418	78		561			2655	② 114.49
115	762	77		854	1845	125.74		
135	931	45		991				
155	719	52		786	1090	160.58		
175	238	51		304			1586	③ 173.04
195	293	53		361	416	200.14		
215	104	16	15	135				

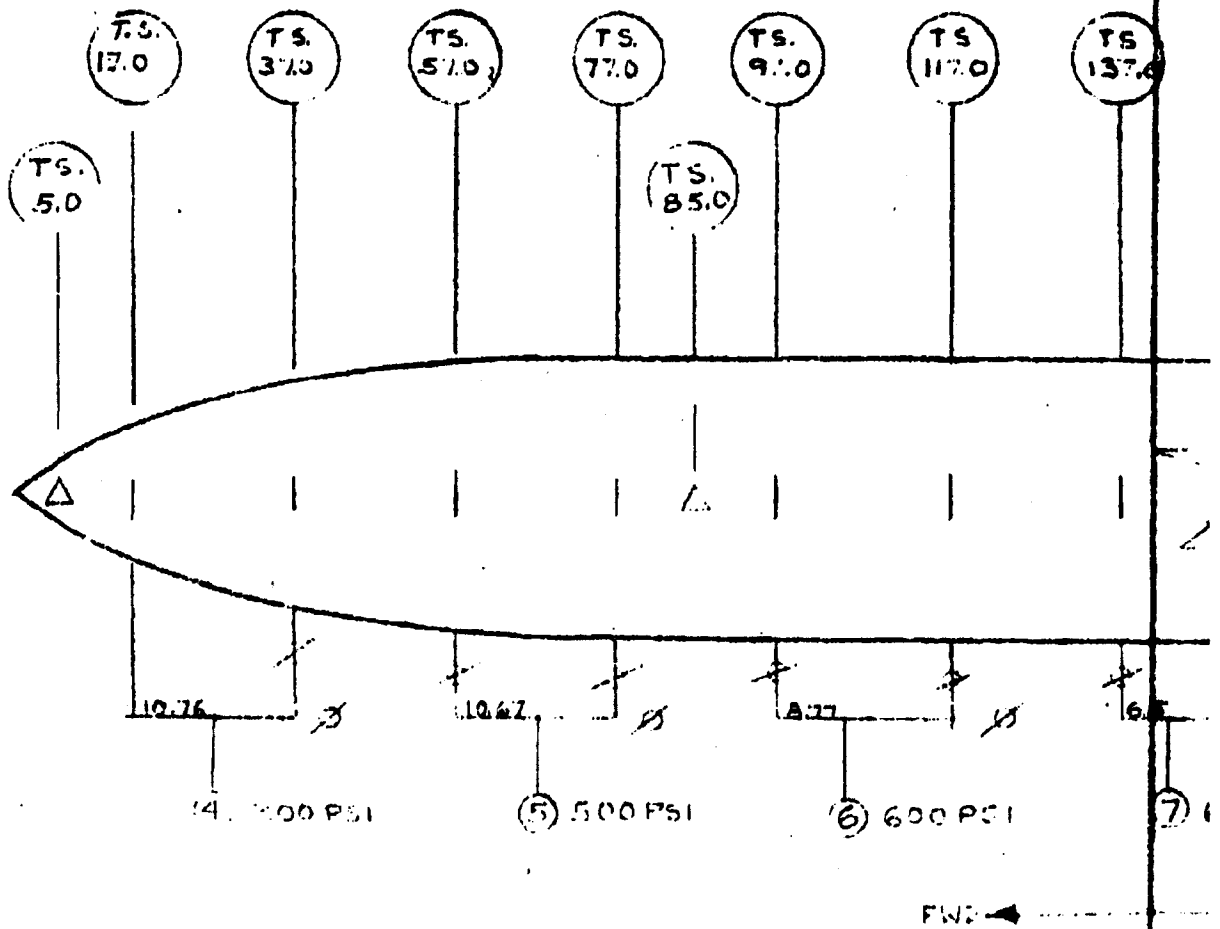
**HORIZONTAL LOADS**

	Sta.	Ult. Ld.	Comb.	Sta.	Comb.	Sta.
④ = Pump and gauge no.	17"	64	270	21.76		④
	3"	148				
	5"	345	941	62.67		⑤
	7"	596				
	9"	763	1672	105.87		⑥
	11"	909				
	13"	930	1570	143.15		⑦
	15"	640				
	17"	195	421	185.74		⑧
	19"	226			442	15750
Drag Load	21"	27	27	215		⑨





HORIZONTAL LOADS COND  
WHIFFLE DIAGRAM

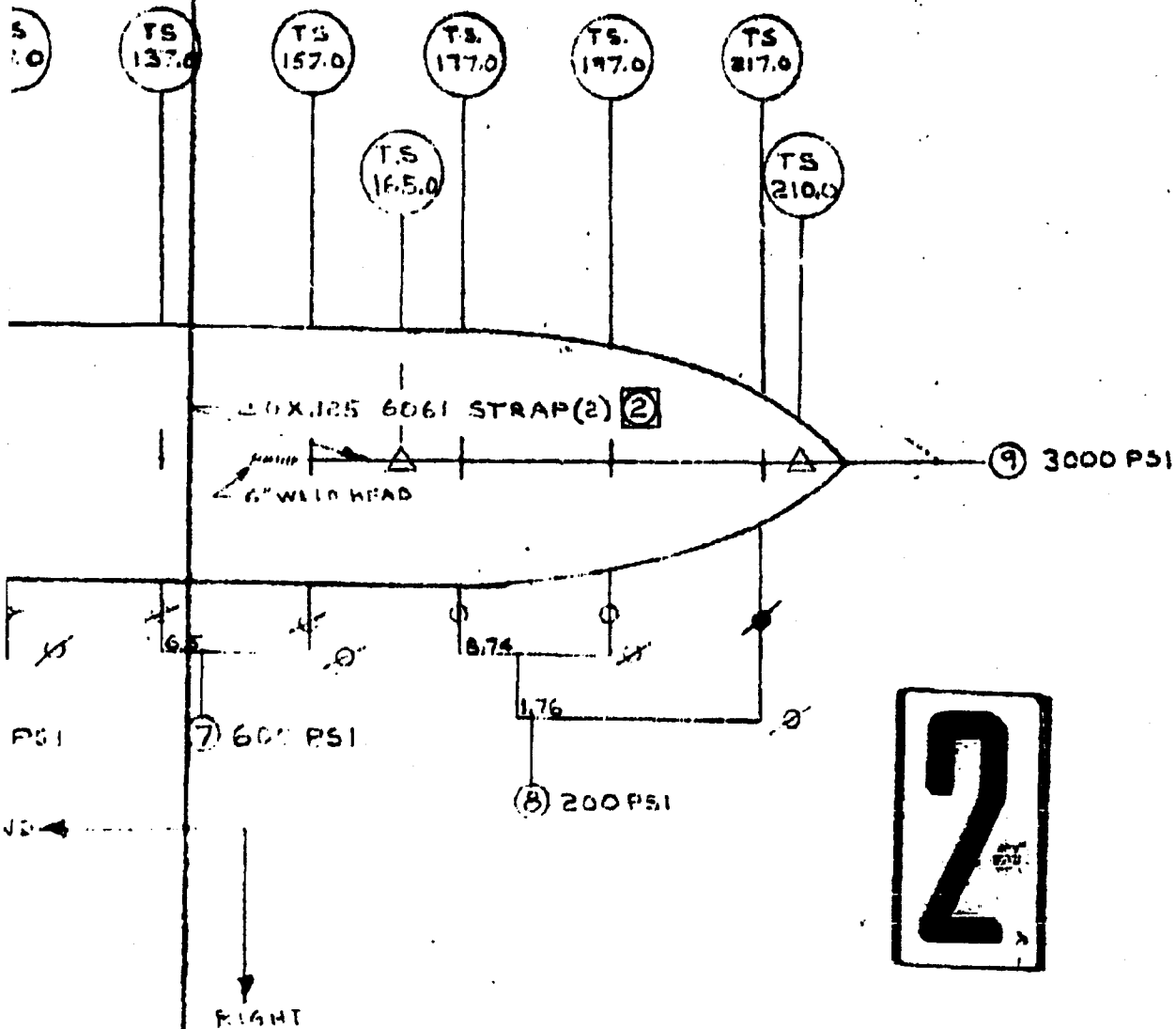


LEGEND:  
SEE PAGE 781

NOTE:

1. INSTALL TANK WITH NOSE POINTING FORWARD
2. INSTALL STRAPS ON HORIZONTAL C/L

SADS CONDITION 25 (CAT TAKE OFF)  
DIAGRAM



PREPARED: R.W. Hill	DATE: 1-9-62	FLETCHER AVIATION CORPORATION	PAGE: 7	TEMP. 110
CHECKED:	TITLE: STATIC TESTS	26-300		
APPROVED:		MODEL: 43.286		
		REPORT No.		

LOAD CONDITION NO. 10 (Flight)      TEST DATE 2-8-62 (3)

REFERENCE DIAGRAM PAGES

GAGE NO.	JACK AREA	PRESSURE GAGE READINGS IN PERCENT OF LIMIT LOAD									
		0	25	50	75	100	0	125	150	0	
1	2.795	0	0	90	180	271	0	362	453	0	
2	10.308	0	124	277	430	584	0	738	891	0	
3	2.795	0	16	91	166	242	0	317	392	0	
4	2.795	0	30	60	90	120	0	150	180	0	
5	2.795	0	28	57	85	113	0	142	170	0	
6	2.795	0	146	293	440	586	0	732	879	0	
7	2.795	0	133	266	398	531	0	664	797	0	
8	2.795	0	28	57	86	114	0	142	171	0	
9	2.795	0	244	488	732	977	0	1221	1465		

PRESSURE      No Pressure

TANK STATION		VERTICAL DEFLECTION READING IN INCHES									
5.0	0	-.03	-.15	-.28	-.41	-.06	-.50	-.62	-.13		
85.0	0	0	.02	.02	.14	0	.07	.10	.02		
165.0	0	.06	.20	.36	.52	.07	.68	.84	.18		
225.0	0	.09	.28	.62	.90	.10	1.20	1.47	.23		

TANK STATION		HORIZONTAL DEFLECTION READING IN INCHES									
5.0	0	+.01	+.02	-.03	-.06	-.06	-.11	-.13	-.11		
85.0	0	.03	.10	.20	.33	.01	.47	.59	.03		
165.0	0	.04	.07	.20	.53	.04	.93	1.18	.07		
225.0	0	.04	.20	.75	1.24	.10	.65	2.02	.26		

ENGINEERING: *Wayne Callahan*

QUALITY CONTROL: *[Signature]*

CUSTOMER: *[Signature]*



JUL 19 2013

PREPARED <b>R.W. Hill</b>	DATE <b>1-9-62</b>	FLETCHER AVIATION CORPORATION	PAGE <b>7.11</b>	FORM <b>7.11</b>						
CHECKED <b>STATIC TESTS</b>			MODEL <b>43.286</b>							
APPROVED			REPORT NO.							
LOAD CONDITION NO. 25 (Cat. T.O.)		TEST DATE <b>2-12-62</b>								
REFERENCE DIAGRAM PAGES										
PRESSURE GAGE READINGS IN PERCENT OF LIMIT LOAD										
GAGE NO.	JACK AREA	0	25	50	75	100	0	125	150	0
1	.7977	0	0	0	56	148	0	239	330	0
2	2.795	59	128	198	267	336	59	406	475	59
3	2.795	42	82	123	163	203	42	244	284	42
4	.7977	0	48	97	146	194	0	242	291	0
5	2.795	0	56	112	168	225	0	281	337	0
6	2.795	0	100	199	299	399	0	498	598	0
7	2.795	0	94	187	281	375	0	468	562	0
8	2.795	0	27	53	80	107	0	133	160	0
9	10.308	0	393	786	1180	1573	0	1966	2359	0
PRESSURE										
TANK STATION		VERTICAL DEFLECTION READING IN INCHES								
5.0	0	-.13	-.25	-.45	-.63	-.08	-.80	-.98	-.08	
85.0	0	-.02	-.02	-.05	-.05	-.02	-.07	-.10	-.04	
165.0	0	.10	.21	.35	.53	.01	.76	.96	.06	
225.0	0	.15	.38	.65	1.00	.02	1.43	1.83	.11	
TANK STATION		HORIZONTAL DEFLECTION READING IN INCHES								
5.0	0	.01	.05	.07	.11	-.02	.24	.30	.04	
85.0	0	0	0	.05	.12	-.03	.30	.44	0	
165.0	0	-.03	0	.11	.22	.01	.47	.67	.03	
225.0	0	.02	.03	.08	.13	0	.48	.90	0	
ENGINEERING:		<i>W. Hill</i>								
QUALITY CONTROL:		<i>[Signature]</i>								
CUSTOMER:		<i>[Signature]</i>								

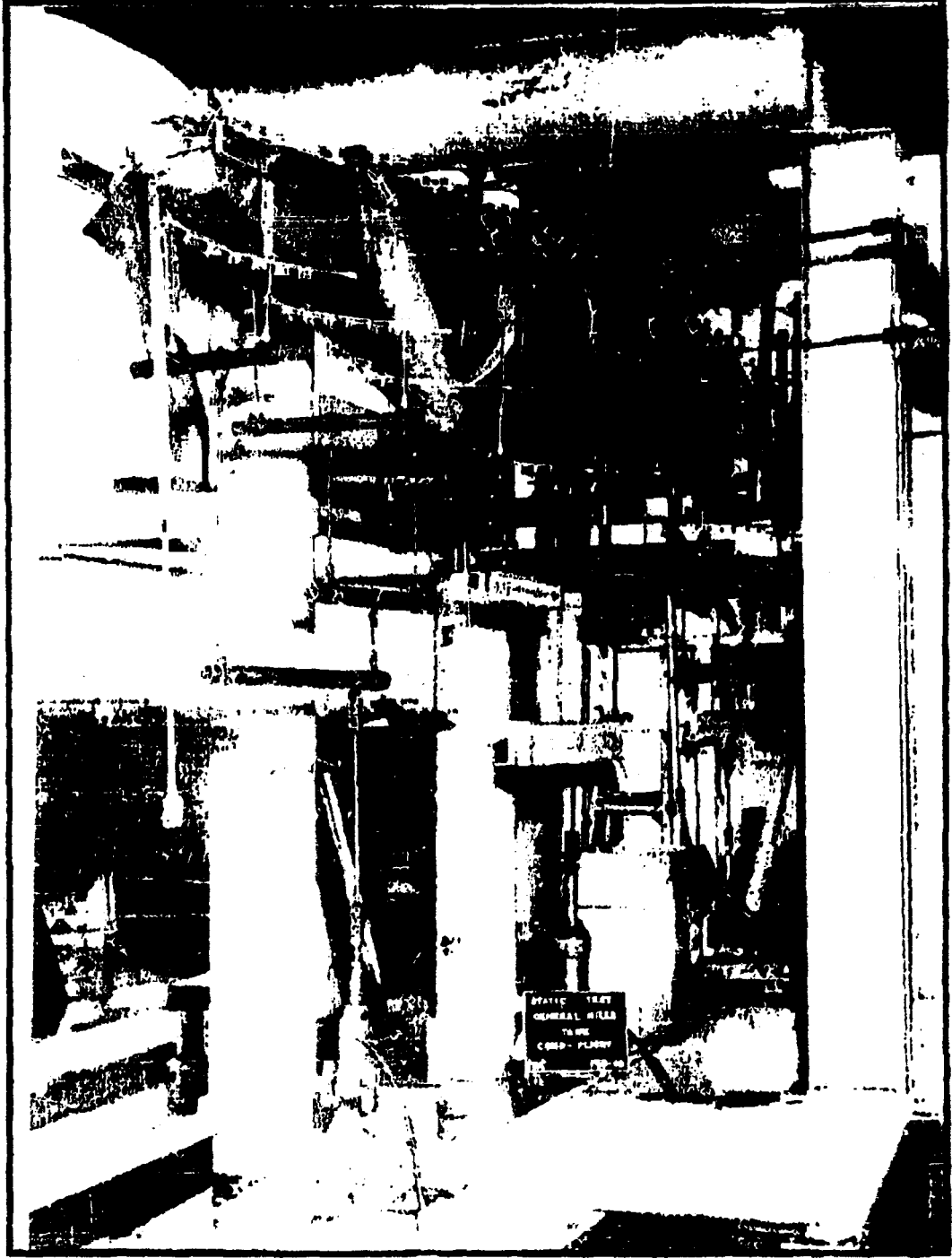
JUL 19 2019

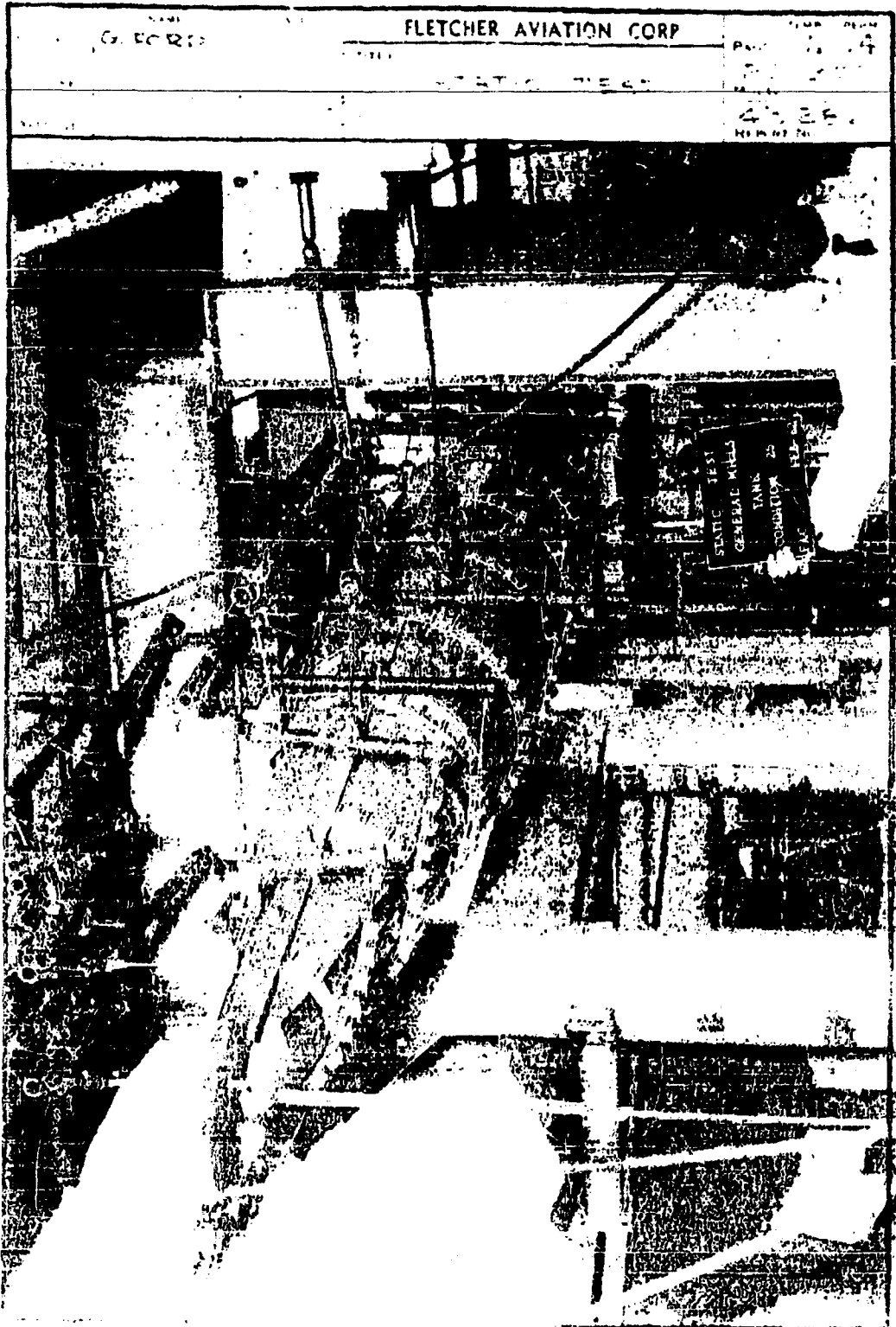
PREPARED	NAME	DATE	FLETCHER AVIATION CORP.	PAGE	TEMP	PERM.
G. FORD			TITLE	26-300		
CHECKED			STATIC TEST	MOB		
APPROVED				43286		
				REPORT NO.		

Page determined to be Unclassified  
Reviewed Chief, RDD, WHS  
IAW EO 13526, Section 3.5  
Date:

JUL 19 2013

PREPARED	NAME <b>G. FORD</b>	DATE	<b>FLETCHER AVIATION CORP.</b>	PAGE	7	PERM. 13
CHECKED			TITLE <b>STATIC TEST</b>	NO. <b>26-300</b>		
APPROVED				REPORT NO. <b>43286</b>		





Page determined to be Unclassified  
Reviewed Chief, RDD, WHS  
IAW EO 13526, Section 3.5  
Date: JUL 19 2013

